

THE IMPACT OF HIGH-RISE RESIDENTIAL BUILDING MORPHOLOGY WITH
CONTROLLED ENVIRONMENT AGRICULTURE (CEA) OF VERTICAL FARMING
ON ENERGY PERFORMANCE

A THESIS SUBMITTED TO
THE FACULTY OF ARCHITECTURE AND ENGINEERING
OF
EPOKA UNIVERSITY

BY

KATERINA LIKA

IN PARTIAL FULFILLMENT OF THE REQUIREMENTS
FOR
THE DEGREE OF MASTER OF SCIENCE
IN
ARCHITECTURE

JUNE, 2023

Approval sheet of the Thesis

This is to certify that we have read this thesis entitled **“The Impact of High-Rise Residential Building Morphology with Controlled Environment Agriculture (CEA) of Vertical Farming on Energy Performance”** and that in our opinion it is fully adequate, in scope and quality, as a thesis for the degree of Master of Science.

Assoc. Prof. Dr. Edmond Manahasa
Head of Department
Date: June 19, 2023

Examining Committee Members:

Prof. Dr. Sokol Dervishi	(Architecture)	_____
Dr. Ina Dervishi	(Architecture)	_____
Dr. Paolo Camilletti	(Architecture)	_____
M.Sc Nerina Baçi	(Architecture)	_____
M.Sc Manjola Logli	(Architecture)	_____

I hereby declare that all information in this document has been obtained and presented in accordance with academic rules and ethical conduct. I also declare that, as required by these rules and conduct, I have fully cited and referenced all material and results that are not original to this work.

Name Surname: Katerina Lika

Signature: _____

ABSTRACT

THE IMPACT OF HIGH-RISE RESIDENTIAL BUILDING MORPHOLOGY WITH CONTROLLED ENVIRONMENT AGRICULTURE (CEA) OF VERTICAL FARMING ON ENERGY PERFORMANCE

Lika, Katerina

M.Sc., Department of Architecture

Supervisor: Prof. Dr. Sokol Dervishi

The incorporation of CEA systems into building design has emerged as a rapidly rising trend as a result of the growing urgency to address global food security and urbanization challenges. Given the significant energy demands associated with these systems, the impact of incorporating them into building design is a critical area of investigation that is yet under-researched. To fill this knowledge gap, this study will provide significant contributions to the field by presenting numerous key findings: Firstly, the primary focus of the research seeks to evaluate the energy efficiency of high-rise residential buildings equipped with controlled environment agriculture (CEA). Secondly, it aims to identify optimal morphological alternatives associated also with food production, which could potentially reduce consumption required for heating, cooling, ventilation, and air conditioning. Finally, the study intends to highlight critical design factors, such as building shape, transparency, and envelope design that have the potential to improve energy performance in three climate contexts. Furthermore, the study endeavors to develop energy simulation and analysis by incorporating meteorological data input parameters and considering different climate settings while providing assumption scenarios about future greenhouse gas emissions. By encouraging creative solutions that meet numerous UN SDGs, the project aligns with its mission to accomplish goals such as affordable and clean energy, sustainable cities and communities, responsible consumption and production, and climate action. This study employs simulation tools, such as Design Builder, Energy Plus and Meteonorm, to analyze the energy efficiency of such structures and

to demonstrate the potential of computational approaches in furthering sustainability practices. The findings indicated a statistically significant correlation between morphology and energy performance. The results underscore the efficiency of implementing geometric design strategies, which could potentially lead to a substantial reduction of up to 42.5% in annual energy consumption. Additionally, shading optimization techniques were found to have a significant impact capable of reducing the demand by a maximum of 25%. By identifying the most suitable building morphologies and design components that maximize energy performance for the right conditions, this study provides valuable insights for building designers, architects, and engineers pursuing to improve the circularity of high-rise residential structures through CEA integration. As a result, this research has significant practical implications given the potential to address global food security, urbanization, and environmental sustainability concerns.

Keywords: *Controlled Environment Agriculture (CEA), Energy efficiency, Vertical Farming, High-Rise Residential Building, Temperature, Shading Optimization, Morphology.*

ABSTRAKT

NDIKIMI I MORFOLOGJISË SË OBJEKTEVE TË LARTA RESIDENCIALE ME AGRIKULTURË TË MJEDISIT TË KONTROLLUAR (AMK) TË FERMAKULTURËS VERTIKALE NË PERFORMANCËN ENERGJITIKE

Lika, Katerina

Master Shkencor, Departamenti i Arkitekturës

Udhëheqësi: Prof. Dr. Sokol Dervishi

Inkorporimi i sistemeve CEA në projektimin e ndërtesave është shfaqur si një prirje në rritje të shpejtë si rezultat i urgjencës të vazhdueshme për të adresuar sfidat globale të sigurisë ushqimore dhe urbanizimit. Duke pasur parasysh kërkesat e rëndësishme për energji që lidhen me këto sisteme, ndikimi i përfshirjes së tyre në projektimin e ndërtesave është një fushë kritike hetimi që është ende e nën-hulumtuar. Për të mbushur këtë boshllëk njohurish, ky studim do të japë një kontribut të rëndësishëm në këtë fushë duke paraqitur gjetje të shumta kyçe: Së pari, fokusi parësor i këtij kërkimi kërkon të vlerësojë efikasitetin energjetik të ndërtesave të larta të banimit të pajisura me Agrokulturë me Mjedis të Kontrolluar (AMK). Së dyti, synon të identifikojë alternativat morfologjike optimale të lidhura edhe me prodhimin e ushqimit, të cilat potencialisht mund të zvogëlojnë konsumin e kërkuar për ngrohje, ftohje, ajrim dhe klimë të kondicionuar. Së fundi, studimi synon të nxjerrë në pah faktorët kritikë të projektimit, si forma e ndërtesës, transparenca dhe dizajni i fasades, që kanë potencialin për të përmirësuar performancën e energjisë në tre kontekste klimatike. Për më tepër, studimi zhvillon simulimin dhe analizën e energjisë duke përfshirë parametrat e të dhënave meteorologjike dhe duke marrë në konsideratë cilësime të ndryshme klimatike dhe skenarë për emetimet e ardhshme të gazeve serrë. Duke inkurajuar zgjidhje kreative që plotësojnë shumë pika nga UN SDGs, projekti përputhet me misionin e tij për të përmbushur qëllime të tilla si “energjia e

përballueshme dhe e pastër”, “qytetet dhe komunitetet e qëndrueshme”, “konsumi dhe prodhimi i përgjegjshëm” dhe “ndryshimi i klimës”. Ky studim përdor mjete simulimi, si Design Builder, Energy Plus dhe Meteonorm, për të analizuar efikasitetin e energjisë të strukturave të tilla dhe për të demonstruar potencialin e qasjeve llogaritëse në avancimin e praktikave të qëndrueshmërisë. Gjetjet treguan një korrelacion statistikisht domethënës midis morfologjisë dhe performancës së energjisë. Rezultatet nënvizojnë efikasitetin e zbatimit të strategjive të projektimit gjeometrik, të cilat potencialisht mund të çojnë në një reduktim të konsiderueshëm deri në 42.5% të konsumit vjetor të energjisë. Për më tepër, teknikat e optimizimit të hijeve u zbuluan se kishin një ndikim të rëndësishëm, të aftë për të reduktuar kërkesën me një maksimum prej 25%. Duke identifikuar morfologjitë më të përshtatshme të ndërtesave dhe komponentët e projektimit që maksimizojnë performancën energjetike për kushtet e duhura, ky studim ofron njohuri të vlefshme për projektuesit, arkitektët dhe inxhinierët e ndërtesave që kërkojnë të përmirësojnë përhapjen dhe zhvillimin e strukturave të larta të banimit përmes integritit të AMK. Si rezultat, ky hulumtim ka implikime praktike të rëndësishme duke pasur parasysh potencialin për të adresuar shqetësimet globale të sigurisë ushqimore, urbanizimit dhe qëndrueshmërisë mjedisore.

Fjalët kyçe: *Agrokulture e Mjedisit të Kontrolluar (AMK), Efikasiteti i Energjisë, Fermat Vertikale, Ndërtesa Rezidenciale të Larta, Temperatura, Optimizimi i Pajisjeve Hijëzuese, Morfologjia,*

I dedicate this thesis to my family, whose unwavering support has been my anchor throughout my academic pursuits. Their motivation and inspiration have driven me to fulfill my ambitions. I am forever grateful for their presence in my life.

I would also like to express my gratitude to my colleagues and friends for their encouragement and support during this challenging journey. Their contributions and enthusiasm have been a constant source of inspiration and motivation. Thank you all for your invaluable support toward the successful completion of this thesis.

Lastly, I am humbled to dedicate this thesis to myself, as it represents the culmination of my hard work, perseverance, and commitment to personal growth. This journey has been challenging, but it has also been a source of immense growth and self-discovery.

ACKNOWLEDGEMENTS

I would like to express my deepest appreciation to my supervisor, Sokol Dervishi and Co-adviser Nerina Baçi, for their guidance and support throughout my research. Your insights, knowledge, and advice have been invaluable, and without your assistance, this project would not have been possible.

I would also like to extend my gratitude to the faculty members of the Department of Architecture for their dedication and commitment to my academic growth. Your courses and teachings have greatly contributed to the development of my research skills and the completion of this thesis.

TABLE OF CONTENTS

ABSTRACT	iv
ABSTRAKT.....	vi
ACKNOWLEDGEMENTS	ix
LIST OF TABLES	xv
LIST OF FIGURES	xvi
LIST OF EQUATIONS	xxii
LIST OF ABBREVIATIONS	xxii
CHAPTER 1	1
INTRODUCTION	1
1.2 Objectives	2
1.3 Motivation	3
1.4 Thesis Outline.....	5
CHAPTER 2 LITERATURE REVIEW.....	6
2.1 Introduction	6
2.2 Morphological Design Impact on Building Energy Demand.....	7
2.2.1 The Importance of Building Form and Orientation	7
2.2.2 Overview of Building Envelope	10
2.3 Theoretical Background	12
2.3.1 Energy Consumption and Fundamental Equations	12
2.3.2 Vertical Farming Yield Governing Equations	17
2.3.3 Overview of Vertical Farming	23

2.3.4	What is Vertical Farming?	23
2.3.5	The Benefits and Challenges of Vertical Farming	24
2.3.6	Vertical Farming Systems and Operational Needs	25
2.3.7	VF Common System Technology	26
2.3.8	VF Crop Types	26
2.3.9	Temperature and Lighting	27
2.3.10	Energy for the HVAC Devices, Humidity and Ventilation	28
2.3.11	Vertical Farming Typologies	29
2.4	Previous Research	31
2.5	Aim and Originality of The Study	35
CHAPTER 3 METHODOLOGY		38
3.1	Overview	38
3.1.1	Data Analysis	38
3.1.2	Ethics	38
3.2	Climate characterization	40
3.2.1	New York, USA	41
3.2.2	Singapore, Asia	42
3.2.3	Athens, Greece	43
3.2.4	Comparison of Selected Climates	44
3.3	Future Predictions	45
3.3.1	Representative Concentration Pathway (RCP) 8.5	46
3.3.2	New York, USA (RCP) 8.5	47
3.3.3	Singapore, Asia (RCP) 8.5	47
3.3.4	Athens, Greece (RCP) 8.5	48
3.3.5	Comparison of Contemporary and Future Weather data	49
3.4	Study Morphologies	50
3.4.1	SQR- Square Morphology	52
3.4.2	ATR- Atrium Morphology	53

3.4.3 REC- Rectangle Morphology	55
3.4.4 CIR-Circle Morphology	56
3.4.5 CRS- Cross Morphology.....	58
3.4.6 LM- “L” Shape Morphology	59
3.4.7 TM-“T” Shape Morphology	61
3.4.8 ZM-“Z” Shape Morphology	62
3.4.9 UM-“U” Shape Morphology.....	64
3.4.10 HM-“H” Shape Morphology.....	65
3.5 Relative Compactness (RC)	67
3.6 Computational Modeling and Simulation	70
3.6.1 Building models	70
3.6.2 Proposed Design Strategy Scenarios.....	74
3.6.3 Simulation Software.....	75
CHAPTER 4 RESULTS	76
4.1 New York (Humid Subtropical Climate)	76
4.1.1 Energy Performance.....	76
4.2 Singapore (Tropical Climate).....	80
4.2.1 Energy Performance.....	80
4.3 Athens (Mediterranean Climate)	83
4.3.1 Energy Performance.....	83
CHAPTER 5 DISCUSSIONS.....	88
5.1 Climate of New York	88
5.1.1 Energy Performance.....	88
5.2 Climate of Singapore.....	91
5.2.1 Energy Performance.....	91
5.3 Climate of Athens.....	94

5.3.1 Energy Performance.....	94
5.4 Climate Comparison.....	97
5.5 Future Prediction Scenarios.....	101
5.5.1 Climate of New York RCP 8.5	101
5.5.1.1 Energy Performance.....	101
5.5.2 Climate of Singapore RCP 8.5.....	104
5.5.2.1 Energy Performance.....	105
5.5.3 Climate of Athens RCP 8.5.....	107
5.5.3.1 Energy Performance.....	107
5.5.4 Comparison of Future and Contemporary Results.....	110
5.6 Cost Estimations.....	111
5.6.1 Background.....	111
5.6.2 Concept Ideation	112
5.6.2.1 One-Square meter Growing Structure.....	112
5.6.3.1 Design Specifications.....	114
5.6.4.1 Space Categorization	114
5.6.5.1 Selected Crops	116
5.6.6.1 System Yield Calculations	118
5.6.7.1 Energy Demand-Profitability Ratio	121
5.6.8.1 Inflation Rates and Food Production	122
CHAPTER 6 OPTIMIZATION.....	124
6.1 Shading Typologies	124
6.2 New York, USA Shading Optimization	125
6.2.1 Optimized Energy Performance.....	125
6.2.2 Comparison of Morphological Optimization.....	133
6.3 Singapore, Shading Optimization.....	135
6.3.1 Optimized Energy Performance.....	135
6.3.2 Comparison of Morphological Optimization.....	142

6.4 Athens, Shading Optimization.....	145
6.4.1 Optimized Energy Performance.....	145
6.3.2 Comparison of Morphological Optimization.....	152
CHAPTER 7 CONCLUSIONS.....	155
7.1 Conclusions	155
7.2 Recommendation for future research	157
REFERENCES.....	159
APPENDIX.....	167

LIST OF TABLES

Table 1. Vertical Farming characteristics around the world.	30
Table 2. A review of the scientific literature on building parameters, with an emphasis on morphology, climate, and energy use. (Methods are SS: simulation study, ES: experimental study, RSM: Real-site measurement, RDO: Real Data Observation).....	33
Table 3. Relative Compactness Calculation.	69
Table 4. Construction properties.....	72
Table 5. Input parameters for HVAC operation.	72
Table 6. Brief for the spatial program.....	72
Table 7. Glazing properties.....	74
Table 8. Scenario description.....	74
Table 9. Simulation results for all the scenarios conducted in the climate of New York.....	90
Table 10. Simulation results obtained for all the scenarios conducted in the climate of Singapore	93
Table 11. Simulation results obtained for all the scenarios conducted in the climate of Athens.	96
Table 12. Best-to-Worst Performing morphologies.....	98
Table 13. Total Morphology Effectiveness (%).	100
Table 14. Future prediction simulation results obtained for all the scenarios in the climate .	103
Table 15. Future prediction simulation results obtained for all the scenarios in the climate of Singapore	106
Table 16. Future prediction simulation results obtained for all the scenarios in the climate of Athens.	109
Table 17. Crop timeline monthly data of different categories and temperature growth.	117
Table 18. Annual Yield profitability and estimates of Base Case scenario of SQR.....	119
Table 19. Total Yield profitability of the morphologies.(€)	119
Table 20. Total Start Up costs and payback period estimates.	120
Table 21. Efficiency in terms of Energy demand and Food Production of the morphologies according to the corresponding climate condition.	121
Table 22. Food distribution % for the residential, local community, and service sectors.	123
Table 23. Shading efficiency results for the climate of New York (%).	135
Table 24. Shading efficiency results for the climate of Singapore (%).	144
Table 25. Shading efficiency results for the climate of Athens (%).	154

LIST OF FIGURES

Figure 1. Relation between photosynthetic rate and temperature, light intensity, and CO2 concentration.....	18
Figure 2. Integrated (CEA) Vertical Farming - Operation and Flow Diagram.....	21
Figure 3. Overview of Three Key Systems in Controlled Environment Agriculture (CEA) Farming: An Explanatory Diagram.....	27
Figure 4. Comparative Visualization of Vertical Farming System Typologies.....	30
Figure 5. Funnel Diagram and Framework of Methodological Process.....	40
Figure 6. Selected locations for Climate Analysis.....	40
Figure 7. Monthly Variation in Air Temperature and Radiation in New York City.....	42
Figure 8. Monthly Variation in Air Temperature and Radiation in Singapore.....	43
Figure 9. Monthly Variation in Air Temperature and Radiation in Athens.....	44
Figure 10. Average temperatures of the selected locations.....	45
Figure 11. Monthly Variation in Air Temperature and Radiation in New York RCP 8.5.....	47
Figure 12. Monthly Variation in Air Temperature and Radiation in Singapore RCP 8.5.....	48
Figure 13. Monthly Variation in Air Temperature and Radiation in Athens RCP 8.5.....	49
Figure 14. Air Temperature variations for contemporary and future weather scenarios under RCP 8.5 in three climates.....	50
Figure 15. The illustrative drawing of all study morphologies.....	51
Figure 16. SQR Morphology, Residential block.....	53
Figure 17. SQR Morphology, Vertical Farming block.....	53
Figure 18. ATR Morphology, Residential block.....	54
Figure 19. ATR Morphology, Vertical Farming block.....	55
Figure 20. REC Morphology, Residential Block.....	55
Figure 21. REC Morphology, Vertical Farming block.....	56
Figure 22. CIR Morphology, Residential Block.....	57
Figure 23. CIR Morphology, Vertical Farming Block.....	57
Figure 24. CRS Morphology, Residential Block.....	58
Figure 25. CRS Morphology, Vertical Farming Block.....	59
Figure 26. LM Morphology, Residential Block.....	60
Figure 27. LM Morphology, Vertical Farming Block.....	60
Figure 28. TM Morphology, Residential Block.....	61

Figure 29. TM Morphology, Vertical Farming Block.	62
Figure 30. ZM Morphology, Residential Block.....	63
Figure 31. ZM Morphology, Vertical Farming Block.	64
Figure 32. UM Morphology, Residential Block.	64
Figure 33. UM Morphology, Vertical Farming Block.....	65
Figure 34. HM Morphology, Residential Block.	66
Figure 35. HM Morphology, Vertical Farming Block.....	66
Figure 36. The illustrative drawing of 3D morphologies and RC values.	69
Figure 37. [RC] Relative Compactness comparison of building morphologies measured in terms of the equation $RC = 6 \times V^{0.66} \times A^{-1}$	70
Figure 38. Occupancy Schedules.	71
Figure 39. Detail call-outs of construction properties.....	74
Figure 40. Evaluation of Simulated Heating results (kWh.m ⁻²) among different morphologies of Vertical Farming.....	77
Figure 41. Evaluation of Simulated Cooling results (kWh.m ⁻²) among different morphologies of Vertical Farming VF.....	78
Figure 42. Evaluation of Simulated Heating results (kWh.m ⁻²) among the Residential morphologies.....	79
Figure 43. Evaluation of Simulated Cooling results (kWh.m ⁻²) among the Residential morphologies.....	79
Figure 44. Evaluation of Simulated Heating results (kWh.m ⁻²) among the morphologies with integrated vertical farming VF in High-rise residential buildings.	79
Figure 45. Evaluation of Simulated Cooling results (kWh.m ⁻²) among the morphologies with integrated vertical farming VF in High-rise residential buildings.	80
Figure 46. Evaluation of Simulated Cooling results (kWh.m ⁻²) among different morphologies of Vertical Farming.....	81
Figure 47. Evaluation of Simulated Cooling results (kWh.m ⁻²) among the Residential morphologies.....	82
Figure 48. Evaluation of Simulated Cooling results (kWh.m ⁻²) among the morphologies with integrated vertical farming VF in High-rise residential. buildings.	82
Figure 49. Evaluation of Simulated Heating results (kWh.m ⁻²) among different morphologies of Vertical Farming.....	84
Figure 50. Evaluation of Simulated Cooling results (kWh.m ⁻²) among different morphologies of Vertical Farming.....	84
Figure 51. Evaluation of Simulated Heating results (kWh.m ⁻²) among the Residential	

morphologies.....	85
Figure 52. Evaluation of Simulated Cooling results (kWh.m-2) among the Residential morphologies.....	86
Figure 53. Evaluation of Simulated Heating results (kWh.m-2) among the morphologies with integrated vertical farming VF in High-rise residential buildings.	86
Figure 54. Evaluation of Simulated Cooling results (kWh.m-2) among the morphologies with integrated vertical farming VF in High-rise residential buildings.	87
Figure 55. Comparison of annual energy demand (kWh.m-2) among all morphologies and their respective study typologies Climate of New York.	89
Figure 56. Comparison of annual energy demand (kWh.m-2) among all morphologies and their respective study typologies_Climate of Singapore.....	92
Figure 57. Comparison of annual energy demand (kWh.m-2) among all morphologies and their respective study typologies_Climate of Athens.	95
Figure 58. Comparison of annual simulated energy consumption (kWh.m-2Y-1) for three specific climatic settings for three typologies.....	99
Figure 59. Suitability gradient of the studied morphologies across their respective typologies in three climatic contexts.	99
Figure 60. Comparison of Annual Heating energy consumption (kWh.m-2Y-1) for future(F) and contemporary(C) predictions of VF, R and VF+R and their associated morphologies in New York.....	102
Figure 61. Comparison of Annual Cooling energy consumption (kWh.m-2Y-1) for future(F) and contemporary(C) predictions of VF, R and VF+R and their associated morphologies in New York.....	103
Figure 62. Comparison of Annual Cooling energy consumption (kWh.m-2Y-1) for future(F) and contemporary(C) predictions of VF, R and VF+R and their associated morphologies in Singapore	105
Figure 63. Comparison of Annual Heating energy consumption (kWh.m-2Y-1) for future(F) and contemporary(C) predictions of VF, R and VF+R and their associated morphologies in Athens.	108
Figure 64. Comparison of Annual Cooling energy consumption (kWh.m-2Y-1) for future(F) and contemporary(C) predictions of VF, R and VF+R and their associated morphologies in Athens.	108
Figure 65. Future Prediction and Contemporary Results Comparison.	111
Figure 66. One Square Meter System Rack Details.....	113
Figure 67. Typical vertical Farming Floor Plan.....	116

Figure 68. 3D illustration of Set Point Temperatures of Veryical Farming Floors.	118
Figure 69. Change in the Inflation rate. (Source: IMF and Harver Analytics).	122
Figure 70. Optimization Shading Typologies S1, S2 and S3.....	125
Figure 71. Comparison of Annual Heating and Cooling energy consumption (kWh.m-2Y-1) for each shading typology on SQR.	126
Figure 72. Comparison of Annual Heating and Cooling energy consumption (kWh.m-2Y-1) for each shading typology on ATR.....	127
Figure 73. Comparison of Annual Heating and Cooling energy consumption (kWh.m-2Y-1) for each shading typology on REC.	128
Figure 74. Comparison of Annual Heating and Cooling energy consumption (kWh.m-2Y-1) for each shading typology on CIR.....	128
Figure 75. Comparison of Annual Heating and Cooling energy consumption (kWh.m-2Y-1) for each shading typology on CRS.....	129
Figure 76. Comparison of Annual Heating and Cooling energy consumption (kWh.m-2Y-1) for each shading typology on LM.	130
Figure 77. Comparison of Annual Heating and Cooling energy consumption (kWh.m-2Y-1) for each shading typology on TM.	130
Figure 78. Comparison of Annual Heating and Cooling energy consumption (kWh.m-2Y-1) for each shading typology on ZM.	131
Figure 79. Comparison of Annual Heating and Cooling energy consumption (kWh.m-2Y-1) for each shading typology on UM.....	132
Figure 80. Comparison of Annual Heating and Cooling energy consumption (kWh.m-2Y-1) for each shading typology on HM.....	132
Figure 81. Comparison of Annual Total energy consumption (kWh.m-2Y-1) for each shading scenario according to all morphologies regarding VF.....	133
Figure 82. Comparison of Annual Total energy consumption (kWh.m-2Y-1) for each shading scenario according to all morphologies regarding R(Residence).	134
Figure 83. Comparison of Annual Total energy consumption (kWh.m-2Y-1) for each shading scenario according to all morphologies regarding VF+R.....	135
Figure 84. Comparison of Annual Heating and Cooling energy consumption (kWh.m-2Y-1) for each shading typology on SQR.	136
Figure 85. Comparison of Annual Heating and Cooling energy consumption (kWh.m-2Y-1) for each shading typology on ATR.....	136
Figure 86. Comparison of Annual Heating and Cooling energy consumption (kWh.m-2Y-1) for each shading typology on REC.	137

Figure 87. Comparison of Annual Heating and Cooling energy consumption (kWh.m-2Y-1) for each shading typology on CIR	138
Figure 88. Comparison of Annual Heating and Cooling energy consumption (kWh.m-2Y-1) for each shading typology on CRS	138
Figure 89. Comparison of Annual Heating and Cooling energy consumption (kWh.m-2Y-1) for each shading typology on LM.....	139
Figure 90. Comparison of Annual Heating and Cooling energy consumption (kWh.m-2Y-1) for each shading typology on TM.....	140
Figure 91. Comparison of Annual Heating and Cooling energy consumption (kWh.m-2Y-1) for each shading typology on ZM.....	140
Figure 92. Comparison of Annual Heating and Cooling energy consumption (kWh.m-2Y-1) for each shading typology on UM.....	141
Figure 93. Comparison of Annual Heating and Cooling energy consumption (kWh.m-2Y-1) for each shading typology on HM.....	141
Figure 94. Comparison of Annual Total energy consumption (kWh.m-2Y-1) for each shading scenario according to all morphologies regarding VF.....	143
Figure 95. Comparison of Annual Total energy consumption (kWh.m-2Y-1) for each shading scenario according to all morphologies regarding R(Residence).....	144
Figure 96. Comparison of Annual Total energy consumption (kWh.m-2Y-1) for each shading scenario according to all morphologies regarding VF+R.....	144
Figure 97. Comparison of Annual Heating and Cooling energy consumption (kWh.m-2Y-1) for each shading typology on SQR.....	146
Figure 98. Comparison of Annual Heating and Cooling energy consumption (kWh.m-2Y-1) for each shading typology on ATR.....	146
Figure 99. Comparison of Annual Heating and Cooling energy consumption (kWh.m-2Y-1) for each shading typology on REC.....	147
Figure 100. Comparison of Annual Heating and Cooling energy consumption (kWh.m-2Y-1) for each shading typology on CIR	148
Figure 101. Comparison of Annual Heating and Cooling energy consumption (kWh.m-2Y-1) for each shading typology on CRS	148
Figure 102. Comparison of Annual Heating and Cooling energy consumption (kWh.m-2Y-1) for each shading typology on LM.....	149
Figure 103. Comparison of Annual Heating and Cooling energy consumption (kWh.m-2Y-1) for each shading typology on TM.....	150
Figure 104. Comparison of Annual Heating and Cooling energy consumption (kWh.m-2Y-1)	

for each shading typology on ZM.....	150
Figure 105. Comparison of Annual Heating and Cooling energy consumption (kWh.m-2Y-1) for each shading typology on UM.....	151
Figure 106. Comparison of Annual Heating and Cooling energy consumption (kWh.m-2Y-1) for each shading typology on HM.....	152
Figure 107. Comparison of Annual Total energy consumption (kWh.m-2Y-1) for each shading scenario according to all morphologies regarding VF.....	153
Figure 108. Comparison of Annual Total energy consumption (kWh.m-2Y-1) for each shading scenario according to all morphologies regarding R (Residence).....	154
Figure 109. Comparison of Annual Total energy consumption (kWh.m-2Y-1) for each shading scenario according to all morphologies regarding VF+R.....	154

LIST OF EQUATIONS

Equation 1. Demonstrates Relative Compactness Ratio.....	9
Equation 2. demonstrates the method to calculate the index of energy consumption (EI) in kWh/m ² •year.	14
Equation 3. calculates the E used in heating.....	14
Equation 4. shows the thermal loads calculation associated with heating for each zone	14
Equation 5. shows the yearly secondary energy for heating.....	15
Equation 6. The E consuming in cooling.....	15
Equation 7. shows the thermal loads associated with cooling for each zone.....	15
Equation 8. shows how to compute yearly secondary energy for cooling.....	15
Equation 9. Typical cooling demand of a building.....	16
Equation 10. is used to determine heat transmission via windows.....	16
Equation 11. and Equation 12. can be utilized to determine how much heat will travel through the exterior walls and roof.....	17
Equation 13. demonstrates how to calculate the total mass of production m.	18
Equation 14. is used for vertical-farming energy conservation.	19
Equation 15. shows the Solar heat gain Q _{solar,gain} as composed of two aspects.	19
Equation 16. The wall temperature may be determined using the following formula.....	19
Equation 17. T _{sky} , may be determined using this particular formula	20
Equation 18. The temperature of the window may be estimated.....	20
Equation 19. depicts the hourly electrical consumption of a standard electric compression chiller chilled by air (COP refers to coefficient of performance).	20
Equation 20. displays the relative compactness formula relative to energy consumption.....	67
Equation 21. depicts the formula for measuring the total crop yield mass in kg.....	118
Equation 22. Depicts the Energy and Yield ratio.....	121

LIST OF ABBREVIATIONS

CEA	Controlled Environment Agriculture	FEW	Food Energy and Water
PL	Plant Factories	(C)	Contemporary Scenario
WWR	Window-to-wall-Ratio	(F)	Future Scenario
FAO	UN Food and Agriculture Organization	FF	Wind Speed
GW	Global Warming	RH	Relative Humidity
RC	Relative Compactness	LCA	Life Cycle Assessment
SHGC	Solar Heat Gain Coefficient	U- Value	Thermal Transmittance
AL	Artificial Lighting	GHG	Green House Gasses
RTG	Roof-Top Garden	UA	Urban Agriculture
CO ₂	Carbon dioxide	VF	Vertical Farm
LED	Light-Emitting Diode	CO ₂	Carbon Dioxide
FP	Food Production	PLC	Production Life Cycle
E	Electric energy (kWh)	EU	European Union
E+	Energy-Plus (Software)	GA	Genetic algorithm
VF+R	CEA Integrated Building	DB	Design Builder
RCP 8.5	Representative Concentration Pathway	E _{tot}	Total Energy Production
H _{Gh}	Annual average global radiation	R	Residence
H _{Bn}	Beam Radiation	AL	Artificial Lighting
H _{Dh}	Diffuse Radiation	NL	Natural Light
T _a	Air Temperature	UN	United Nations
		BC	Base Case Scenario
		S/V	Surface-to-Volume ratio
FEW	Food Energy and Water		
(C)	Contemporary Scenario		
(F)	Future Scenario		
ISO	International Standard Organisation		
AENOR	Spanish Association		
IMF	International Monetary Standardization and Certification		
UNE-EN	Spanish National Adoption of ISO Standards		
ASHRAE:	American Society of Heating, Refrigerating, and Air-Conditioning Engineers		
IRAM	Argentine Institute of Standardization and Certification		
HVAC	Heating, Ventilation, and Air Conditioning		

CHAPTER 1

INTRODUCTION

1.1 Introduction

High-rise buildings have gained popularity in urbanized areas as a result of population expansion as a way to vertically expand the city (Bromfield, 2018; Saroglou, T et al, 2017). Urban areas around the world are inadequately unable to embrace vertical density. The transportation of a high quantity of food to feed a large population will be a major issue in cities of the future. In 2050, the Food and Agriculture Organization of the United Nations (FAO) predicts that just one-third of the agricultural land per capital in 1970 will be accessible (FAO, 2021). One environmentally friendly method of feeding people in very crowded cities that can enhance the quantity of arable land while reducing emissions and transit lengths for agricultural goods is to incorporate vertical farms onto high-rise buildings (Al-Kodmany, K., 2018; Bogomolova et al., 2018; Harada and Whitlow, 2020; Renmark, 2021; O'Sullivan et al., 2020).

Notably, vertical farming has experienced significant global upscaling, technical advancements, and expansion (Armanda et al., 2019; Appolloni et al., 2020). Besides the several widely used long vertical farming systems, commonly known as "plant factories," that have received significant attention in recent years (Pinstrup-Andersen, 2018; Bryce, 2019; McDougall et al., 2019), urban farming has been creating and testing new strategies to engage with their clients in various ways. In association with residential, commercial, and retail areas, smaller-scale adaptable, in-store cultivation systems have also grown in popularity and quantity recently (Bustamante, 2020; Butturini and Marcelis, 2020).

In dense and high-rise environments, farming has become more prevalent over time in and around these urban structures, particularly residential buildings (Khan, Aziz, & Ahmed, 2018; Kim, Lee, Lee, & Lee, 2018; Kosorić, Huang, Tablada, Lau, & Tan, 2019; Song, Tan, & Tan, 2018). This is mainly due to the fact that these

facilities provide underused horizontal and vertical areas that may be suitable for farming in the context of the constrained amount of land accessible for agriculture (Palliwal, A. et al,2021). Despite their advantages, one of the key shortcomings of such systems is their disproportionately higher energy consumption when compared to residences or offices (Graamans, L., 2020; van Delden 2021).

This study looks into how to make high-rise residential buildings more efficient in terms of energy use and food production while yet maintaining self-sufficiency subject to geometric factors such as plan shape, height, and window-to-wall ratio for optimal design solutions that would make vertical farming systems successful in high-rise settings.

1.2 Objectives

The purpose of this study is to investigate the feasibility of using vertical farming to produce food and improve energy efficiency in high-rise residential structures. The study will concentrate on how various morphologies affect high-rise residential buildings with integrated Controlled Environment Agriculture (CEA) systems in terms of energy performance. The main objective is to determine how much energy can be saved by the form choice and how that impacts integrated CEA systems' ability to produce food.

Vertical farming is an increasingly popular urban agricultural technique that is gaining popularity due to its ability to provide fresh, healthy food while utilizing a limited amount of resources and space. The research will take into account and assess the energy consumption patterns of high-rise buildings that incorporate vertical farming.

The study's goal is to determine the most sustainable and energy-efficient high-rise building design for vertical farming utilizing CEA systems. The research will employ a combination of case studies and simulation analysis to evaluate the energy performance, with the simulation analysis being carried out using the building energy simulation tools such as DesignBuilder and Energy Plus as primary mediums. More particularly, this study seeks to:

1. Evaluate the potential of using vertical farming in high-rise structures as a sustainable alternative to conventional agricultural practices.
2. To evaluate the possible advantages and difficulties of integrating vertical farming onto high-rise buildings in urban settings, taking into account elements like land usage, energy use, and food security or transportation.
3. Determine how much energy is consumed by high-rise residential structures when vertical farming is used.
4. Examine how building shape affects energy efficiency with integrated CEA Vertical Farming.
5. Provide suggestions for decision-makers and construction developers that will help them optimize the energy efficiency of high-rise residential structures that feature vertical farming for CEA.
6. Provide suggestions for investors on the amount of food that can be generated from each morphology and the cost of energy for their VF operation throughout each month of year-round production and possible payback time.
7. Identify design parameters that may be utilized to optimize the energy performance of high-rise residential buildings in various climates, such as building envelope design.
8. To identify the optimal building morphology for high-rise residential structures with integrated CEA systems, taking into account both food production and energy efficiency.

The findings from this research will aid in determining the best building morphology for incorporating controlled environment systems with vertical farming, which can result in a reduction of energy needed for heating, ventilation, and air conditioning. The overall goal of the study is to contribute to the development of sustainable building techniques and urban agriculture by providing a thorough examination of the effect of building morphology with vertical farming on the energy performance of high-rise residential structures.

1.3 Motivation

Food production and energy efficiency have emerged as critical concerns for urban growth as a result of the world's expanding population. In urban areas, high-rise residential structures are a typical kind of housing, that need a lot of energy for heating, ventilation, and air conditioning (HVAC). On the other hand, conventional farming practices need a lot of space and use a lot of resources to grow food, including water and fossil fuels. In this context, vertical farming has emerged as a promising answer to some of the present global issues. The concept of growing crops in vertical layers and applying controlled environment agriculture (CEA) technology offers several advantages that can help overcome food insecurity, environmental degradation, and climate change.

First off, by increasing crop yields per unit area, vertical farming makes optimal use of available space. Secondly, vertical farming uses a lot less water, pesticides, and fertilizers than traditional farming, which can lessen the environmental effect of agriculture. Furthermore, because the crops may be produced closer to the customer, it can help lower transportation emissions. Thirdly, vertical farming may increase food security by supplying fresh produce all year round, regardless of the time of year or the weather. Finally, may improve urban surroundings' visual appeal while simultaneously fostering job possibilities, healthy food education, and awareness. By optimizing building morphology and architectural elements and encouraging food production in urban areas, the integration of such CEA systems into high-rise residences can result in more sustainable and self-sufficient communities and reduce energy usage.

Yet, it is still unknown how the shape of high-rise buildings affects the energy efficiency in buildings with integrated CEA systems for vertical farming. Building morphology describes the size, form, and orientation of a structure as well as its architectural features, such as the façade and envelope. The energy efficiency of a structure and its connection with CEA systems for vertical farming can be significantly impacted by various morphologies.

This study is motivated by the need to identify the optimum building morphology for CEA system integration as well as the necessity to comprehend the

possible advantages and disadvantages of combining vertical farming with high-rise residential structures. The project will advance knowledge of vertical farming's potential to lessen the environmental effect of high-rise residential structures and to encourage more sustainable urban development. Moreover, this research might provide light on how design elements like building orientation and exterior design parameters affect energy efficiency in various regions.

The overall goal of this study paper is to provide a thorough examination of the effects of CEA of vertical farming and high-rise building morphology on energy performance. The project will contribute to a greater understanding of the potential of vertical farming to lessen the environmental effect of tall residential structures and to encourage more environmentally friendly urban development with an emphasis on energy. The results of this study can enhance and expand urban agriculture and sustainable building techniques, which are both essential for creating more resilient and sustainable communities.

1.4 Thesis Outline

This thesis is divided in 7 chapters. The organization is done as follows:

In Chapter 1, the introduction to the research topic is given, which is then followed by a thorough explanation of the study's objectives and motivation. Chapter 2, includes the literature review, with a particular emphasis on the influence of building shape on energy performance. Moreover, it investigates theoretical background of energy and vertical farming. Chapter 3, consists of the methodology employed in this study, including climate and framework details. In Chapter 4, the computation simulation results and outputs are presented. Chapter 5, emphasizes discussions and main findings on the effect of high-rise residential building morphology with CEA of Vertical Farming on energy performance. Chapter 6 examines optimization strategies while taking into consideration the findings and suggestions of the research. Chapter 7, highlights important conclusions and their wider implications.

CHAPTER 2

LITERATURE REVIEW

2.1 Introduction

The building industry consumes 40% of the total global energy demand (EU, 2021). The design of high-performance buildings has increased enormously and efforts are being made by engineers and architects to conserve resources and secure our energy future. The growing global population, which has a detrimental impact on energy consumption, agricultural land, and CO₂ emissions, has prompted the development of sustainable dwelling alternatives (D.W. Yarbrough et al., 2019; Benke. K et al., 2017; M. Zahorski et al., 2021).

High-rise structures use more energy than low-rise buildings (G. Shimizu. et al, 2018). New ideas, technologies, techniques, and procedures for both food production and consumption are required to ensure long-term sustainability and resilience. Self-sufficient high-rise structures that combine power generation and efficient resource use in dense populations can be a viable future urbanization option. The current study looks at building morphology and its impact on energy performance. However, there is an insufficient number of studies to demonstrate a link between energy performance and food production capacity in buildings. The overall structure's layout is critical for lowering energy loads and enabling passive design approaches. The key factors influencing building energy efficiency include building form and orientation, as well as the overall design of the envelope. Furthermore, for self-sufficiency in vertical farming integrated buildings, an immense number of design elements linked to the number of farming levels, form, and the property of the suggested façade skin are carefully explored.

This chapter presents a summary of the literature reviewed in preparation for this research. It is divided into two main sections which will focus on morphology and vertical farming potential and impact in high-rise buildings. Section 2.2 and subtopics

examine the literature on the current understanding of relationships between building morphology and energy, identifying that these relationships center on heat transfer and solar access. Section 2.3 reviews varying approaches to the study of vertical farming, its advantages, challenges, and contributions to today's global challenges.

2.2 Morphological Design Impact on Building Energy Demand

Given the emergence of building performance simulation tools, the influence of building shape on energy performance has been extensively researched. Several studies have demonstrated a link between the compactness of a structure and its energy usage (Zhang, J. 2020; Boccalatte, A. 2020; Leng, H. 2020; Zhu, D, 2021). According to the findings, compact forms might result in decreased energy use, particularly in hot and cold areas (Yang, Z., et al, 2020). They propose that building shapes, such as aspect ratio, footprint form, orientation, and positioning of structural vertical core and walls, may be established to optimize passive approaches. In addition, they discovered that the degree of insulation in the building envelope had a substantial influence (Kumar, D., 2020). Numerous research has also been conducted to determine the best building form using numerical calculations such as GA (Feng, J. 2021; Jalali, Z., 2020; Chen, Y., 2018).

According to a review of prior studies, building shape is not the sole building layout measure impacting energy consumption, albeit it may be one of the most relevant parameters in climates with a high need for heating or cooling. The three-dimensional massing of a structure's design, including aspects like self-shading, the transparency of the building enclosure in terms of the number and distribution of windows, and the general orientation of a building all contribute to its energy consumption. It is critical to evaluate these aspects as they might result in both energy gains and losses. By carefully accounting for these design decisions, it can be assessed their influence on energy usage and devise solutions to increase energy efficiency.

2.2.1 The Importance of Building Form and Orientation

The main areas of research focus on improving the performance of the building envelope and technology to boost building energy efficiency. Nonetheless, according to Zhang et al. (2017), the process of optimizing the building shape is only briefly covered in a small number of studies. The energy efficiency of a structure is strongly dependent on the shape and height of the building, which is planned in the early design phase. Many studies have been undertaken to investigate the link between the morphology of a building and its energy operation. Building geometry, when appropriately selected based on location and purpose, has the potential to significantly reduce operating and energy expenses. The building form has been shown in studies to have a considerable influence on heating and cooling loads via the building shell (Zhu, D. 2020; Feng J., 2020).

The shape and attributes of a building are modified by temperature, solar gain, wind power, and humidity. As a result, architects face a problem in establishing an adequate connection between structures and climate. Several building types have the same volume but a varied surface area. As is well known, the overall loss of heat varies with building shape. Even if a structure's floor area remains constant, the façade area may alter as a result of changes in building design. Furthermore, larger façade areas may necessitate larger window areas for daylighting, increasing heat loss via glass. Consequently, building shape is thought to be a major element influencing overall heat loss and thermal comfort. It is one of the most important components in the beginning stages of design since it directly influences the building size and orientation and envelope. Building shape can impact several elements of building performance, including energy efficiency, construction costs, and aesthetic benefits (Košir, M., 2018). Furthermore, the effect of building orientation on energy performance is affected by its shape (Gan, V.J., 2020; Chen, X. 2019).

Choosing an appropriate orientation would have a favorable impact on a building's energy usage. According to these study findings, four major aspects can influence the effect of building form on energy efficiency: relative compactness (RC) of the shape, window-to-wall ratio (WWR), and solar heat gain coefficient (SHGC) of the glazing. The geometric indicator (RC) may be used to determine how compact a building is. A greater RC value indicates that the structure is more compact, whereas a lower RC value indicates the opposite.

Equation 1. Demonstrates Relative Compactness Ratio.

(Equation 1)

$$RC = \frac{\left(\frac{Volume}{Surface\ area}\right) Reference\ cube}{\left(\frac{Volume}{Surface\ area}\right) Building}$$

The RC value is calculated by comparing the volume-to-surface area ratio of the building to that of a cube of the same volume. Additionally, research has shown that building form and orientation can play a significant role in natural ventilation and lighting strategies (Mallick, T., 2019; Sivakumar, A., 2018). For example, a study by Lee and Kim (2017) found that building orientation and form can greatly affect the effectiveness of natural ventilation in buildings and that buildings with a more compact form and an orientation that maximizes wind flow had the highest potential for natural ventilation. Another study (Petrucci and Barazzetti, 2019; Wang et al. 2018) found that building form and orientation can greatly affect the potential for natural lighting in buildings, with buildings that have a more compact form and an orientation that maximizes solar exposure having the greatest potential for natural lighting. These studies highlight the importance of considering building form and orientation in the early design stages to optimize the energy performance and sustainability of a building. A study by Li et al. (2019) found that building form and orientation have a significant impact on the effectiveness of natural ventilation in high-rise buildings, with buildings that have a more compact shape and east-west orientation performing better. Another study by Chen et al. (2021) found that building orientation can greatly affect the performance of passive cooling strategies, with buildings that have a south-facing orientation performing the best in terms of reducing cooling energy consumption.

Furthermore, research has also highlighted the importance of building form and orientation in terms of visual comfort. A study by Wang et al. (2018) found that compact building forms and east-west orientations perform the best in terms of providing a well-lit and visually comfortable environment. In addition, studies have shown that building form and orientation can play a key role in reducing energy consumption and greenhouse gas emissions. For example, studies (Park et al. 2020; Xu et al. 2019) found that building form and orientation can greatly affect the energy

consumption of a building, with buildings that have a more compact shape and south-facing orientation performing the best in terms of reducing energy consumption and reduction of greenhouse gas emissions.

Overall, it is clear from these investigations that building form and orientation play a crucial role in the energy performance, natural ventilation, passive cooling, day-lighting, visual comfort, energy consumption, and greenhouse gas emissions of a building. It is important for architects and building designers to consider these factors in the early design stages to create buildings that are energy-efficient, comfortable, and sustainable.

2.2.2 Overview of Building Envelope

Due to the vast surface area of the structure's façade in high-rise buildings, the building envelope plays an important role in energy efficiency (Košir, M., 2018; Chen, X.; 2019). As the thermal resistance of the façade decreases, the energy consumption of these structures rises as a result of their high transparency ratio. It has been discovered that an exterior wall with a double-layered air corridor may provide the residents with the highest level of residential comfort. According to research, the building exterior with an air corridor also saves energy use by 30% when opposed to the same-sized structures (AYDIN, D., 2020). Thermal loads in Controlled Environment Agriculture may be considerably reduced before considering passive or active heating and cooling systems by taking into account appropriate orientation, the use of sufficient thermal mass, materials, and shading throughout the design phase. Transparent facades have been shown to reduce lighting requirements and power consumption. Building shade typologies can cut operational costs by as much as 30% and HVAC expenditures by half (El-Darwish., 2017).

Moreover, the design of the building's exterior with natural ventilation is preferable over the mechanical one. The greater the height of high-rise structures, the more major the issue that influences both the natural ventilation conditions of the building as well as the heating and cooling loads (Košir, M., 2018). Ascending in height for high-rise structures, particularly in hot and cold regions, increases heating loads while decreasing cooling loads (Godoy-Shimizu 2018; Chen X., 2019). Heat

movement gets complicated by factors such as season, building type, and building activity. When cooling a building during periods of high outside temperatures, the windows must-have features that allow for optimum thermal control. This involves keeping heat within the building with high U-values, efficiently blocking heat from the sun with low Solar Heat Gain Coefficient (SHGC) or g-values, and facilitating heat drainage from the structure with low SHGC or g-values (Yarbrough, 2019). Several main elements have a substantial influence on building energy use. Building orientation is critical, as is efficient thermal insulation, which has been shown to save more than 20% on energy in residential settings. Choosing the proper glass type and orientation in heavily glazed office buildings has been observed to result in energy savings of up to 55%.

Addressing concerns like high light levels and glare also helps with energy efficiency. In industrial settings, utilizing natural ventilation systems can result in significant energy savings ranging from 30% to an astonishing 79% (El-Darwish, 2017; Kumar, D., 2020; Jalali, Z., Leng H., 2020; Ref Giouri, 2019). Furthermore, research has demonstrated that building envelope materials, such as the use of high-performance insulation materials in building envelopes, may play an important role in energy efficiency (Kim et al., 2016) as well as glazing materials with outstanding performance (Li et al., 2018; Wang et al. 2018; Kato, T., 2019; Kurniawan, D., 2020) may significantly minimize heat loss and solar heat gain while increasing energy efficiency. Green roofs and walls in building facades may enhance energy efficiency significantly by lowering heat loss and solar energy gain, while also delivering additional environmental advantages such as reducing stormwater runoff and increasing air quality (Li, Y., 2019; Chen, L., 2020). Moreover, building envelopes with excellent thermal insulation and low solar heat gain coefficients (SHGC) can significantly reduce building energy usage (Kurniawan, T., 2019; Li, J., 2018). Combining high-performance glass and thermal insulation in building envelopes can contribute to a reduction in building energy usage (Park et al. 2020).

According to studies, building envelopes with high insulation values and low (SHGC) may significantly cut energy usage in buildings (Kurniawan, T., 2019; Li, J., 2018). According to a study done by Petrucci and Barazzetti (2019), the use of high-performance glazing and shading materials in building envelopes can result in a 45%

decrease in energy usage. The energy efficiency of a structure is determined by carefully examining its building envelope, which includes the roof, walls, windows, and foundation, as these components have a substantial impact on its total energy performance. Insulated walls and roofs are one technique to increase the energy efficiency of a building's envelope. According to research published in the *Journal of Building Envelope Construction*, integrating insulated walls can result in significant energy savings. Insulated walls, for instance, were discovered to reduce heat loss during the winter by up to 50% and heat gain during the summer by up to 25% (Choi and Roaf, 2018). Insulated roofs can contribute to a reduction in winter heat loss by up to 25% and summer heat gain by up to 20% (Lstiburek, 2017). Furthermore, the adoption of high-efficiency windows, designed to reduce heat loss in the winter and gain heat, may considerably increase a building's energy performance. According to the National Fenestration Rating Council, installing high-efficiency windows can result in significant energy savings. These windows, in particular, can reduce heat loss by up to 25% during colder months and heat gain by up to 30% during warmer months (National Fenestration Rating Council, 2021).

To improve the energy efficiency of a building's envelope, reflective roofing materials are an efficient method. According to research undertaken by the Lawrence Berkeley National Laboratory, the use of reflective roofing materials may significantly reduce the heat absorbed by a building's roof, with possible savings of up to 40% (Levinson, 2010). This can result in considerable energy savings, particularly in hotter areas. The findings convincingly show that the design of building envelopes has a significant impact on building energy performance. In the design of building envelopes, architects and building designers must emphasize the use of high-performance materials, insulation, glass, and shading systems. This method guarantees the construction of energy-efficient and environmentally friendly structures.

2.3 Theoretical Background

2.3.1 Energy Consumption and Fundamental Equations

Designing energy-efficient buildings requires careful consideration of cooling

and heating demands. Both sensible and latent loads, which are influenced by elements including the building envelope, internal sources, and infiltration, are taken into consideration in the computation of the cooling load. Analytical approaches are used to validate the accuracy of numerical simulations for cooling and heating load estimations. The introduction of the IRAM Standard 11900 in 2018 supported the development of building labeling based on energy efficiency and environmental effect. The UNE-EN ISO 1370 methodology, as specified by AENOR in 2011 and other sources like ASHRAE Fundamentals Handbook 2013. Energy use in heating and cooling was calculated using average monthly data, allowing calculations to be done to measure overall energy usage. The major parameters considered when estimating thermal loads for heating and cooling are sensible heating and cooling. These components are critical in estimating the amount of energy necessary to sustain desirable temperature levels within a structure.

Building energy analysis requires the following inputs:

- Solar gain and Internal Heat
- Emission and ventilation characteristics
- Climate data
- Building specification, elements systems, and usage data
- Systems for heating, cooling, air conditioning, and lighting
- Energy waste and reclaimable energy inside the building
- The ventilation supply, temperature, and airflow rate
- Requirements for comfort (set-point values and ventilation settings)



The outcomes of building energy analysis include:

- Yearly energy requirement for heating and cooling (kWh/m²).
- Annual Secondary energy defined as the airflow rate used for space heating and cooling in kWh/m².

- Monthly data for major energy balancing aspects such as conductivity, internal heat gains, and ventilation.
- Monthly data on energy demand and energy use.
- Cost recovery from the building's heating, cooling, ventilation, and lighting.

Although conversion factors for E calculation are dependent on the local energy framework, which might change depending on building location, they are balanced to decrease variables and focus entirely on analyzing the form of the building.

Equation 2. demonstrates the method to calculate the index of energy consumption (EI) in kWh/m²•year.

(Equation 2)

$$EI = \frac{E_{Heat} + E_{Cool}}{A}$$

Where E_{heat} is the principal energy consumed for heating (in kWh). E_{cool} = main cooling energy usage (kWh). A = net usable area of the building (m²), which is the interior area.

Equation 3. calculates the E used in heating.

(Equation 3)

$$E_{Heat} = \sum_{j=1}^M \left[\sum_{i=1}^N \frac{Q_{Heat;i,j}}{\eta_{Heat;i,j}} \times f_{p;i} \right]$$

Where $Q_{heat;l,j}$ = average efficiency of the heating system is 0.7, $f_{p;i}$ = for each thermal zone, the conversion ratio from secondary to primary energy is 1.25, M = amount per month that requires heating, N = nr of thermal zones, with each solid.

Equation 4. shows the thermal loads calculation associated with heating for each zone.

(Equation 4)

$$Q_{Heat} = Q_{env,rad,vent} - \eta_g \times (Q_{Intg} + Q_{Sol})$$

In which Q_{heat} represents kWh of heating energy, $Q_{\text{env;rad;vent}}$ = heat energy transported through the shell and sent to space, as well as energy lost through ventilation, η_g = gains factor, Q_{intg} = (equipment, illumination, occupancy) and Q_{sol} = Solar gains (kWh).

Equation 5. shows the yearly secondary energy for heating.

(Equation 5)

$$E_{\text{Sec.Heat}} = \sum_{j=1}^M \left[\sum_{i=1}^N \frac{Q_{\text{Heat};i;j}}{\eta_{\text{Heat};i;j}} \right]$$

The references are identical to those used in Equation 3.

Equation 6. The E consuming in cooling.

(Equation 6)

$$E_{\text{Cool}} = \sum_{j=1}^M \left[\sum_{i=1}^N \frac{Q_{\text{Cool};i;j}}{\eta_{\text{Cool};i;j}} \times f_{p;i} \right]$$

Where $Q_{\text{cool};i;j}$ = energy for cooling, monthly $\eta_{\text{cool};i;j}$ = cooling system efficiency: 3.2. M=nr of months that require cooling. N = number of thermal areas, and $f_{p;i}$ = The change of secondary to primary energy.

Equation 7. shows the thermal loads associated with cooling for each zone.

(Equation 7)

$$Q_{\text{Cool}} = Q_{\text{Intg}} + Q_{\text{Sol}} - \eta_g \times Q_{\text{env,rad,vent}}$$

Where Q_{cool} = cooling thermal energy in kW, Q_{intg} = (occupancy, illumination, and equipment), Q_{sol} = Heat gains (kWh), η_{disp} = dispersion usage factor and $Q_{\text{env;rad;vent}}$ = dispersion via façade area.

Equation 8. shows how to compute yearly secondary energy for cooling.

(Equation 8)

$$E_{\text{Sec.Cool}} = \sum_{j=1}^M \left[\sum_{i=1}^N \frac{Q_{\text{Cool};i;j}}{\eta_{\text{Cool};i;j}} \right]$$

The references are identical to those used in Equation 4.

Other governing equations that account for conduction, convection, and radiation are used to explain heat transport through windows, walls, and roofs. The formula also takes into account several other variables, including the ground-reflected irradiance, the direct solar heat gain coefficient, the area, the normal indoor and outdoor air temperatures, the direct and diffuse irradiance, and the heat transfer coefficient. These equations may be used to provide precise forecasts regarding the energy performance of buildings (Burdick, A. 2011; Javanroodi, K et al 2018). A typical building's cooling demand is determined using the:

Equation 9. Typical cooling demand of a building.

(Equation 9)

$$Q_{All} = \sum Q_W + \sum Q_R + \sum Q_{Wd}$$

Where Q_W , Q_R , and Q_{Wd} represent heat transfer via windows, walls, and roofs, respectively, all in Watt and taking into account conduction, convection, and radiation

The following formula Equation 10. is used to determine heat transmission via windows.

(Equation 10)

$$Q_{Wd} = \sum Q_{Con} + \sum Q_{Dir} + \sum Q_{Dif}$$

The symbols Q_{Con} , Q_{Dir} , and Q_{Dif} signify three types of heat acquisition via windows: conductive, direct solar, and diffuse solar heat transmission.

$$Q_{Con} = U_{Wd} \times A(T_o - T_i)$$

$$Q_{Dir} = A \times E_{Dir} \times SHGC(\theta)IAC$$

$$Q_{Dif} = A \times (E_{Dir} + E_r) \times (SHGC)_{Dif} \times IAC$$

Where U_{wd} = r coefficient for heat transmission (W/m² K), A = window surface (m²), T_o and T_i = typical interior and exterior air temperatures, E_{Dir} = irradiance (W/m²), SHGC = solar gain coefficient, E_{Dif} = diffuse irradiation (W/m²), E_r = albedo radiation (W/m²).

Equation 11. and Equation 12. can be utilized to determine how much heat will travel through the exterior walls and roof.

(Equation 11)

$$Q_W = \sum U_w \times A(T_o - T_i)$$

(Equation 12)

$$Q_R = \sum U_R \times A(T_o - T_i)$$

Where U_w and U_R , the walls and the roof's respective U-values (W/m² /K), are estimated based on the thickness and composition of the levels that made up those structures.

2.3.2 Vertical Farming Yield Governing Equations

The collecting of data is critical in the modeling, assessment, and optimization of vertical farming systems, and it is an important stage in the process. The suggested outline in this research necessitates some key parameter groups, which include the fundamental consumption of energy or input, as well as the fundamental yield data.

Plants use photosynthesis to transform solar energy into biomass. Estimating plant output frequently entails evaluating the photosynthetic process efficiency, which is impacted by parameters such as temperature, CO₂ concentration, and light intensity, all of which contribute to the plant's productivity. Each plant, as shown in *Figure 1*, has an ideal growth temperature at which its output is maximized. A temperature increase or decrease reduces the rate of photosynthesis.

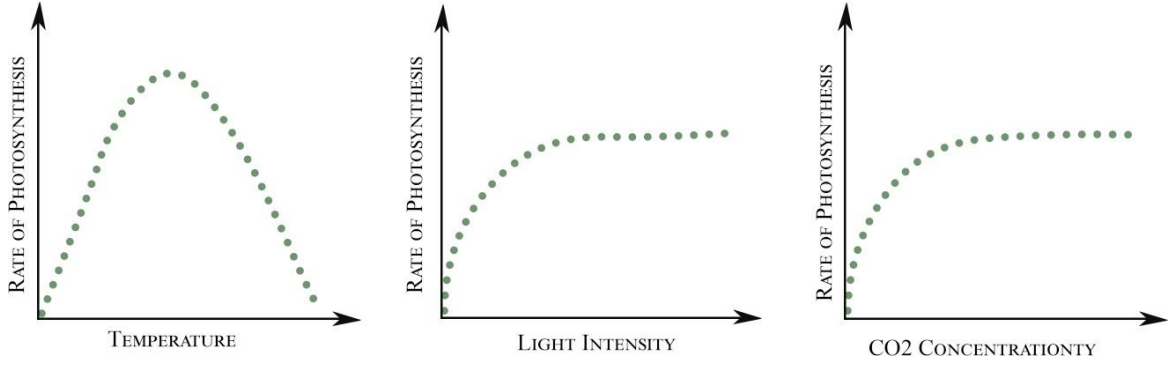


Figure 1. Relation between photosynthetic rate and temperature, light intensity, and CO2 concentration.

Equation 13. demonstrates how to calculate the total mass of production m .

(Equation 13)

$$\begin{aligned}
 m &= Y_{max} \times A \times n_{cropmax} \times \eta_{yield} \quad (1) \\
 \eta_T &= \frac{r}{R_{max}} = \left(\frac{T_{max}-T}{T_{max}-T_{opt}} \right) \times \left(\frac{T}{T_{opt}} \right)^{\frac{T_{max}-T_{opt}}{T}} \quad (2) \\
 \eta_{CO_2} &= 1 - \exp(-k_{CO_2} \times (C_{CO_2} - C_{CO_2,0})) \quad (3) \\
 \eta_L &= 1 - \exp(-k_I \times (I_{PAR} - I_{PAR,0})) \quad (4) \\
 \eta_{yield} &= \min \times (\eta_T, \eta_{CO_2}, \eta_L) \quad (5)
 \end{aligned}$$

As a result, when operating circumstances are not optimal, total production mass (m) is lowered, which is defined by the crop's maximum yield (Y_{max}) under ideal conditions, planting area (A), and number of crop turns each year ($n_{crop, max}$) (as shown in **Equation 1**). Photosynthesis efficiency is estimated by dividing the actual rate of photosynthesis (r) by the rate under ideal conditions (R_{max}). Using **Equations 2-4** can be calculated the effect of suboptimal temperature, CO2 concentration, and light intensity on photosynthetic efficiency. The component that restricts the rate of photosynthesis, which is the least value among r , T , r , CO2, and r , L (as indicated in **Equation 5**), determines the total efficiency of photosynthesis (r , yield). Indoor vertical farming's energy consumption is mostly constituted of two components: (1) Heating, ventilation, and air-conditioning (HVAC) systems consume the most energy, mostly for temperature adjustment. (2) Lighting energy consumption is especially tied to

aiding plant development. Considering that various plants demand varied indoor environmental factors temperature and humidity, a simpler method of calculation is established.

Equation 14. is used for vertical-farming energy conservation.

(Equation 14)

$$\begin{aligned} Q_{appliance,gain} + Q_{solar,gain} + Q_{person,gain} + Q_{vap,gain} + Q_{infiltration} \\ = Q_{ven,out} + Q_{loss} + Q_{cooling} \end{aligned}$$

Where $Q_{appliance,gain}$ - energy gains contributed by the appliances in the indoor environment, $Q_{solar,gain}$ - energy gains contributed by solar radiation in the indoor environment, $Q_{person,gain}$ - energy gains contributed by persons in the indoor environment, $Q_{ven, in}$ in energy input of the fresh air supplied by the ventilation device, $Q_{vap,gain}$ - energy input of the vapor from both the fogging device and the evaporation of the plants, $Q_{ven, out}$ - energy loss of the exhaust gas, $Q_{cooling}$ - cooling load of the indoor environment of vertical farming and lastly, $Q_{infiltration}$ - leakage of air through unsealed gaps in the indoor environment.

Equation 15. shows the Solar heat gain $Q_{solar,gain}$ as composed of two aspects.

(Equation 15)

$$\begin{aligned} Q_{solar,gain} &= Q_F + Q_U \\ Q_F &= A_F U_F (T_{Wall} - T_{indoor}) \\ Q_U &= A_U U_U (T_{Window} - T_{indoor}) \end{aligned}$$

In this context, A_F represents the wall's surface area, whereas U_F and U_U indicate the total heat transfer coefficients of the wall and window, respectively. The temperature of the wall's exterior surface is represented by the symbol T_{wall} . The window's surface area is denoted by A_U , whereas the surface temperature is denoted by T_{window} .

Equation 17. The wall temperature may be determined using the following formula.

(Equation 16)

$$I_{SRG} \alpha A_{ap} = Q_F + \alpha \varepsilon_F A_F F_F (T_{Wall}^4 - T_{sky}^4) + U_F A_F (T_{wall} - T_{air})$$

I_{SRG} signifies sun irradiance in this application, whereas 'a' specifies the absorptivity of the wall's outer surface. A_{ap} denotes the aperture area of a vertical farming module. The Stefan-Boltzmann constant is represented by the symbol ' σ '. ε_F = thermal emissivity, while the view factor for thermal radiation connected to the wall is denoted by F_F . The temperature of the sky is represented by T_{sky} .

Equation 17. T_{sky} , may be determined using this particular formula.

$$T_{sky} = 0.0552 T_{air}^{1.5} \quad \text{(Equation 17)}$$

Equation 18. The temperature of the window may be estimated.

(Equation 18)

$$N_U N_S I_{SRG} A_U = Q_U + \sigma \varepsilon_U A_U F_U (T_{Window}^4 - T_{sky}^4) + U_U A_U (T_{window} - T_{air})$$

Where N_U is the factor used for glazing, N_s is the shading factor and F_U the view factor.

Equation 19. depicts the hourly electrical consumption of a standard electric compression chiller chilled by air (COP refers to coefficient of performance).

(Equation 19)

$$U_T = \frac{Q_{Cooling}}{COP}$$

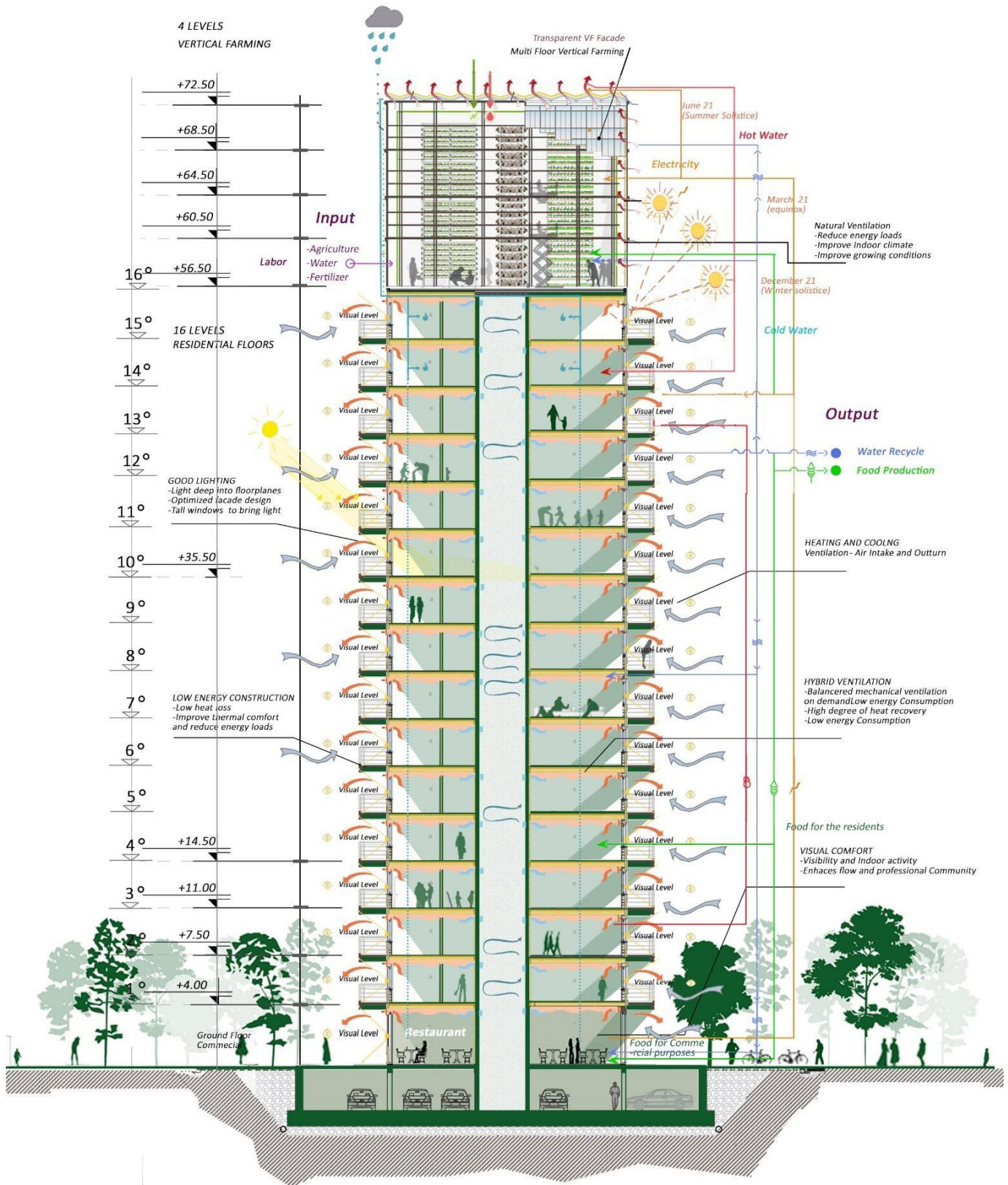


Figure 2. Integrated (CEA) Vertical Farming - Operation and Flow Diagram.

2.3.3 Overview of Vertical Farming

Expanding in popularity around the world, vertical farming, or VF, is a recent phenomenon in urban areas, producing crops on vertically structured surfaces stacked in numerous layers, fully capable of functioning in a controlled indoor setting (Avgoustaki, 2020; Khandaker et al, 2018). There is a narrow range of identified crops ideal for enclosed climate-controlled farms, smaller crops, and a short production lifecycle (Popkova et al, 2022). Hydroponics and aeroponics, which utilize nutritionally water in comparison to the soil for plant growth, are the two major agricultural techniques that are frequently used in vertical farming. As a result, unlike traditional farming methods, VF consumes less water and occupies a smaller area while still being productive as it does not require fertile ground. Moreover, since the overall procedure is in a protected closed loop with total environmental control, it is feasible to accomplish a year-long growth cycle in VF that is undisturbed by externally occurring weather conditions (Mahkeswaran et al, 2021; Krishnan et al, 2020). The VFs also incorporate a variety of technologies that allow for complete condition monitoring as well as rapid and accurate traceability. Typically, the farm cells include thermally regulated growth spaces, cooling fans, irrigated pumps, CO2 filters, LED lighting systems, and other types of sensors (Sharma et al, 2020; Talaviya et al, 2020). Many farms are contemplating energy management strategies to lower the dependencies regarding excessive energy demand to assure sustainable development in the vertical farm systems (Rohit et al, 2021).

2.3.4 What is Vertical Farming?

Vertical farms are a type of Controlled Environment Agriculture (CEA). Thereby, the plant production is multiplied by the vertical farm's number of stories for a certain number of floor spaces utilized. With the same footprint, a vertical farm that is higher produces more food. To elevate crops vertically, vertical farms (VFs) frequently employ scissor lifts, ladders, stairs, or stacked A-frames. VFs can enhance

agricultural yields by 10-100 times by arranging these plant beds in comparison to what a regular farm might do with the same space. Consequently, they can currently produce millions of tons annually. According to reports (Woltering, E, 2021; Butturini, M., 2020), VFs use between 70 and 95 percent less water while growing at a rate that is almost two times that of conventional farming each year. Even while the concept of a vertical farm may have existed for many years before 2010, it might not have received the publicity necessary for its growth and continuation. However, vertical farms are currently finding success because of several global problems that demand the use of such systems. Vertical farming is becoming increasingly important in the transformation of food production and consumption into new, more sustainable patterns.

2.3.5 The Benefits and Challenges of Vertical Farming

Vertical farming evolved as a strategic method to increase agricultural capacity via the use of vertical space. It is an extension of the hydroponic farming approach used in controlled conditions like greenhouses, addressing soil use issues such as the use of fertilizers, pesticides, and herbicides. Vertical farms' closeness to end consumers provides for lower transportation costs while providing year-round output suited to demand. Optimal growth conditions may be accomplished by methodically regulating temperature, humidity, and illumination factors, resulting in optimum crop output (Appolloni, E., 2020; O'Sullivan C.A.,2020; Armanda, D., 2019; Renmark, A.,2021). As indoor farming re-uses gray water and evaporates less than outdoor farming, indoor farming is also much more water efficient (Avgoustaki, D, 2020) than outdoor farming. When there is a significant demand for food in arid regions that simultaneously experience severe pollution and soil erosion, vertical farming is especially promising. According to many studies of vertical farming, the benefits of VF can be categorized also as economic, environmental, social, and political (Harada, Y., 2020; Pinstrup-Andersen, P. 2018). There are several financial benefits to vertical farming, including selling upscale products and export opportunities and protecting crops from floods, droughts, and sun damage. Significant environmental advantages include the provision

of fresh and healthy, uncontaminated organic food. Furthermore, because the technology supports both adaptation and mitigation activities, vertical farming has the potential to aid compliance with climate change obligations. Vertical farming's closed-system concept adds to improved bio-security by providing stronger protection against invading pest species. Along with all the positives, VF also has several downsides and challenges. The complexity of establishing a VF and the expensive start-up expenditures are two main challenges. High energy demands and maintenance costs can contribute significantly to operating costs. According to various research on consumer behavior, people went out of their way to buy food that was grown or manufactured nearby because they believed it would be fresh (Al-Kodmany, K., 2018; Benke K., 2017). However, even though vertical farming has been around for a while, few customers are aware of it. Additionally, because customers are unsure of what artificiality in the farming process means, they are often skeptical.

The research supports this trend by demonstrating that consumers still view food produced by vertical farms as being less natural than food produced by traditional and alternative agricultural methods (Benke, K., 2017). As a result, it appears from the material supplied in the literature that there has not been enough investigation of the market's acceptability of vertical farming. Despite the market's promise, there is barely enough data for all of Europe or other countries (Butturini, M., and Marcelis, 2020).

2.3.6 Vertical Farming Systems and Operational Needs

Currently, the VF efforts are concentrated on integrating agricultural methods within the current urban environment. However, there are more chances for urban agriculture to succeed when it is connected with architecture. Growing in popularity are rooftop farms, especially in tall buildings. Rooftop gardens (RTG) may be climate-controlled or not. They are constructed on rooftops that already exist in densely populated areas where real estate costs are typically too high to construct a conventional indoor farm (Gibson T. 2018). As they normally do not even weigh much, constructing them usually will not require significant structural alterations.

Since RTGs can reduce a building's exposure to heat gains and losses through the roof, which in turn reduces a building's summer cooling and winter heating loads, they are also promoted as energy-efficient design features. Greening rooftops could help to lessen the effects of urban heat islands if implemented on numerous buildings (Mancebo F, 2018). This type of urban agriculture smoothly integrates agriculture and architecture by utilizing available, underutilized, and prospective space within the built environment. It entails assessing crucial elements of a vertical farm to make it ecologically sustainable.

2.3.7 VF Common System Technology

A hydroponic system involves growing plants without soil and providing nutrients and water. Due to the high efficiency of hydroponic systems, the deployment of this technique at several CEA plants has greatly reduced water usage (Avgoustaki, D, 2020; Woltering, E, 2021; Butturini, M., 2020). It should be mentioned that the cost of these systems typically varies depending on their design, functionality, and dependability. Aeroponics is a way of growing plants in an air-based environment, with frequent water and fertilizer sprays directly onto their floating roots. This configuration promotes adequate aeration around the roots, resulting in greatly accelerated plant development that is about ten times quicker than traditional soil-based production (Ampim, 2022). Furthermore, aeroponic systems provide plants with exactly what they need, reducing waste and enabling optimal nutrient consumption, optimizing nutrient usage efficiency. To maximize results, however, aeroponic systems need precise sensing technologies. As is *Figure 3*. Aquaponics is a production method that combines the method of growing plants without soil, with the production of fish. Aquaponic farms are primarily employed in climate-controlled indoor settings that are ground-based (O'Sullivan C.A.,2019). Hydroponics, aquaculture, and maintaining microbes and nutrients are crucial to the success of aquaponics systems.

2.3.8 VF Crop Types

Many assert that, in theory, any crop may be produced in a greenhouse for vertical farming. Strawberries, tomatoes, and various lettuce species make up the majority of today's produce (Benke, K.;2017; Ampim, P.A., 2022). Additionally, viable possibilities are grains, grapes, and tree fruits. Such tree crops require more time, equipment, and labor to produce. The reason why leafy greens are such a popular crop is that they offer a high-profit margin since this method of cultivation requires less time and space between the growing modules to allow for taller crop production (O'Sullivan C.A.,2020). The crop quality and yield can be impacted by many indoor factors as briefly covered in the sections below.

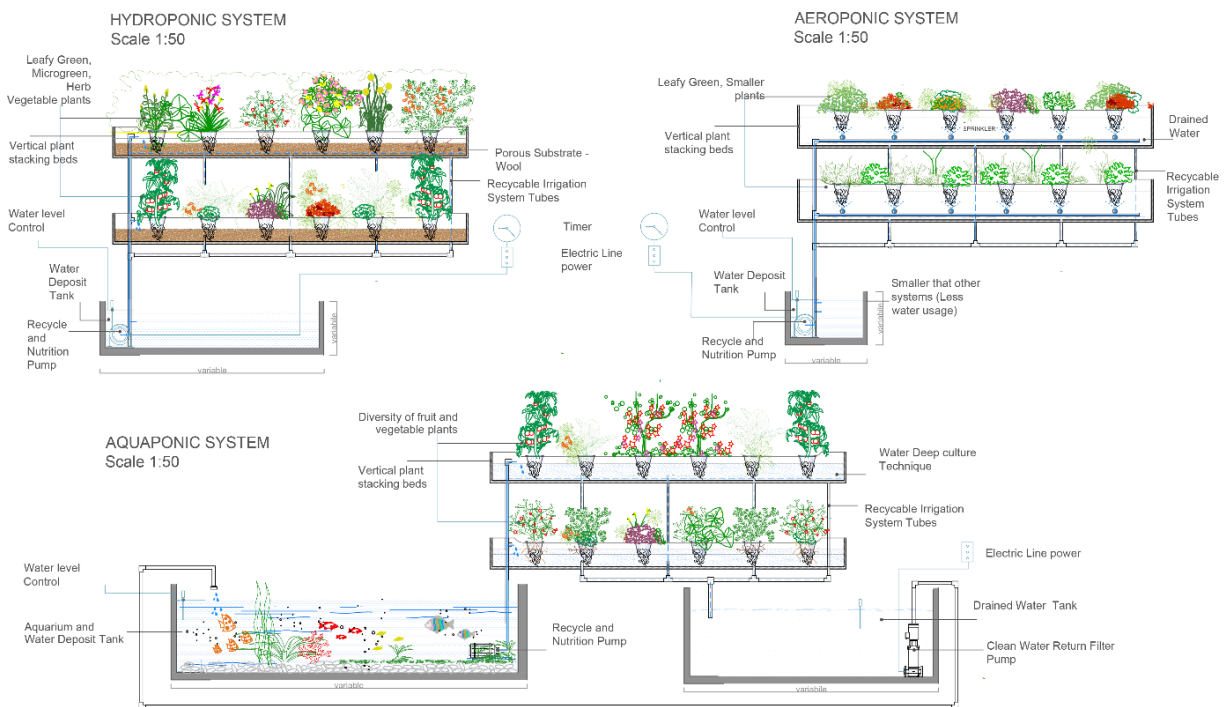


Figure 3. Overview of Three Key Systems in Controlled Environment Agriculture (CEA) Farming: An Explanatory Diagram

2.3.9 Temperature and Lighting

The exact control of ambient air temperature and light conditions has a

significant impact on crop quality and growth rate in indoor production systems. To attain maximum development and productivity, each plant species requires a different temperature range. Deviations from these temperature ranges, whether too low or too high, can hamper plant development, decreasing crop yield and quality owing to nutritional and hormone imbalances, protein misfolding, and other physiological issues. Furthermore, temperature influences the solubility of oxygen in water, which affects root zone health. Elevated nutrient solution temperatures can cause stress and represent a key limiting factor in hydroponic crop growth (Al-Kodmany, 2018; Avgoustaki, D. 2020). Light, on the contrary, has a direct impact on many elements of plant growth, including stem thickness, branching, roots, and critical developmental processes like seed germination and blooming. Due to their low heat production and energy consumption, modern indoor cultivation depends on light-emitting diodes (LEDs) as a preferred light source, making them well-suited for fostering plant growth and development (Ampim, 2022). However, for crops to develop effectively and naturally, sunlight is essential. This exposure type is more useful when VF placement is on a rooftop or an open-air farm.

2.3.10 Energy for the HVAC Devices, Humidity and Ventilation

To encourage evapotranspiration rates of plants, which frequently leads to a significant increase in HVAC-related energy consumption, it is specifically important to maintain low humidity levels for the majority of VF applications (Benke, K.,2017). Moisture is released into the air by plants, which cools it and reduces the sensible load. Lowering indoor humidity levels can be accomplished by drastically chilling supply air and then warming it before giving it to thermally controlled zones (Woltering, E.2021; O’Sullivan, 2019). In northern latitudes and difficult climates, HVAC systems are said to be responsible for 70-85% of total running costs (Appolloni, E., 2020). When radiant heating cannot adequately heat the space during the winter, other heating methods, such as overhead air heaters should be taken into consideration. Additionally, ventilation can prevent overheating in the top rows of a CEA facility through natural convection.

2.3.11 Vertical Farming Typologies

Rooftop gardens (RTGs) are divided into two types: climate-controlled and non-climate-controlled. These gardens are erected on existing rooftops, which is especially important in densely populated places where property prices frequently prevent the establishment of typical indoor farms (Gibson 2018). They typically don't have much weight, thus building them usually does not always require major structural changes. Moreover, RTGs are marketed as energy-efficient construction elements because they may lower a structure's exposure to heat gains and losses via the roof, which lowers heating and cooling loads in the winter and during the summer (Specht, 2013; Mancebo, 2018; Benis, 2017).

To facilitate vertical cultivation, vertical farms (VFs) frequently use scissor lifts, ladders, stairs, or stacked A-frames, the particular choice of which relies on the VF type. VFs may successfully stack plant beds by leveraging these structures, leading to dramatically improved agricultural yields ranging from 10 to 100 times greater than traditional farms occupying the same footprint. According to reports, VFs grow almost twice as quickly each year as conventional farming while consuming between 75% and 90% less water (Liu 2017; Tong 2016). As illustrated in **Figure 4**, vertical space use is the primary distinction between multi-floor vertical farming and single-floor vertical farming.

In a single-floor vertical farming system, plants are cultivated on the same floor in layers or columns that are vertically stacked and often reach heights of several meters. This indicates that the system has a bigger horizontal footprint than a multi-floor system, but needs less structural support and could be easier to handle (Naqvi,2022). In a multiple-floor vertical farming system, plants are produced on several levels, with one or more growth layers present on each level. Elevators or steps can be used to reach the levels, which are typically a few meters apart. As a result, space may be used more effectively since the system can make use of a building or other structure's vertical height (Mancebo, 2018). Nevertheless, this kind of system needs additional structural support, lighting, and administration in addition to perhaps having more complicated logistics, such as the need to carry water and fertilizers to

various levels (Touliato, 2019; Agritecture, 2019). The quantity of growth area each plant has access to is another variable. The growth space for each plant is often smaller in a multi-level vertical farming system than it is in a single-floor setup. Nevertheless, this may be made up for by adding extra levels and utilizing the given area to its fullest. When compared to conventional farming techniques, both kinds of vertical farming systems may produce large yields while using less water. Moreover in **Table 1** are provided the main characteristics of the most popular vertical farming around the world and their operational features as per the typology to which they belong to.

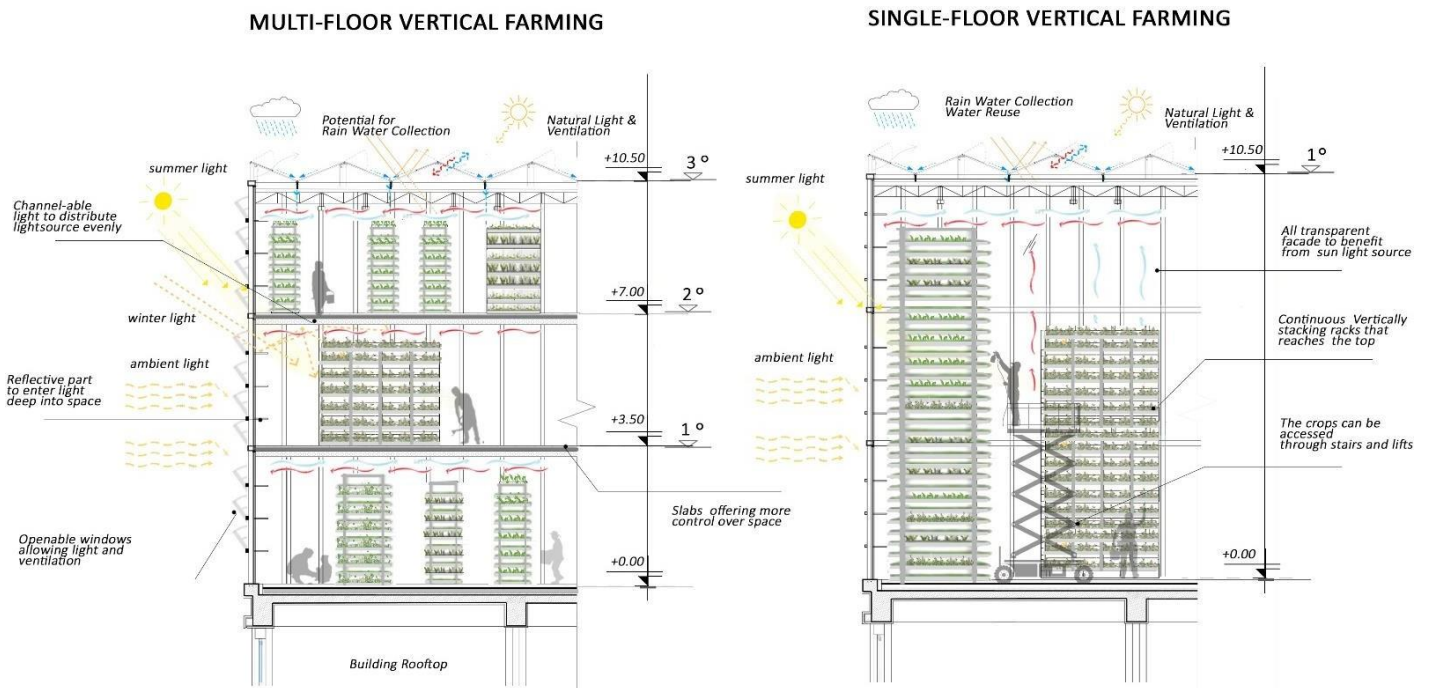


Figure 4. Comparative Visualization of Vertical Farming System Typologies.

Table 1. Vertical Farming characteristics around the world.

VF Name	Location	Area per m ²	VF Design	Building Type	Crops Produced	Year	Lighting	Growing System	Source
SkyGreen Farms	Singapore	650 m ²	SF (3-9 m) A-frame	BS	Leafy greens, microgreens, herbs	2010	NL	Hydrop	www.skygreens.com
Freight Farms	Boston, USA	30 m ²	SF Stacked Bed	SC	Corn, leafy greens, vegetables	2011	AL	Hydrop	www.freightfarms.com
Republic of	South Korea	450 m ²	3 MF Stacked Bed	IBS Tunnel	Leafy greens, fruit greens such as	2011	C	Hydrop	www.cityfarmer.info

Sout Korea VF									strawberries
VertiCrop TM	Canada	350 m ²	SF(column stacked)	RT	Leafy green and vegetables	2009	NL	Hydrop	www.Verticrop.com
Planned VF	Sweden	-	17 MS Stacked Bed	BS	Leafy green and vegetables	2012	C	Hydrop	www.plantagon.com
Aero Farms	New Jersey	13000 m ²	SF Stacked Bed	BS	Variety of leafy greens and herbs	2012	C	Aerop	www.aerofarms.com
PlanetLab VF	Netherland	-	3 MS Stacked Bed	UEB	Vegetables, leafy greens	2011	AL	Aerop	www.plantlab.nl
Vertical Harvest	Wyoming, USA	420 m ²	3 MS Stacked Bed	BS	Lettuce, leafy greens, micro greens, tomato	2012	NL	Hydrop	www.verticalharvestjackson.com
Lufa Farms	Montreal, Canada	2970m ²	3 MS Stacked Bed	RT	Vegetables and leafy greens	2013	C	Hydrop	www.montreal.lufa.com
The Plant VF	Chicago, Illinois, USA	92800 m ²	MF Stacked Bed	BS	Breweries, mushrooms, aculture products	2013	C	Aquap	www.plantchicago.com
Nuvege VF	Japan	25 000 m ²	SF Stacked Bed	BS	Leafy greens	-	AL	Hydrop.	www.nuvege.com
GreenSense	Shenzhen, China	1850 m ²	SF Stacked Bed	BS	Leafy Greens, Lettuces and herbs	2014	C	Hydrop.	www.greensensefarms.com
Mirai Group	Japan	25 000 m ²	SF Stacked Bed	BS	Vegetable, leafy greens	2015	AL	Hydrop	www.mirai-group.jp

Note: SF: Single floor; MF; Multi-floor; BS: New Building Structure; RT: Rooftops of a building; SC: Shipping container; UEB: Underground of an existing building. IBS: Integrated to a Building Structure; NL: Natural light; AL: Artificial Light; C: Combination of both.

2.4 Previous Research

Previous research on buildings have primarily centered on improving energy efficiency through building systems and envelope design. However, this study takes a unique approach particularly on high-rise residential buildings by incorporating building-integrated vertical farming as a means of promoting sustainability, as a result reducing the building's ecological footprint. By considering agriculture as a central aspect of the building's design, this study aims to provide a more comprehensive approach to achieving sustainability and self-sufficiency in high-rise residential

buildings, an approach that has been largely neglected in former research. Nevertheless, several notable authors have made major contributions to the topic of examining building design factors and their influence on energy efficiency in diverse climatic zones.

Aydin and Mihlayanlar (2020) conducted a study on high-rise residential constructions to explore the impact of building envelope design on energy consumption. They discovered that upgrading the design of the building envelope, which includes features like shading devices, insulation materials, glass, and orientations, may result in a 30% reduction in energy use.

Saroglou et al. (2017) also did significant work on the climatically sensitive design for high-rise structures. The authors demonstrated, using thermal simulations and energy modeling, that applying measures such as improved insulation, shading, and ventilation systems may significantly reduce energy consumption.

Li, Liu, et al (2019) investigated the effect of building orientation and design on cooling loads and energy consumption in Tianjin, China, in a continental climate. Their research found that shifting the direction of the building from east-west to north-south can result in considerable energy savings, with cooling loads reduced by 20%.

Benke, K. et al. (2017) investigated the potential benefits of vertical farming and controlled-environment agriculture as alternative food-production systems in research. To assess the practicality and commercial success of vertical farming, they examined various elements such, as profitability, and life-cycle analyses.

Engler N. and Moncef K. (2017) conducted qualitative research on a variety of controlled-environment agriculture (CEA) case studies. They explored how changes to a facility's facade, HVAC systems, lighting, and the use of distributed generating technologies might drastically cut power usage, potentially saving up to 75% of the energy used.

Additionally, Gan, V., et al. (2019) explored the use of simulation-based evolutionary optimization in high-rise residential constructions connected to vertical farming. Proved that employing genetic algorithms and energy simulations may

discover ideal high-rise building layout plans, resulting in significant energy savings of up to 30%-40%.

Table 2. A review of the scientific literature on building parameters, with an emphasis on morphology, climate, and energy use. (Methods are SS: simulation study, ES: experimental study, RSM: Real-site measurement, RDO: Real Data Observation).

Study and Climate locations	Research theme	Building Design Parameters		Morphology and energy	Method	Tools	Main Findings Description	Future Research
		Envelope	Environ. Parameters					
	High-Rise Mid-Rise Low-Rise Vertical	Transparency Shading Devices Thermal Performance Materials Roof/green systems	Temperature Orientation Lighting/solar access Ventilation	Building shape/form Window-to-wall ratio Building floor/height/volume/RC Energy Consumption				
<i>No specific Climate</i>								
AYDIN, D., & MIHLAYANLAR, E. (2020).	•	•	•	•	•	SS Design Builder, Energy-Plus	According to the study, high-rise residential structures with high transparency ratios consume more energy, while improving building envelope design can lower energy consumption by up to 30%.	Shading devices, insulation materials, glazing, orientations, HVAC systems, occupant behavior etc.
Butturini, M (2020) Europe		•				RDO Qualitative Data	The study emphasizes the need of lowering product costs and energy use in the next years. In Europe it is still in its early phases and requires upgrades to become profitable, thus predicting its long-term commercial success is premature.	Potential for diversification with other crops, cost calculations.
T. Saroglou et al. (2017)	•		•	•	•	SS Energy-Plus, Thermal simulations	The study discovers that a climatically responsive design can decrease energy consumption in high-rise buildings through enhanced insulation, shading, and ventilation measures.	Building shapes/forms; window-to-wall ratios; solar panels; impact of ventilation
Benke, K. et al. (2017)		•			•	RDO Qualitative Data	The report investigates the potential benefits and limitations of vertical farming and controlled-environment agriculture as alternative food-production systems.	Detailed analysis, cost and profitability, and life-cycle analysis.
Engler, N and Moncef K. (2017)		•	•		•	ES/ RDO Qualitative Data	According to multiple CEA case studies, alterations to a facility's exterior, HVAC, lighting, and the adoption of distributed generating technologies can cut power use by up to 75%.	Orientation, lighting, and limited measurements of energy efficiency in CEA facilities.
<i>Tropical Climate- (Af)</i>								
Pathirana, Sh. et al. (2019)				•	•	SS Design Builder V5, Energy-Plus	The difference in lighting energy need between the best and worst orientation for rectangular structures is 8.5-9.5%, whereas a WWR of 40% decreases adaptive thermal discomfort hours by 15-20% compared to a WWR of 20%.	Shading devices glazing, mechanical ventilation systems weather patterns.
Jayaweera, N et al. (2021)	•		•	•	•	SS/ RSM Rhino GH, Diva4, Archsim, Energy-Plus	The optimal solar access for a perimeter zone in a high-rise residential structure is specified as 75 sDA (300lx 50), with corresponding yearly energy savings of 28%-36% in the east-west and 8%-12% in the north-south directions.	Climate variations, construction data, building materials.

Song, et al. (2018) Singapore																	RSM	Spectroradiometer, quantum sensor, hemispherical camera	The research looked at the feasibility of growing leafy vegetables on the vertical surfaces of high-rise urban buildings by analyzing sunlight sufficiency and discovered that leaf physiological properties may be utilized to determine plant light requirements.	Use of artificial lighting to supplement natural light, different growing systems, and vertical farming impact	
Palliwal et al. (2021) Singapore																	SS/ RSM	3D GIS, Solweig, Python, Open Street Map	The paper proposes a framework for measuring the potential of urban farming in high-rise buildings that may be adapted to other structures and help unlock underutilized urban farming locations.	Economic feasibility, cost, energy, other building typology,	
Gan, V. et al. (2019) Subtropical-Hong Kong																	SS	GA, Energy Simulation	The study demonstrates that simulation-based evolutionary optimization may uncover optimal layout plans for high-rise residential structures, resulting in energy savings of up to 30%-40%.	Limited in case study, optimization approach, occupant behavior on energy consumption, etc.	
<i>Continental Climate-(Dwa-Dfa)</i>																					
Li, Liu, et al (2019). Tianjin, China																		SS	DesignBuilder, DOE-2, EnergyPlus, TRNSYS, BLAST, DEST, PKPM	Expanding floor space by 10% increased cooling loads and energy consumption by 6.5% and 5.8%, Increasing WWR ratio by 10%, they increased by 4.3% and 3.9%, respectively. Orientation from east-west to north-south can lower cooling loads and energy by 20% and 18% respectively.	Shading devices, insulation materials, glazing, orientations, HVAC systems, occupant behavior etc.
Khamma, T. R. et al. (2017) Chicago																		SS	Energy modeling	The study demonstrates that building shape and orientation, as well as climatic considerations, are critical elements in obtaining maximum energy performance.	varying window-wall ratios, daylighting and different locations on energy performance
<i>Subtropical Climate-(Cfa)</i>																					
Zhu, et al. (2020) Shanghai																		SS	Rhinoceros3D, LadyBug, GH, Energy Plus	The study discovered that the morphology of high-density residential buildings has a considerable influence on their solar potential and that raising building height, decreasing building spacing, and boosting the sky view factor can all help to increase solar potential.	Varying typologies, non-homogeneous building heights, balconies, roof forms
<i>Temperate Climate-(Cfb)</i>																					
Ekici, B (2021). Rotterdam																		SS/ RSM	Honeybee (HB) and Ladybug (LB) plug-ins in GH	Artificial intelligence is being used to improve self-sufficient high-rise buildings, especially in terms of energy usage and food production. The Euro-point complex (case study) could offer lettuce for 27,000 inhabitants within a 1.67 km radius at the highest value of Fp (food production).	Different climate zones, systems of food production, Usage of alternative renewable energy sources
Camporeale, P. E. et al. (2019)																		SS/ RDO	Rhino6, GH, GA Octopus, Energy-Plus	The study suggests that designing building forms with a multi-objective Genetic Algorithm can minimize primary energy consumption while minimizing PE consumption per m2 (PEI), maximizing passive volume ratio (PVR), and maximizing the sum of roofs and best-oriented surfaces (RBOS).	WWR variables, energy savings, and GHG emissions reduction
<i>Tropical Subtropical and Temperate Climate-(Af-Cfa-Cfb)</i>																					
Raji B. et al. (2017) Singapore, Sidney, Amsterdam																		SS	Design Builder and Energy Plus	The study found that the early design of high-rise structures can impact energy usage by up to 32%. In subtropical conditions, the biggest disparity between best and worst solutions occurred with geometric considerations having the greatest effect on energy performance in this setting. Building orientation has a 62% influence. Plan form and plan depth exhibited substantial effects as well, with up to 27% and 25%.	Building typology, considered only single zone open plan layout, plan layout variables, occupant behavior, etc.
<i>Semi-Arid Climate-(Bsk)</i>																					
Javanroodi (2018). Tehran, Iran																		SS	Rhino, GH, Diva, Archsim, Autodesk Inventor, Energy-Plus	Discovered that urban density, building form, and pattern all have significant effects on cooling load reduction and ventilation potential enhancement, with high-density urban form, cubic building form, and pattern P03 being identified as the best urban configuration for achieving these outcomes. The analysis found the top 35 and top 100 instances with the lowest cooling demand and maximum ventilation possibilities.	Orientation, shading materials, climate, comparative analysis
<i>Mediterranean-(Csa-Csb)</i>																					
Vartholomaios, A. et al (2017) Thessaloniki																		SS	Parametric simulations, Python, Regressor algorithm	The study discovered that, assuming constant climatic, construction, and occupancy characteristics, a combination of morphological indicators such as seasonal SA, WWR, and exposed wall/roof S/V ratio can accurately estimate heating and cooling loads for simplified rectangular zone geometries in the studied climate.	Explore other parameters such as materials, transparencies, shape variables, ventilation, etc

Giouria et al. (2019). Piraeus, Athens	•	•	•	•	•	•	•	•	•	•	•	•	•	•	SS	Design Builder Energy-Plus, FRONTIER	The results demonstrate that by optimizing the building's design, orientation, envelope, and systems, attain zero-energy performance. Increased WWR results in increased energy demand for cooling and heating, whilst increased insulation thickness in decreased energy demand.	Impact of occupancy patterns, integrating renewable energy, natural ventilation strategies...
<i>Hot deserted climate, Temperate and Continental -(BWh-Cfb-Dfc)</i>																		
Graamans L. et al (2020). Abu Dhabi, Netherlands, Sweden	•	•	•	•	•	•	•	•	•	•	•	•	•	•	SS	Energy Plus and Crop transpiration model	The study aimed to determine how façade structure influences lettuce output in plant factories, in which opaque facades with high U-values cut energy consumption by up to 30.4%, while transparent facades can reduce electricity usage by up to 9.4%	Different façade variables, renewable energy, economic feasibility, plant growth, and yield
<i>Humid Subtropical, Tropical, and Mediterranean Climate – (Cfa-Af-Csa)</i>																		
<i>This Paper</i>	•	•	•	•	•	•	•	•	•	•	•	•	•	•	SS	Design Builder, Energy Plus, Meteonorm	Efficient geometric design strategies have been shown to reduce annual energy consumption by up to 42.5% and shading techniques by 25%. Integrated models of controlled-environment agriculture (CEA) have the potential to meet 70% of neighborhood food needs, achieving a favorable payback time of 2.3 years.	Impact of different CEA systems, high factor, renewable energy, building typology, etc.

2.5 Aim and Originality of The Study

In today's world, achieving energy efficiency and food self-sufficiency in buildings is of utmost importance. This study aims to provide a novel model of high-rise building integrated farming that is based on the self-sufficiency attained by the initial building shape morphology. A small range of industrial sectors engages in the practice of integrating efficient energy use in the production of goods. As a result, a limited number of research has been done on this subject. The originality of this study lies in the following points:

- Unlike previous works (AYDIN, D., 2020; Sarogloue, T., 2017; Jayaweera, N., 2021; Gan, V., 2019) that focused solely on energy sufficiency, this study takes into account several self-sufficiency factors such as food production and energy usage in high-rise residential buildings as a more holistic approach that considers multiple factors.
- The study employs simulation methods to examine a large number of design aspects concerning the number of farming floors, shape, and properties of the proposed façade skin with shading devices. This approach has not been used before in the context of building integrated CEA.
- The study is the first of its kind to investigate the advantages of vertical farming in high-rise residential structures and the integration of such farming into the concept of energy efficiency for agricultural uses.

- There have been no studies done on energetic performing stimulation and measures with new agricultural purposes in buildings in the context of the Mediterranean and Humid Subtropical and Tropical climates. This study takes into account different climates and ensures that it can be applied to other nations with comparable conditions.
- The morphological analysis of energy performance in high-rise residential buildings has been limited to simple calculations of shape and surface area (Pathirana, Sh. 2019; Gan, V. 2019; Li, Liu, 2019; Khamma, T. 2017; Zhu. 2020). This study aims to provide deep analytical data regarding the other related components of overhang balconies, window-to-wall ratio (WWR), shading devices, future weather predictions, cost analysis, and food production.
- Another original contribution of this study lies in the consideration of the feasibility of the proposed designs. The study by focusing on achieving self-sufficiency for both energy and food production and also considers the cost-effectiveness, and optimization of the proposed solutions. This is an important factor to consider, since solutions that are not economically viable may not be adopted by building owners or developers. By including a more complete picture analysis, this study has the potential impact of the proposed designs on building stakeholders.
- The proposed designs do hold a potential impact on the social well-being and quality of life of the building's inhabitants. The incorporation of integrated Vertical Farming is not only aimed at achieving self-sufficiency but also holds great potential for offering shared community job opportunities, promoting local year-round food production, and providing food supplies on a large scale regardless of weather conditions. This can promote a sense of community and environmental stewardship among residents, creating a more livable and thriving community.

The research will gather input data on the climate setting, agricultural background, building typology, and other factors to find the best possible scenario for

energy efficiency and food self-sufficiency with the fewest investments that can be applied to other building-integrated agricultures. The results will contribute to the growing body of knowledge on CEAI in buildings, particularly in the context of high-rise residential buildings for policymakers, building owners, as well as researchers and academics, who are interested in promoting sustainable living and exploring innovative solutions to the global challenges of the 21st century.

CHAPTER 3

METHODOLOGY

3.1 Overview

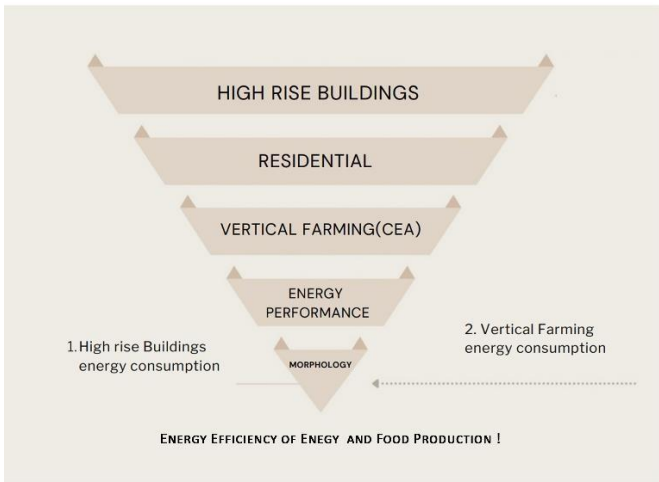
The research will use a mixed-method research design. The study will have three components: selection of building morphology shapes for different climates, modeling of the selected high-rise residential blocks, and case study data collection. The investigation of residential and vertical farming's impact on food production and energy performance is done accordingly, taking into consideration three different climates. Data inputs such as the footprint of each morphology, construction properties, transparencies, and other parameters are kept constant to evaluate their comparison.

3.1.1 Data Analysis

The data analysis process will involve a comprehensive examination of the data collected from the simulation analysis and case study data collection. A combination of qualitative and quantitative methods will be employed to extract meaningful insights from the data. Descriptive statistics will be used to present a clear picture of the energy performance of the various building morphologies. The qualitative data are firstly analyzed to identify the key themes and factors related to the effectiveness of the CEA systems.

3.1.2 Ethics

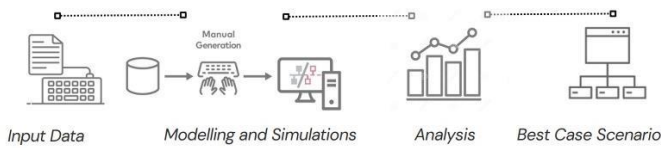
Particularly in the simulation analysis and case study method, ethical issues will be of paramount significance. As there will be no inclusion of human participants, the use of simulation modeling tools will guarantee that the research is non-invasive. Overall, this research will emphasize the preservation and respect for the privacy and safety of all individuals or parties participating in the research and will be done following the highest professional standards.



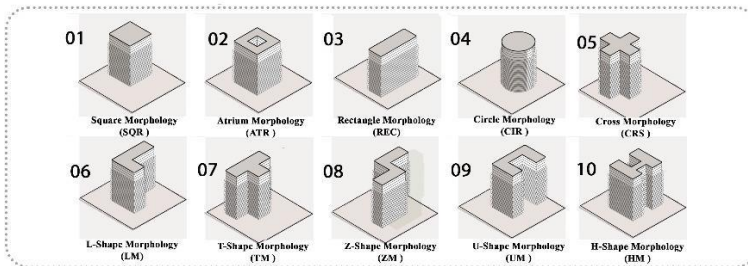
INPUT ASPECTS ON THREE DISTINCT CLIMATES

A-Subtropical	B-Tropical	C-Mediterranean
BUILDING MORPHOLOGIES (10 Total Study Shapes)		
Footprint Area sqm 1800		
WINDOW TO WALL RATIO (60%, 100%)		
GLAZING - DOUBLE GLAZING LoE (e2=1) clear 6mm/13mm Air		
CONSTRUCTION PROPERTIES		
SHADING DEVICES		
OCCUPANCY PATTERNS		
VENTILATION-HVAC SYSTEMS		

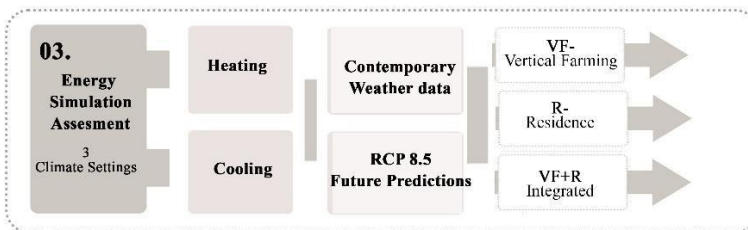
COMPUTING ENERGY SIMULATION



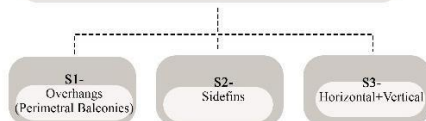
01. Study Morphology Selection and Modelling



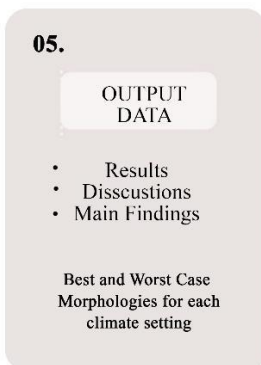
High-Rise Blocks with Integrated CEA- Same floor plan area =1800 sqm
 Residential Block- 16 floors , 3.5 m each
 Vertical Farming Block- 4 floors , 4 m each



04. Optimization Scenarios



05.



06.

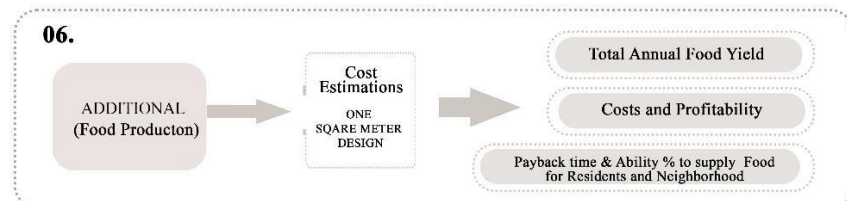


Figure 5. Funnel Diagram and Framework of Methodological Process.

3.2 Climate characterization

To make it easier to generate accurate assessments of the energy performance of high-rise structures, the current study aims to get a greater understanding of varied climates in different geographic areas. Giving a detailed assessment of the climatic conditions in the chosen places is an essential part of this attempt. Thus, these data form a fundamental basis for this analysis and offer vital insights into the climatic conditions that are known to have an impact on the study area. To that purpose, Meteonorm 8.0.3 was used as the source software to collect trustworthy and accurate data on regional weather and climate patterns. By using this method, it is ensured that the descriptions of the climate that result are supported by actual data, giving a clear explanation of the dominant meteorological aspects that guide the subsequent analyses. In addition to the aforementioned details, it is significant to point out that New York in the United States, Singapore in Asia, and Athens in Greece are the cities selected for climate investigation in this study. It was crucial to consider a wide range of climatic aspects unique to each site that affected the selection of these regions.

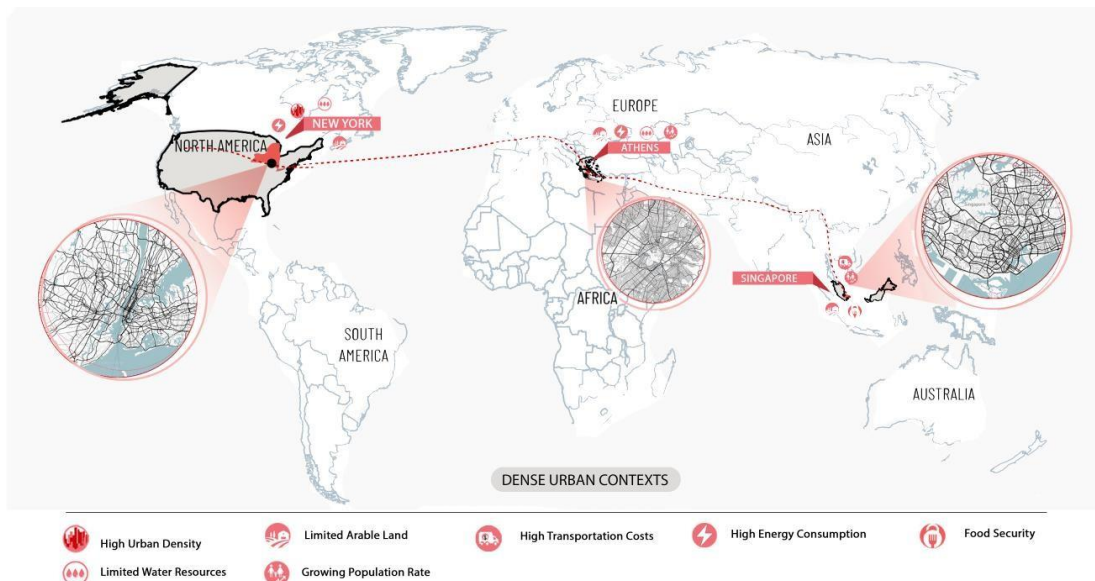


Figure 6. Selected locations for Climate Analysis.

Additionally, these areas were included as a result of their considerable impact on global problems including energy consumption and carbon emissions. The research paper's findings may offer new perspectives that may help shape sustainable building practices and regulations in these areas and beyond.

3.2.1 New York, USA

The Climate of New York is classified as Cfa by Köppen-Geiger climate classification system classifies New York's climate as Cfa. It stands for humid subtropical climate (Cfa) characterized by mild to hot summers and cool to mild winters, and rainfall is relatively evenly distributed throughout the year, with a slight decrease in the winter month. The city has an average temperature of 24.9°C in July, which is the warmest month, and an average temperature of 0°C in January, which is the coldest month. The humid subtropical zone in which New York falls has a mean annual temperature above 0°C and less than 10 months with a mean temperature above 10°C, which is classified as zone III, 8.

The city's annual global radiation averages 1428 kWh/m², with 1342 kWh/m² of beam radiation and 686 kWh/m² of diffuse radiation horizontal. The average temperature throughout the year is 12.8°C, and the relative humidity in New York averages 61%. The average annual air pressure is 1009 hPa, and the wind speed ranges from 2.4 m/s in August to 3.7 m/s in February and March. The prevailing wind direction is from the northeast.

Due to New York's geographic location, the city experiences a range of weather events, including hurricanes, snowstorms, and thunderstorms. Precipitation is distributed evenly throughout the year, with an average of 124.5 cm of rain and 76.2 cm of snow annually. The consistent rainfall is beneficial for the city's vegetation, and New York is known for its lush greenery in the summer months. *Figure 7.* displays a monthly chart of the air temperature and radiation data, with the vertical axis indicating the values. Overall, the climate in New York City can be characterized as having moderate to high levels of solar radiation and temperature, particularly during the summer months. Despite some variability in radiation and temperature values throughout the year, the city's climate is generally characterized by ample sunlight and

relatively warm temperatures, which can have significant implications for energy use.

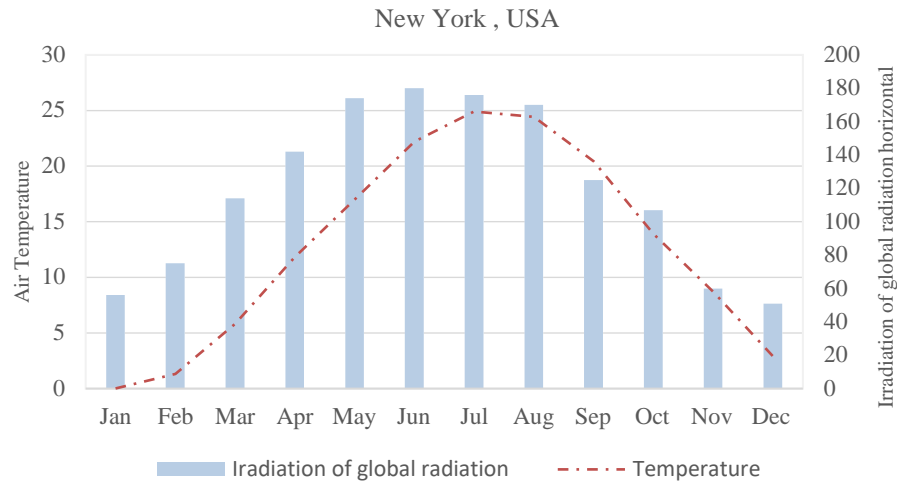


Figure 7. Monthly Variation in Air Temperature and Radiation in New York City.

3.2.2 Singapore, Asia

The Climate of Singapore is classified as Am by the Köppen-Geiger climate classification system. It is characterized by a tropical monsoon climate (Am) with uniformly high temperatures and high humidity throughout the year, along with frequent rainfall. The city-state has an average temperature of 27.7°C in May, which is the warmest month, and an average temperature of 26.1°C in January, which is the coolest month. The tropical climate zone in which Singapore falls has a mean annual temperature above 18°C and no dry season, which is classified as zone A. The city's annual global radiation averages 1945 kWh/m², with 1885 kWh/m² of beam radiation and 1180 kWh/m² of diffuse radiation horizontal. The average temperature throughout the year is 27°C, and the relative humidity in Singapore averages 84%. The average annual air pressure is 1008 hPa, and the wind speed ranges from 2.4 m/s in June to 3.6 m/s in February and March. The prevailing wind direction is from the southeast. Due to Singapore's geographic location, the city experiences a range of weather events, including heavy rainfall, thunderstorms, and occasional haze from forest fires in neighboring countries. Precipitation is distributed unevenly throughout the year, with an average of 234 cm of rain annually. **Figure 8.** displays a monthly chart of the air temperature and radiation data. Overall, the climate in Singapore can be characterized

as having high levels of solar radiation and temperature throughout the year, along with high humidity and frequent rainfall.

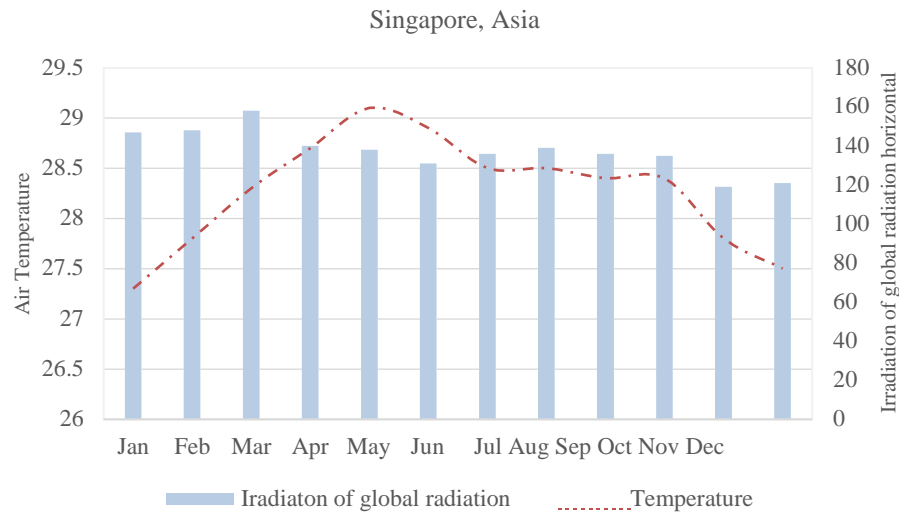


Figure 8. Monthly Variation in Air Temperature and Radiation in Singapore.

3.2.3 Athens, Greece

Athens, the capital of Greece, has a Mediterranean climate (Csa) according to the Köppen-Geiger climate classification system. The city experiences hot, dry summers and mild, wet winters. The average temperature in Athens is 28°C in July, which is the warmest month, and 10°C in January, which is the coldest month. The Mediterranean zone in which Athens is located has a mean annual temperature above 0°C and more than 10 months with a mean temperature above 10°C, which is classified as zone IV, 10. The city's annual global radiation averages 1793 kWh/m², with 1381 kWh/m² of beam radiation and 1012 kWh/m² of diffuse radiation horizontal. The average temperature throughout the year is 18.6°C, and the relative humidity in Athens averages 63%. The average annual air pressure is 1014 hPa, and the wind speed ranges from 2.6 m/s in August to 4.4 m/s in February. The prevailing wind direction is from the northwest. Athens experiences occasional thunderstorms and hailstorms in the summer and occasional snowfall in the winter. The city receives an average of 393 mm of precipitation annually, with the heaviest rainfall occurring in the winter months. Athens' vegetation is relatively dry, especially during the summer months, due to the

low levels of rainfall.

Figure 9. displays Athens' climate which is characterized by abundant solar radiation and high temperatures, particularly during the summer months, highlighting the potential for solar energy utilization and the need for effective heat mitigation strategies.

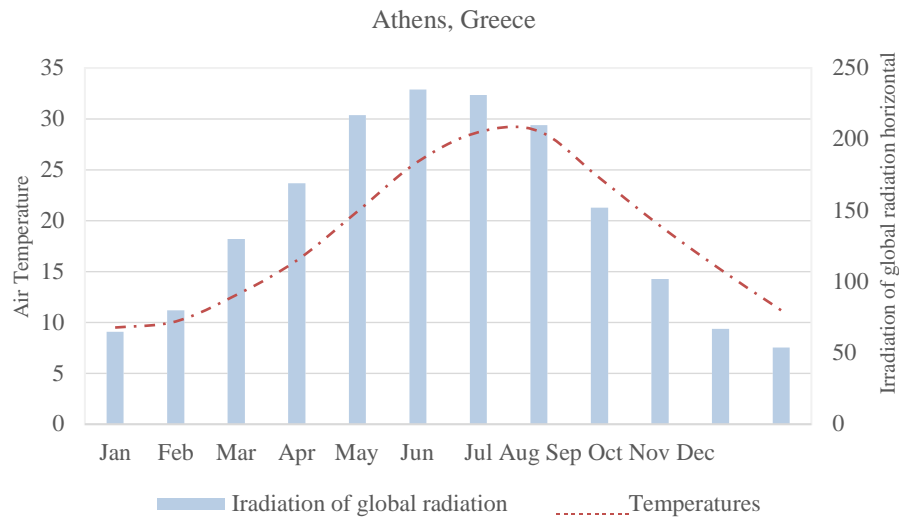


Figure 9. Monthly Variation in Air Temperature and Radiation in Athens.

3.2.4 Comparison of Selected Climates

New York, Singapore, and Athens have distinct climate characteristics. New York has a humid subtropical climate (Cfa) with relatively mild to hot summers and cool to mild winters, while Singapore has a tropical monsoon climate (Am) characterized by uniformly high temperatures and high humidity throughout the year. Athens, on the other hand, has a Mediterranean climate (Cs) with hot, dry summers and mild, wet winters. All cities experience precipitation throughout the year, except for Athens, which has a distinct dry season in the summer months. As depicted in **Figure 10**, New York has a relatively even distribution of precipitation throughout the year, while Singapore experiences uneven distribution with frequent rainfall, and Athens experiences heavy rainfall during the winter months. In terms of solar radiation and temperature, Singapore and New York have higher levels throughout the year compared to Athens. Singapore has the highest annual global radiation average,

followed by New York and then Athens. Nonetheless, Athens has cooler temperatures throughout the year experiencing an average annual temperature of 17.2°C. In contrast, Singapore and New York have warmer temperatures, with Singapore having an average temperature of 27°C and New York at 12.8°C. Wind speeds also vary across the cities, with Singapore having the highest wind speed and Athens having the lowest. Despite these differences, all cities have their unique weather events. New York experiences hurricanes, snowstorms, and thunderstorms, while Singapore has heavy rainfall, thunderstorms, and occasional haze from forest fires. Moreover, Athens has hot, dry summers with occasional heat waves and heavy rain during the winter months. Overall, the different climate characteristics of these cities have significant implications for energy use, vegetation, and the local lifestyle.

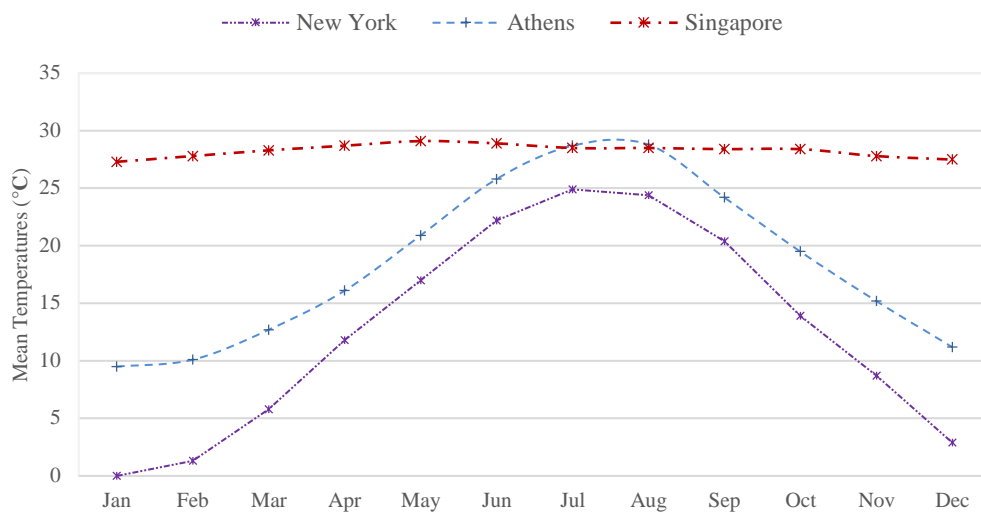


Figure 10. Average temperatures of the selected locations.

3.3 Future Predictions

This study aims to not only conduct a complete analysis of the current situation but also to expand its contributions to the area of future implications for the energy performance of the researched morphologies. The investigation includes future weather scenarios for New York, Singapore, and Athens and intends to identify the possible effects on energy consumption following major temporal shifts, especially

over a centennial timeframe (100 years), by including these new dimensions. The research will examine the complex relationship between changing climatic circumstances and the energy needs of the analyzed morphologies employing Meteorom data associated with the Representative Concentration Pathway (RCP) 8.5. The research seeks to enhance the comprehensive nature of its findings and develop a more thorough knowledge of the energy performance dynamics inherent to the examined morphologies by integrating future weather scenarios and performing a long-term prediction of energy demand changes. By incorporating future weather scenarios and carrying out a long-term projection of energy demand changes, the study enables the enhancement of the comprehensive nature of its results and provides a more in-depth understanding of the energy performance dynamics inherent to the assessed morphologies.

3.3.1 Representative Concentration Pathway (RCP) 8.5

A crucial paradigm in climate research, the Representative Concentration Pathways (RCPs) examine probable future greenhouse gas concentration trajectories and their ensuing effects on the Earth's climate system. RCPs, which were created as an extensive collection of scenarios, allow for the evaluation of probable repercussions resulting from different amounts of greenhouse gas emissions. Each RCP reflects a unique radiative forcing pathway, which measures the change in the Earth's atmosphere's energy balance brought on by outside factors, mostly greenhouse gas emissions. RCP 8.5, which depicts a scenario in which greenhouse gas concentrations continue to rise consistently throughout the 21st century, assumes a high-emission trajectory.

This scenario demonstrates a future with sustained reliance on fossil fuels and assumes minimal mitigation measures, leading to a significant rise in radiative forcing by 2100. For researchers to comprehend and improve awareness of the effects of such a scenario on various aspects, including energy demand, climate change, and sustainability, RCP 8.5 provides a basis for exploring the potential outcomes and challenges associated with a future that involves significant greenhouse gas emissions.

3.3.2 New York, USA (RCP) 8.5

The information given in *Figure 11* provides a succinct summary of the expected climatic conditions in New York for the year 2100 under the RCP 8.5 scenario. Changes in radiation, temperature, humidity, wind, and precipitation are indicated. According to estimates, the annual average global radiation (H_Gh) will be 1493 kWh/m², with beam radiation (H_Bn) averaging around 1471 kWh/m² and diffuse radiation (H_Dh) averaging about 676 kWh/m². The dataset shows that the annual average air temperature (Ta) is around 19.1 °C. The average annual wind speed (FF) is thought to be around 3.1 m/s, while the relative humidity (RH) stays constant at about 61%.

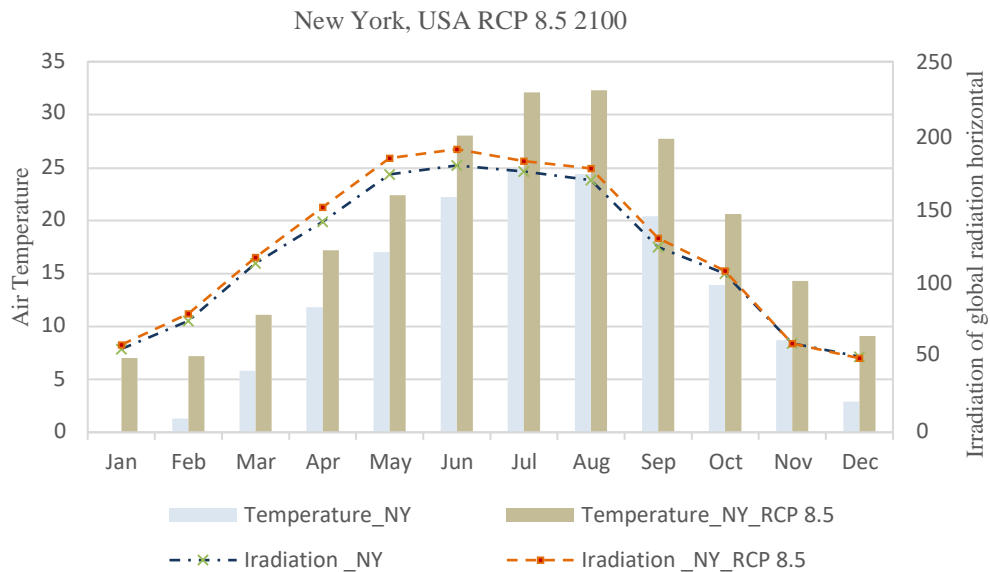


Figure 11. Monthly Variation in Air Temperature and Radiation in New York RCP 8.5.

3.3.3 Singapore, Asia (RCP) 8.5

Important facts describing the expected climatic conditions are shown in the dataset for Singapore in the year 2100, as described in **Figure 12**. Peak temperatures will occur in May and June, with average temperatures being persistently high. The relative humidity will remain constant, and the wind speed will change seasonally. According to the statistics, cloud cover and precipitation patterns are generally consistent. With beam radiation (H_{Bn}) averaging 1127 kWh/m² and diffuse radiation (H_{Dh}) averaging 915 kWh/m², the yearly average global radiation (H_{Gh}) is expected to be about 1703 kWh/m². The annual average air temperature (T_a) is predicted to be about 32.2 °C, with relative humidity (RH) that stays largely constant at 79% and the average wind speed (FF) to be about 2.3 m/s.

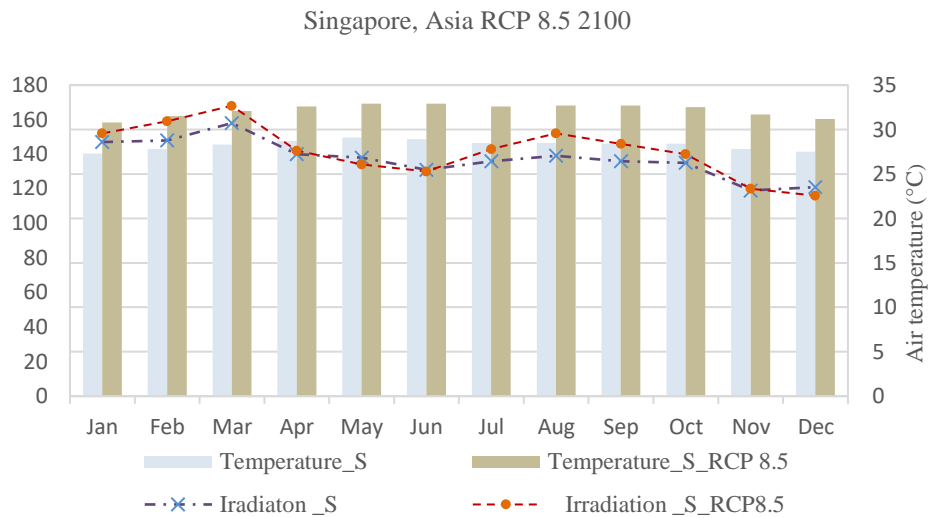


Figure 12. Monthly Variation in Air Temperature and Radiation in Singapore RCP 8.5.

3.3.4 Athens, Greece (RCP) 8.5

Under the RCP 8.5 scenario, the information shown in **Figure 13** regarding Athens in the year 2100 offers important insights into the anticipated climatic conditions. Radiation-wise, it is anticipated that the average annual global radiation (H_{Gh}) will be roughly 1769 kWh/m². This comprises an average diffuse radiation (H_{Dh}) of around 624 kWh/m² and a typical beam radiation (H_{Bn}) of roughly 1921 kWh/m². The dataset provides monthly average air temperature (T_a) information for

temperature, Athens is expected to have an average annual air temperature of about 23.8 °C in 2100. The average relative humidity (RH), in terms of moisture content, is about 57%. while the expected average wind speed (FF) is 2.7 m/s.

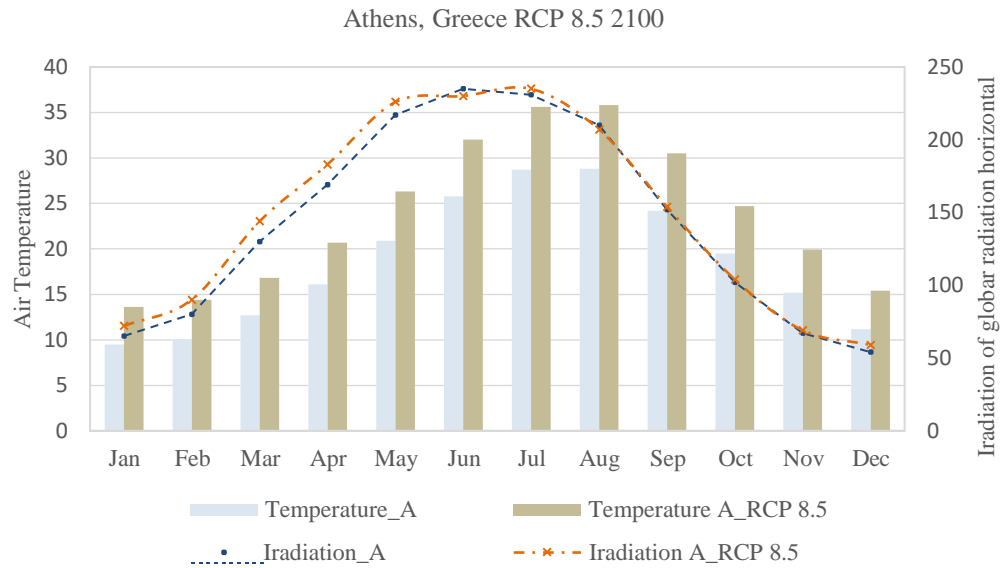


Figure 13. Monthly Variation in Air Temperature and Radiation in Athens RCP 8.5.

3.3.5 Comparison of Contemporary and Future Weather data

Significant temperature differences may be seen when contrasting the climatic data for New York, Singapore, and Athens in both the present and future estimates made by RCP 8.5. It is clear from comparing the predicted climatic conditions that Singapore will have the highest average annual air temperature of about 32.2 °C, making it much hotter than Athens, which is predicted to have an average temperature of 23.8 °C, and New York is predicted to have a temperature of 19.1 °C. **Figure 14** suggests that Singapore is likely to experience more severe heat-related problems in the future. In terms of radiation levels, Athens is anticipated to have the highest average global radiation of around 1769 kWh/m², followed by Singapore (1703 kWh/m²) and New York (1493). According to this, Athens and Singapore will presumably get more solar radiation than New York, which may have an impact on the regional climate, energy production, and farming practices in these areas.

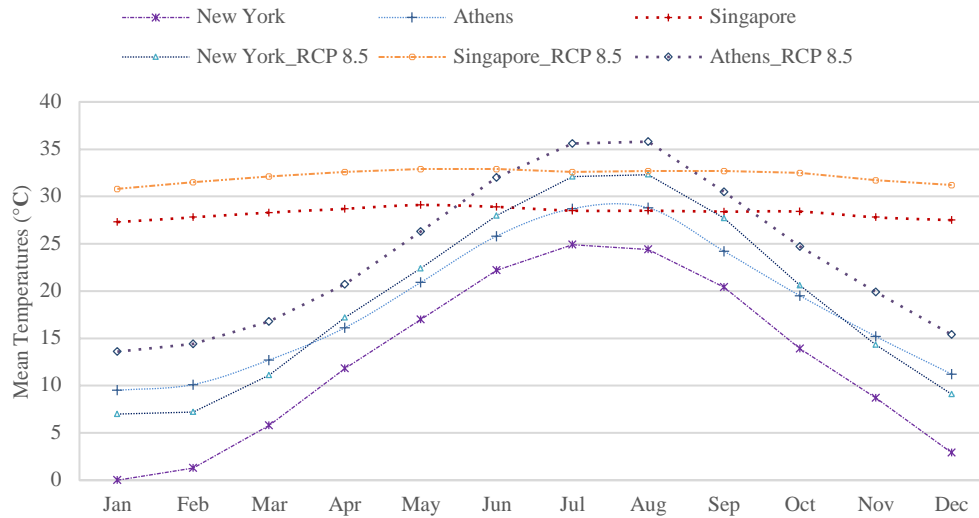


Figure 14. Air Temperature variations for contemporary and future weather scenarios under RCP 8.5 in three climates.

3.4 Study Morphologies

High-rise buildings are identifiable and distinctive elements in urban contexts all over the world due to their imposing verticality and architectural significance. Due to the interaction of numerous aspects, such as structural stability, solar exposure, and spatial efficiency, choosing an acceptable morphology for high-rise building design is a challenging issue. Therefore, to successfully achieve their goals, architects, engineers, and urban planners must carefully assess the morphological characteristics of various geometrical shapes. This paper investigates common geometrical forms seen in high-rise constructions focusing on their implications for energy performance. Given their effective use of space, simplicity in construction, and suitability for urban environments, the data show that rectilinear designs are frequently used in high-rise constructions. Therefore 10 distinctive and prevalent morphologies as illustrated in **Figure 15**, are selected to be evaluated in three climate contexts.

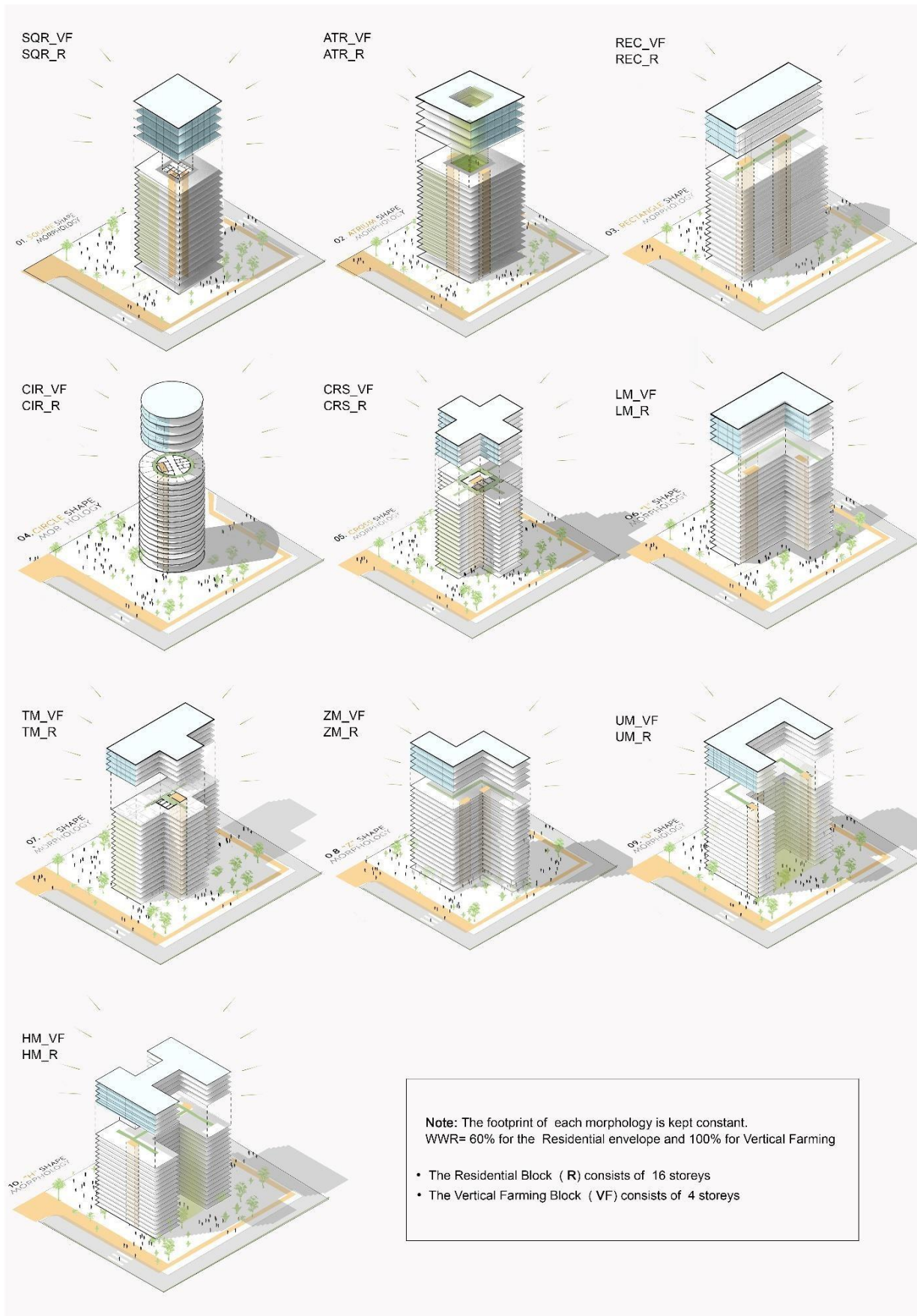


Figure 15. The illustrative drawing of all study morphologies.

3.4.1 SQR- Square Morphology

The SQR, or Square Morphology, is a striking architectural concept centered on a square-shaped structure as shown in **Figure 16**. Efficiency, use, and aesthetic appeal are all embodied in this unique morphology, which results in an exceptionally inviting urban structure. The square form, which serves as the cornerstone for its spatial arrangement, is at the core of the SQR Morphology. The square shape provides a symmetrical architecture that maximizes internal space usage and makes it easier for a fluid circulation system to operate. The building's seamless integration of residential blocks within this square provides practical living quarters.

Schematically illustrated in **Figure 17**, alongside having outstandingly widespread residential architecture, in this research it supports sustainability and innovation by incorporating vertical farming on its upper floors, making the most of the building's vertical space to accommodate a modern day agricultural system that enables the growing of a wide variety of crops. It encourages food self-sufficiency and adds to the community's general sustainability, and it does it through an inventive integration of agriculture into the urban fabric. Furthermore, the presence of the vertical farming block improves the building's aesthetic appeal by bringing a distinctive contrast of greenery against the urban setting.

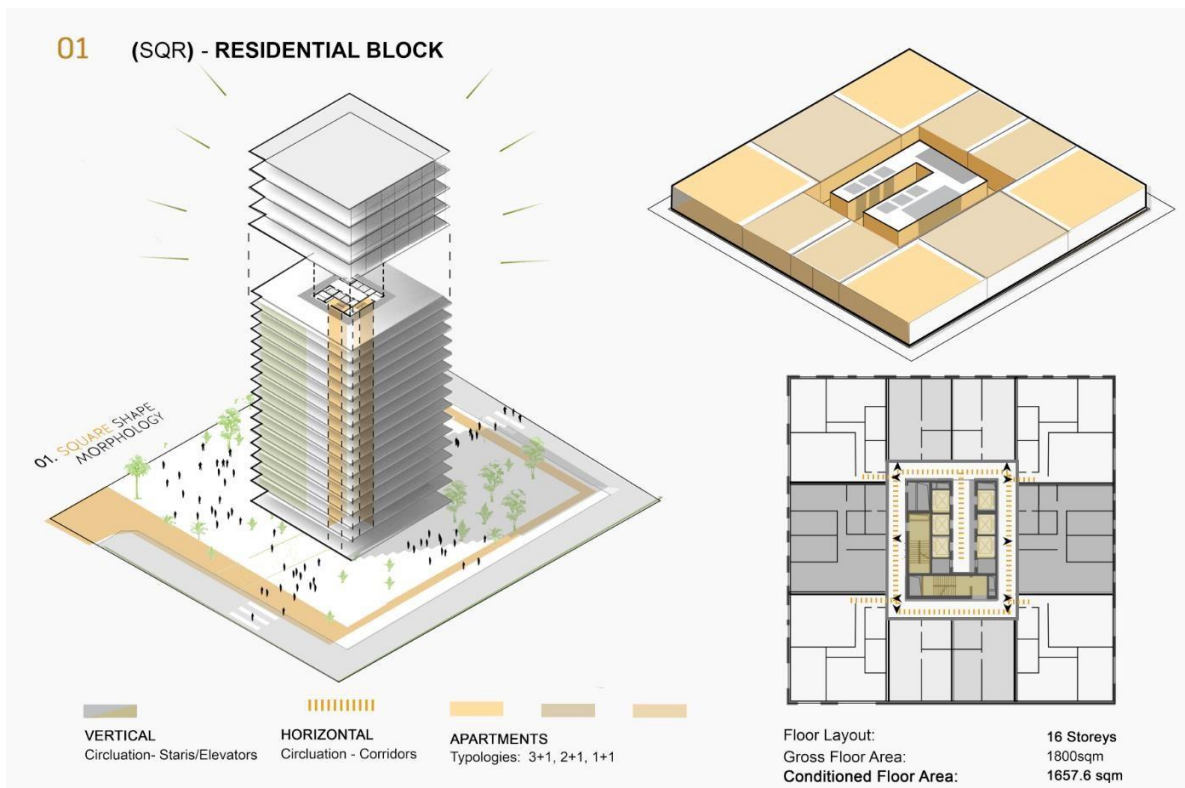


Figure 16. SQR Morphology, Residential block.

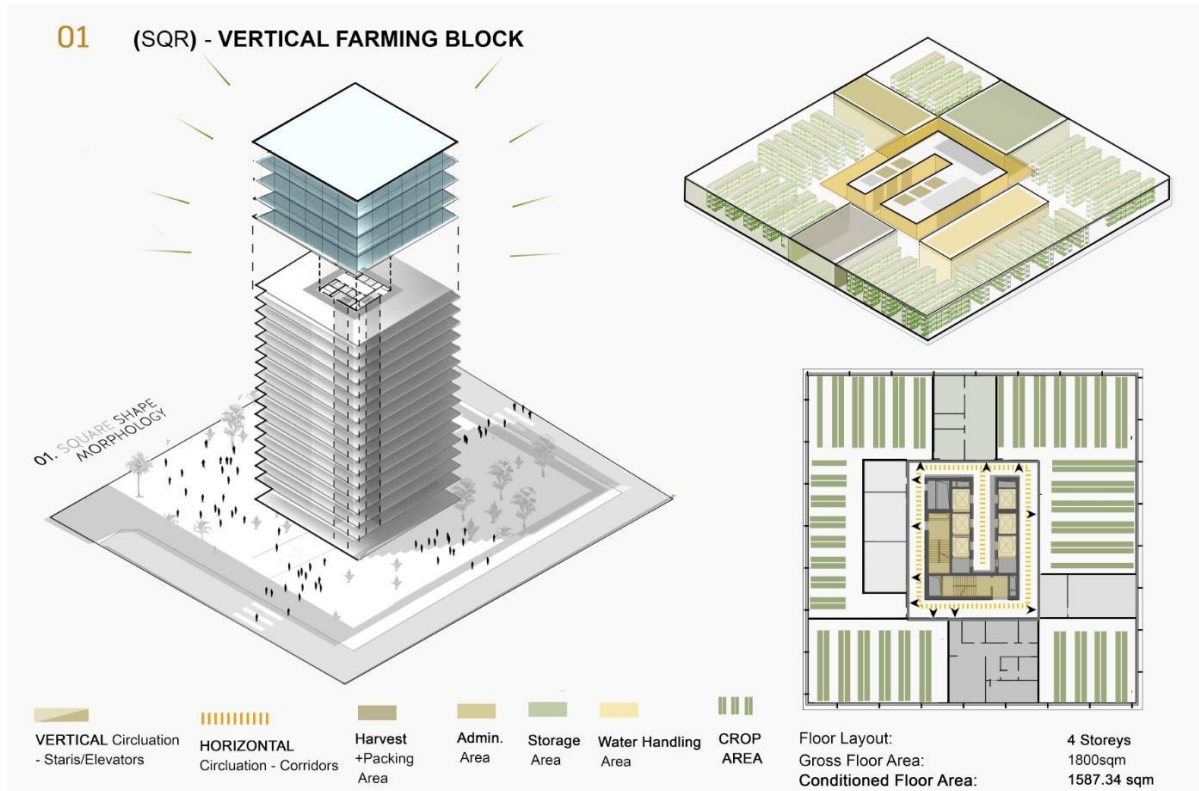


Figure 17. SQR Morphology, Vertical Farming block.

3.4.2 ATR- Atrium Morphology

The ATR, Atrium Morphology, is built around the idea of a significant central atrium (**Figure 18**). This architecture fosters openness, natural light, and the seamless fusion of interior and outdoor spaces, resulting in a warm and motivating ambiance. The atrium functions as a dynamic meeting space, encouraging a sense of community and connection among its occupants with regard to its exceptional height and abundance of natural light. Effective circulation is made possible by the central atrium, which also serves as a landmark for navigation and aids in internal orientation. Vertical farming is incorporated into the ATR Morphology as an integral part of the building as in **Figure 19**.

02 (ATR) - RESIDENTIAL BLOCK

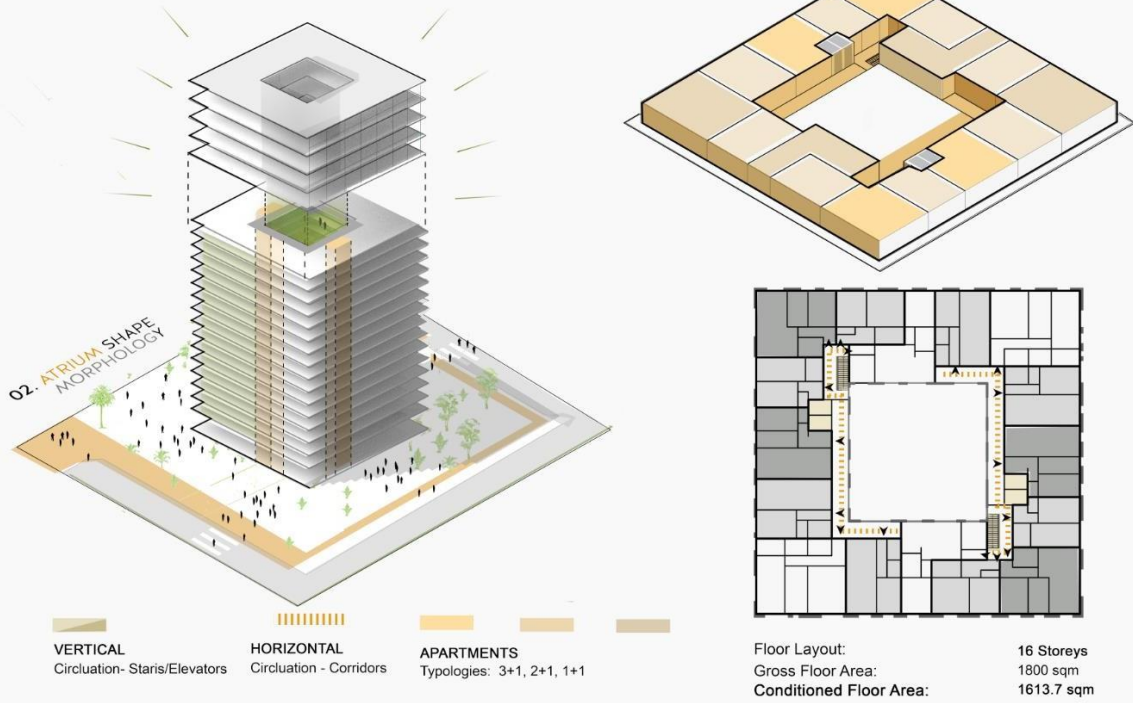


Figure 18. ATR Morphology, Residential block.

02 (ATR) - VERTICAL FARMING BLOCK

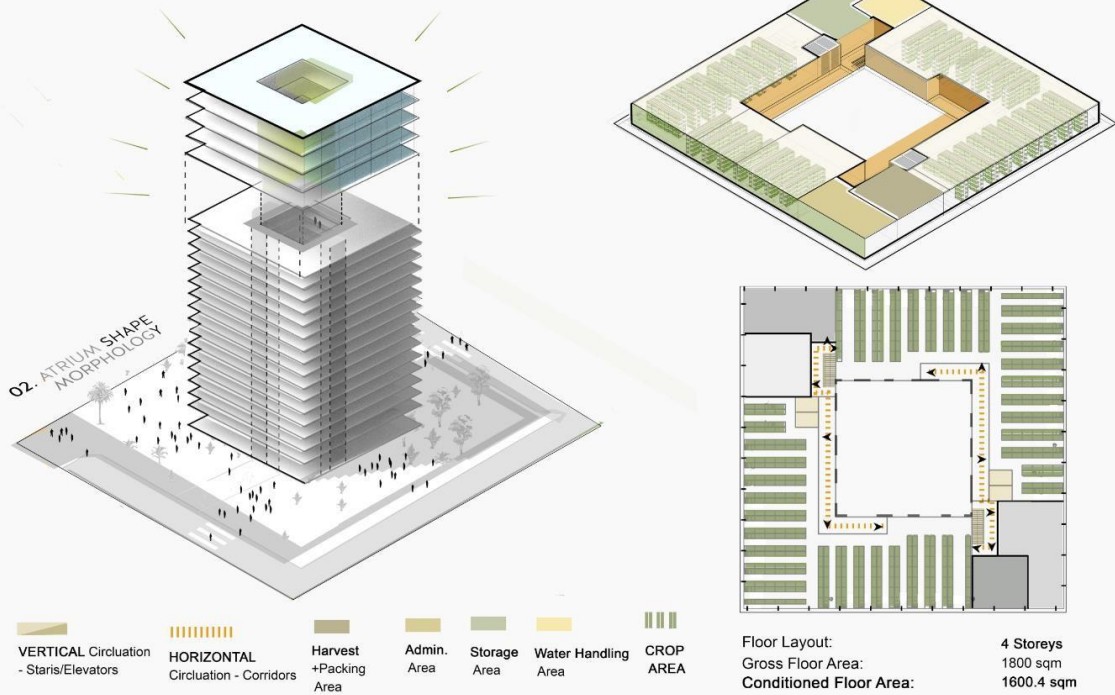


Figure 19. ATR Morphology, Vertical Farming block.

3.4.3 REC- Rectangle Morphology

The versatility and adaptability of the REC Morphology is one of its main benefits. It has the ability to accommodate a range of floor layouts and configurations, the rectangle shape lends itself well to addressing varied housing demands and preferences. As a result, a wide variety of residential structures, including townhomes and flats, can be easily included into the morphology. It also enables effective movement within the facility. Due to the units' elongated and straight edges, it is possible for each apartment to be placed in a way that maximizes natural light and ventilation while also maximizing comfort.

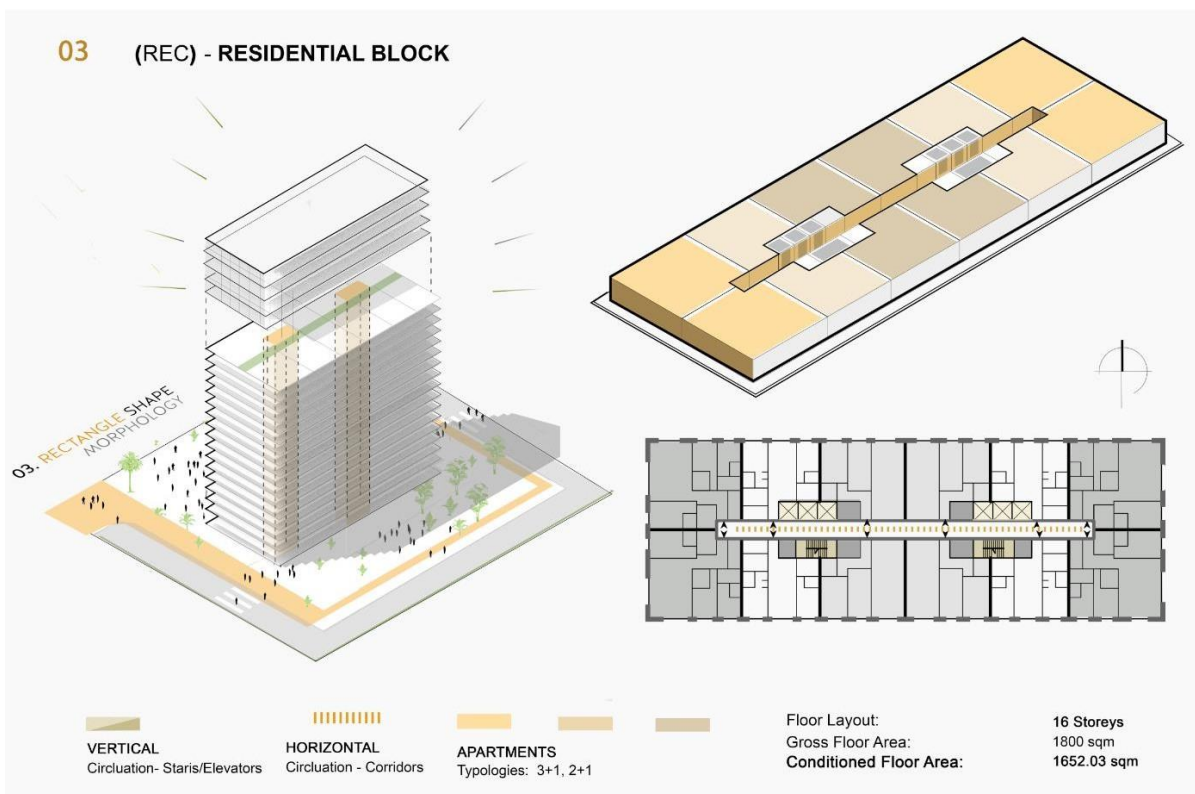


Figure 20. REC Morphology, Residential Block.

As in the other morphologies Vertical Farming floors are incorporated in the uppermost levels, dedicated to advanced agricultural systems and food production as visually presented in **Figure 21**, which can allow also residents to actively engage in sustainable production practices. This cutting-edge integration encourages self-

sufficiency while minimizing the environmental impact of conventional farming practices.

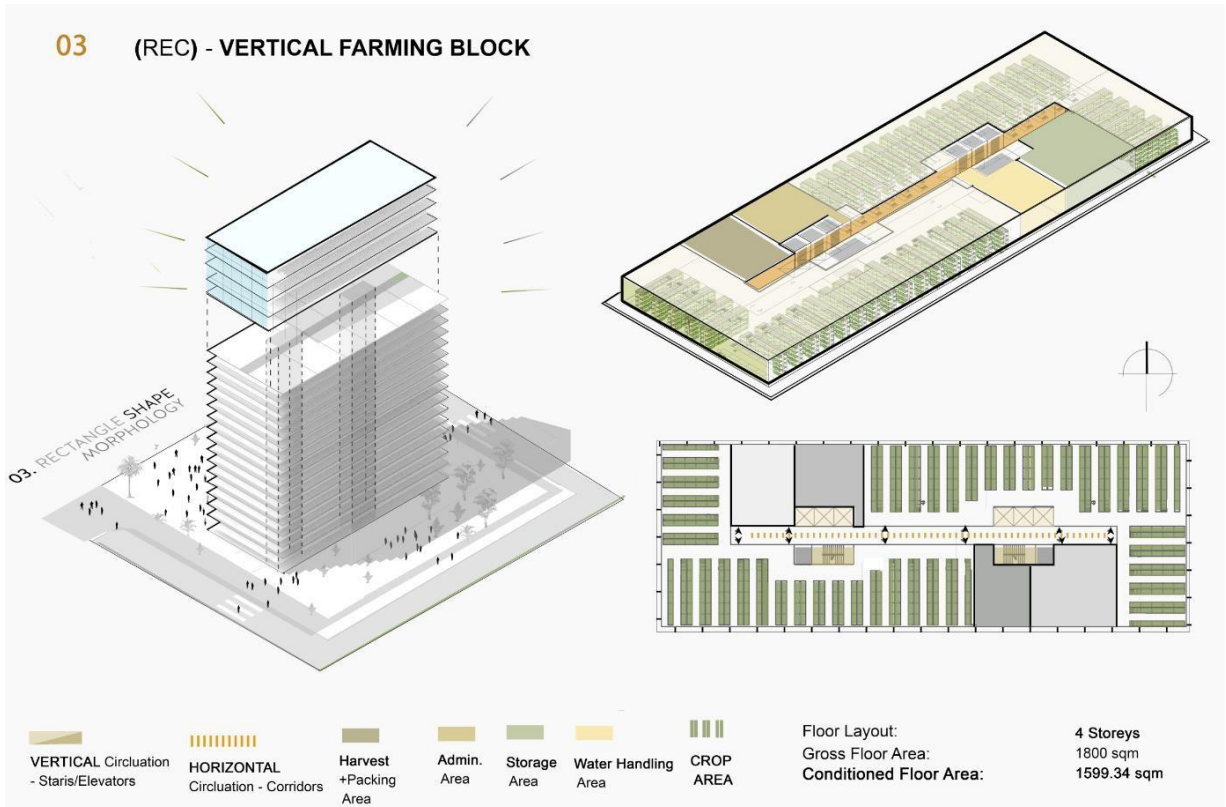


Figure 21. REC Morphology, Vertical Farming block.

3.4.4 CIR-Circle Morphology

The Circle Morphology illustrated in **Figure 22**, represents a distinctive design distinguished by a very compact and circular building construction. While encouraging a sense of cohesion and connectivity among its users, its shape maximizes internal space utilization. In addition to maximizing ventilation and natural light throughout the structure, the circular design enables effective circulation. The CIR Morphology offers an eye-catching and practical architectural solution for domestic life given to its unusual circular form.

Additionally, the circular shape offers expansive views and an abundant sense of sustainability when incorporated with Vertical Farming as in **Figure 23**.

04 (CIR) - RESIDENTIAL BLOCK

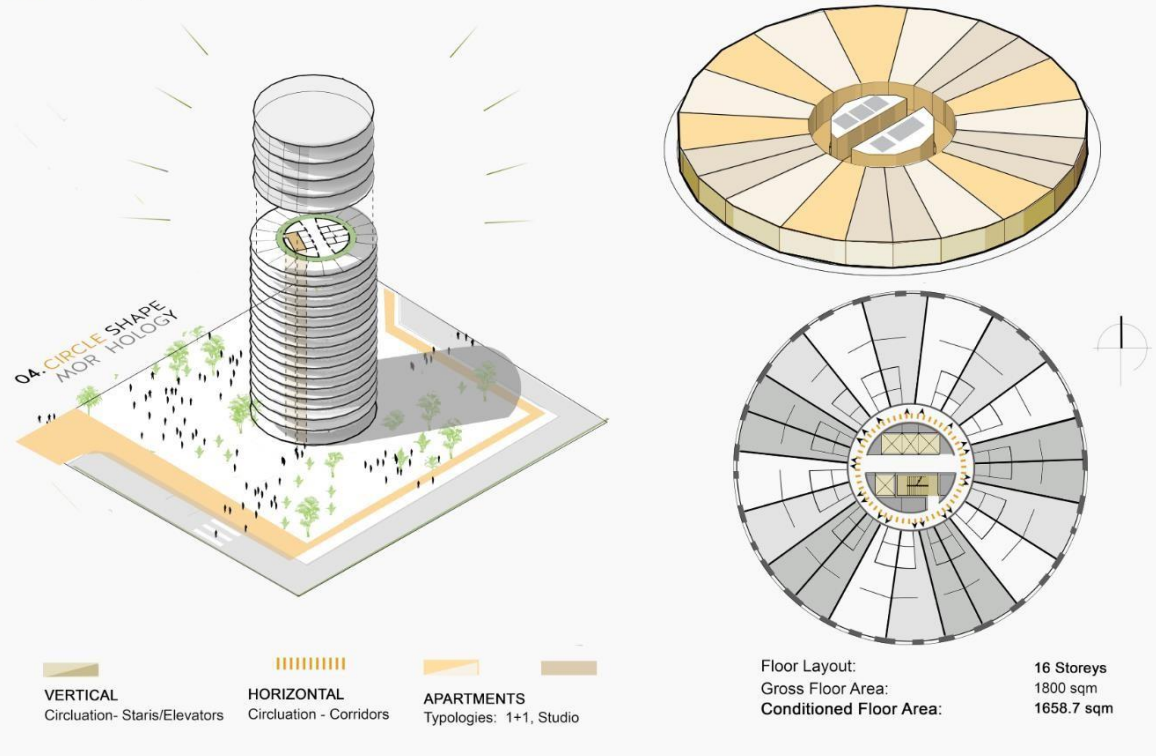


Figure 22. CIR Morphology, Residential Block.

04 (CIR) - VERTICAL FARMING BLOCK

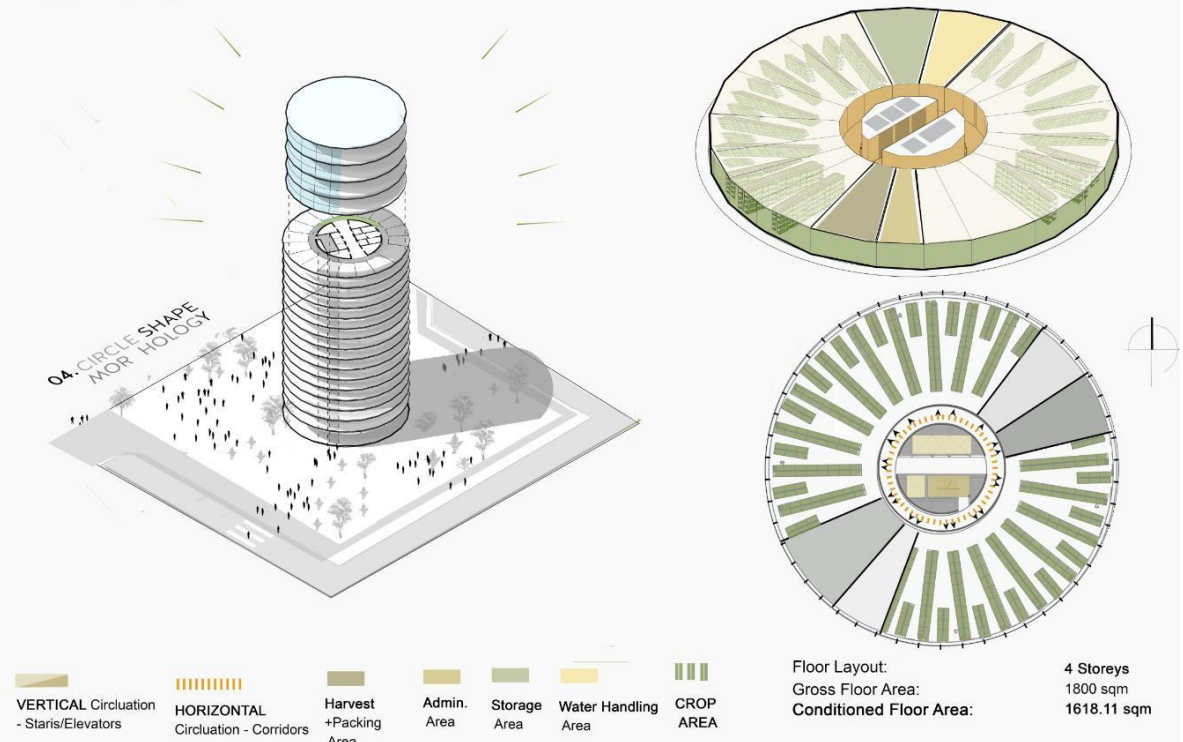


Figure 23. CIR Morphology, Vertical Farming Block.

3.4.5 CRS- Cross Morphology

The CRS Morphology's design flexibility is another morphology shown in *Figure 24*. The cross-shaped layout enables flexible residential unit configuration, supporting a range of floor patterns and housing options. This adaptability can accommodate various housing preferences, like apartments, townhouses, or duplexes, making it possible for the morphology to accommodate the various demands of its occupants. The architectural composition benefits from symmetry and clear lines. The movement inside the building is made easier by the logical pathways that are created by the cross's arms. Residents' living quarters are easily navigable, and they need little effort to use communal amenities in this case the vertical farming floors which can be accessible to the residents displayed in *Figure 25*.

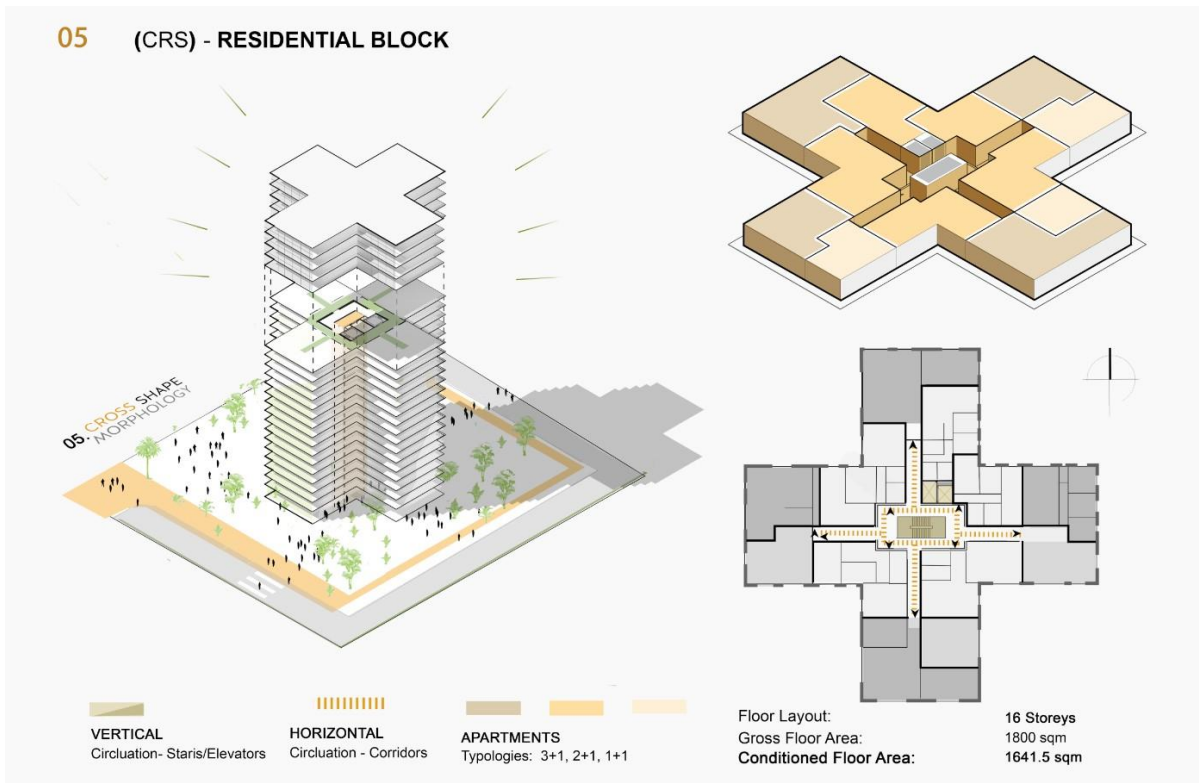


Figure 24. CRS Morphology, Residential Block.

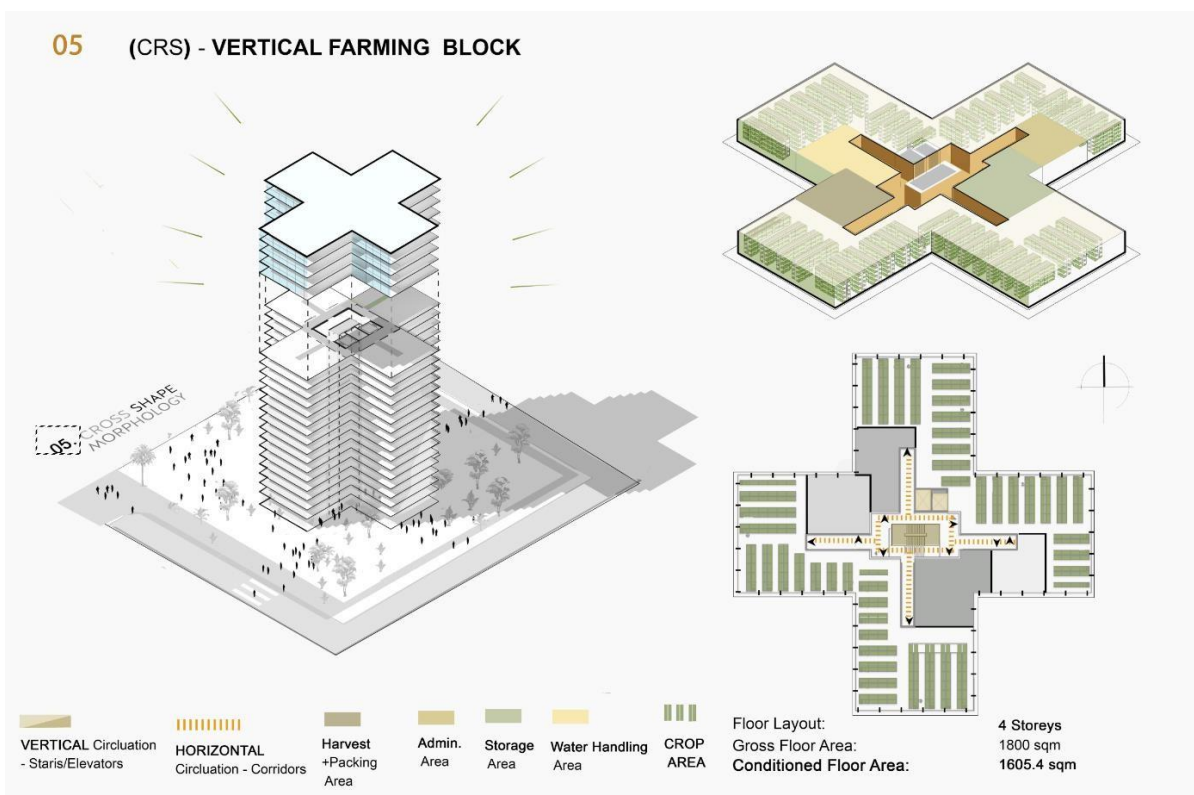


Figure 25. CRS Morphology, Vertical Farming Block.

3.4.6 LM- “L” Shape Morphology

The LM Morphology creates a sense of openness and adaptability because of its L-shape, which allows natural light to enter deep into the structure and create warm and welcoming living areas. The interiors have great airflow because of the thoughtful positioning of windows and openings, which improves ventilation. As depicted in **Figure 27**, the vertical Farming floor plans give the structure more architectural interest, making it more aesthetically pleasing and dynamic. Such distinctive form and practices stand out and add to the residential block's overall enticing appearance.

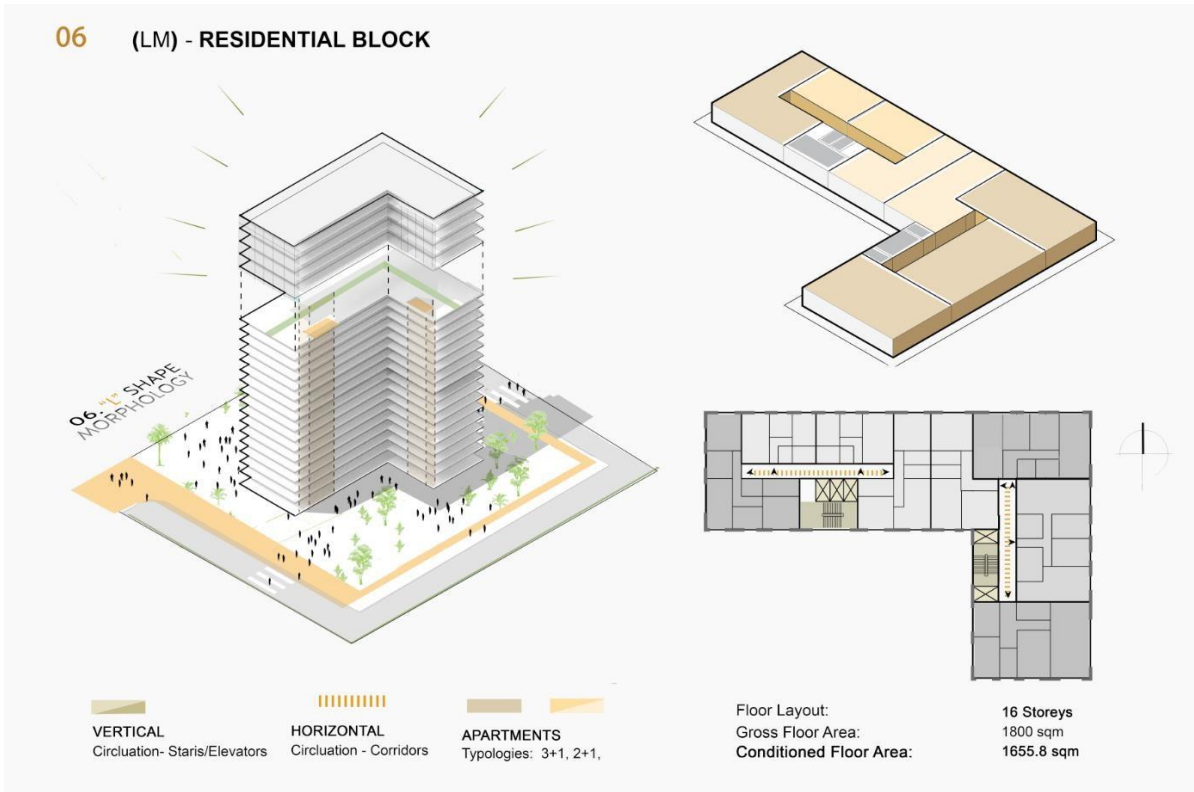


Figure 26. LM Morphology, Residential Block.

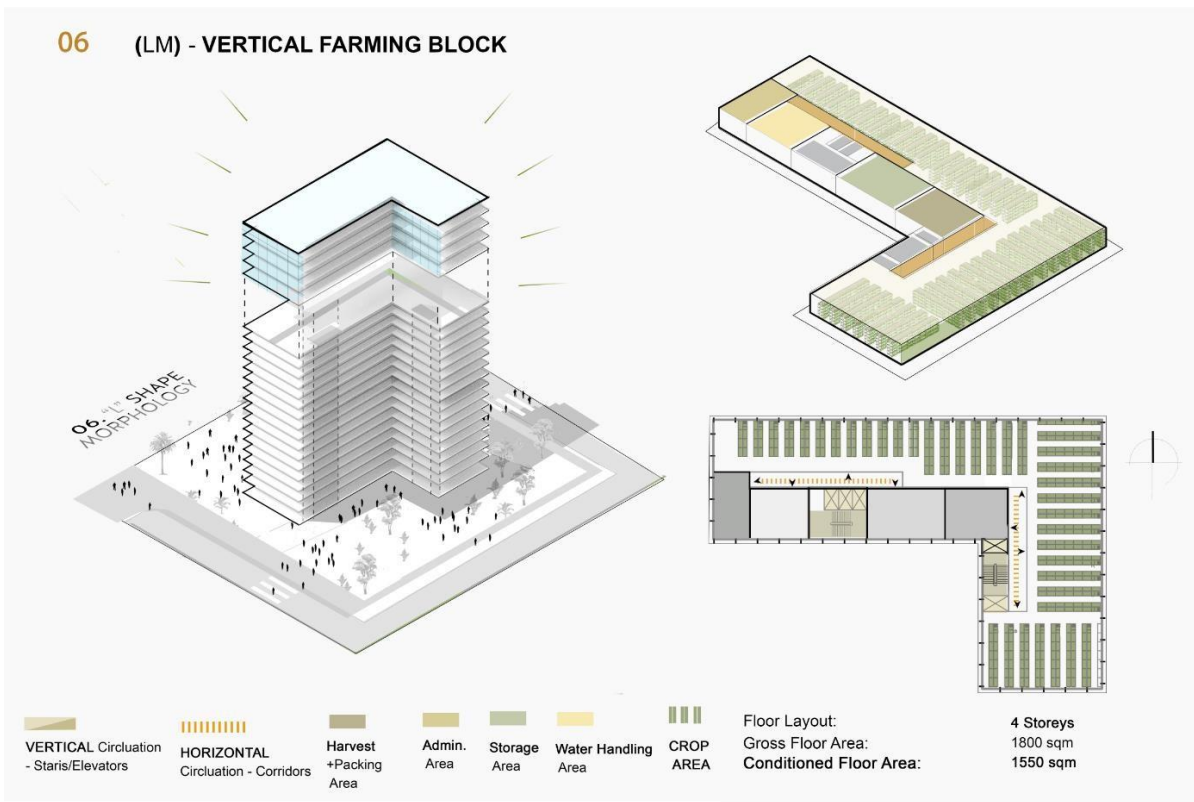


Figure 27. LM Morphology, Vertical Farming Block.

3.4.7 TM-“T” Shape Morphology

The T-Shaped Morphology represents a distinctive residential building form, characterized by its geometric arrangement that mimics the letter "T". This morphology exhibits a variety of unique geometrical traits that support both its aesthetic appeal and functional advantages. The T-shaped floor plan makes a strong architectural statement by drawing attention to the conspicuous intersection of vertical and horizontal lines as illustrated in *Figure 28*. With this arrangement, distinct living areas or wings can accommodate various building functions. Residents can set apart sections for various activities since it fosters a feeling of seclusion and division. The T-shaped architecture also improves ventilation and natural light penetration throughout the entire building. The T's extended arms make it possible for windows and openings to receive light from numerous directions by increasing the exposure of the outer wall. This design feature produces light and airy interiors that improve the occupants' general comfort and well-being.

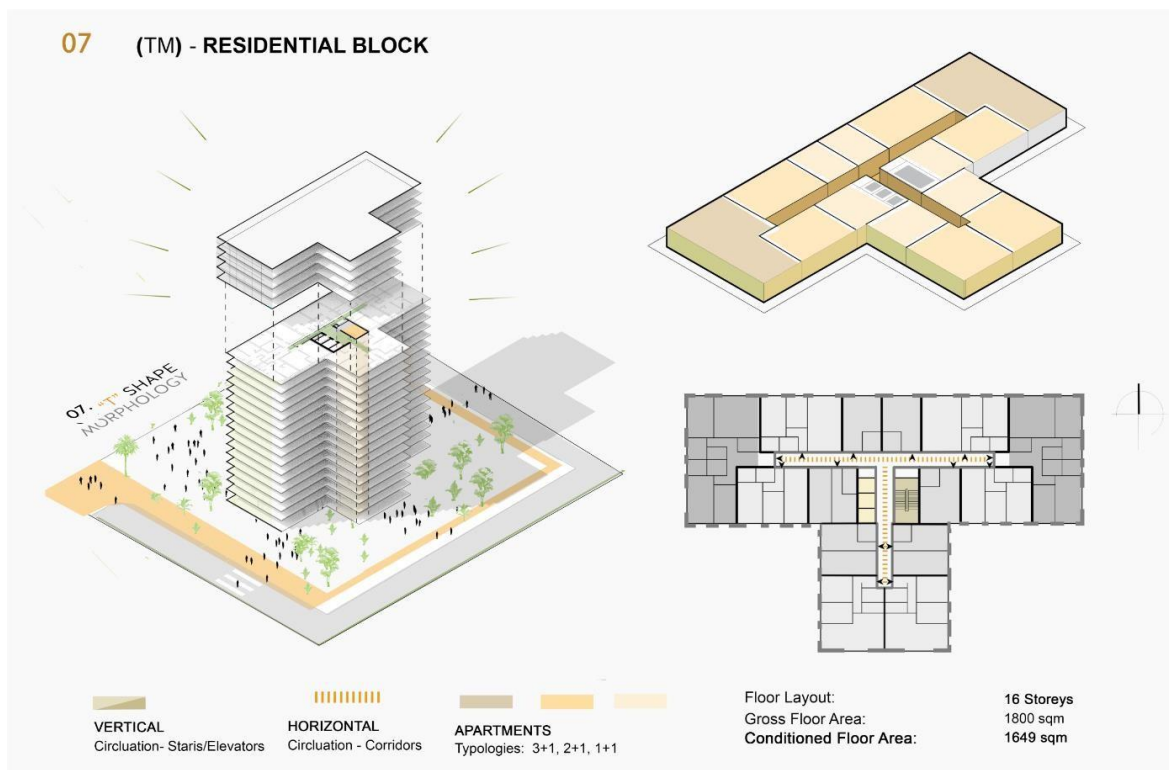


Figure 28. TM Morphology, Residential Block.

The T-Shaped Morphology additionally employs vertical farming, making use of the building's vertical area to incorporate sustainable agricultural systems as in **Figure 29**. Residents can actively participate in agricultural growing which encourages self-sufficiency and environmentally responsible behavior in addition to the food production for the whole neighborhood.

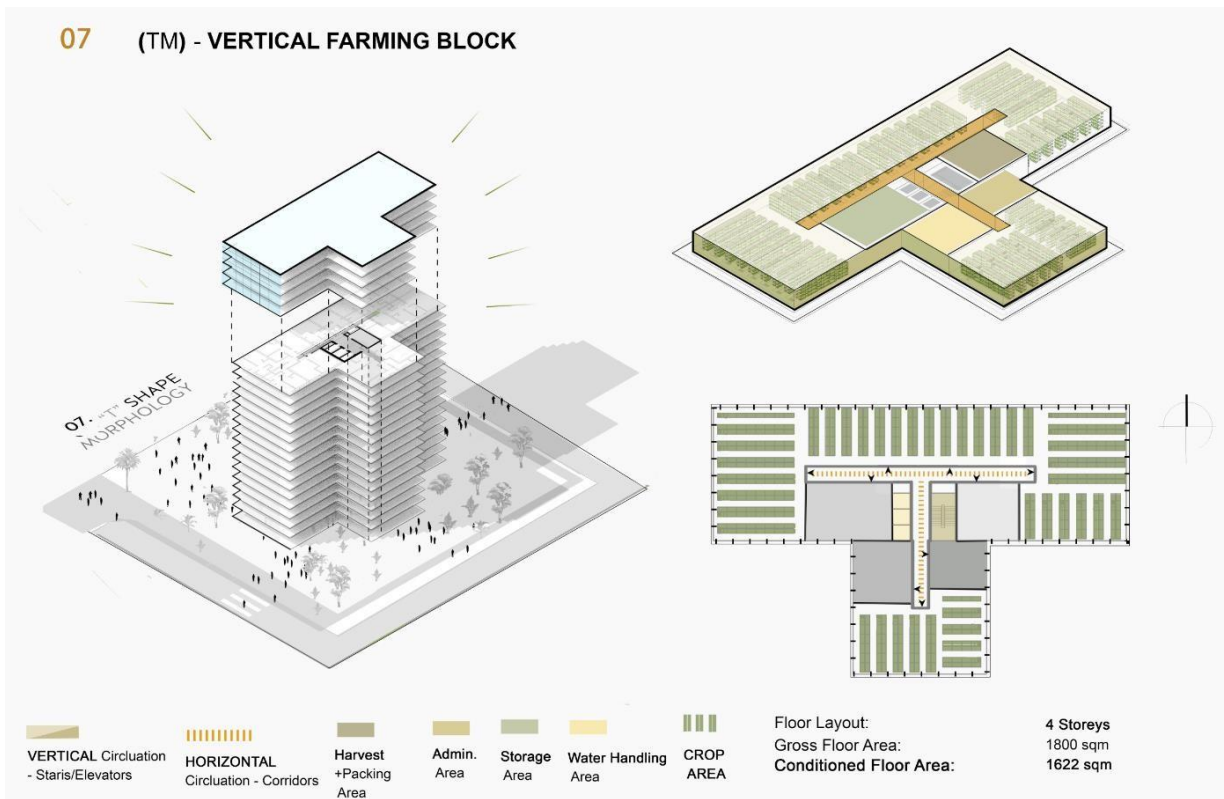


Figure 29. TM Morphology, Vertical Farming Block.

3.4.8 ZM-“Z” Shape Morphology

The Z-Shaped Morphology offers a distinctive Z arrangement for a residential design, as well as distinct geometrical elements. Sharp angles and clean lines that give the Z-shaped floor plan a sense of architectural appeal and distinctiveness produce a visually dynamic structure. With multiple orientations and plenty of ventilation along the various Z segments, the Z layout also encourages exceptional natural light penetration for living areas and Vertical farming producing spaces demonstrated in

Figure 30 and Figure 31.

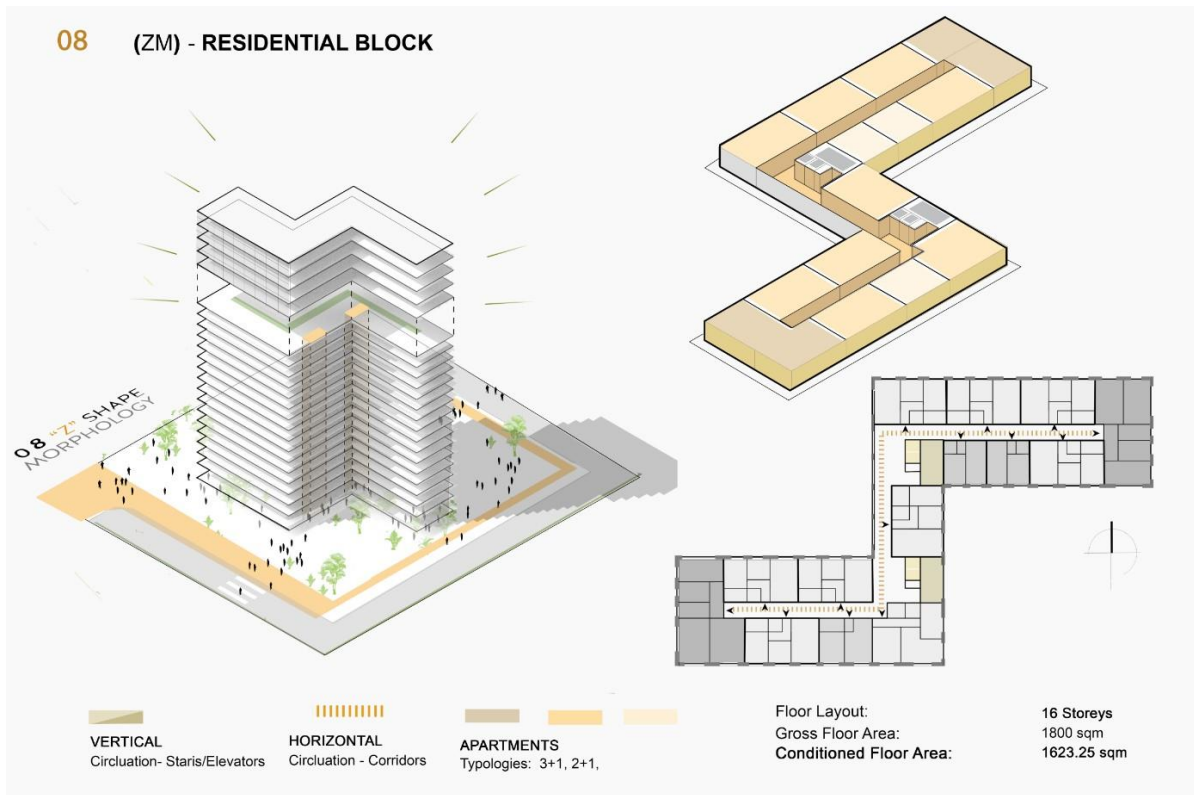


Figure 30. ZM Morphology, Residential Block.

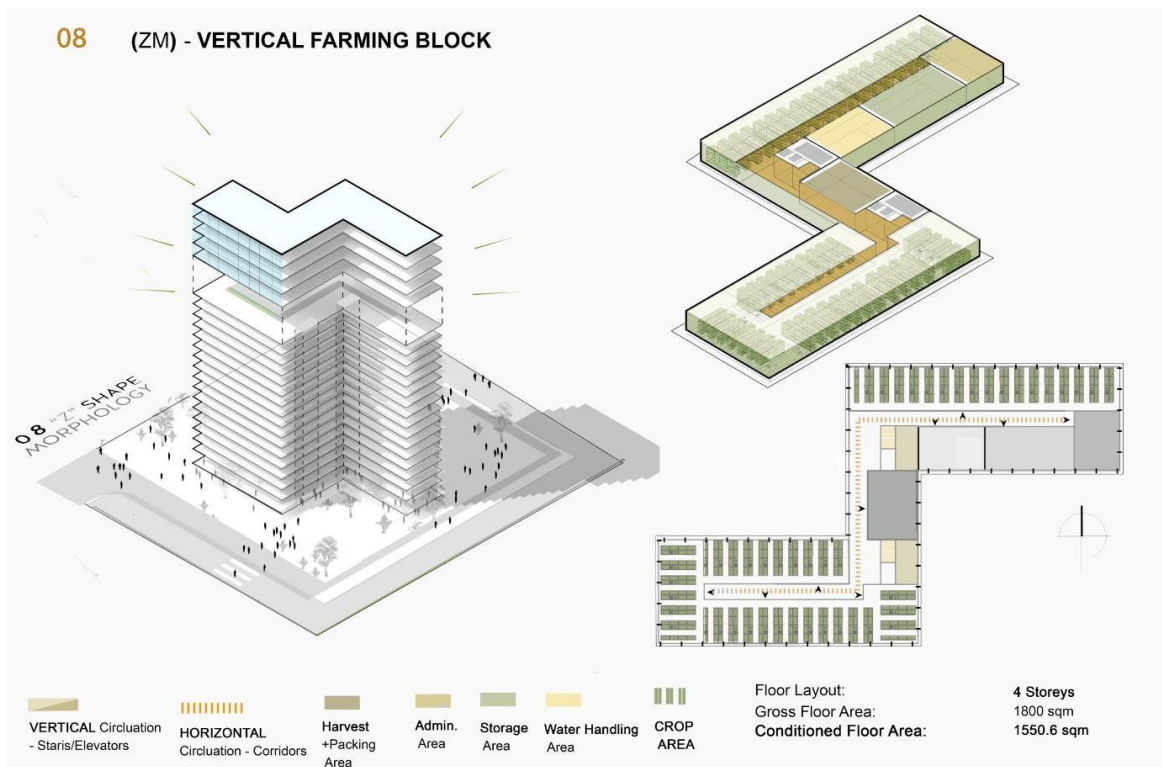


Figure 31. ZM Morphology, Vertical Farming Block.

3.4.9 UM-“U” Shape Morphology

European and Mediterranean-style residences frequently utilize the U-shaped building form. By including a central courtyard, which serves as the main outdoor area, the U-shape provides a conventional rectangular residence with an inviting twist as displayed in *Figure 32*. In order to have complete views and easy access to the outdoor space, every apartment is often placed alongside the courtyard and equipped with sizable windows. Overall, the emphasis of a U-shaped dwelling is on the spatial relationships between rooms, the smooth connection between the interior and outside regions, and the flow of circulation. The main rooms and various spaces are connected by an extended corridor. The courtyard is used also as a partition that works as a natural buffer from noises and disturbances.

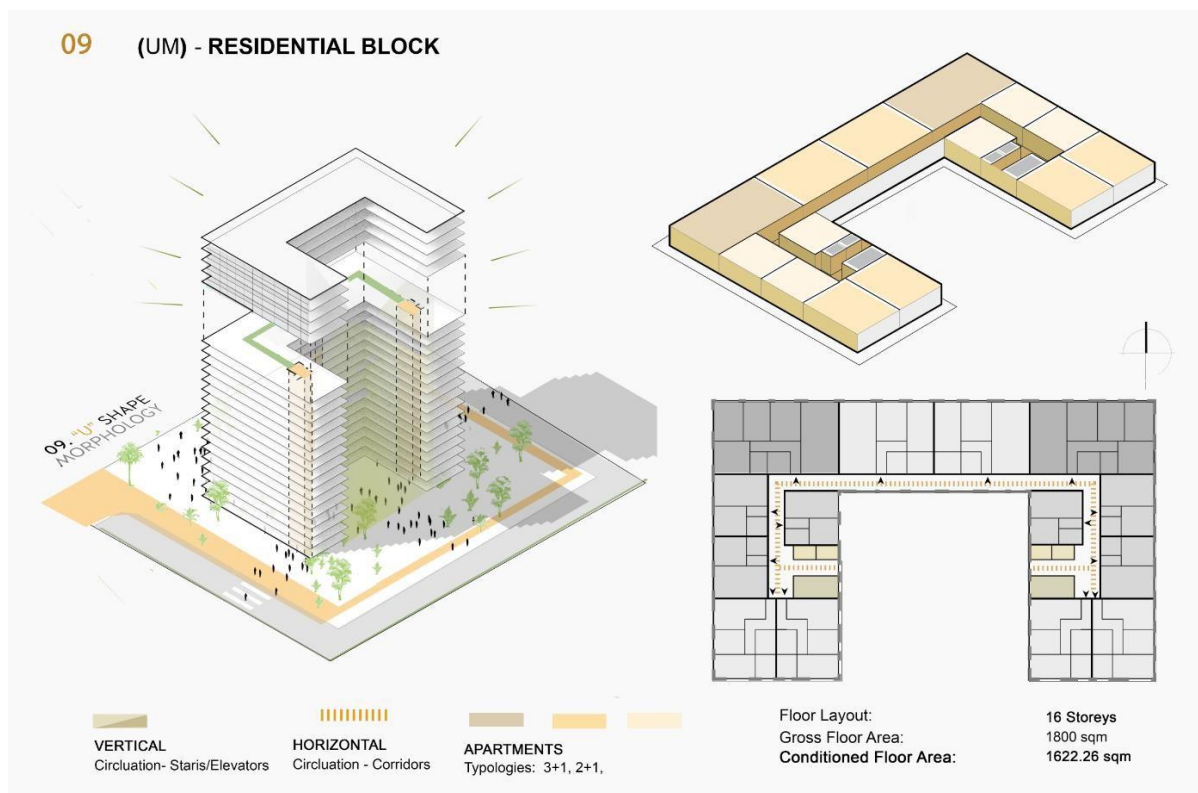


Figure 32. UM Morphology, Residential Block.

As in *Figure 33*, vertical farming operations can benefit from its level of

flexibility and access to natural light that enables effective space usage and optimizes functional flow.

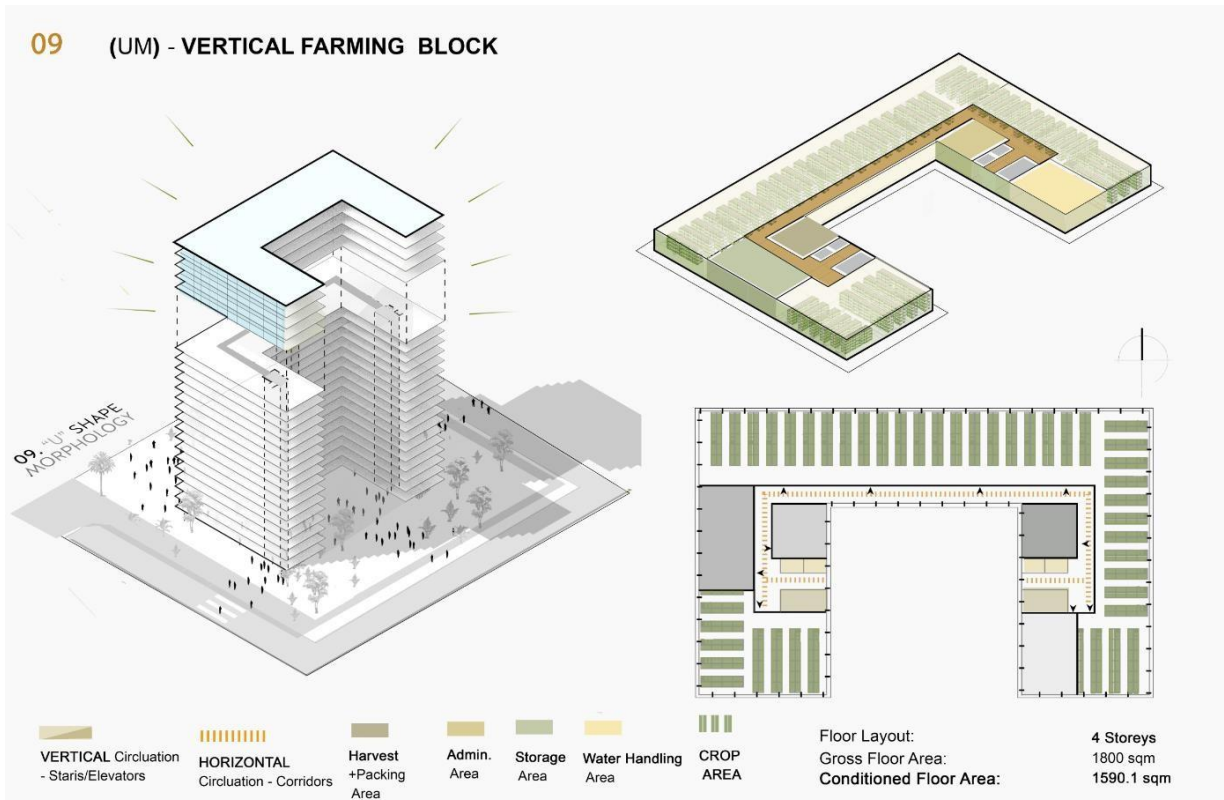


Figure 33. UM Morphology, Vertical Farming Block.

3.4.10 HM-“H” Shape Morphology

The H-shape offers multiple wings for a sizable number of living spaces, which are typically found in residential settings. The advantages of H-shaped floor plans include easy circulation and enough of light as represented in **Figure 34**. Dead space and dark nooks are minimized. Even though it is elongated and spacious, the two parallel wings that are perpendicular to the central hall block increase functionality and allow for ample light and ventilation. H-shaped structures frequently have two courtyards facing in opposite directions or other outside areas that act as focal points. Through the provision of cross-ventilation between the wings, the H-shaped form encourages natural cross-ventilation. This airflow contributes also to the food production practices for the vertical farming block as in **Figure 35**.

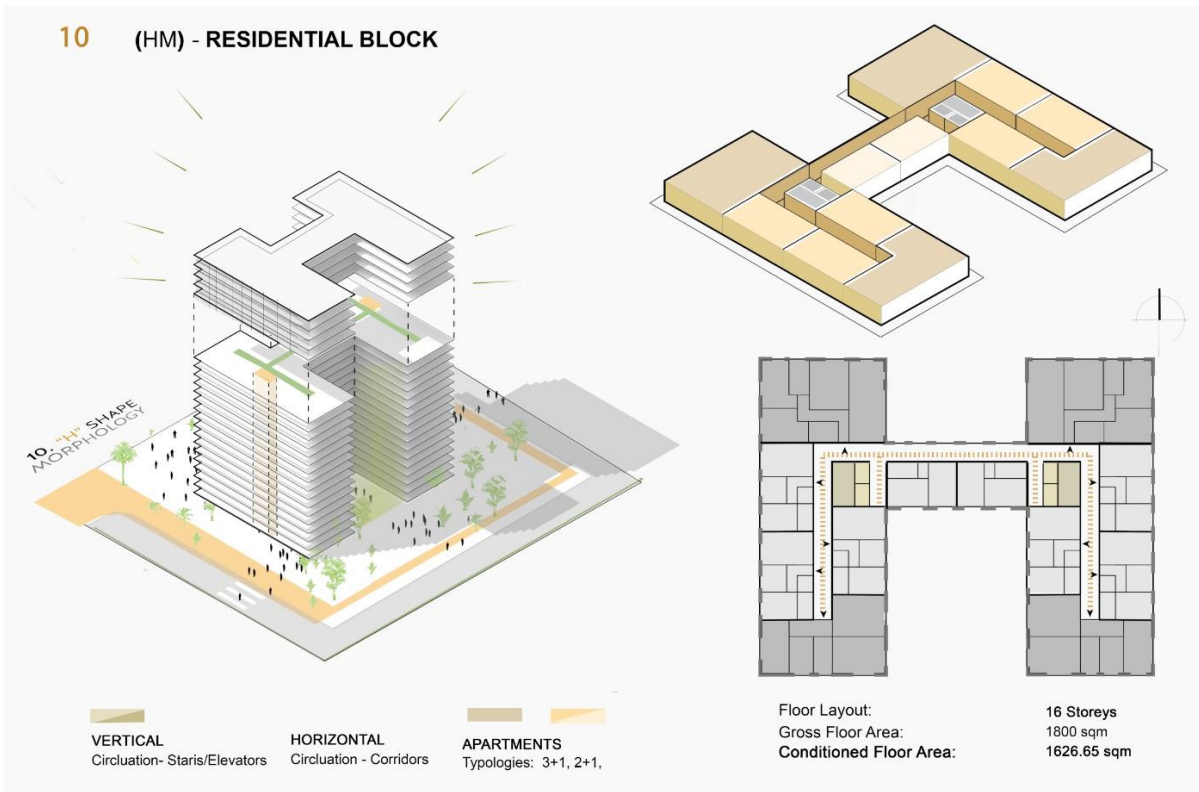


Figure 34. HM Morphology, Residential Block.

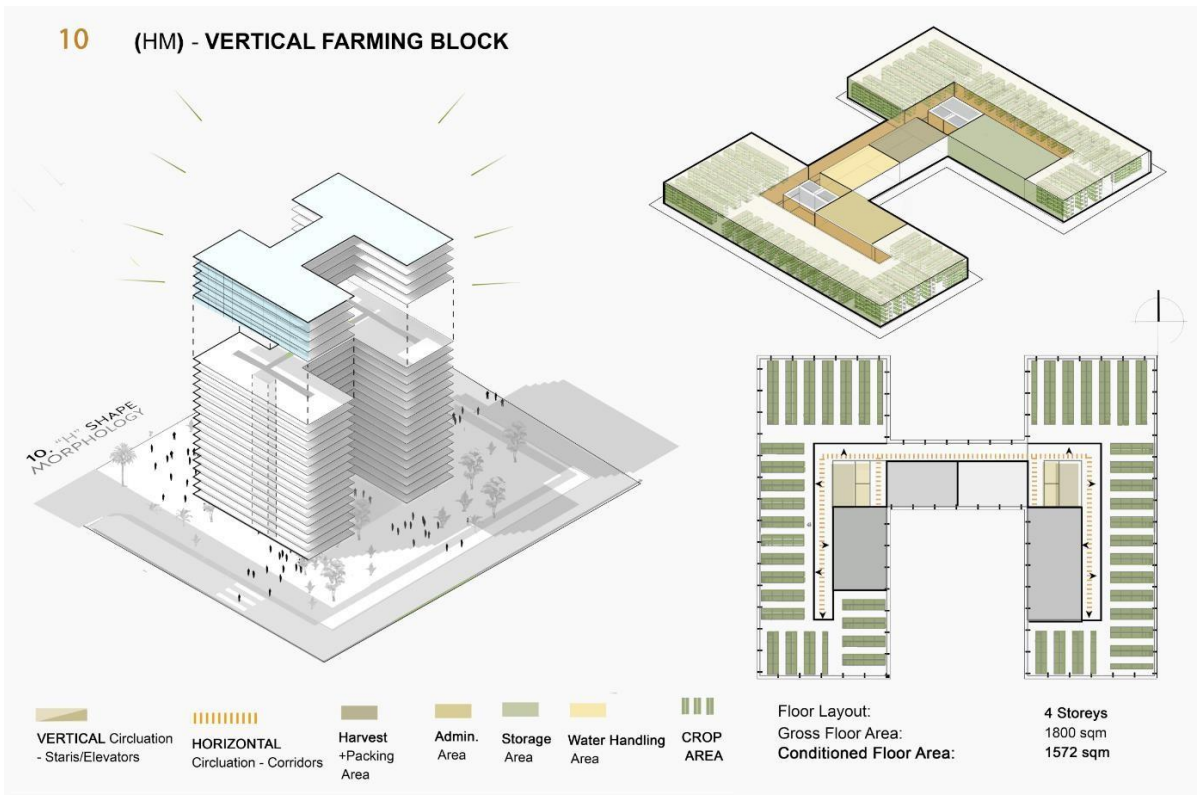


Figure 35. HM Morphology, Vertical Farming Block.

3.5 Relative Compactness (RC)

Relative Compactness (RC) is a geometric indicator that measures a building's compactness. It is determined by dividing the exposed surface area of a structure, including the total of roofs, walls, and ground floor surfaces, by the surface area of a cube of the same volume as the building (RamziOurghi et al 2007 and Mahdavi, Gurtekin 2002). A higher RC number suggests a more compact building layout, which can result in improved energy efficiency. Because most buildings are orthogonal forms, the cube is utilized as the reference shape, resulting in the following definition of RC.

Equation 20. displays the relative compactness formula relative to energy consumption.

(Equation 20)

$$RC = 6 \times V^{0.66} \times A^{-1}$$

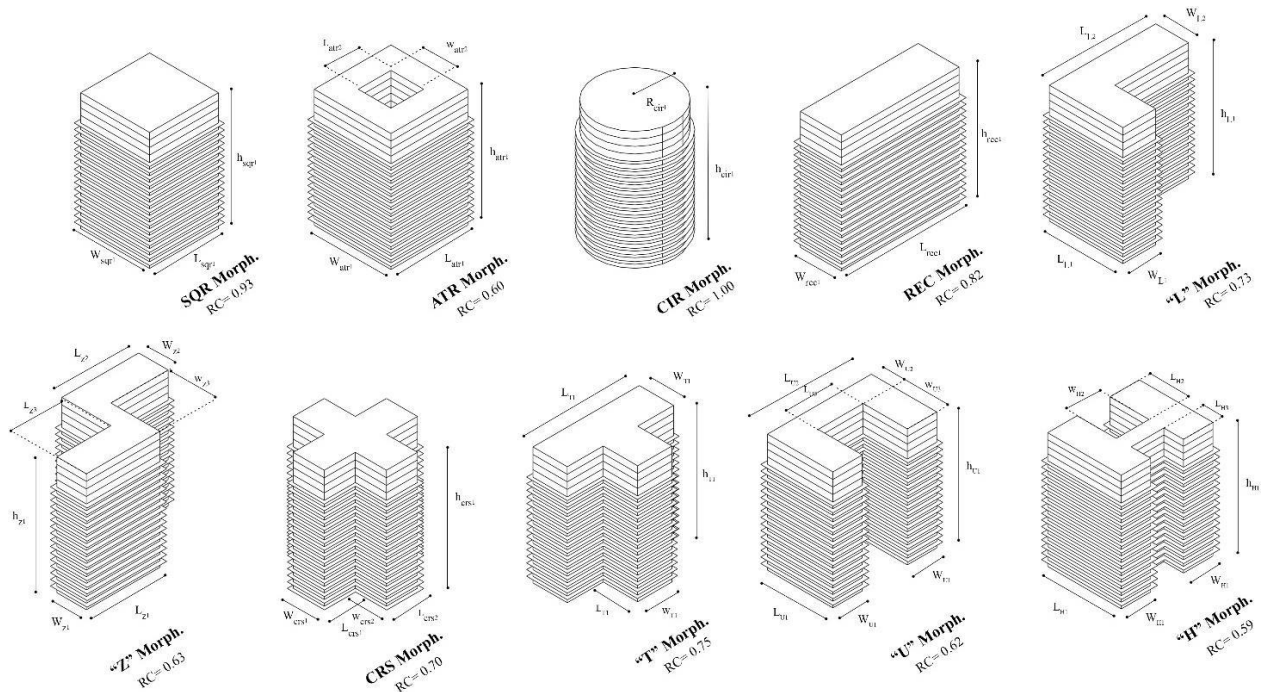
Several research have looked into the effect of building shape and height on energy performance, emphasizing the relevance of RC in building design. Werner et al. (2003) studied the dependability of compactness indicators for energy-related assessments using parametric thermal simulations, discovering a substantial relationship between RC and simulated heating loads of structures with varied forms, glazing %, and orientation. Albatici et al. (2010) proposed that including a bioclimatic approach in the early design phase, taking into account elements like orientation, openings, and exposure to atmospheric agents, might result in more effective outcomes.

Camporeale et al. (2019) adjusted high-rise dwelling typologies based on local climatic needs by evaluating criteria such as passive volume ratio, total roofs, and best-oriented surfaces. Ciardiello et al. (2020) used a genetic algorithm to construct a multi-objective optimization strategy to maximize the energy consumption of a case study building in a Mediterranean environment. They discovered that geometry optimization could save 60% of the yearly energy demand and that after the geometry was determined, passive and active techniques could save 23% of the annual energy expenditure. Chaganti et al. (2021) observed that RC, surface area, and wall area all

played a part in determining the best cooling and heating load for a structure. Khamma et al. (2017) stated that RC is a superior measure of designers' subjective categorization of form compactness since it is an indication of the geometric compactness of the building. Building shape has a considerable influence on both construction and energy expenditures, and studies have been conducted to explore the impact of building shape on thermal performance in various regions.

Hassan et al. (2020) discovered that different building morphologies with varying RC had a significant impact on pollutant dispersion, with an estimated reduction of 30%-90% demonstrating the importance of building morphology in improving outdoor air quality. As a result, RC is a crucial aspect to consider in building design to improve energy efficiency and performance.

As shown in **Figure 36** the energy performance of 10 distinct typical morphologies of high-rise residential buildings is examined in this study using the building energy consumption formula. To compute the overall energy consumption of the structure, the formula takes into consideration aspects such as the building envelope surface gross roof area and overall object volume.



Note: The footprint area and height of each morphology is kept constant.

Figure 36. The illustrative drawing of 3D morphologies and RC values.

The prospective results will be achieved by applying this formula to different building morphologies, allowing for a comparison of the energy efficiency of different building designs. This data may be utilized to guide future building design and construction processes, resulting in more energy-efficient and sustainable high-rise residential structures.

Table 3. Relative Compactness Calculation.

Code	Footprint Surf. Area	Lateral Wall Surf. Area	Area _{Total}	Volume	Width			Length			Height	RC
					W ₁	W ₂	W ₃	L ₁	L ₂	L ₃		
SQR Morph.	1800 m ²	12211 m ²	14011 m ²	129600 m ³	42.4	—	—	42.4	—	—	72	0.93
ATR Morph.	1800 m ²	18732 m ²	20532 m ²	129600 m ³	46.9	20	—	46.9	20	—	72	0.60
CIR Morph.	1800 m ²	10525 m ²	12325 m ²	129600 m ³	r= 23.9			72	—	—	72	1.00
REC Morph.	1800 m ²	13580 m ²	15380 m ²	129600 m ³	25	—	—	72	—	—	72	0.82
“L” Morph.	1800 m ²	15400 m ²	17200 m ²	129600 m ³	20	20	—	45	65	—	72	0.73
“Z” Morph.	1800 m ²	17885 m ²	19685 m ²	129600 m ³	18	18	30	45	47	33	72	0.63
CRS Morph.	1800 m ²	15960 m ²	17765 m ²	129600 m ³	19	19	—	19	19	—	72	0.70
“T” Morph.	1800 m ²	14980 m ²	16786 m ²	129600 m ³	21	21	—	65	21	—	72	0.75
“U” Morph.	1800 m ²	18270 m ²	20070 m ²	129600 m ³	18	13	27	40	63.5	27.5	72	0.62
“H” Morph.	1800 m ²	19180 m ²	20980 m ²	129600 m ³	18	20	—	45	24	12	72	0.59

Based on the characteristics and geometric measurements of each morphology as displayed in **Figure 37**, the circular morphology was found to be the most compact building geometry.

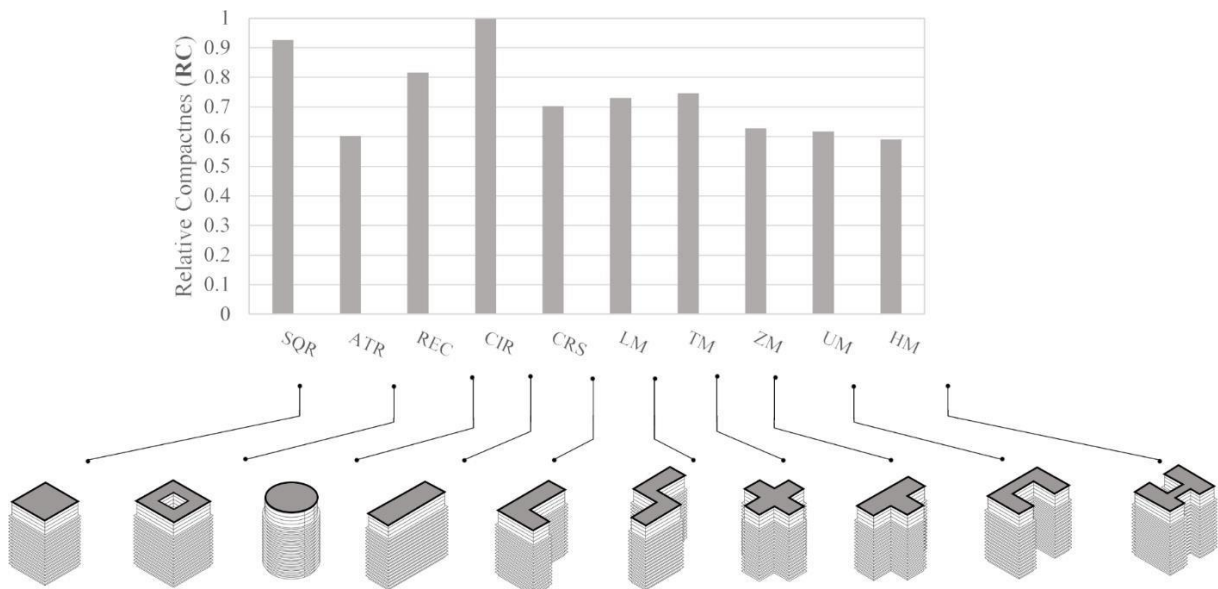


Figure 37. [RC] Relative Compactness comparison of building morphologies measured in terms of the equation $RC = 6 \times V^{0.66} \times A^{-1}$.

When compared to other morphologies, the round shape has the smallest surface area, which results in a smaller envelope area and less exposure to external climatic conditions, eventually expected to result in decreased energy usage. The square and rectangular morphologies were placed second and third in terms of architectural geometry compactness. The next most compact morphologies were T and L shapes. The H shape and atrium morphologies, on the other hand, were the least compact. Because the H shape morphology has a big envelope area, it consumes more energy. Likewise, the atrium shape has a big volume, which leads to greater heating and cooling areas.

3.6 Computational Modeling and Simulation

3.6.1 Building models

Common floor plan configurations will be modeled using Design-Builder software for the examination of energy-efficient designs of integrated CEA high-rise residential structures. Hypothetical twenty-story high-rise building models are chosen for this research purpose to examine the effectiveness of various morphologies. The structure of the residential area has a floor-to-floor height of 3.5 meters and a footprint of 1800 square meters. Although all building types have the same conditioned area, the surface-to-volume ratio changes depending on the shape. The modeling includes the layout of apartment spaces for the residential block and vertical farming operational spaces that correspond to the functions of harvesting, storing, administrating, water management, and crop growing area. The floor-to-floor area of the vertical farming area is set to be 4m, overall, with 16 floors for residential purposes and 4 for vertical farming food production purposes. The core area is kept similar throughout the morphologies occupying around 15 % of the total space.

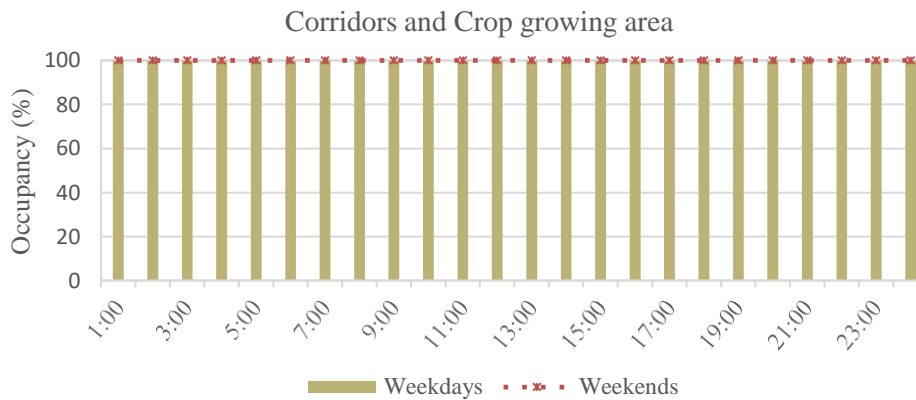
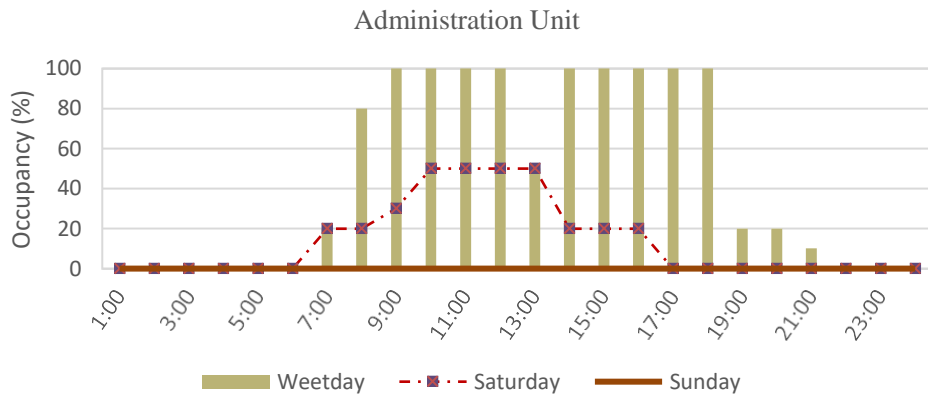
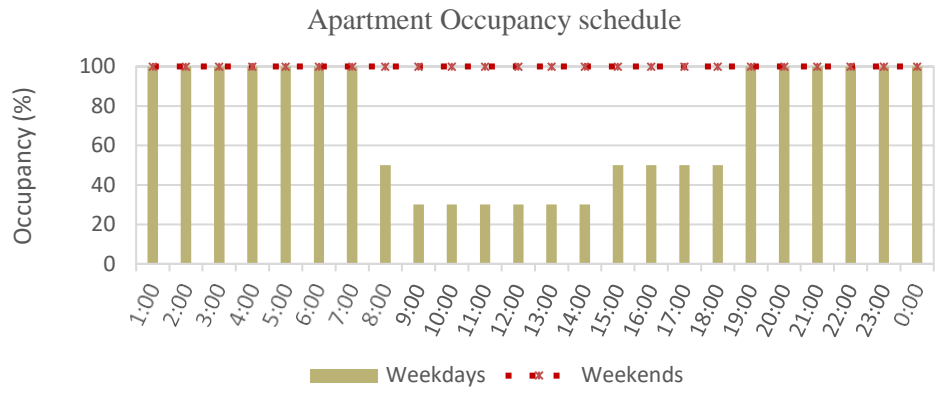


Figure 38. Occupancy Schedules.

The building construction parameters, glass type, illumination, HVAC characteristics, and internal loads remain unaltered, as shown in **Tables 4, 5, and 6.** **Figure 39.** depicts the specifics of the building attributes.

Table 4. Construction properties.

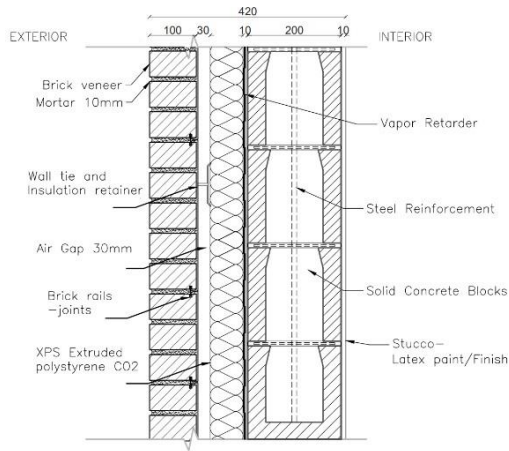
		Density [kg/m ³]	Conductivity [W/m °C]	Specific heat [J/kg °C]	Thickness [m]
External wall U-value= 0.338 [W/m ² .K] D=[0.42m]	Solid brick	1920	0.72	840	0.10
	Air Gap 30mm	-	-	-	0.03
	Insulation - XPS Extruded Polystyrene CO2 Blowing	35	0.034	1400	0.07
	Vapor Barrier-Polyethylene foam	70	0.05	2300	0.01
	Concrete- Solid grouted	1841.1	1.04	921.1	0.20
	Cement plaster	1760	0.72	840	0.01
Internal wall U-value= 0.50 [W/m ² .K] D=[0.27m]	Cement Plaster (10 mm)	1760	0.72	840	0.01
	Brickwork Inner (100 mm)	1700	0.62	800	0.10
	MW Glass Wool standard board	20	0.036	840	0.05
	Brickwork Inner (100 mm)	1700	0.62	800	0.10
	Cement Plaster (10 mm)	1760	0.72	840	0.01
Insulated flat roof U-value= 0.344 [W/m ² .K] D=[0.25m]	Roof Screed	1200	0.41	840	0.05
	XPS Extruded Polystyrene - CO2 Blowing	35	0.034	1400	0.08
	Cast Concrete-Lightweight	2000	1.13	1000	0.10
	Gypsum plaster	1120	0.51	960	0.02
Ground floor U-value= 0.509 [W/m ² .K] D=[0.43m]	Timber Flooring	650	0.14	1200	0.02
	Floor Screed	1200	0.41	840	0.07
	Cast Concrete	2000	1.13	1000	0.30
	XPS Extruded Polystyrene	35	0.034	1400	0.04

Table 5. Input parameters for HVAC operation.

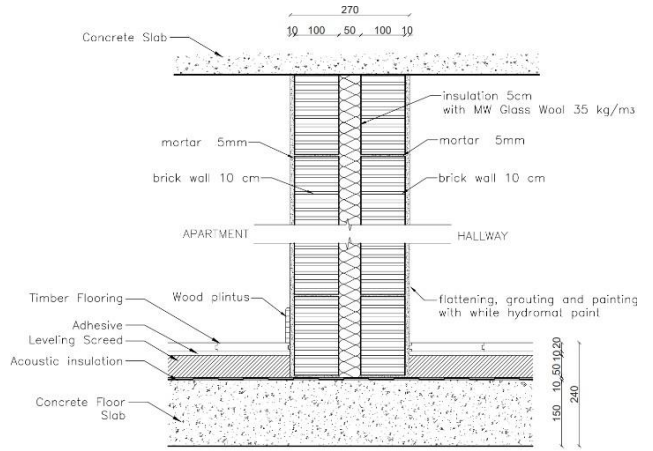
Input parameters	
Fan coil unit	(4 pipes) chiller economizer
Heating/cooling system	Electricity from grid
Coefficient of Performance for Heating [CoP]	3.8
Coefficient of Performance Cooling [CoP]	3.4
Heating set back [°C]	12
Cooling set back [°C]	28
Natural ventilation setpoint [°C]	15

Table 6. Brief for the spatial program.

Area	Space [m ²]	Nr of Units	Fresh Air flow rate for person [l/s]	Air Exchange Rate [Ac/h]	Power Density[W/m ²]	Illuminance [lux]	Heating Temp Set Point [°C]	Cooling Temp Set Point [°C]	Occupancy Density [p/m ²]
Apartment	150	-	10	10	10	300	20	24	0.027
Corridors	210	-	2.5	5	5	100	20	28	0.02
Admin. Unit	70	1	8	6	15	500	20	24	0.014
Crop Prod.	1215	1	7	4	50	2500	7-10	20-27	0.016
Harvesting + Packing	90	1	8	8	20	500	20	26	0.07
Storage + Refregerator	125	1	1.5	2	30	100	5	10-16	0.012
Water and Fertilizer	90	1	4	6	10	150	18	26	0.04

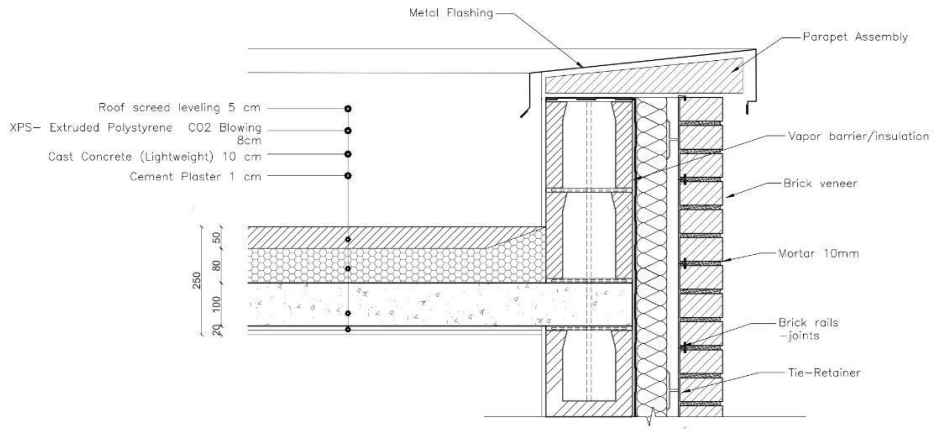


1 **EXTERIOR WALL**
 SCALE: 1:5 RESIDENTIAL WALL
 U-Value= 0.338

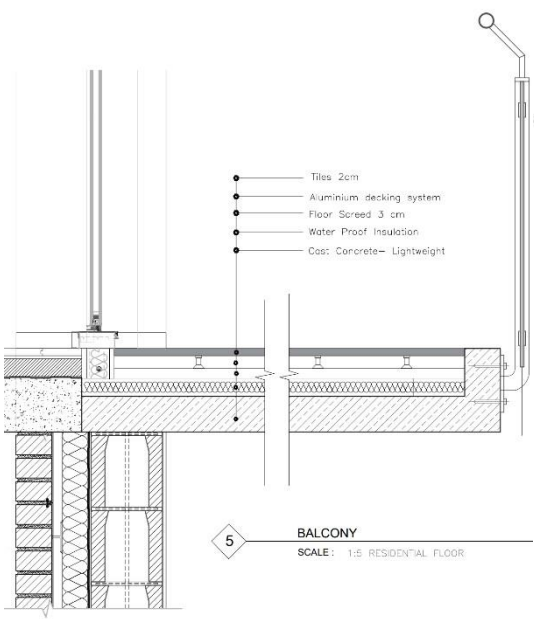


2 **INTERIOR WALL- FLOOR TO CEILING**
 SCALE: 1:5 RESIDENTIAL WALL
 U-Value= 0.50

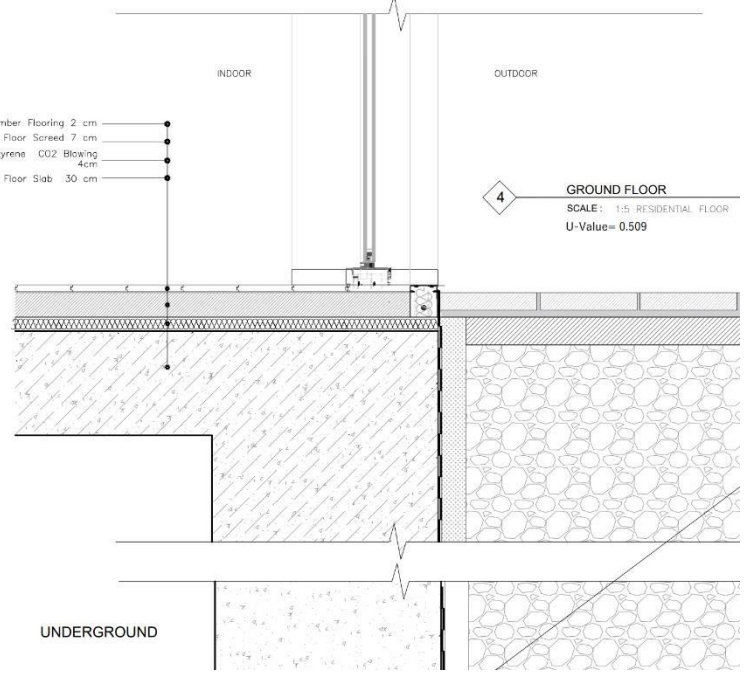
1. Exterior Walls
2. Interior Walls
3. Roof
4. Ground Floor
5. Overhang Balcony



3 **ROOF FLOOR**
 SCALE: 1:5 RESIDENTIAL FLOOR
 U-Value= 0.344



5 **BALCONY**
 SCALE: 1:5 RESIDENTIAL FLOOR



4 **GROUND FLOOR**
 SCALE: 1:5 RESIDENTIAL FLOOR
 U-Value= 0.509

Figure 39. Detail call-outs of construction properties.

The window-to-wall ratio (WWR), or the amount of glazing material on the external wall is set to be 60 % for the residential floors (R) and 100% for the vertical farming (VF) to make use of the natural solar gain for food production. **Table 7** lists the properties of the glazing materials.

Table 7. Glazing properties

Glazing properties	
Glazing type	Double LoE (e2=1) clear 6mm/13mm Air
Frame properties	Aluminum window frame with thermal break
SHGC (Total solar transmission)	0.568
U-value of glass [W/m ² .K]	1.761
Opening position	Middle
Glazing area opens [%]	30
Airtightness [ac/h]	0.5

3.6.2 Proposed Design Strategy Scenarios

In the computation for the ten building configurations, several variables are altered to evaluate the impact of different design parameters on energy consumption and performance. The models are analyzed in three different climate settings with a WWR_VF of 100% and WWR_R of 60 % for three typologies, vertical farming, residence, and when the two operate as one integrated building. On the other hand **Table 8** lists the simulation scenarios and their specific conditions.

Table 8. Scenario description.

Code name	Scenario	Description
SQR	Square morphology, 16 residential floors, and 4 vertical farming floors, south-oriented	High-rise structure with a square form and a basic symmetrical design, with units placed in a grid pattern.
ATR	Atrium morphology, 16 residential floors, and 4 vertical farming floors, Central courtyard south-oriented	High-rise structure with a central atrium for natural light and ventilation, with apartments arranged around it.
CRC	Circle morphology, 16 residential floors, and 4 vertical farming floors, compact structure	A circle-shaped high-rise structure with apartments organized in a circular configuration, providing optimal structural stability.
REC	Rectangle morphology, 16 residential floors, and 4 vertical farming floors elongated, south-oriented	A very common high-rise structure, characterized by a straight rectangular and elongated form, offering enough vertical support and stability while maximizing floor area.

LM	“L”-shaped morphology, 16 residential floors, and 4 vertical farming floors, elongated, southwest-oriented	High-rise structure with an L-shaped form that creates two different wings, with units placed in a linear arrangement.
ZM	“Z”-shaped morphology, 16 residential floors, 4 vertical farming floors, two elongated wings, south-oriented	High-rise structure with a Z-shaped design that allows for flexibility in apartment layouts and is distinguished by a sequence of angled setbacks or extensions that create a zigzag form.
CRS	Cross-shaped morphology, 16 residential floors, 4 vertical farming floors, four symmetrical wings, south-oriented	A cross-shaped high-rise structure with apartments organized in a cruciform four-armed configuration, with various corner units and balconies and diverse viewpoints.
TM	“T”-shaped morphology, 16 residential floors, and 4 vertical farming floors, longer side south-oriented	High-rise T-shaped design with a core joined by two perpendicular wings, with apartments distributed in a linear arrangement around the arms.
UM	“U”-shaped morphology, 16 residential floors, and 4 vertical farming floors, courtyard south-oriented	U-shaped design in which apartments are located along the perimeter of the building, along a front courtyard
HM	“H”-shaped morphology, 16 residential floors and 4 vertical farming floors, two courtyards in the east-west axis	A high-rise building design with two elongated volumes joined by a third, generating two courtyards that form an H-shape design.

3.6.3 Simulation Software

The Design-Builder software is used as the main medium to run simulations in the selected climatic conditions. This program provides an interface that enables the virtual modeling of the geometrical features of buildings, taking into account specific details about the building's architecture, HVAC systems, occupants, glazing, and energy loads. The local weather information relevant to each particular climate is taken from Meteonorm 8.0.3 and used in the Design-Builder software simulations. These weather files are automatically incorporated into the program and used as inputs for the simulations. The transmission of hourly input data between Meteonorm and Design-Builder is made possible by the Energy Plus simulation engine, enabling precise and thorough simulations.

CHAPTER 4

RESULTS

Upon the completion of the rigorous methods indicated in the research, the results are obtained and subjected to a thorough examination and interpretation procedure. To aid in the analysis, visual representations such as charts are used.

The study includes 10 different morphologies that are exposed to three different climatic situations. The following illustrations will be divided into 3 different scenarios to evaluate the energy consumption of Vertical Farming, Residential buildings and when these two different typologies function as one respectively. The findings of this evaluation help to break down the relationship between the morphological aspect, function, and their associated energy performance.

4.1 New York (Humid Subtropical Climate)

An examination is carried out to analyze the influence of New York's climate on the studied morphologies, taking into account the specific characteristics of this weather pattern. Insights are gained for each of the 10 analyzed morphologies by comparing annual active energy consumption and thermal comfort. The graphical representations that follow effectively express this analysis.

4.1.1 Energy Performance

The energy performance is assessed through a monthly analysis of heating and cooling statistics, as shown in *Figures 40* and *41* respectively.

Figure 40 focuses on the monthly heating demand, providing an in-depth overview of the performance of each shape. Notably, the UM and SQR shapes have

the highest heating consumption in January (4.47- 4.45 kWh.m⁻² respectively), with demand steadily decreasing throughout the year. The ATR and REC morphologies, on the other hand, showed decreased heating demands, indicating more potentially energy-efficient designs which can be reasoned by their greater S/V ratios. Comparing the total energy consumption values LM seems to be the most efficient among all in heating for Vertical Farming practices possibly attributed to its geometry and aspect ratios as opposed to HM as the least followed by UM, and SQR morphologies, as a consequence of their inefficient heat transfer outer layers. As the winter progresses, the heating demand generally decreases among all morphologies.

Figure 41 depicts the monthly cooling demand for various shapes. According to the calculations, the morphology with ATR configuration exhibits a rise in cooling demand peaking at 13.84 kWh.m⁻² in August leading to the least efficient configuration as a result of high façade area exposed to solar gain and 100% WWR transparent surfaces which are primarily needed for the natural food production of this building typology. On the other hand, the morphology with the lowest overall cooling energy consumption is SQR (64.91 kWh.m⁻²) as associated with its compactness. Overall cooling demand tends to be higher in the summer months (June to August) and lower in the winter months (December to February).

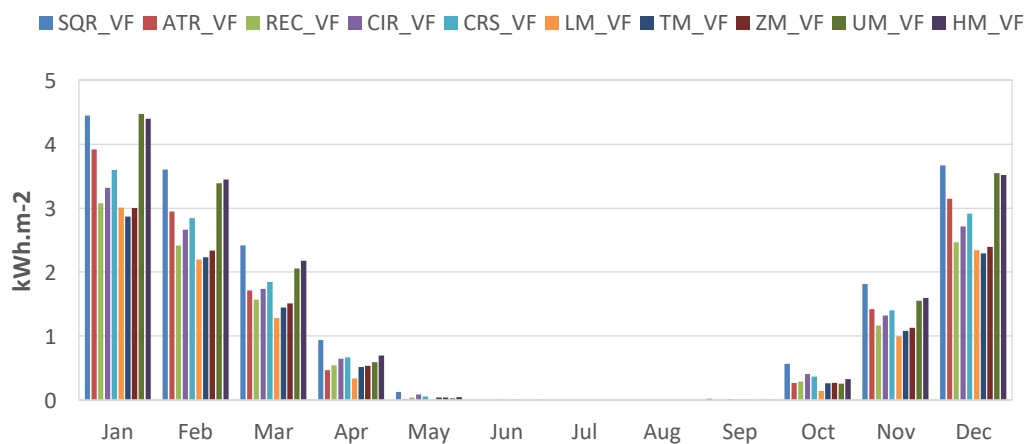


Figure 40. Evaluation of Simulated Heating results (kWh.m⁻²) among different morphologies of Vertical Farming.

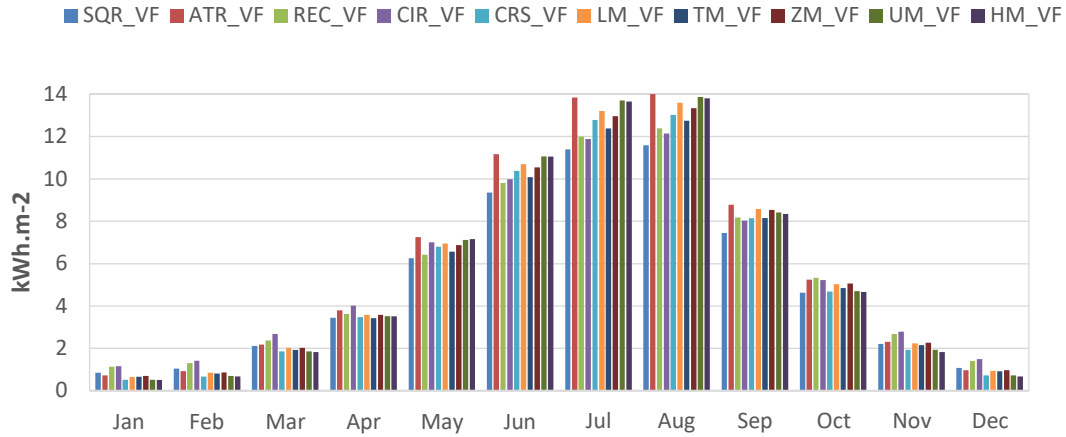


Figure 41. Evaluation of Simulated Cooling results (kWh.m-2) among different morphologies of Vertical Farming VF.

Figure 42 indicates the monthly heating consumption while **Figure 43** the monthly cooling energy demand for each morphology. The most efficient for heating the residential block is LM, which consumes 91.09 kWh.m-2 yearly, while the least efficient are CRS and ATR which in contrast to the former have poor air circulation especially due to their pocket layouts acting as thermal bridges. Similarly, for cooling, the optimal morphology is SQR, ascribed to the shape efficiency allowing optimized airflow and consuming 30.83 kWh.m-2 per year, in sharp contrast to ATR as the least. In terms of seasonal variation, the findings suggest that heating energy use is higher during the winter months, notably in January and December, across all morphologies.

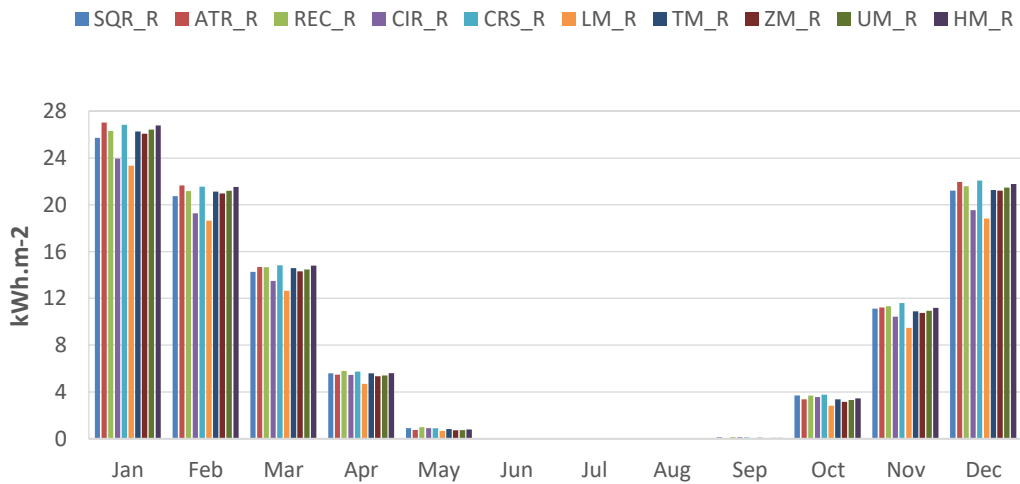


Figure 42. Evaluation of Simulated Heating results (kWh.m⁻²) among the Residential morphologies.

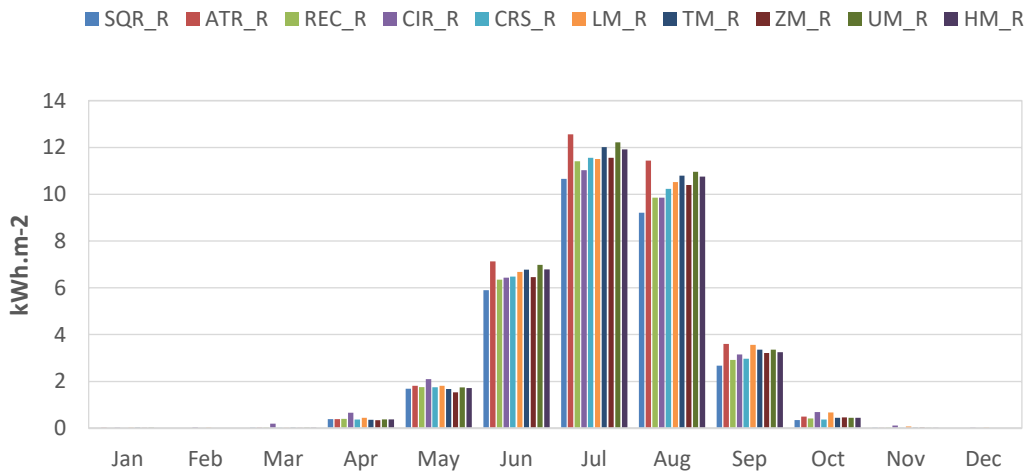


Figure 43. Evaluation of Simulated Cooling results (kWh.m⁻²) among the Residential morphologies.

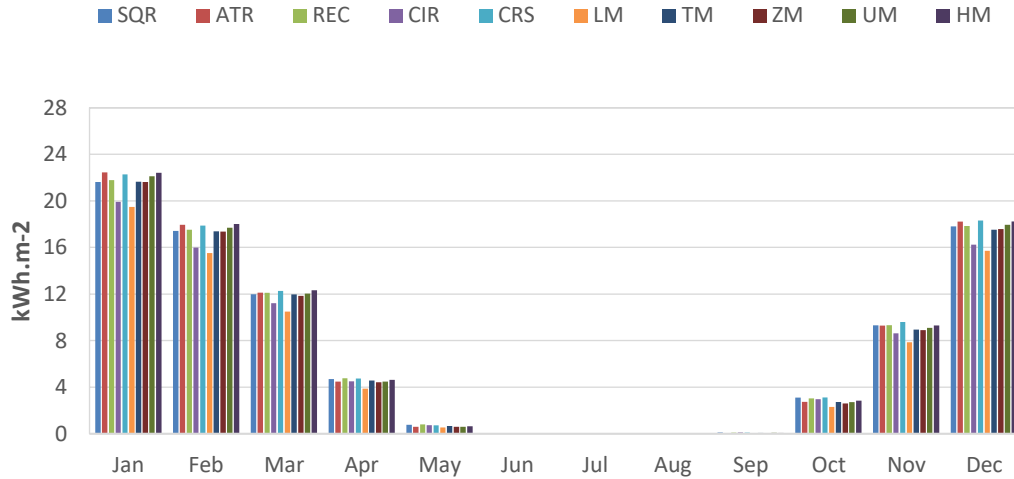


Figure 44. Evaluation of Simulated Heating results (kWh.m⁻²) among the morphologies with integrated vertical farming VF in High-rise residential buildings.

Figure 44 represents the monthly heating demand for all the morphologies. **Figure 45** represents the monthly cooling demand respectively. According to the

calculations, the best overall energy performance for heating and cooling among the integrated models resulted in LM morphology. Whereas the worst scenario in ATR and HM morphology is due to their larger amount of glazing façade surface area exposed to solar gains.

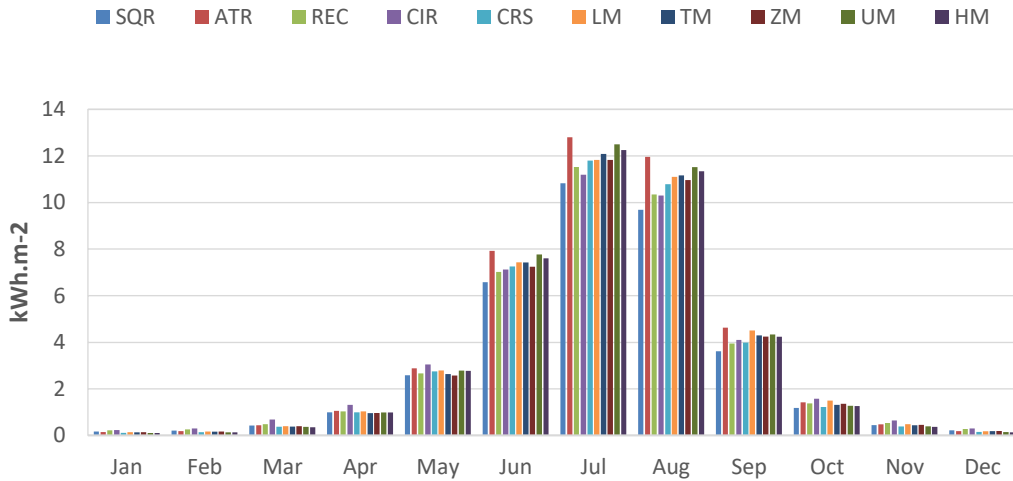


Figure 45. Evaluation of Simulated Cooling results (kWh.m⁻²) among the morphologies with integrated vertical farming VF in High-rise residential buildings.

4.2 Singapore (Tropical Climate)

The data below provide a comparison of annual energy usage and thermal comfort inside the proposed study models to examine the influence of Singapore's tropical and humid climate on the suggested designs.

4.2.1 Energy Performance

The figures below show the monthly consumption for heating and cooling loads of the study morphologies for vertical farming, residential block, and integrated model accordingly.

Figure 46 compares the monthly cooling demand for all morphologies focusing on only vertical farming. Due to the effect of the constant heat weather patterns of

Singapore's climate, there is no requirement for heating yearly.

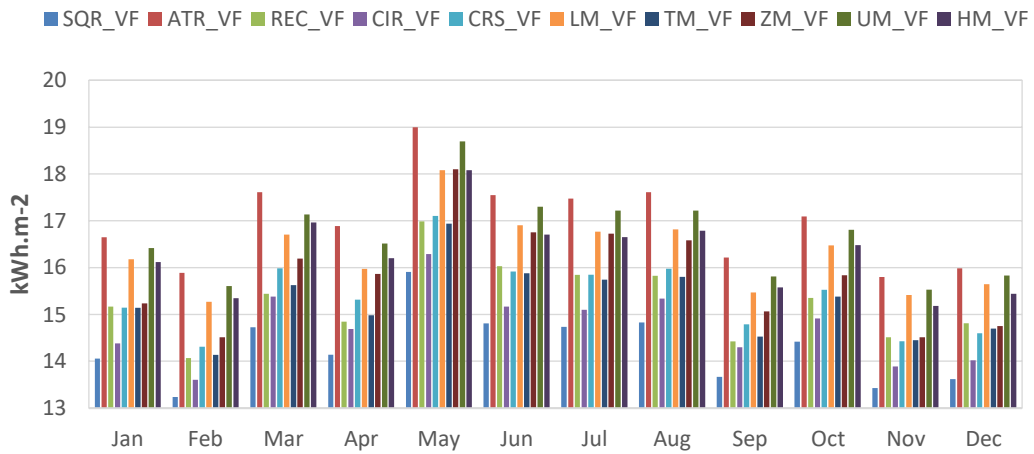


Figure 46. Evaluation of Simulated Cooling results (kWh.m⁻²) among different morphologies of Vertical Farming.

In comparison with the other climate contexts, Singapore does consume much more annual energy among all morphologies. When it comes to monthly cooling energy consumption, the summer months (May, June, July, and August) generally have the highest values, reaching a peak in May with a consumption of over 19 kWh.m⁻² by ATR morphology associated with its fully transparent atrium. This pattern is consistent with the projected tendency, since the requirement for cooling rises during the warmer months. By comparing these values the SQR morphology has the lowest cooling demand with a value of 14.06 kWh.m⁻² as the most compact shape.

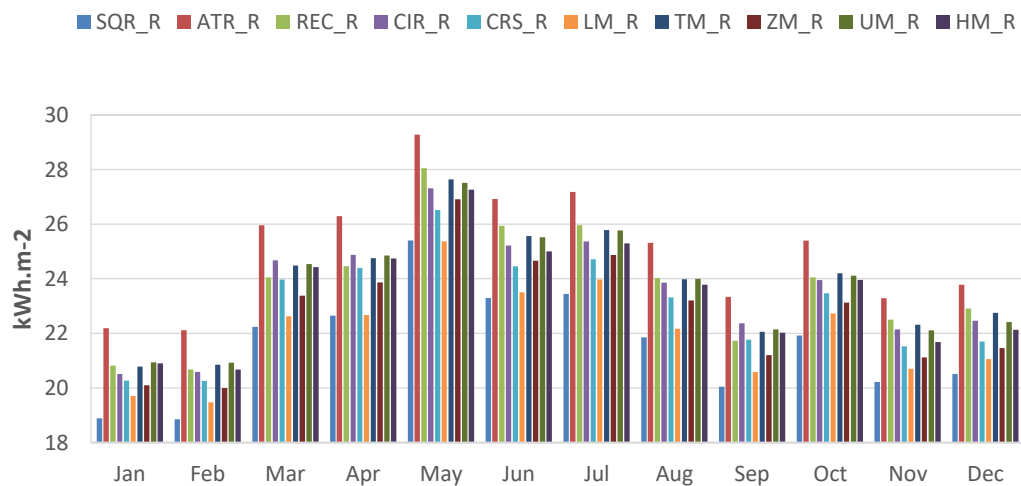


Figure 47. Evaluation of Simulated Cooling results (kWh.m⁻²) among the Residential morphologies.

Firstly, as with the prior graph, there is no reported energy usage for heating in any of the buildings or spaces throughout the observed months. This implies that heating was neither necessary nor used during this time period.

Figure 47. show that the residential morphology of SQR and LM consume the least amount of cooling energy due to their efficiency in spatial utilization, airflow, and thermal performance, whereas ATR consumes the most overcoming 300 kWh.m⁻² yearly consumption attributed to its surface-to-volume area, complex shape, and limited natural ventilation options. The summer months have the largest cooling demand, while the winter months have the lowest although the values are relatively high annually. When compared to the prior report, total cooling energy usage across all buildings has risen. Furthermore, the findings reveal an approximate 30 % increase in cooling values as compared to vertical farming demands for the same climate context. These findings highlight the importance of energy-efficient cooling systems and the necessity for adaptive control solutions to properly regulate and minimize cooling energy usage.

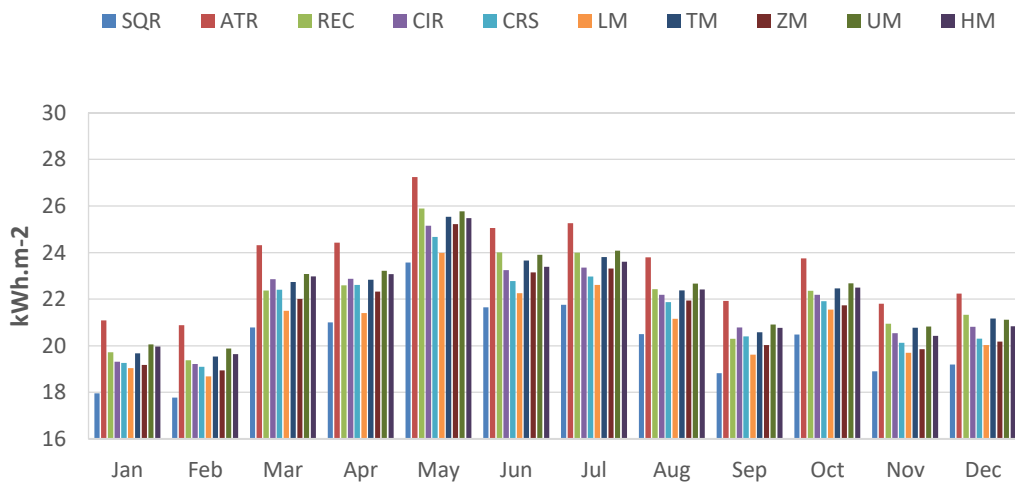


Figure 48. Evaluation of Simulated Cooling results (kWh.m⁻²) among the morphologies with integrated vertical farming VF in High-rise residential. buildings.

Figure 48 illustrates the results in different morphologies considering that there is no need for heating in this scenario either. What can be emphasized here is that the total heating and cooling energy usage across all buildings decreases slightly when vertical farming performs integrated with the high-rise residential morphologies which may be linked to the ability of passive heat exchange. In this case, once again, the SQR shape morphology demonstrates the best overall results and ATR the least.

4.3 Athens (Mediterranean Climate)

A carried investigation was done to analyze the impact of the Mediterranean climate on the suggested morphologies, which included a comparison of yearly energy usage and thermal comfort levels responding to the unique climatic conditions prevalent in Athens. The figures that resulted give a visual depiction of the data, giving insight into the probable influence of the local climate on the studied morphologies.

4.3.1 Energy Performance

The energy performance of various vertical farming morphologies is assessed by evaluating monthly heating and cooling statistics, as shown in *Figures 49* and *50*, respectively.

The data in *Figure 49* represent the energy consumption for heating purposes. By comparing the results across the categories, it can be observed that the heating values are relatively very low for all morphologies which is highly influenced by the climate context and insulation properties. For instance, the highest heating energy consumption is observed in the ZM shape with a value of 1.63 kWh.m⁻² in January with less favorable orientation concerning its geometrical attributes, as opposed to LM which is 40 % more heat efficient.

Similarly, the highest annual heating energy consumption is observed in the SQR morphology, while the lowest is in the LM shape which occupies 5.5% of the

total energy consumption, with the raining 94.5 % for cooling. Such differences can be attributed to the SQR morphology having a larger surface relative to its volume leading to increased heat loss requires a significant quantity of air conditioning for cooling throughout the summer, casting questions on the efficiency of this shape in this specific context. This trend is also observed in other categories, indicating that cooling generally requires more energy than heating as displayed in *Figure 50*.

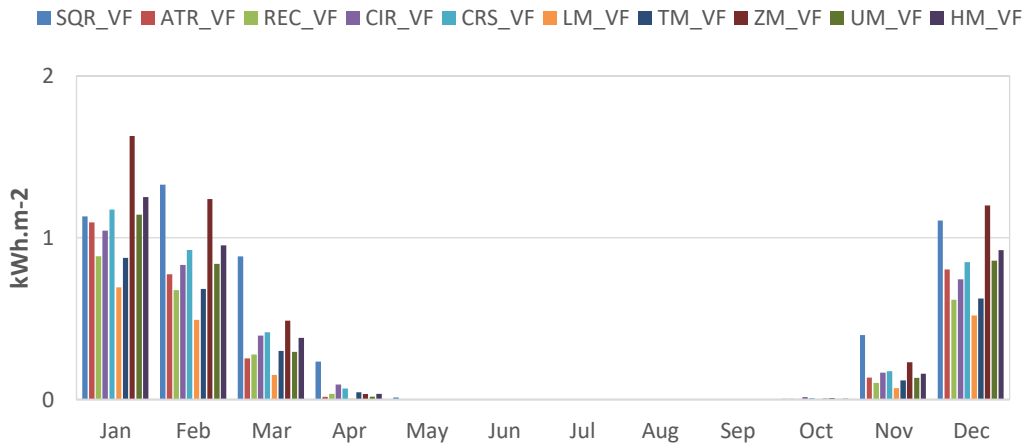


Figure 49. Evaluation of Simulated Heating results (kWh.m-2) among different morphologies of Vertical Farming.

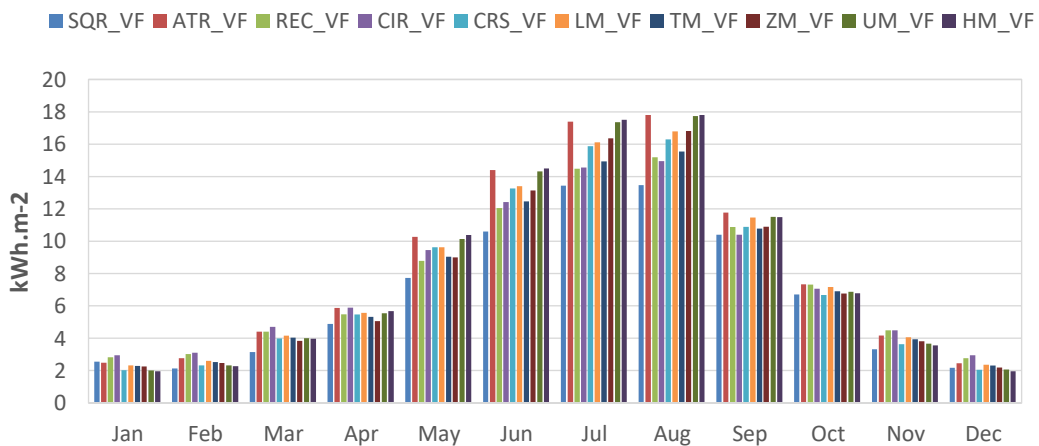


Figure 50. Evaluation of Simulated Cooling results (kWh.m-2) among different morphologies of Vertical Farming.

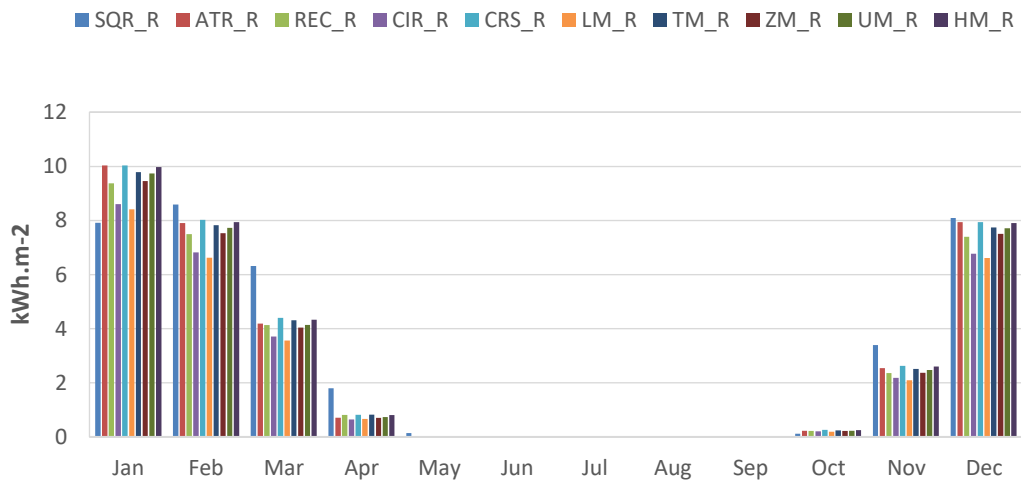


Figure 51. Evaluation of Simulated Heating results (kWh.m-2) among the Residential morphologies.

Figure 51 compares the monthly heating requirement for all morphologies for the residential block calculations. **Figure 52** depicts the monthly cooling demand for all accordingly. The data display a consistent pattern of higher energy consumption for cooling than heating. However, when comparing these results with the previous conclusions on the Vertical Farming block it is evident that the residential typology consumes approximately 50 % more energy for heating. This disparity can be due to the fact of having a smaller WWR of 70 % when compared to vertical farming block.

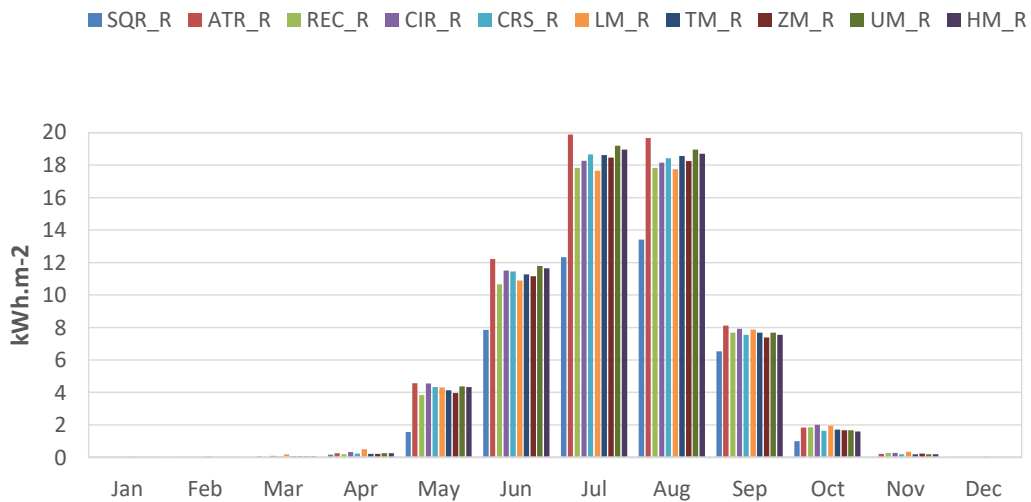


Figure 52. Evaluation of Simulated Cooling results (kWh.m-2) among the Residential morphologies.

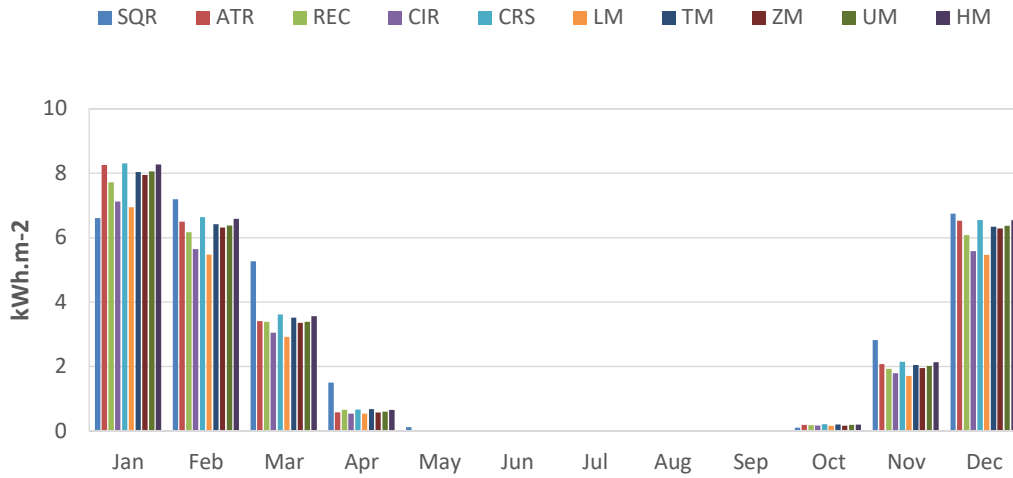


Figure 53. Evaluation of Simulated Heating results (kWh.m-2) among the morphologies with integrated vertical farming VF in High-rise residential buildings.

The monthly heating requirement for all morphologies of High-rise residential models with integrated VF are as depicted in **Figure 53**. The monthly heating demand for each type has slightly decreased by 20 % among all morphologies relative to earlier outcomes. In this scenario, the overall optimal performance for heating it had CIR followed by LM morphology as more compact shapes in contrast to SQR as the worst efficient due to its attributes related to S/V ratio layout or aspect ratio. The VF block might emit some heat, which contributes to the building's total heating requirements. This integration may have resulted in better balanced and optimal heating performance throughout the building as a whole system.

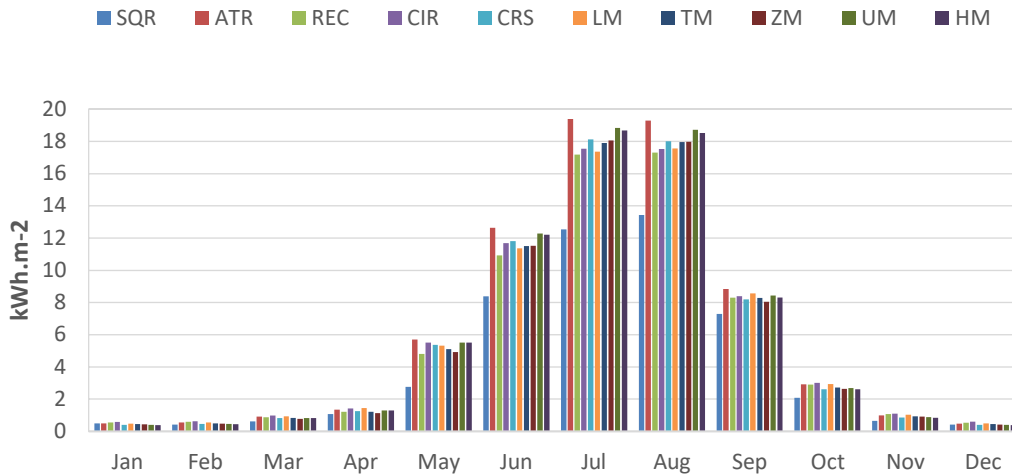


Figure 54. Evaluation of Simulated Cooling results (kWh.m-2) among the morphologies with integrated vertical farming VF in High-rise residential buildings.

Figure 54 indicates the monthly cooling consumption. What can be highlighted here is that the SQR morphology although having poor heating performance compared to other morphologies it's the most efficient by at least 13 % when it comes to cooling demands and overall performance among all others for yearly cooling and heating sum results. Conversely, ATR leads as the worst-case scenario in this climate context once again, succeeded by UM and HM morphology as a result of their limited airflow circulation relevant to their complex configurations and lower relative compactness values.

CHAPTER 5

DISCUSSIONS

5.1 Climate of New York

A comprehensive investigation was undertaken to compare the yearly active energy consumption of the study high rise and vertical farming typologies in New York's climate setting. The study's conclusions are graphically represented in the illustrative figures presented below.

5.1.1 Energy Performance

Figure 55 depicts a graphic representation of useful insights into the yearly predicted energy demand across all morphologies as per their performance associated with their typologies, specifically VF_Vertical Farming, R_Residence, and VF+R (a combination of the two). The analysis focuses on the amounts of energy consumption linked with distinct morphological attributes in this particular climatic scenario.

Among the examined morphologies, ATR and LM have the most noticeable variances in energy demand in all the typologies, consuming the most and the least energy accordingly. Commonly the Residential typology (R_ATR) consumes the greatest amount with an overall 143.47 kWh.m-2Y-1 annual energy consumed. Conversely, the Vertical Farming typology consumes the least with only ± 80.24 kWh.m-2Y-1 on average across all morphologies. Further examination of individual morphologies reveals that LM is at least 12 % more energy efficient than all other morphologies for the climate of New York. On the contrary, ATR, UM, and HM result as the least efficient because of their higher S/V ratios exposed to the solar gains.

Making use of the natural light for food production and minor air conditioning

system consumption the VF_TM but also generally all the morphologies of vertical farming result as the most energy-optimized. It is worth being noted that slight differences in energy usage have been found throughout REC and TM in all studied typologies with a difference between the greatest and lowest energy usage of roughly $\pm 0.55 \text{ kWh.m}^{-2}\text{Y}^{-1}$, demonstrating similar fluctuation.

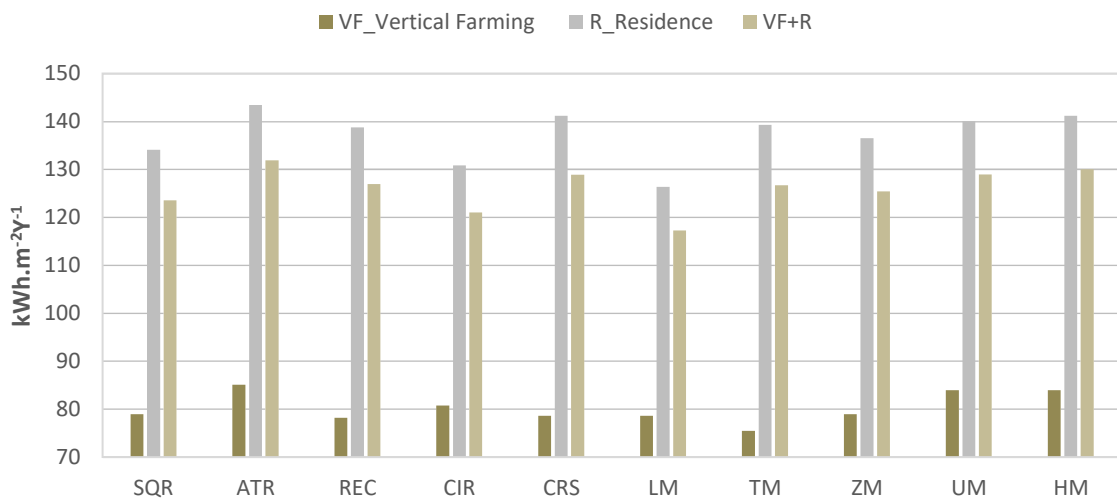


Figure 55. Comparison of annual energy demand (kWh.m^{-2}) among all morphologies and their respective study typologies Climate of New York.

Table 9 presents a thorough breakdown of the simulation results for all scenarios run under New York's climatic conditions. The data show that carefully selecting a suitable architectural morphology matched to the individual climatic setting may result in a profound energy demand decrease of over 41.5%. Notably, the LM morphology is the most efficient in terms of energy performance, especially for heating demands. The layout and shape configuration and compactness result in better space and energy efficiency. ATR, on the other hand, has the lowest energy demand performance, raising concerns about the viability of this morphology layout and its associated attributes such as the central atrium, for New York's humid subtropical climate.

Table 9. Simulation results for all the scenarios conducted in the climate of New York

Annual Heating Demand			Annual Cooling Demand			Annual Energy Demand		
Total Heating [kWh]	Heating/ conditioned area [kWh/m ²]	Morphology effectiveness [%]	Total Cooling [kWh]	Cooling/ conditioned area [kWh/m ²]	Morphology effectiveness [%]	Total Energy [kWh]	Total Energy conditioned area [kWh/m ²]	Morphology effectiveness [%]
111807.7	17.6	-	393850.6	62.0	-	505658.3	79.6	-
88984.4	13.9	21.1	455891.3	71.2	-14.8	544875.7	85.1	-6.9
74150.2	11.6	34.2	426005.7	66.6	-7.4	500155.9	78.2	1.8
83544.6	12.9	26.7	438967.7	67.8	-9.3	522512.3	80.7	-1.4
88009.4	13.7	22.2	416845.2	64.9	-4.6	504854.6	78.6	1.3
63910.7	10.3	41.5	423490.2	68.3	-10.1	487400.9	78.6	1.3
69675.9	10.7	39.0	419814.8	64.7	-4.3	489490.7	75.4	5.3
69675.9	11.2	36.2	419814.8	67.7	-9.1	489490.7	78.9	0.9
101096.7	15.9	9.7	432676.6	68.0	-9.7	533773.3	83.9	-5.4
101948.0	16.2	7.9	425778.5	67.7	-9.2	527726.6	83.9	-5.4
171182.5	103.3	-	51098.5	30.8	-	222281.0	134.1	-
171222.5	106.1	-2.7	60302.2	37.4	-21.2	231524.7	143.5	-7.0
174574.5	105.7	-2.3	54647.0	33.1	-7.3	229221.5	138.8	-3.5
160295.7	96.6	6.4	56719.2	34.2	-10.9	217014.8	130.8	2.4
176390.2	107.5	-4.1	55362.3	33.7	-9.4	231752.5	141.2	-5.3
150820.3	91.1	11.8	58366.9	35.3	-14.3	209187.2	126.3	5.8
171359.0	103.9	-0.6	58350.6	35.4	-14.8	229709.6	139.3	-3.9
166478.9	102.6	0.7	55144.0	34.0	-10.2	221622.9	136.5	-1.8
168690.4	104.0	-0.7	58455.7	36.0	-16.9	227146.0	140.0	-4.4
172400.3	106.0	-2.6	57268.4	35.2	-14.2	229668.7	141.2	-5.3
2850728.	86.7	-	1211426.1	36.9	-	4062154.6	123.6	-
2828544.	87.8	-1.2	1420726.8	44.1	-19.6	4249271.6	131.9	-6.7
2867342.	87.3	-0.7	1300357.7	39.6	-7.5	4167700.1	126.9	-2.7
2648275.	80.2	7.5	1346474.3	40.8	-10.7	3994749.6	121.0	2.1
2910252.	89.0	-2.7	1302641.8	39.9	-8.1	4212894.0	128.9	-4.3
2477035.	75.8	12.6	1357360.2	41.5	-12.7	3834395.3	117.3	5.1
2811420.	85.5	1.4	1353424.8	41.2	-11.7	4164844.9	126.7	-2.5
2733337.	85.0	2.0	1302118.5	40.5	-9.8	4035456.3	125.4	-1.5
2800142.	86.6	0.1	1367967.3	42.3	-14.9	4168110.1	129.0	-4.4
2860353.	88.5	-2.1	1342072.5	41.5	-12.7	4202425.8	130.0	-5.2

It's noteworthy to mention also that SQR morphology leads with the best performance among all morphologies of each typology with an efficiency that does reach up to 21.2% in annual cooling demand only. The compact shape leads to better airflow and less heat collected lowering the cooling demand.

In terms of the overall energy performance of VF, the morphological efficiency ranges $\pm 12.13\%$, for R ± 12.8 and 11.7% for VF+R from worst to best case scenario. When compared to alternative morphologies with larger surface-to-volume ratios, the LM_VF+R morphological design performs better in terms of yearly heating and cooling needs, with an efficacy above 12%. Surprisingly, LM_VF+R delivers a significant reduction in energy usage, equivalent to 117.3 kWh/m² per year.

5.2 Climate of Singapore

A thorough examination was conducted to compare the yearly active energy consumption of the study high rise and vertical farming typologies in the climatic setting of Singapore. The study's findings are visually illustrated in the figures shown below.

5.2.1 Energy Performance

Figure 56 displays a graphical depiction of important insights into the yearly expected energy consumption for all morphologies based on their performance concerning their typologies. The analysis focuses on the amounts of energy consumption linked with distinct morphological attributes in this particular climatic scenario.

First and foremost it is of essential importance to mention that the climate of Singapore in comparison to the New York' or Athen's climate does not require cooling due to its constant weather temperatures throughout the year. Thus, there are no energy

demands for cooling among all the study morphologies. As previously shown in the New York climate analysis, ATR exhibits the most substantial discrepancies in energy usage among all evaluated morphologies. ATR is the largest energy user, whereas SQR followed by LM is at the other end of the range with the lowest energy consumption. The Residential type (R_ATR) typically consumes the most energy, totaling 259.27 kWh.m-2Y-1 each year. Vertical Farming, on the other hand, consistently has the lowest energy usage, averaging roughly 188.56 kWh.m-2Y-1 across all morphologies. The examination of the various morphologies indicates that SQR is at least 15.8 % more energy efficient than all other morphologies, resulting in the best scenario for Singapore's setting. ATM and UM, on the other hand, are the least efficient due to factors such as suboptimal thermal mass distribution, lower compactness, and more complex configuration.

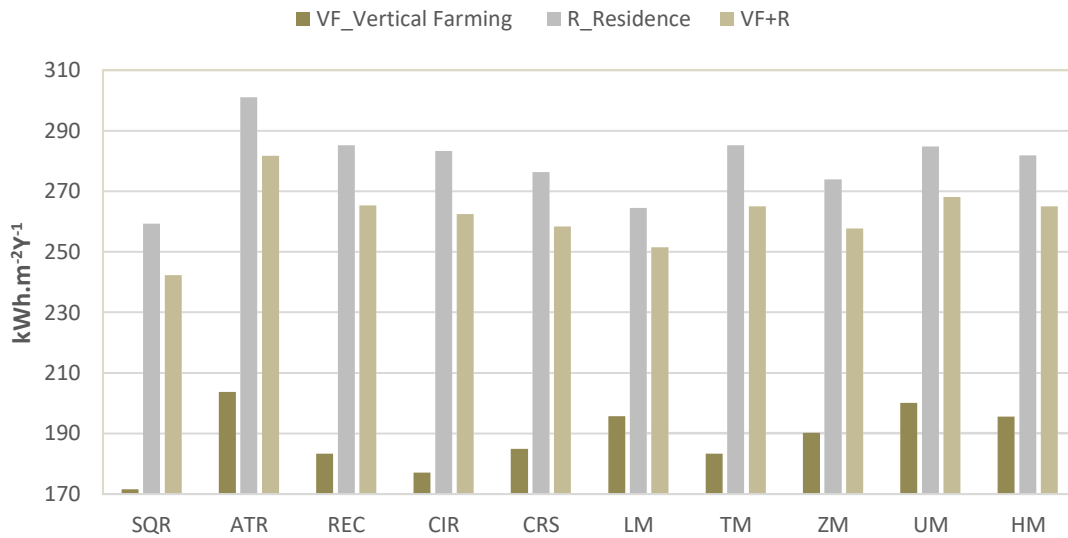


Figure 56. Comparison of annual energy demand (kWh.m-2) among all morphologies and their respective study typologies_Climate of Singapore.

Table 10 presents a thorough breakdown of the simulation results for all scenarios run under Singapore's climatic conditions. The data show that carefully selecting a suitable architectural morphology matched to the individual climatic setting may result in a profound energy demand decrease of over 18.7 %.

Remarkably the SQR shape outperforms all others in terms of energy performance for all typologies, particularly cooling needs. Its compact form reduces heat intake and loss by minimizing surface area. Furthermore, the lack of heating requirements strengthens its position as the most efficient morphology. In contrast, ATR has the least efficient energy demand performance, requiring almost 20% more energy than other morphologies. This is due to certain characteristics such as the existence of a central atrium and greater facade surface area, which may lead to greater energy usage for cooling. The energy efficiency of the ATR shape is further constrained by Singapore's specific tropical environment. It's noteworthy to state that LM morphology is the second best scenario in this climate conditions which makes it an optimal choice in terms of overall energy efficiency in different climates.

In terms of total energy performance, the morphological efficiency for the VF, R, and VF+R typologies spans from around -2% to +20.76%, reflecting the worst-case to best-case situations.

Table 10. Simulation results obtained for all the scenarios conducted in the climate of Singapore

Scenarios	Annual Heating Demand			Annual Cooling Demand			Annual Energy Demand		
	Total Heating [kWh]	Heating/conditioned area [kWh/m ²]	Morphology effectiveness [%]	Total Cooling [kWh]	Cooling/conditioned area [kWh/m ²]	Morphology effectiveness [%]	Total Energy [kWh]	Total Energy conditioned area [kWh/m ²]	Morphology effectiveness [%]
SQR _{vf}	0.0	0.0	-	1089338.6	171.6	-	1089338.6	171.6	-
ATR _{vf}	0.0	0.0	0.0	1304355.6	203.8	-18.8	1304355.6	203.8	-18.8
REC _{vf}	0.0	0.0	0.0	1172860.1	183.3	-6.9	1172860.1	183.3	-6.9
CIR _{vf}	0.0	0.0	0.0	1146211.4	177.1	-3.2	1146211.4	177.1	-3.2
CRS _{vf}	0.0	0.0	0.0	1187455.9	184.9	-7.8	1187455.9	184.9	-7.8
LM _{vf}	0.0	0.0	0.0	1213387.2	195.7	-14.1	1213387.2	195.7	-14.1
TM _{vf}	0.0	0.0	0.0	1189424.3	183.3	-6.9	1189424.3	183.3	-6.9
ZM _{vf}	0.0	0.0	0.0	1179445.6	190.2	-10.8	1179445.6	190.2	-10.8
UM _{vf}	0.0	0.0	0.0	1272727.8	200.1	-16.6	1272727.8	200.1	-16.6

HM _{vf}	0.0	0.0	0.0	1229761.6	195.6	-14.0	1229761.6	195.6	-14.0
SQR _R	0.0	0.0	-	429771.1	259.3	-	429771.1	259.3	-
ATR _R	0.0	0.0	0.0	485864.1	301.1	-16.1	485864.1	301.1	-16.1
REC _R	0.0	0.0	0.0	471125.9	285.2	-10.0	471125.9	285.2	-10.0
CIR _R	0.0	0.0	0.0	469861.0	283.3	-9.3	469861.0	283.3	-9.3
CRS _R	0.0	0.0	0.0	453539.7	276.3	-6.6	453539.7	276.3	-6.6
LM _R	0.0	0.0	0.0	437968.8	264.5	-2.0	437968.8	264.5	-2.0
TM _R	0.0	0.0	0.0	470257.7	285.2	-10.0	470257.7	285.2	-10.0
ZM _R	0.0	0.0	0.0	444631.7	273.9	-5.6	444631.7	273.9	-5.6
UM _R	0.0	0.0	0.0	461991.7	284.8	-9.8	461991.7	284.8	-9.8
HM _R	0.0	0.0	0.0	458480.0	281.9	-8.7	458480.0	281.9	-8.7
SQR _{VF+R}	0.0	0.0	-	7965675.9	242.3	-	7965675.9	242.3	-
ATR _{VF+R}	0.0	0.0	0.0	9078180.4	281.7	-16.3	9078180.4	281.7	-16.3
REC _{VF+R}	0.0	0.0	0.0	8710874.3	265.3	-9.5	8710874.3	265.3	-9.5
CIR _{VF+R}	0.0	0.0	0.0	8663987.3	262.5	-8.3	8663987.3	262.5	-8.3
CRS _{VF+R}	0.0	0.0	0.0	8444090.3	258.3	-6.6	8444090.3	258.3	-6.6
LM _{VF+R}	0.0	0.0	0.0	8220888.2	251.5	-3.8	8220888.2	251.5	-3.8
TM _{VF+R}	0.0	0.0	0.0	8713547.5	265.1	-9.4	8713547.5	265.1	-9.4
ZM _{VF+R}	0.0	0.0	0.0	8293552.8	257.8	-6.4	8293552.8	257.8	-6.4
UM _{VF+R}	0.0	0.0	0.0	8664594.9	268.1	-10.6	8664594.9	268.1	-10.6
HM _{VF+R}	0.0	0.0	0.0	8565441.6	265.1	-9.4	8565441.6	265.1	-9.4

5.3 Climate of Athens

A thorough examination was conducted to compare the yearly active energy consumption of the study high rise and vertical farming typologies in the climatic setting of Athens. The study's findings are visually illustrated in the figures shown below.

5.3.1 Energy Performance

Figure 57 displays a graphical depiction of important insights into the yearly expected energy consumption for all morphologies based on their performance in

relation to their typologies. The analysis focuses on the amounts of energy consumption linked with distinct morphological attributes in this particular climatic scenario. It is noteworthy that, after Singapore, the Mediterranean climate of Athens ranks as the second warmest for this study. As a result, the energy demand for heating is substantially lower than for cooling, showing that cooling requirements are prioritized.

As demonstrated in the Singapore climate analysis, ATR morphology exhibits the most significant fluctuations in energy usage when compared to other analyzed morphologies. In this environment, ATR is the largest energy user, whereas SQR is the lowest energy consumer among all typologies. In comparison, the most energy-consuming type, ATR_VF, consumes 104.11 kWh.m-2Y-1. The average yearly energy usage generally differs across the VF, R, and VF_R typologies by around ± 3.79 kWh.m-2Y-1 between best or worst scenarios. The examination of several morphologies suggests that the SQR morphology has a significant energy efficiency advantage of at least 21% over all other morphologies. As a result, it is the most beneficial scenario for Athens' climate. In contrast, ATM, UM, and HM exhibited lower levels of efficiency similar to the other analyzed climates, resulting in the worst-case scenarios overall.

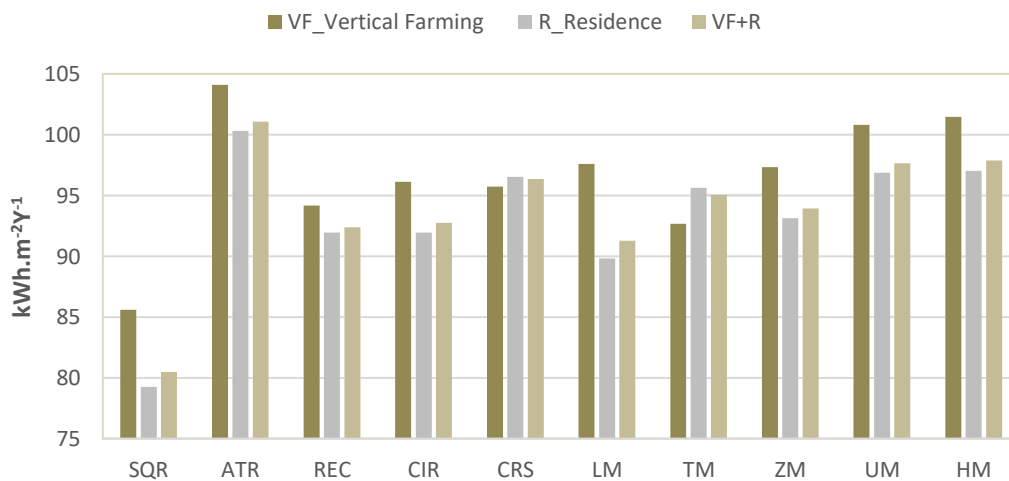


Figure 57. Comparison of annual energy demand (kWh.m-2) among all morphologies and their respective study typologies_Climate of Athens.

Table 11 presents a thorough breakdown of the simulation results for all

scenarios run under Athens climatic conditions. The data show that carefully selecting a suitable architectural morphology matched to the individual climatic setting may result in a profound energy demand decrease of over 67.5 %. Notably, the SQR morphology is the most efficient in terms of energy performance, especially for heating and cooling demands. The layout and shape configuration and compactness result in better space and energy efficiency. In contrast, based on prior climatic examinations, ATR stands out as the shape with the largest energy consumption. This raises questions regarding the layout's feasibility and viability, as well as its accompanying features, such as the central atrium, in Athens' Mediterranean climate. ATR's considerable energy consumption peaking at 104.1 kWh.m-2Y-1 for yearly cooling indicate possible obstacles in attaining energy efficiency and point to the necessity for additional research and optimization of its design elements in this unique climatic environment.

It is worth noting that the SQR morphology stands out with an exceptional average performance of 51% across all typologies. In the instance of the VF typology, LM outperforms other morphologies with an outstanding heating efficiency of around 62%. This is due, in part, to its compact form and arrangement, which results in lower surface-to-volume (S/V) ratios. As a consequence, LM also delivers the second-best scenario for these environmental conditions, proving its efficacy in optimizing energy performance.

Table 11. Simulation results obtained for all the scenarios conducted in the climate of Athens.

Scenarios	Annual Heating Demand			Annual Cooling Demand			Annual Energy Demand		
	Total Heating [kWh]	Heating/conditioned area [kWh/m2]	Morphology effectiveness [%]	Total Cooling [kWh]	Cooling/conditioned area [kWh/m2]	Morphology effectiveness [%]	Total Energy [kWh]	Total Energy conditioned area [kWh/m2]	Morphology effectiveness [%]
SQR _{vf}	32425.7	5.1	–	511044.6	80.5	–	543470.2	85.6	–
ATR _{vf}	19766.4	3.1	39.5	646695.9	101.0	-25.5	666462.3	104.1	-21.6
REC _{vf}	16621.9	2.6	49.1	585831.2	91.6	-13.8	602453.1	94.2	-10.0
CIR _{vf}	21277.5	3.3	35.6	600942.7	92.8	-15.4	622220.2	96.1	-12.3
CRS _{vf}	23242.9	3.6	29.1	591455.2	92.1	-14.4	614698.0	95.7	-11.8
LM _{vf}	11977.1	1.9	62.2	593061.6	95.7	-18.9	605038.7	97.6	-14.0

TM _{vf}	17198.2	2.7	48.1	584029.2	90.0	-11.8	601227.4	92.7	-8.3
ZM _{vf}	29973.7	4.8	5.4	573750.7	92.5	-14.9	603724.4	97.3	-13.7
UM _{vf}	20904.1	3.3	35.6	620242.8	97.5	-21.2	641146.9	100.8	-17.8
HM _{vf}	23317.9	3.7	27.4	614711.8	97.8	-21.5	638029.8	101.5	-18.5
SQR _R	60306.1	36.4	-	71077.5	42.9	-	131383.5	79.3	-
ATR _R	54173.0	33.6	7.7	107723.6	66.8	-55.7	161896.6	100.3	-26.6
REC _R	52522.6	31.8	12.6	99366.7	60.1	-40.3	151889.3	91.9	-16.0
CIR _R	47948.0	28.9	20.5	104563.3	63.0	-47.0	152511.3	91.9	-16.0
CRS _R	55984.0	34.1	6.3	102461.9	62.4	-45.6	158445.9	96.5	-21.8
LM _R	46670.4	28.2	22.5	102036.2	61.6	-43.7	148706.6	89.8	-13.3
TM _R	54819.5	33.2	8.6	102888.1	62.4	-45.5	157707.6	95.6	-20.7
ZM _R	51633.8	31.8	12.6	99529.8	61.3	-43.0	151163.6	93.1	-17.5
UM _R	53164.9	32.8	9.9	103994.3	64.1	-49.5	157159.2	96.9	-22.2
HM _R	55003.1	33.8	7.1	102809.4	63.2	-47.4	157812.5	97.0	-22.4
SQR _{VF+R}	997323.1	30.3	-	1648283.8	50.1	-	2645606.8	80.5	-
ATR _{VF+R}	886534.9	27.5	9.3	2370272.9	73.6	-46.7	3256807.8	101.1	-25.6
REC _{VF+R}	856983.3	26.1	14.0	2175698.0	66.3	-32.2	3032681.2	92.4	-14.8
CIR _{VF+R}	788446.0	23.9	21.3	2273955.7	68.9	-37.4	3062401.7	92.8	-15.3
CRS _{VF+R}	918986.8	28.1	7.3	2230846.1	68.3	-36.1	3149832.9	96.4	-19.7
LM _{VF+R}	758703.8	23.2	23.5	2225640.2	68.1	-35.8	2984343.9	91.3	-13.4
TM _{VF+R}	894310.8	27.2	10.3	2230238.1	67.8	-35.3	3124548.9	95.0	-18.1
ZM _{VF+R}	856115.2	26.6	12.3	2166226.8	67.3	-34.3	3022342.0	93.9	-16.7
UM _{VF+R}	871543.0	27.0	11.1	2284151.1	70.7	-41.0	3155694.1	97.6	-21.3
HM _{VF+R}	903367.9	28.0	7.9	2259662.6	69.9	-39.5	3163030.5	97.9	-21.6

5.4 Climate Comparison

Figure 58 compares the predicted energy demand (kWh.m-2Y-1) for three distinct climatic settings for each typology and their belonging morphological configuration. It is essential to note that Singapore's tropical climate has the greatest energy demand, secondly followed by Athens's hot Mediterranean climate, which has a comparable performance.

Conversely, in New York's humid subtropical climate, the typologies of VF, R and VF+R show had the lowest annual energy consumption making these models

ideally suited to these climatic conditions. Among the investigated typologies and climates, the SQR shape consistently outperforms the others in terms of energy efficiency. It continually displays the lowest energy requirements across several situations, including New York, Singapore and Athens, nonetheless, its performance alternates best according to the typologies in different weather scenarios. ATR morphology, on the other hand, has the greatest energy needs, making it the least efficient alternative for all climate settings. Moreover, the LM morphology also outperforms in terms of energy performance, especially in the Singapore_VF and Athens_VF and other situations. The main highlights of the results on energy performance for each climate and typology are as follows:

Table 12. Best-to-Worst Performing morphologies.

	Climate_Type	Best Performing	Worst Performing
N	New York_VF	TM, LM, CRS	ATR, UM, HM
	New York_R	LM, CIR, SQR	ATR, HM, CRS
	New York_VF+R	LM, CIR, SQR	ATR, UM, HM
S	Singapore_VF	SQR, CIR	ATR, UM, LM, HM
	Singapore_R	SQR, LM	ATR
	Singapore_VF+R	SQR, LM, ZM	ATR
A	Athens_VF	SQR, TM, REC	ATR, HM, UM
	Athens_R	SQR,LM	ATR, HM,UM,CRS
	Athens_VF+R	SQR,LM	ATR, HM,UM

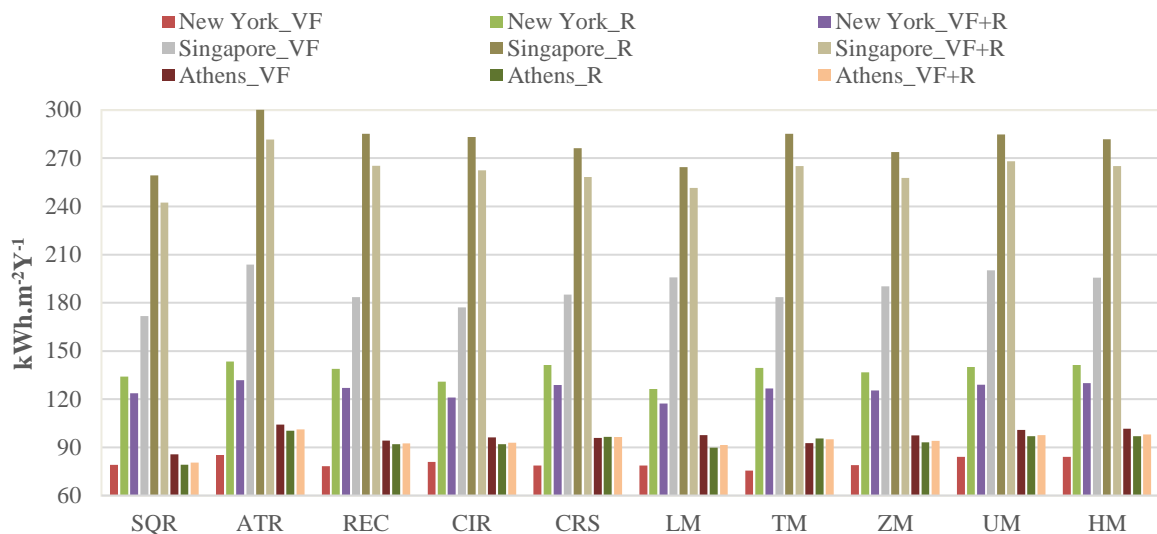


Figure 58. Comparison of annual simulated energy consumption (kWh.m-2Y-1) for three specific climatic settings for three typologies.

The findings highlight the need of taking unique morphology and climate into account when aiming for maximum energy efficiency in architectural design.

According to the suitability gradient presented in **Figure 59**, and the findings of the simulation scenarios, the ATR typology is overall not well-suited for areas with climates similar to Singapore and Athens, or New York. However, may be considered better performing for the humid subtropical climate of VF typology since it's a cooler climate and needs less energy consumed for cooling. Typologies with greater Surface-to-Volume ratios (S/V) and lower compactness, such as HM, UM, and CRS are commonly less appropriate in all three climates. On the contrary, SQR and LM outperform consistently all other morphologies.

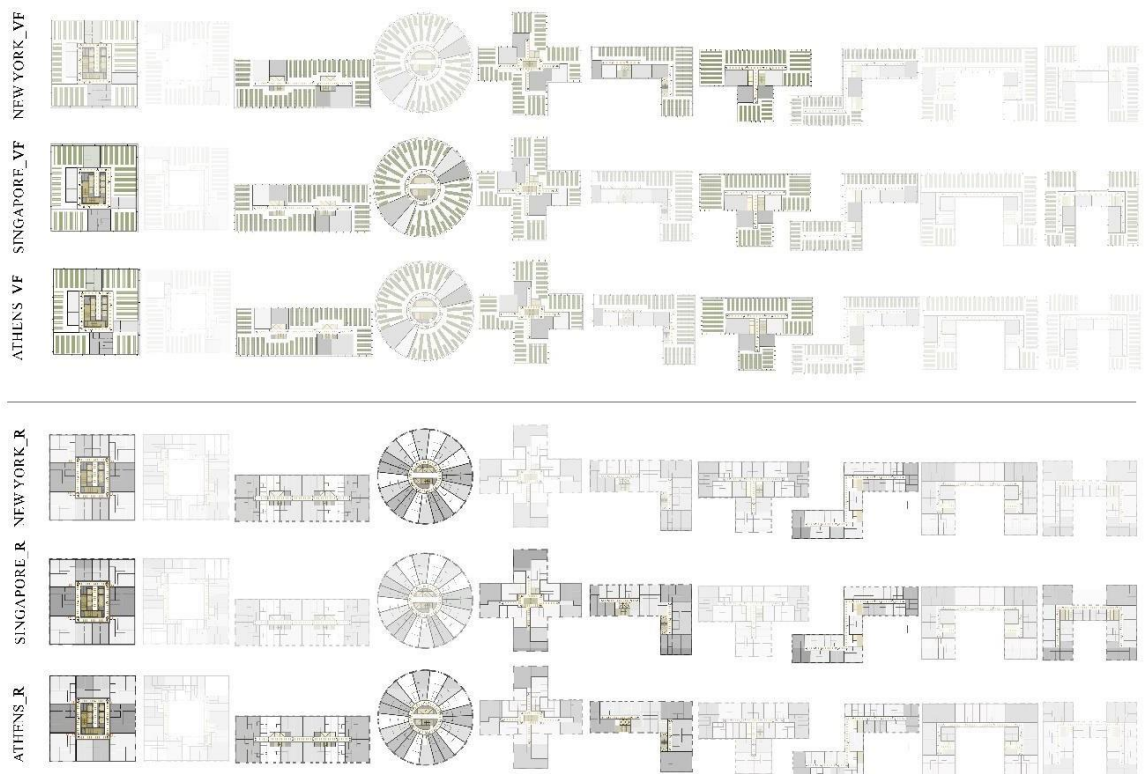


Figure 59. Suitability gradient of the studied morphologies across their respective typologies in three climatic contexts.

Table 13 displays the total efficacy (%) of morphologies in different climates. New York has the greatest optimization value of +5.8 % (LM_R) compared to the other morphologies in this setting which is linked to the low cooling demands for humid subtropical climates. Furthermore while considering morphology choices, Singapore has the highest energy consumption and thus least effectiveness percentage values. Such an occurrence can be linked to the year-round high temperatures, which result in large cooling demands across all typologies. It is worth noting that SQR morphology shows the best performance for the climate of Singapore and Athens with LM as the second-best scenario for all settings.

Table 13. Total Morphology Effectiveness (%).

	New York	Singapore	Athens
SQR _{vf}	–	–	–
ATR _{vf}	-6.9	-18.8	-21.6
REC _{vf}	1.8	-6.9	-10.0
CIR _{vf}	-1.4	-3.2	-12.3
CRS _{vf}	1.3	-7.8	-11.8
LM _{vf}	1.3	-14.1	-14.0
TM _{vf}	5.3	-6.9	-8.3
ZM _{vf}	0.9	-10.8	-13.7
UM _{vf}	-5.4	-16.6	-17.8
HM _{vf}	-5.4	-14.0	-18.5
SQR _R	–	–	–
ATR _R	-7.0	-16.1	-26.6
REC _R	-3.5	-10.0	-16.0
CIR _R	2.4	-9.3	-16.0
CRS _R	-5.3	-6.6	-21.8
LM _R	5.8	-2.0	-13.3
TM _R	-3.9	-10.0	-20.7
ZM _R	-1.8	-5.6	-17.5
UM _R	-4.4	-9.8	-22.2
HM _R	-5.3	-8.7	-22.4

SQR_{VF+R}	–	–	–
ATR_{VF+R}	-6.7	-16.3	-25.6
REC_{VF+R}	-2.7	-9.5	-14.8
CIR_{VF+R}	2.1	-8.3	-15.3
CRS_{VF+R}	-4.3	-6.6	-19.7
LM_{VF+R}	5.1	-3.8	-13.4
TM_{VF+R}	-2.5	-9.4	-18.1
ZM_{VF+R}	-1.5	-6.4	-16.7
UM_{VF+R}	-4.4	-10.6	-21.3
HM_{VF+R}	-5.2	-9.4	-21.6

5.5 Future Prediction Scenarios

5.5.1 Climate of New York RCP 8.5

To evaluate the potential energy efficiency for future predictions (2100) of various high-rise structures and vertical farming typologies under the peculiar climatic conditions anticipated for New York, a thorough analysis was conducted.

5.5.1.1 Energy Performance

The following data shown in **Figure 60** depict the heating energy consumption for the typologies VF (vertical farming), R (residential), and VF+R (integrated) in both C-contemporary and F-future scenarios. According to the estimations, there will be a significant decrease across all morphologies and their associated typologies. As to the VF typology, the F-future scenario's heating energy usage (7.44 kWh.m-2Y-1) is significantly lower than the C-contemporary scenario's (17.61 kWh.m-2Y-1), by about 57.83%. Similarly, the R typology exhibits a large reduction of roughly 55.38% and the VF+R typology 55.43% in heating energy consumption in contrast to the C-contemporary scenario (103.27 kWh.m-2Y-1, 86.72 kWh.m-2Y-1 respectively).

Conversely, **Figure 61** depicts the cooling results in which there is an increase of 41.5%, 70.2%, and 64.6% for VF, R and VF+R accordingly for future scenarios.

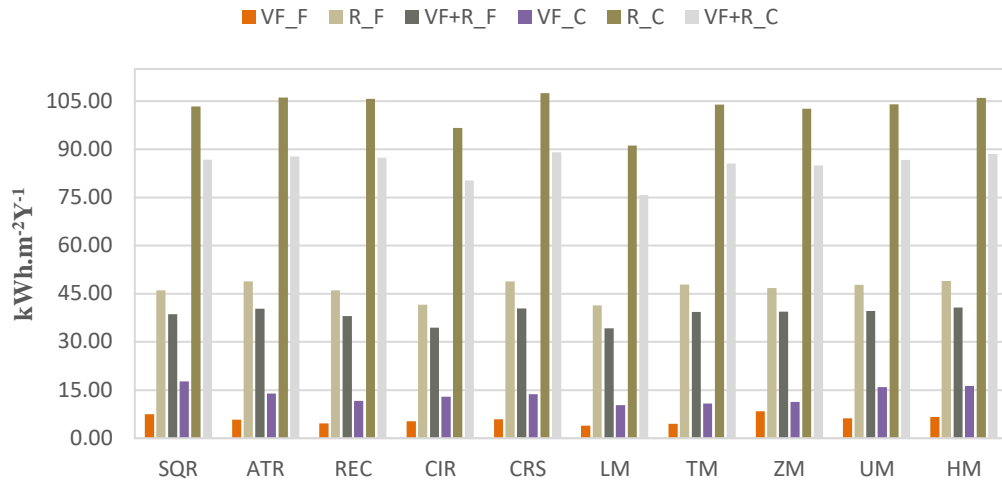


Figure 60. Comparison of Annual Heating energy consumption (kWh.m-2Y-1) for future(F) and contemporary(C) predictions of VF, R and VF+R and their associated morphologies in New York.

Table 14 displays the total efficacy (%) of morphologies for this climate setting. What is interesting to mention is that the morphological suitability gap across best-to-worst morphologies does increase by at least 30% for the following years. If the LM did outperform the rest in contemporary scenarios, in future prediction SQR seems to be the most resilient followed secondly by LM morphology, and ATR as the ultimate worst case. SQR has the greatest optimization value of +14.4% as compared to LM with 5.8% for contemporary estimates.

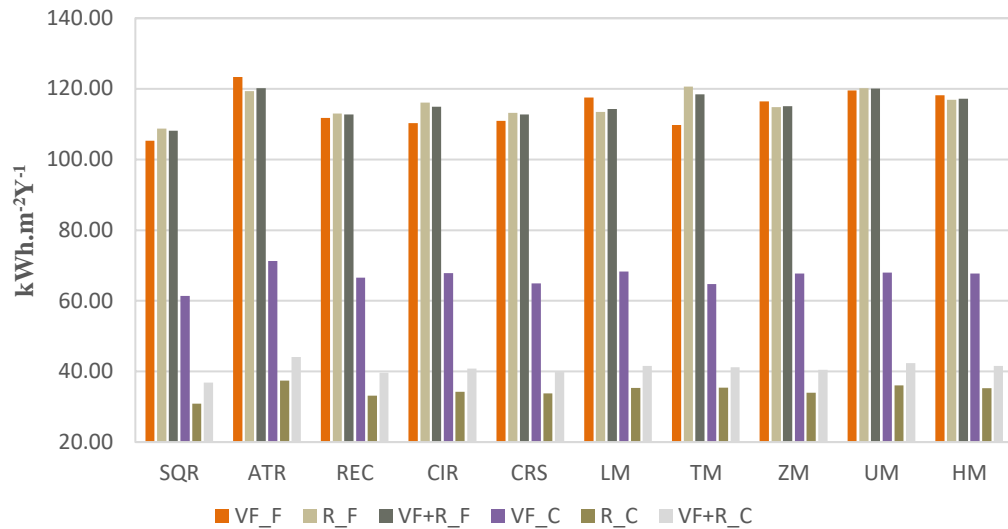


Figure 61. Comparison of Annual Cooling energy consumption (kWh.m⁻²Y⁻¹) for future(F) and contemporary(C) predictions of VF, R and VF+R and their associated morphologies in New York.

Table 14 displays the total efficacy (%) of morphologies for this climate setting. What is interesting to mention is that the morphological suitability gap across best–to–worst morphologies does increase by at least 30% for the following years. If the LM did outperform the rest in contemporary scenarios, in future prediction SQR seems to be the most resilient followed secondly by LM morphology, and ATR as the ultimate worst case. SQR has the greatest optimization value of +14.4% as compared to LM with 5.8% for contemporary estimates.

Table 14. Future prediction simulation results obtained for all the scenarios in the climate of New York.

Scenarios	Annual Heating Demand			Annual Cooling Demand			Annual Energy Demand		
	Total Heating [kWh]	Heating/conditioned area [kWh/m ²]	Morphology effectiveness [%]	Total Cooling [kWh]	Cooling/conditioned area [kWh/m ²]	Morphology effectiveness [%]	Total Energy [kWh]	Total Energy conditioned area [kWh/m ²]	Morphology effectiveness [%]
SQR _{vf}	47264.4	7.4	–	668870.2	105.3	–	716134.6	112.8	–
ATR _{vf}	36763	5.7	22.9	789447.6	123.3	-17.1	826210.5	129.1	-14.4
REC _{vf}	29086.2	4.5	38.9	714978.9	111.8	-6.1	744065	116.3	-3.1
CIR _{vf}	34270.7	5.3	28.9	714150	110.3	-4.7	748420.7	115.6	-2.5
CRS _{vf}	38011.9	5.9	20.5	712272.9	110.9	-5.3	750284.8	116.8	-3.6
LM _{vf}	24187.7	3.9	47.6	728709.1	117.5	-11.6	752896.8	121.4	-7.7
TM _{vf}	29307.2	4.5	39.3	711933.4	109.7	-4.2	741240.6	114.2	-1.3
ZM _{vf}	51805.8	8.4	-12.2	722436	116.5	-10.6	774241.7	124.8	-10.7
UM _{vf}	39569.8	6.2	16.4	760138.7	119.5	-13.4	799708.5	125.7	-11.5
HM _{vf}	41307.1	6.6	11.8	743177.7	118.2	-12.2	784484.8	124.8	-10.6
SQR _R	76399.6	46.1	–	180366.3	108.8	–	256766	154.9	–
ATR _R	78806.2	48.8	-6	192680	119.4	-9.7	271486.2	168.2	-8.6
REC _R	76112.3	46.1	0	186736	113	-3.9	262848.3	159.1	-2.7
CIR _R	68910.3	41.5	9.9	192589.6	116.1	-6.7	261499.8	157.7	-1.8
CRS _R	80217.8	48.9	-6	185848.4	113.2	-4.1	266066.2	162.1	-4.6
LM _R	68434	41.3	10.3	187960	113.5	-4.3	256394	154.8	0
TM _R	78847.9	47.8	-3.7	198882.1	120.6	-10.8	277729.9	168.4	-8.7
ZM _R	75867.9	46.7	-1.4	186383	114.8	-5.5	262250.9	161.6	-4.3
UM _R	77450.7	47.7	-3.6	195027.6	120.2	-10.5	272478.3	168	-8.4
HM _R	79584.1	48.9	-6.2	190265.9	117	-7.5	269850	165.9	-7.1
SQR _{VF+R}	1269658.71	38.6	–	3554731.412	108.1	–	4824390.1	146.8	–
ATR _{VF+R}	1297662.628	40.3	-4.3	3872327.808	120.2	-11.1	5169990.4	160.4	-9.3
REC _{VF+R}	1246882.727	38	1.7	3702755.378	112.8	-4.3	4949638.1	150.8	-2.7
CIR _{VF+R}	1136835.107	34.4	10.8	3795582.932	115	-6.3	4932418	149.4	-1.8
CRS _{VF+R}	1321497.02	40.4	-4.7	3685846.774	112.8	-4.3	5007343.8	153.2	-4.4
LM _{VF+R}	1119131.736	34.2	11.4	3736069.035	114.3	-5.7	4855200.8	148.5	-1.2
TM _{VF+R}	1290872.968	39.3	-1.7	3894046.391	118.5	-9.5	5184919.4	157.7	-7.5
ZM _{VF+R}	1265692.698	39.3	-1.8	3704563.424	115.1	-6.5	4970256.1	154.5	-5.3
UM _{VF+R}	1278780.935	39.6	-2.4	3880580.817	120.1	-11	5159361.8	159.7	-8.8
HM _{VF+R}	1314652.543	40.7	-5.3	3787432.741	117.2	-8.4	5102085.3	157.9	-7.6

5.5.2 Climate of Singapore RCP 8.5

To evaluate the potential energy efficiency for future predictions (2100) of various high-rise structures and vertical farming typologies under the peculiar climatic

conditions anticipated for Singapore, a thorough analysis was conducted.

5.5.2.1 Energy Performance

The following data shown in **Figure 62** depicts the cooling energy consumption for the typologies VF (vertical farming), R (residential), and VF+R (integrated) in both C-contemporary and F-future scenarios. It is noteworthy to mention again that there are to heating demands in this climate as per previous estimates. According to the calculations, there will be a significant increase in cooling demands across all morphologies and their associated typologies. The average cooling energy consumption in the F-future scenario of the VF typologies (260.8 kWh.m⁻²Y⁻¹) is around 27.7% greater than in the C-contemporary scenario. Similar to the C-contemporary scenario, the VF+R typology shows a significant rise in energy use of about 35.6% (406.6kWh.m⁻²Y⁻¹). In comparison to the C-contemporary scenario (279.5 kWh.m⁻²Y⁻¹), the F-future scenario (441.9 kWh.m⁻²Y⁻¹) for the R typology exhibits a considerable rise of around 36.7 %.

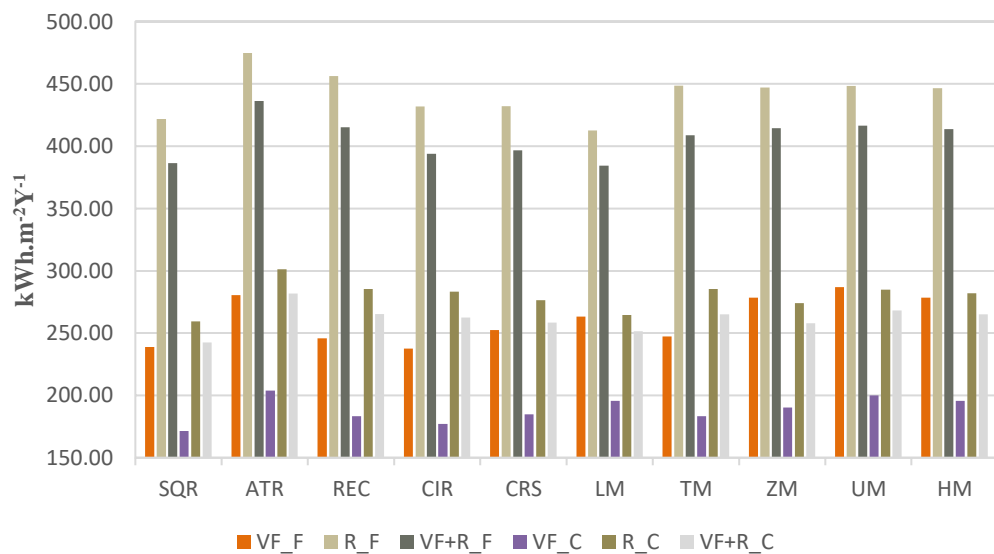


Figure 62. Comparison of Annual Cooling energy consumption (kWh.m⁻²Y⁻¹) for future(F) and contemporary(C) predictions of VF, R and VF+R and their associated morphologies in Singapore.

Table 15 displays the total efficacy (%) of morphologies for this climate setting. It is noteworthy to mention that the morphological suitability gap across best-to-worst morphologies do increase by at least 46.8% for the following years in this climate setting. There is also a change in the morphological suitability effectiveness percentage between morphologies. If the SQR did outperform the rest in contemporary scenarios, in future prediction LM seems to be slightly more resilient followed secondly and ATR in the ultimate worst case. LM has an energy efficiency of 2.2% more than SQR for future estimates.

Table 15. Future prediction simulation results obtained for all the scenarios in the climate of Singapore.

Scenario	Annual Heating Demand			Annual Cooling Demand			Annual Energy Demand		
	Total Heating [kWh]	Heating/conditioned area [kWh/m ²]	Morphology effectiveness [%]	Total Cooling [kWh]	Cooling/conditioned area [kWh/m ²]	Morphology effectiveness [%]	Total Energy [kWh]	Total Energy conditioned area [kWh/m ²]	Morphology effectiveness [%]
SQR _{vf}	0	0	–	1516767.8	238.9	–	1516767.8	238.9	–
ATR _{vf}	0	0	0	1795371.4	280.5	-17.4	1795371.4	280.5	-17.4
REC _{vf}	0	0	0	1571758.8	245.7	-2.8	1571758.8	245.7	-2.8
CIR _{vf}	0	0	0	1536855.7	237.4	0.6	1536855.7	237.4	0.6
CRS _{vf}	0	0	0	1620989.4	252.4	-5.7	1620989.4	252.4	-5.7
LM _{vf}	0	0	0	1631786.9	263.2	-10.2	1631786.9	263.2	-10.2
TM _{vf}	0	0	0	1603561.1	247.2	-3.5	1603561.1	247.2	-3.5
ZM _{vf}	0	0	0	1726803.5	278.4	-16.5	1726803.5	278.4	-16.5
UM _{vf}	0	0	0	1823815.4	286.7	-20	1823815.4	286.7	-20
HM _{vf}	0	0	0	1750258.5	278.4	-16.5	1750258.5	278.4	-16.5
SQR _R	0	0	–	699178.7	421.8	–	699178.7	421.8	–
ATR _R	0	0	0	766311	474.9	-12.6	766311	474.9	-12.6
REC _R	0	0	0	753647.9	456.2	-8.2	753647.9	456.2	-8.2
CIR _R	0	0	0	716377.1	431.9	-2.4	716377.1	431.9	-2.4
CRS _R	0	0	0	709320.3	432.1	-2.4	709320.3	432.1	-2.4
LM _R	0	0	0	683375.3	412.7	2.2	683375.3	412.7	2.2
TM _R	0	0	0	739721.2	448.6	-6.3	739721.2	448.6	-6.3
ZM _R	0	0	0	725635	447	-6	725635	447	-6
UM _R	0	0	0	727367.2	448.4	-6.3	727367.2	448.4	-6.3
HM _R	0	0	0	726182.4	446.4	-5.8	726182.4	446.4	-5.8
SQR _{VF+R}	0	0	–	12703627. ₃	386.5	–	12703627. ₃	386.5	–
ATR _{VF+R}	0	0	0	14056347. ₄	436.2	-12.9	14056347. ₄	436.2	-12.9
REC _{VF+R}	0	0	0	13630125. ₇	415.2	-7.4	13630125. ₇	415.2	-7.4

CIR _{VF+R}	0	0	0	12998888. ₈	393.8	-1.9	12998888. ₈	393.8	-1.9
CRS _{VF+R}	0	0	0	12970113. ₉	396.8	-2.7	12970113. ₉	396.8	-2.7
LM _{VF+R}	0	0	0	12565791. ₂	384.4	0.5	12565791. ₂	384.4	0.5
TM _{VF+R}	0	0	0	13439100. ₆	408.8	-5.8	13439100. ₆	408.8	-5.8
ZM _{VF+R}	0	0	0	13336963	414.5	-7.3	13336963	414.5	-7.3
UM _{VF+R}	0	0	0	13461690. ₁	416.6	-7.8	13461690. ₁	416.6	-7.8
HM _{VF+R}	0	0	0	13369176. ₁	413.7	-7.1	13369176. ₁	413.7	-7.1

5.5.3 Climate of Athens RCP 8.5

To evaluate the potential energy efficiency for future predictions (2100) of various high-rise structures and vertical farming typologies under the peculiar climatic conditions anticipated for Athens, a thorough analysis was conducted.

5.5.3.1 Energy Performance

The following data shown in *Figure 63* depict the heating energy consumption for the typologies VF (vertical farming), R (residential), and VF+R (integrated) in both C-contemporary and F-future scenarios. Based on the estimates there will be a significant decrease in energy demand values by the year 2100. Regarding

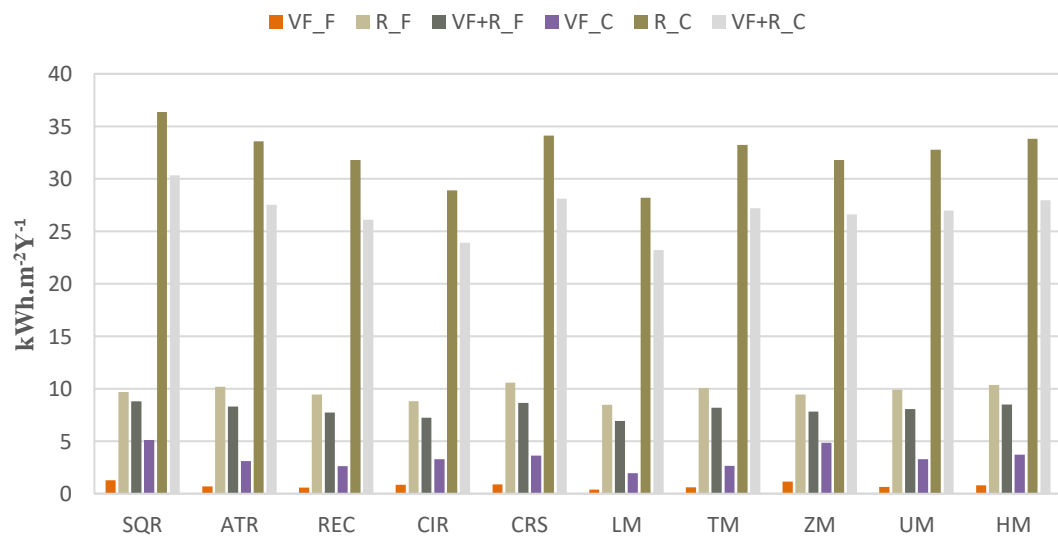


Figure 63. Comparison of Annual Heating energy consumption (kWh.m-2Y-1) for future(F) and contemporary(C) predictions of VF, R and VF+R and their associated morphologies in Athens.

VF typology, the F-future scenario's heating energy usage (0.077 kWh.m-2Y-1) is a lot lower than the C-contemporary scenario's (3.41 kWh.m-2Y-1), by about 77.4%, although such amounts are not significant consummation rates.

Similarly, the R typology exhibits a large reduction of roughly 70.1% and the VF+R typology 69.8%. Conversely, **Figure 64** depicts the cooling demands in which there is an average increase of 34.4%, 56%, and 59.2% for VF, R and VF+R accordingly for future scenarios.

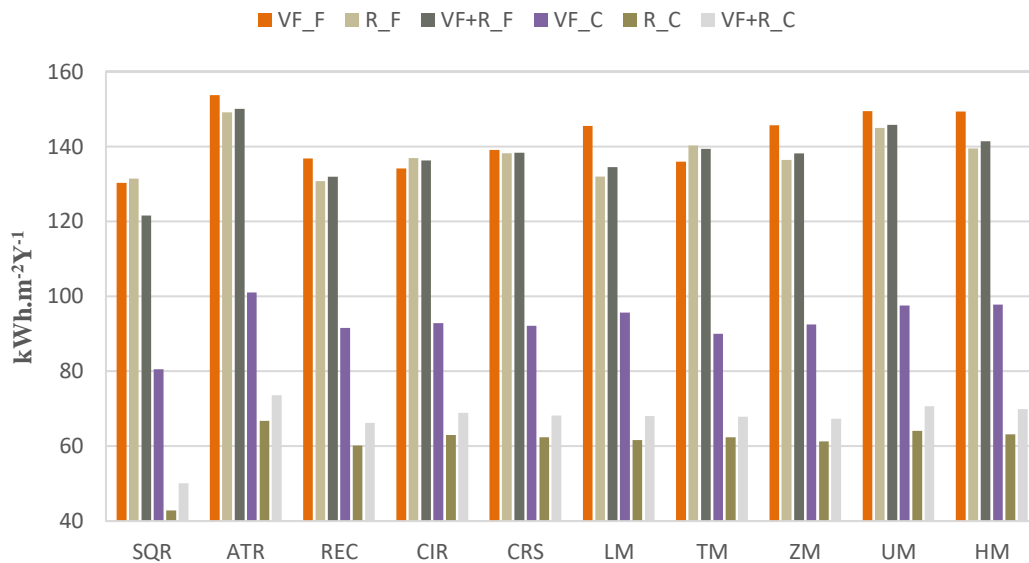


Figure 64. Comparison of Annual Cooling energy consumption (kWh.m-2Y-1) for future(F) and contemporary(C) predictions of VF, R and VF+R and their associated morphologies in Athens.

Table 16 displays the total efficacy (%) of morphologies for this climate setting. The morphological suitability gap across best-to-worst morphologies does increase by at least 23.1% in between the morphologies from contemporary to future scenarios. There is also a change in the morphological suitability effectiveness percentage

between morphologies. According to the estimates if SQR was priorly the best performing in this climate too, for future prediction the priority as the best scenario has surprisingly shifted to REC morphology for the R_Residential typology, nevertheless, SQR continues to provide the best efficiency overall of 17.3% more than other morphologies.

Table 16. Future prediction simulation results obtained for all the scenarios in the climate of Athens.

Scenarios	Annual Heating Demand			Annual Cooling Demand			Annual Energy Demand		
	Total Heating [kWh]	Heating/conditioned area [kWh/m ²]	Morphology effectiveness [%]	Total Cooling [kWh]	Cooling/conditioned area [kWh/m ²]	Morphology effectiveness [%]	Total Energy [kWh]	Total Energy conditioned area [kWh/m ²]	Morphology effectiveness [%]
SQR _{vf}	8013.9	1.3	–	827527.4	130.3	–	835541.3	131.6	–
ATR _{vf}	4406.8	0.7	45.5	983826.1	153.7	-17.9	988232.9	154.4	-17.3
REC _{vf}	3670	0.6	54.5	875106.2	136.8	-5	878776.2	137.4	-4.4
CIR _{vf}	5498	0.8	32.7	868526.7	134.2	-3	874024.7	135	-2.6
CRS _{vf}	5666.7	0.9	30.1	893455.8	139.1	-6.8	899122.4	140	-6.4
LM _{vf}	2357.5	0.4	69.9	902108.6	145.5	-11.6	904466.1	145.9	-10.9
TM _{vf}	3954.2	0.6	51.7	881940	135.9	-4.3	885894.1	136.5	-3.8
ZM _{vf}	7164.2	1.2	8.5	903855.4	145.7	-11.8	911019.6	146.9	-11.6
UM _{vf}	3991.7	0.6	50.3	950327.6	149.4	-14.6	954319.3	150	-14
HM _{vf}	4808.8	0.8	39.4	939162.4	149.4	-14.6	943971.2	150.1	-14.1
SQR _R	16035.8	9.7	–	217843.7	131.4	–	233879.6	141.1	–
ATR _R	16439.4	10.2	-5.3	240669.8	149.1	-13.5	257109.2	159.3	-12.9
REC _R	15614.1	9.5	2.3	215992.9	130.7	0.5	231607	140.2	0.6
CIR _R	14619.3	8.8	8.9	227003.1	136.9	-4.1	241622.3	145.7	-3.2
CRS _R	17333.5	10.6	-9.2	226789.1	138.2	-5.1	244122.6	148.7	-5.4
LM _R	14000.6	8.5	12.6	218467.9	131.9	-0.4	232468.4	140.4	0.5
TM _R	16568	10	-3.9	231269.4	140.2	-6.7	247837.4	150.3	-6.5
ZM _R	15311.6	9.4	2.5	221319.1	136.3	-3.7	236630.7	145.8	-3.3
UM _R	16039.3	9.9	-2.2	235129.9	144.9	-10.3	251169.2	154.8	-9.7
HM _R	16846.7	10.4	-7.1	226888.1	139.5	-6.1	243734.8	149.8	-6.2
SQR _{VF+R}	264587.2	8	–	4313027.2	131.2	–	4577614.4	139.3	–
ATR _{VF+R}	267436.9	8.3	-3.1	4834543.2	150	-14.3	5101980.1	158.3	-13.7
REC _{VF+R}	253495.4	7.7	4.1	4330992.2	131.9	-0.5	4584487.6	139.6	-0.3
CIR _{VF+R}	239406.1	7.3	9.9	4500575.5	136.3	-3.9	4739981.7	143.6	-3.1
CRS _{VF+R}	283003	8.7	-7.6	4522080.9	138.4	-5.4	4805083.9	147	-5.6
LM _{VF+R}	226366.6	6.9	14	4397594.5	134.5	-2.5	4623961	141.4	-1.6

TM _{VF+R}	269043	8.2	-1.7	4582250.1	139.4	-6.2	4851293	147.6	-6
ZM _{VF+R}	252150.2	7.8	2.6	4444961.3	138.2	-5.3	4697111.5	146	-4.8
UM _{VF+R}	260621.1	8.1	-0.2	4712406.1	145.8	-11.1	4973027.2	153.9	-10.5
HM _{VF+R}	274355.3	8.5	-5.5	4569372.3	141.4	-7.8	4843727.6	149.9	-7.6

5.5.4 Comparison of Future and Contemporary Results

It is crucial to take into account the percentages of these values concerning one another when comparing the annual total energy consumption values for the studied typologies in New York (NY), Singapore (S), and Athens (A) for F-future scenarios as opposed to C-Contemporary ones. VF_{NY_F} is 33.2% higher in energy demand than in the contemporary climate. Furthermore, 15.3% and 18.6% are the comparable values for energy consumption, indicated by the R_{NY_} and VF_{NY_F} respectively. Moving on to Singapore, the VF_{S_F} representation of this climate's yearly total energy consumption reads 53.9% over the contemporary ones. R_{S_F} and VF+R_F on the other hand result in 36.7% and 35.6%. A total energy consumption figure of 35.6% for Singapore is produced by combining VF_S and R_S.

Finally based on the examinations for Athens, VF_{A_F}, R_{A_F}, and VF+R_{A_F} yield 32.3, 36.8, and 35.6 respectively. Overall, the future climate might be affected by a rise in energy consumption. Higher values of VF in future scenarios serve as an indicator of this rise. In comparison to Singapore, there are smaller percentage variances in NY and Athens. The results in *Figure 65* indicate that major consideration must be given to the implementation of energy-efficient measures, and sustainable practices to meet future forecasts for energy consumption in these climates. The disparities that have been found highlight the necessity of adaptation and mitigation techniques to successfully manage the rising energy demand and tackle climate change issues.

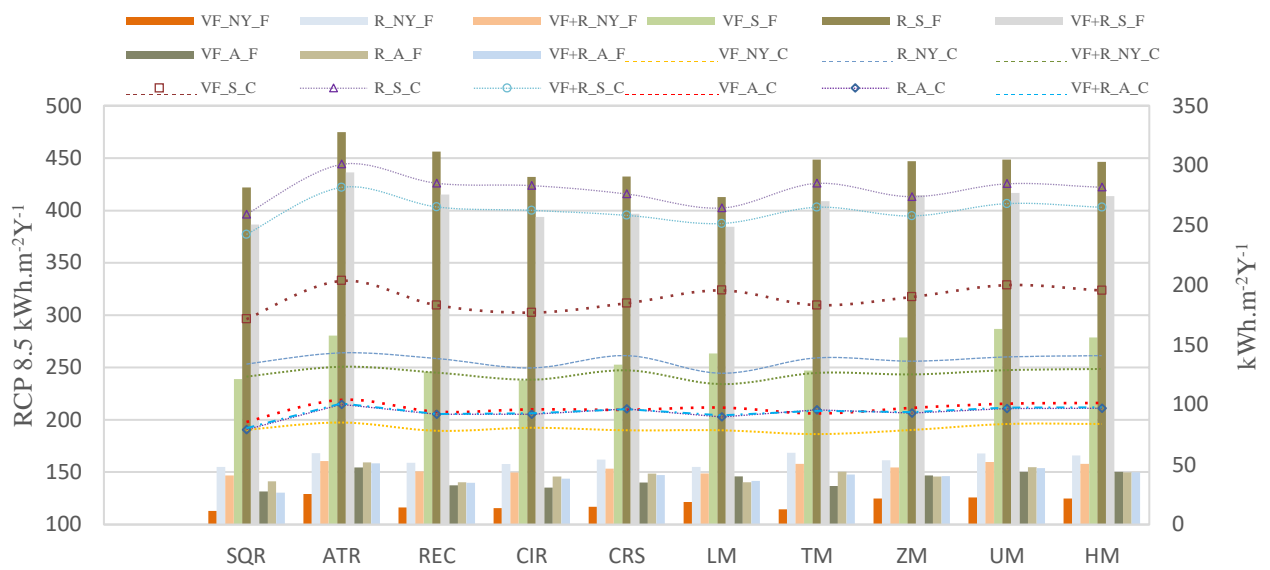


Figure 65. Future Prediction and Contemporary Results Comparison.

5.6 Cost Estimations

5.6.1 Background

Vertical farming has emerged as a possible method for long-term food production, particularly in urban regions with limited land conditions. This novel method involves planting crops in vertically stacked layers or shelves, maximizing vertical space use. Vertical farms attempt to improve yields while reducing resource consumption and environmental effect by employing sophisticated technology and optimum farming techniques. Nevertheless, the profitability of these prototype models must be explored to determine the viability of these vertical farming systems in meeting food production targets. This investigation looks at the economic aspect, with an emphasis on yearly yields, to understand their potential of earning profits. To acquire a quantitative grasp of their prospective food production capacity, simple methodologies are used.

5.6.2 Concept Ideation

5.6.2.1 One-Square meter Growing Structure

A rack design based on the notion of generating food for a one-square-meter area is designed to enable correct basic calculations and establish the entire output potential of a food-growing structure. By adhering to this notion, the capacity of the rack arrangement may be used to predict overall production. The rack's design takes into account the morphological characteristics of the building models employed, allowing for an evaluation of their relative area capacities. The selected growth method for the food production system will be restricted to a hydroponic system due to its acknowledged benefits in terms of cost-effectiveness and ease of initial investment.

As illustrated in *Figure 66* the prototype's structural design includes a rectangular model with 5 distinct levels of vertical growth area. Each level is offset by 60 cm from the next, allowing for adequate sunlight penetration and sufficient area for the development of crops of varied heights.

Taller crops may be accommodated at the highest level, which capitalizes on available vertical space and maximizes light exposure for maximum growth. The dimensions of the structure are derived from considerations based on the ISO 1006 building construction basic module.

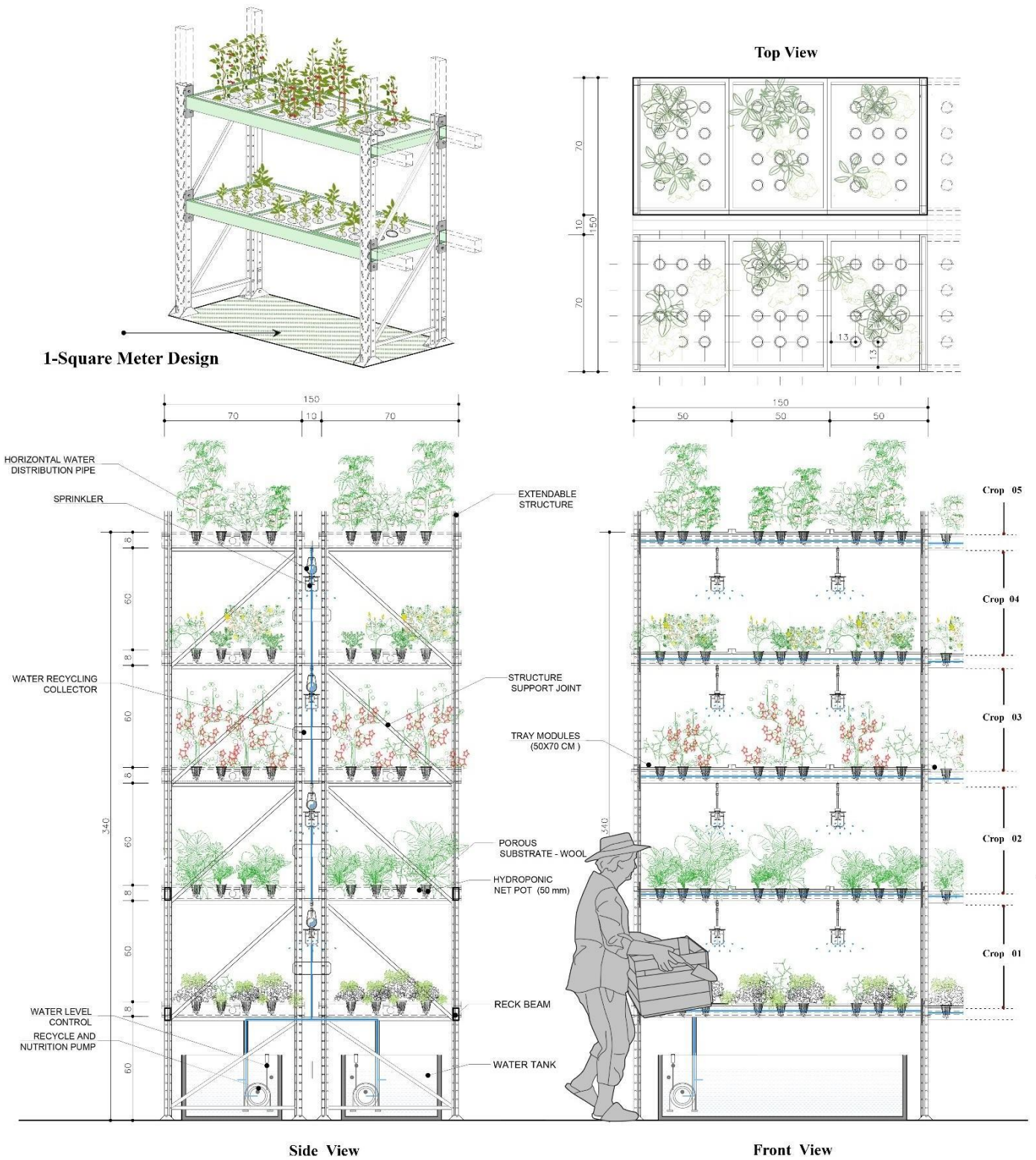


Figure 66. One Square Meter System Rack Details.

5.6.3.1 Design Specifications

The vertical farming model has four stories, each measuring four meters in height. The farming floor of each morphology comprises an approximate total area of 1215 square meters. While the overall area covered by the farming floor stays consistent across all morphologies, crop production capacity will vary depending on the number of 1 square meter unit systems that each morphology configuration can accommodate, taking into account fundamental design needs and distance requirements. The ISO 1006 building construction basic module recommends a minimum horizontal spacing of 90 cm between each rack system. For design purposes, the horizontal distance is kept at 120 cm and a minimum of 150 cm for the main aisles. This spacing allows workers to navigate easily between the racks while doing important duties such as planting, harvesting, trimming, and maintenance. It additionally permits the flow of equipment such as carts or trolleys.

5.6.4.1 Space Categorisation

The design of the CEA (Controlled Environment Agriculture) vertical farming prototype as shown in *Figure 67*. contains five fundamental zones, each responding to distinct demands closely linked to the farming process's output:

1. ***Crop Production Area (70 % of total space)***: On each level of the vertical farm, this is the principal space dedicated solely to crop production(1215 sqm).
2. ***Water and Fertilizer Area***: This area of around 90 sqm is critical for giving water and nutrients to plants. It contains germination chambers and nurseries, as well as facilities for the early phases of seed sprouting. When the seeds reach a size of 2-3 centimeters, they are moved to the main production area to continue growing.
3. ***Harvesting and packing***: After the crops have fully matured, they are harvested

and packaged when ready for delivery to customers. (90 sqm)

4. **Storage and Refrigerator room:** A separate storage and refrigerator room is incorporated in the layout to maintain the quality and retain the bio characteristics of the produce. To increase the shelf life of harvested crops, this area provides optimal conditions, including temperature control and storage options(125 sqm).
5. **Administration Area:** This area comprises the working labor as well as the necessary places for administrative tasks. It provides workforce amenities such as washing areas and monitoring spaces where personnel can undertake farm management, crop monitoring, and quality control operations (70 sqm).









LEGEND				
	Non-Edible Plants -Overhang balcony	1. Crop Production Area	1215 m²	4. Storage and Refregerator 125 m²
	1 Square Meter System Rack	2. Harvest and Packing	90 m²	- Germination Chamber - Sowing Room - Main Storage - Refregerator Rooms
	Growing Crops	- Main Packing Room - Fresh refreerator storage - Temporary storage - Washing station		5. Water and Nutritions 90 m²
	Hydroponic watering system	3. Administration	70 m²	- Water Supply Room - Nutriton Room - Equipment Room
	Crop Sprinklers	- Main Office Room - Control-Monitoring Room		
	Water Pump Supplier			Total Floor Area 1800 m²

Figure 67. Typical vertical Farming Floor Plan.

5.6.5.1 Selected Crops

Vertical farming offers the potential to develop a broad variety of crops if certain conditions are met. The fundamental goal of this research is to look at the reasoning behind the original design of vertical farming on numerous levels, which allows for increased productivity, improved crop management efficiency, and, most importantly, the cultivation of a varied array of crops. As a result, the modular system rack with five levels allows for the simultaneous development of different crops on each level.

To maximize natural light use and facilitate the cultivation of a wide range of crops, the temperature set points of each floor are strategically established depending on crop production requirements. Temperature settings are modified based on the temperature range required for optimal crop development. According to this strategy, the upper levels of the vertical farming structure, which get higher solar gains and enhanced light intensity, are earmarked for crops that flourish in well-lit surroundings. Lower levels, on the contrary, which receive less direct sunshine and milder temperatures, are allocated for crops that are more light tolerant and thrive in cooler growth conditions as shown in **Figure 68**.

Table 17 demonstrates general information about the majority of crops that can be found in the global market as well as their specific characteristics for growth such as optimal temperature for growth, height, storing days, cultivation, and availability of different categories of produce.

Table 17. Crop timeline monthly data of different categories and temperature growth.

Crop name	Winter			Spring			Summer			Fall			Avg. Height (cm)	Temp. Range (°C)	Avg. Temp (°C)	Moisture (%)	Convent. Harvest (Days)	VF Harvest (Days)	Conv. Yield (kg/m2)	Max storage
	Jan	Feb	Mar	Apr	May	Jun	Jul	Aug	Sep	Oct	Nov	Dec								
Leafy Greens																				
Lettuce													15-30 cm	4-30°C	18°C	95-98	40-80	28-40	3-4	7-10 days
Spinach													30-35 cm	5-25°C	18°C	90-95	40-50	28-35	3-5	5-7 days
Kale													60-90 cm	15-25°C	20°C	90-95	50-70	40-60	3-5	7-10 days
Arugula													20-30 cm	10-25°C	18°C	90-95	30-40	21-28	3-5	3-5 days
Chard													30-50 cm	10-25°C	18°C	90-95	50-60	35-50	3-4	5-7 days
Mustard													20-50 cm	10-30°C	20°C	90-95	30-40	21-28	3-4	3-5 days
Collard													60-90 cm	10-30°C	20°C	90-95	60-75	45-60	3-4	5-7 days
Watercress													5-10 cm	5-25°C	15-20°C	90-95	30-45	21-28	4-5	3-5 days
Herbs																				
Basil													15-30 cm	4-30°C	18°C	95-98	40-80	28-40	4-6	7-10 days
Mint													30-35 cm	5-25°C	18°C	90-95	40-50	28-35	4-6	5-7 days
Oregano													60-90 cm	15-25°C	20°C	90-95	50-70	40-60	4-5	7-10 days
Thyme													20-30 cm	10-25°C	18°C	90-95	30-40	21-28	4-5	3-5 days
Parsley													30-50 cm	10-25°C	18°C	90-95	50-60	35-50	3-4	5-7 days
Cilantro													20-50 cm	10-30°C	20°C	90-95	30-40	21-28	3-4	3-5 days
Sage													60-90 cm	10-30°C	20°C	90-95	60-75	45-60	3-4	5-7 days
Rosemary													5-10 cm	5-25°C	15-20°C	90-95	30-45	21-28	3-4	3-5 days
Dill													60-150 cm	10-30°C	20°C	70-80	70-90	30-50	3-4	5-7 days
Microgreens																				
Radish													5-30	10-25°C	18°C	80-90	20-30	12-20.	2-3	2-3 days
Broccoli													60-90	10-25°C	20°C	70-80	60-100	35-50	2-3	7-10 days
Sunflower													180-300	15-30 °C	20 °C	60-70	80-120	60-80	2-3	3-4 days
Pea													30-120	4-25 °C	18°C	70-80	60-80	30-40	2-3	5-7 days
Wheatgrass													10-20	15-25	20°C	70-80	45-117	7-10.	2-3	5-7 days
Beet													30-60	7-27 °C	20°C	80-90	50-70	40-50	2-3	2-3 days
Mustard													20-30	10-30°C	20°C	80-90	20-30	12-20.	2-3	2-3 days
Vegetables																				
Tomatoes													100-300	15-35°C	21-24	60-70	60-120	50-70	5-7	14-21days
Peppers													45-120	18-30°C	24-27	60-80	60-90	50-60	4-6	14-21 days
Cucumbers													100-200	18-30°C	24-27	70-80	50-70	35-45	5-7	10-14 days
Eggplant													60-150	20-35°C	24-27	60-80	80-120	60-70	4-6	14-21 days
Beans													100-200	15-30°C	20°C	60-70	50-70	35-45	2-4	6-12 days
Other Veggies																				
Peas													100-200	10-25 °C	15°C	60-70	60-90	40-50	2-4	5-7 days
Carrots													30-60	15-25°C	15°C	70-80	60-80	45-55	2-3	2-4 weeks
Beets													30-60	10-25 °C	18°C	70-80	60-80	45-55	2-3	2-4 weeks
Turnips													30-60	10-25 °C	15°C	70-80	60-80	45-55	2-3	1-2 weeks
Radishes													10-30	10-25 °C	15°C	70-80	20-60	14-20	2-3	1-2 weeks
Onions													30-90	10-25 °C	15°C	70-80	100-150	60-70	2-3	2-3 months
Mushrooms																				
Button													10-15	10-18 °C	15 °C	75-85%	35-42	30-35	2-3	7-10 days
Shiitake													5-10	12-25 °C	20 °C	85-95%	80-120	60-90	15-20	7-10 days
Oyster													5-10	10-20 °C	15 °C	85-95%	20-25	15-20	12-15	5-7 days
Enoki													7-10	10-20 °C	15 °C	80-90%	35-45	30-35	5-7	7-10 days

(Note: The color indication shows also the time or period of the year when these crops are found available globally in markets despite all of them being generally year-round crops).

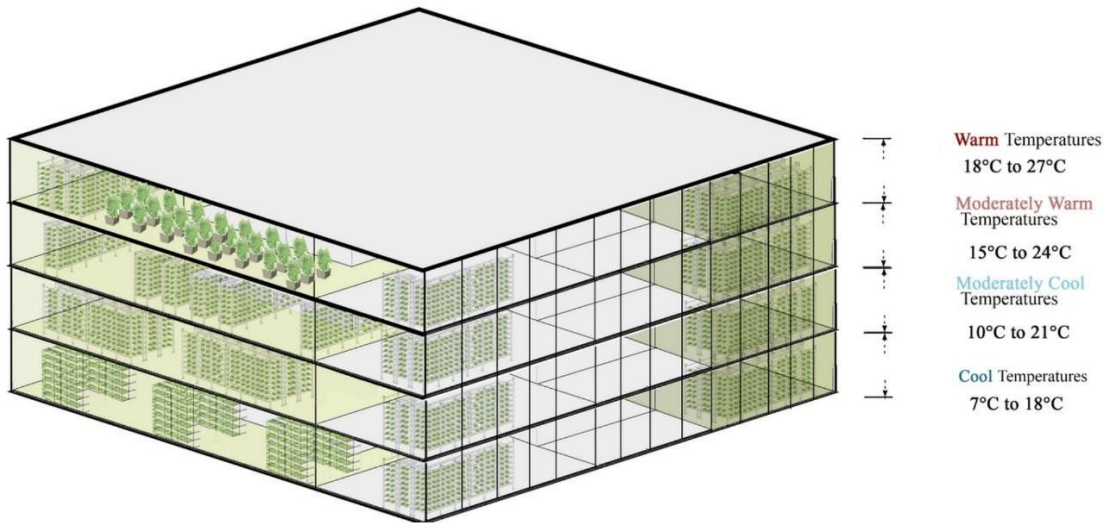


Figure 68. 3D illustration of Set Point Temperatures of Vertical Farming Floors.

5.6.6.1 System Yield Calculations

Table 18 depicts the calculations according to configurations for each floor and their selected crops and specific conditions. This investigation seeks to create an understanding of the total annual profit in EUR based on the common market price values for each crop. Note that these conclusions are very relative to the prices and inflation rates. The calculations are based following a straightforward method based on the formula below:

Equation 21. depicts the formula for measuring the total crop yield mass in kg.

(Equation 21)

$$Total\ mass(\mathbf{kg}) = \frac{Year - around\ cycle(\mathbf{days}) \times Total\ nr\ of\ crops(\mathbf{kg})}{Harvest\ (\mathbf{days})}$$

The presented formula estimates the total number of crops that may be cultivated while taking into consideration the particular harvest days of each crop.

Table 18. Annual Yield profitability and estimates of Base Case scenario of SQR.

SQR	Crop name	Height range[cm]	Maturing [days]	Nr of crop per 1 system level	Crop mass [kg]	Yield/ mature days [kg]	Annual yield[kg. Y ⁻¹]	Price [€/kg]	Profit[€/ year]
First Floor(10-18 °C)	Leaf lettuce	10-20 cm	35	13896	0.2	2779.2	28983.1	4.50 €	130,423.89 €
	spinach (Spinacia oleracea)	20-30 cm	20	13896	0.1	1389.6	25360.2	22.95 €	582,016.59 €
	Arugula (Eruca sativa)	30-60 cm	30	13896	0.02	277.92	3381.4	17.50 €	59,173.80 €
	Pea(Tom Thumb)	20-45	55	13896	0.3	4168.8	27665.7	6.29 €	174,017.08 €
	Fava Beans microgreen	8-15 cm	14	13896	0.15	2084.4	54343.3	7.50 €	407,574.64 €
Second Floor(18-21 °C)	chives microgreen	10-15 cm	14	13896	0.02	277.92	7245.8	4.50 €	32,605.97 €
	Bok Choy	15-60 cm	30	13896	0.84	11672.64	142017.1	1.21 €	171,840.72 €
	Mustard greens (Brassica juncea)	30-50 cm	40	13896	0.058	805.968	7354.5	11.63 €	85,532.35 €
	Cilantro (Coriandrum sativum)	30-60	45	13896	0.05	694.8	5635.6	5.67 €	31,953.85 €
	Mint	30-45	30	13896	0.25	3474	42267.0	12.00 €	507,204.00 €
Third Floor(20-24 °C)	Kale(Dwarf Blue Curled)	35-50	50	13896	0.5	6948	50720.4	7.75 €	393,083.10 €
	Dwarf Broccoli	30-55	55	13896	0.35	4863.6	32276.6	8.27 €	266,927.63 €
	Strawberries	20-30	45	13896	0.25	3474	28178.0	5.31 €	149,625.18 €
	Baby Carrots	20-25	50	13896	0.03	416.88	3043.2	3.35 €	10,194.80 €
	Radish Microgreen	3-7cm	7	13896	0.015	208.44	10868.7	20.20 €	219,546.87 €
Fourth Floor(21-27 °C)	Dwarf cherry tomatos	45-60	50	13896	1.35	18759.6	136945.1	3.25 €	445,071.51 €
	Dwarf Eggplant	30-50	45	13896	0.4	5558.4	45084.8	2.75	123,983.20 €
	Dawrf Pepers	20-60	60	13896	0.3	4168.8	25360.2	2.19	55,538.84 €
	Swiss Chard	20-60	45	13896	0.35	4863.6	39449.2	6.25	246,557.50 €
	Parsley	20-35	60	13896	0.2	2779.2	16906.8	3.34	56,468.71 €
Total Profit [Y-1]								4149340.232	

Table 19. Total Yield profitability of the morphologies.(€)

	Module No.	Tot. Pots/ 1 System level	Total nr of Treys	Total nr of Pots / 1 level of Growing rack	Yield/maturing days [kg]				Total Annual yield[kg.Y-1]/floor				Total Yield Profit [€/ year]
					F1_y	F2_y	F3_y	F4_y	F1_Ty	F2_Ty	F3_Ty	F4_Ty	
SQR	386	36	1158	13896	10699.92	16925.328	15910.92	36129.6	10699.92	16925.328	15910.92	36129.6	4149340.232
ATR	478	36	1434	17208	13250.16	20959.344	19703.16	44740.8	13250.16	20959.344	19703.16	44740.8	5138302.153
REC	460	36	1380	16560	12751.2	20170.08	18961.2	43056	12751.2	20170.08	18961.2	43056	4944809.603

CIR	402	36	1206	14472	11143.44	17626.896	16570.44	37627.2	11143.44	17626.896	16570.44	37627.2	4321333.61
CRS	464	36	1392	16704	12862.08	20345.472	19126.08	43430.4	12862.08	20345.472	19126.08	43430.4	4987807.948
LM	468	36	1404	16848	12972.96	20520.864	19290.96	43804.8	12972.96	20520.864	19290.96	43804.8	5030806.292
TM	392	36	1176	14112	10866.24	17188.416	16158.24	36691.2	10866.24	17188.416	16158.24	36691.2	4213837.749
ZM	388	36	1164	13968	10755.36	17013.024	15993.36	36316.8	10755.36	17013.024	15993.36	36316.8	4170839.404
UM	432	36	1296	15552	11975.04	18942.336	17807.04	40435.2	11975.04	18942.336	17807.04	40435.2	4643821.193
HM	364	36	1092	13104	10090.08	15960.672	15004.08	34070.4	10090.08	15960.672	15004.08	34070.4	3912849.338

The aforementioned method is used to determine the total yield profit across all morphologies, and the results are shown in *Table 19*. These calculations enable a comparison of the profitability of various morphologies based on their relative footprints. Due to their equal footprint area, the morphologies demonstrate roughly similar earnings. Nonetheless, the ATR arrangement stands out since it allows for the most agricultural production area while yielding the maximum profit closely followed by LM, CRS, and REC.

The approach goes beyond simply looking at earnings based on total yearly returns. *Table 20* presents a more complete view by including estimates of investment expenses, revenue, and the probability of obtaining a payback time. These additional characteristics help to provide a more comprehensive knowledge of the overall economic implications associated with the morphologies.

Table 20. Total Start Up costs and payback period estimates.

General Information		Calculations per month	
Average Landing (growing) area size	2 136 m²	Avg Yield	221 605 pots
Required power	513 kW	Avg Yield kg	9 652 kg
Average daily electricity consumption	4 330 kW	Revenue	212 643 EUR
Average daily water consumption	15 m³	Cost of raw materials	33 527 EUR
Investment amount:	2 778 003 EUR	Electricity cost	20 784 EUR
Investment in farm technology	2 178 442 EUR	Labor costs	35 752 EUR
Building Construction	-	Rent	0 EUR
Delivery of equipment and travel cost	174 275 EUR	Farm maintenance	5 981 EUR
Working capital	425 286 EUR	EBITDA	82 562 EUR
Total Investment Amount	2 778 003 EUR	Payback period	2.37 years

(Note: The investment estimate does not include prices for packaging and seedling equipment,

unique crop economics, alternatives for individual facilities, or any costs involved with leasing and building construction. These calculations are based on iFarm **Startup Cost Calculator** ([_www.ifarm.fi/ifarm_calculators.com](http://www.ifarm.fi/ifarm_calculators.com))

5.6.7.1 Energy Demand-Profitability Ratio

Table 21 illustrates a comparison of the ratio between Average Annual Energy consumption and Yield Profitability as per **Equation 22** to determine the best-performing morphology in terms of both energy consumption and capacity for yielding profits. A greater ratio shows that the building's energy usage is relatively higher than its profitability. A smaller ratio, on the other hand, indicates a more advantageous balance between energy use and profitability. As a result, deeper color indicators imply better case scenarios across the typologies. It is worth noting that New York and Athens deliver the best outcomes when compared to the Singapore climatic setting.

Equation 22. Depicts the Energy and Yield ratio.

(Equation 22)

$$\text{Ratio} = \frac{\text{Average Annual Energy Demand}}{\text{Total Annual Yield Profitability}}$$

Table 21. Efficiency in terms of Energy demand and Food Production of the morphologies according to the corresponding climate condition.

Climate_Typology	SQR	ATR	REC	CIR	CRS	LM	TM	ZM	UM	HM
New York_VF	12.2	10.6	10.1	12.1	10.1	9.7	11.6	11.7	11.5	13.5
Singapore_VF	26.3	25.4	23.7	26.5	23.8	24.1	28.2	28.3	27.4	31.4
Athens_VF	13.1	13.0	12.2	14.4	12.3	12.0	14.3	14.5	13.8	16.3
New York_VF+R	97.9	82.7	84.3	92.4	84.5	76.2	98.8	96.8	89.8	107.4
Singapore_VF+R	192.0	176.7	176.2	200.5	169.3	163.4	206.8	198.8	186.6	218.9
Athens_VF+R	63.8	63.4	61.3	70.9	63.2	59.3	74.1	72.5	68.0	80.8

5.6.8.1 Inflation Rates and Food Production

The interconnection of the food-energy-water (FEW) allows fluctuations in prices to be transmitted across sectors, becoming a difficult problem. Inflationary tendencies in one sector might impact the others both directly and indirectly. Food inflation currently outpaces that of water and electricity. Climate change, increased water, and fuel demands, and rising transportation costs, on the other hand, are set to have a substantial influence on growing conditions, consequently influencing future food supply. The International Monetary Fund (IMF) and Food and Agriculture Organization (FAO) have reported greater food inflation rates than water and energy (as illustrated in *Figure 69*), and they forecast continuing inflation tendencies until 2050. Higher pricing, on the other hand, may encourage greater income and profitability, stimulating investments in vertical farming and supporting operation development, particularly in these countries with limited arable land and right climate conditions like New York and Athens in this case. Through which it can lower transportation costs and decrease water demand since vertical farming practices can save up to 90 %, as opposed to its consumption in conventional terms.

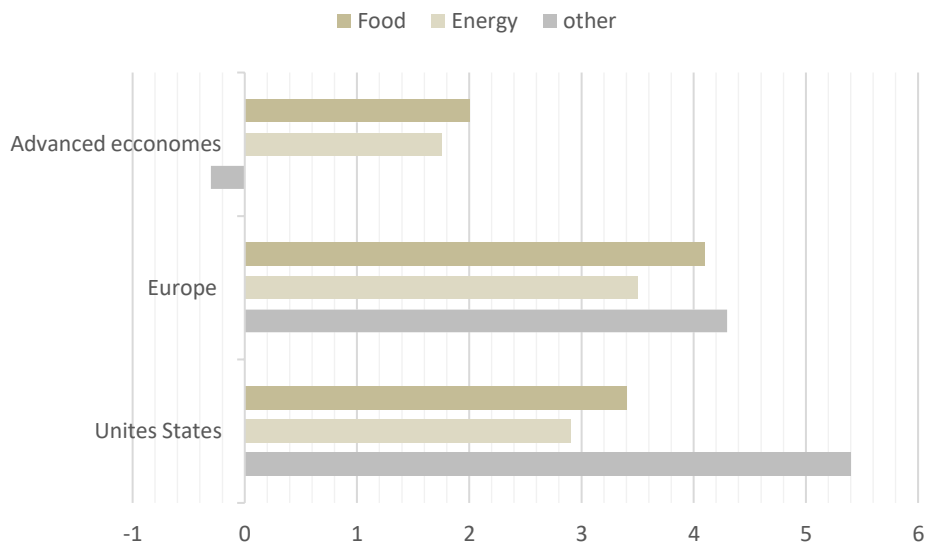
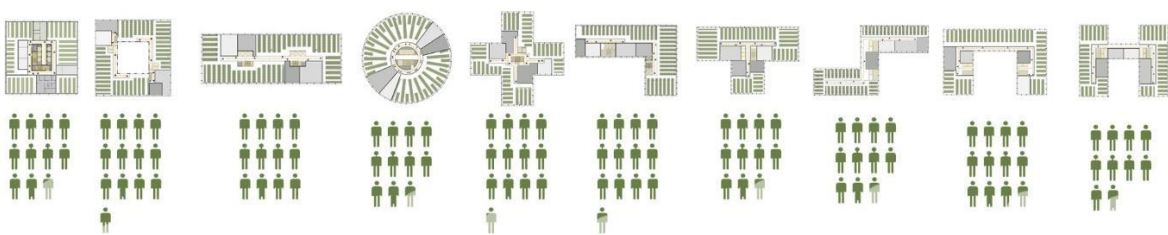


Figure 69. Change in the Inflation rate. (Source: IMF and Harver Analytics).

Table 22 demonstrates the expected annual food production for each shape, emphasizing the potential effect. According to the findings, almost 70% of the average total food generated in kilograms may be distributed to the neighboring communities, including sectors such as restaurants, retail, catering, and others that experience significant demand for fresh food. Therefore, just around 30% of food production is required to fulfill the nutritional demands of people in each typology yearly. These findings highlight the self-sufficiency of vertical farming practices, as they not only generate profits but also contribute significantly to feeding both the local population and the service sectors, demonstrating their potential to foster long-term and mutually beneficial relationships within communities.

Table 22. Food distribution % for the residential, local community, and service sectors.

	Total Annual Yield (kg)	Average Yearly Consumption/ Person (kg)	Nr.of People Fed Yearly	Average Family Size	Total Nr. of Families Fed Yearly	Neighborhood food gain(%)
SQR	733086.5	774	2036	4	509	(68.6)
ATR	907811.8	774	2522	4	630	(74.6)
REC	873626.4	774	2427	4	607	(73.6)
CIR	763473.5	774	2121	4	530	(69.8)
CRS	881223.2	774	2448	4	612	(73.9)
LM	888819.9	774	2469	4	617	(74.1)
TM	744481.7	774	2068	4	517	(69.1)
ZM	736884.9	774	2047	4	512	(68.7)
UM	820449.2	774	2279	4	570	(71.9)
HM	691304.4	774	1920	4	480	(66.7)



 = 200 PEOPLE OR 50 FAMILIES IN TOTAL TO FEED YEARLY

CHAPTER 6

OPTIMIZATION

6.1 Shading Typologies

Implementing different typologies is a common strategy for optimizing shading components in building design in order to improve energy efficiency and occupant comfort. In order to reduce direct sunlight penetration during peak hours, the first typology, S1-overhang, relies on horizontal shade devices installed above windows or openings. While efficiently reducing solar heat gain, this shading technique also allows natural light to reach the interior rooms. The second typology, S2, incorporates vertical shading components of side fins like. These elements are thoughtfully positioned on the building's outer façade to regulate the amount of sunlight and glare entering the structure while yet allowing for good solar gain. This typology is mostly seen for vertical farming practice facilities. S3, the third typology, further integrates horizontal and vertical shading components to produce a complete shading solution. This shading typology maximizes shade efficacy by preventing direct solar radiation from various angles through the use of horizontal overhangs and vertical fins. The incorporation of these typologies into building design offers a comprehensive strategy to optimizing shading, enhancing energy performance, and producing a comfortable indoor atmosphere for both occupants and plant optimal growth.

Figure 70 illustrates the three different typologies of shading devices used for optimizing the morphology impact, overhangs can also be considered as the effect of a perimeter balcony, the distances for each of them are given as follows:

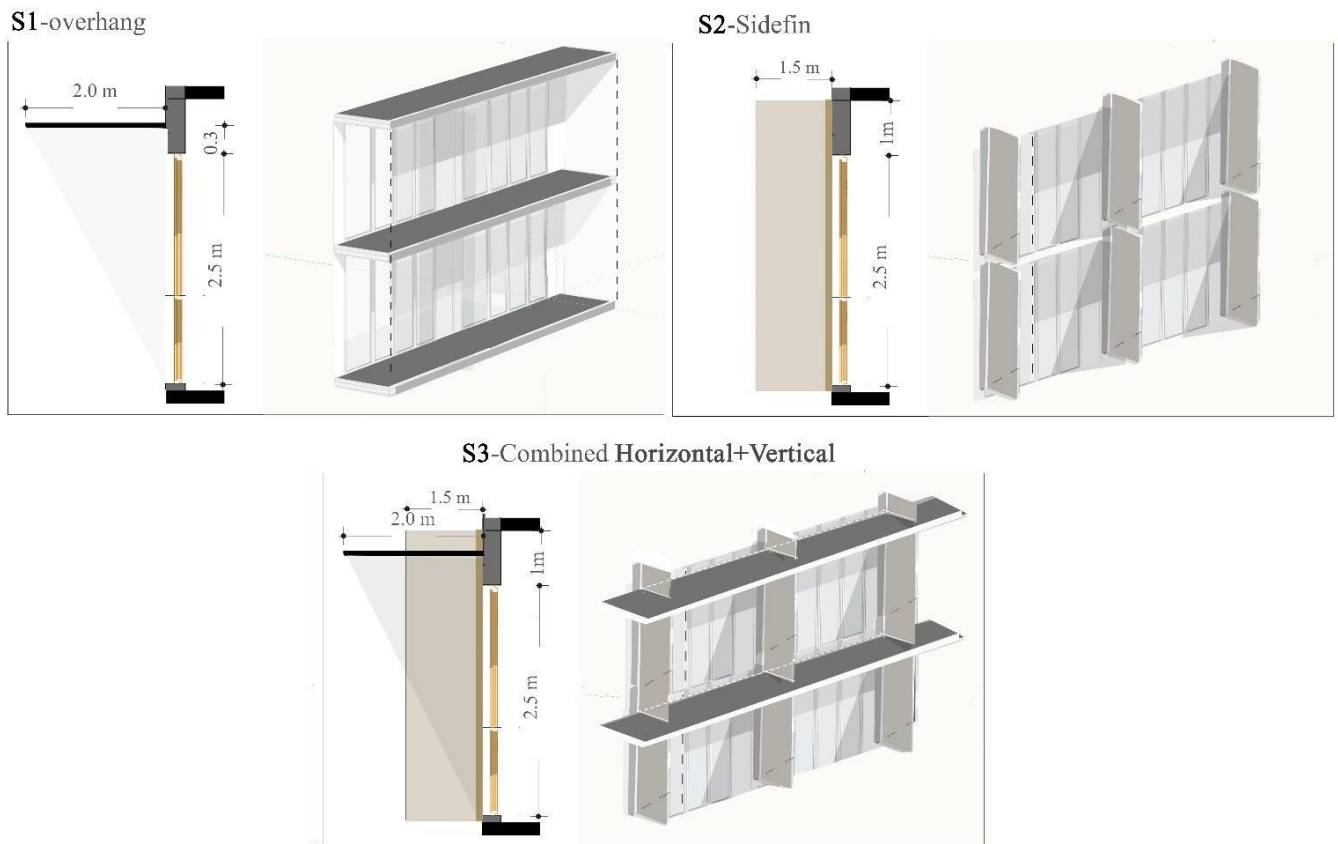


Figure 70. Optimization Shading Typologies S1, S2 and S3.

6.2 New York, USA Shading Optimization

A further study was conducted to examine the effects of the three topologies of shading devices of S1, S2 and S3 over the base case scenario BC, on each of the researched morphologies, which were developed in response to the particular climatic circumstances found in New York. The figures include information on each morphology's annual heating and cooling energy performance as well as that of their corresponding building typology(building typology_heating/cooling).

6.2.1 Optimized Energy Performance

The following data shown in **Figure 71** depict the heating and cooling energy consumption optimization for all shading typologies and their associated building type for SQR morphology. Based on the estimates there is a slight decrease in average heating demands of only ± 0.18 kWh.m-2Y-1. among all shading typologies. Conversely, will be a significant average decrease + 5.52 kWh.m-2Y-1 of cooling energy demand values or 17.1%, 6.9%, and 10.2 % for VF, R and VF+R respectively in which the greatest optimization is provided by S3 shading typology followed by S1 and lastly by S2.

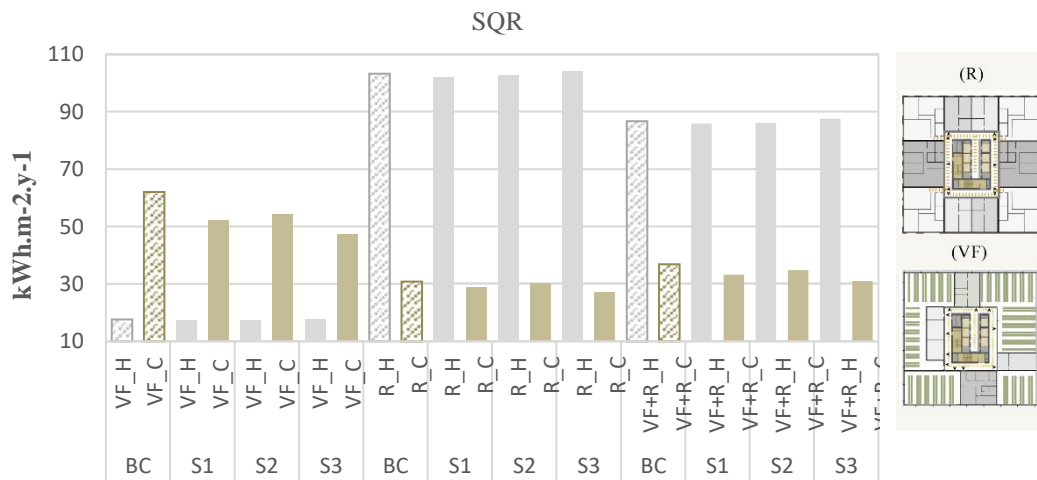


Figure 71. Comparison of Annual Heating and Cooling energy consumption (kWh.m-2Y-1) for each shading typology on SQR.

Figure 72 depict the heating and cooling energy consumption optimization for all shading typologies and their associated building type for ATR morphology. Based on the estimates there is an increase in average heating demands of only ± 2.59 kWh.m-2Y-1. among all shading typologies.

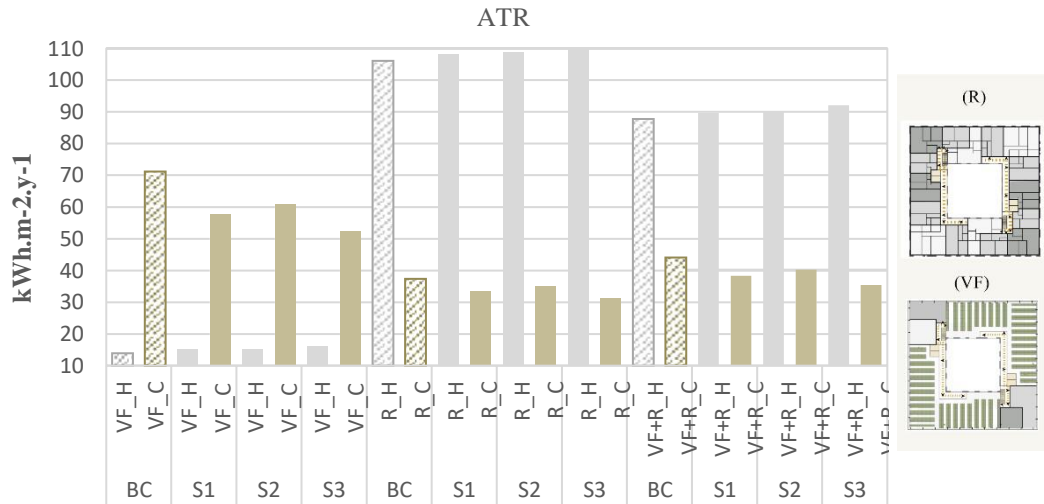


Figure 72. Comparison of Annual Heating and Cooling energy consumption (kWh.m-2Y-1) for each shading typology on ATR.

Conversely, will be a significant average decrease + 6.16 kWh.m-2Y-1 of cooling energy demand values or 20%, 11%, and 13.8 % for VF, R and VF+R respectively in which the greatest optimization is provided by S3 shading typology followed by S1 and lastly by S2.

Figure 73 depict the heating and cooling energy consumption optimization for all shading typologies and their associated building type for REC morphology. Based on the estimates there is an insignificant decrease in average heating demands of ± 0.68 kWh.m-2Y-1. among all shading typologies. Conversely, will be a substantial average decrease + 6.28 kWh.m-2Y-1 of cooling energy demand values or 18.4%, 6.9%, and 10.7 % for VF, R and VF+R respectively in which the greatest optimization is provided by S3 shading typology followed by S1 and lastly by S2.

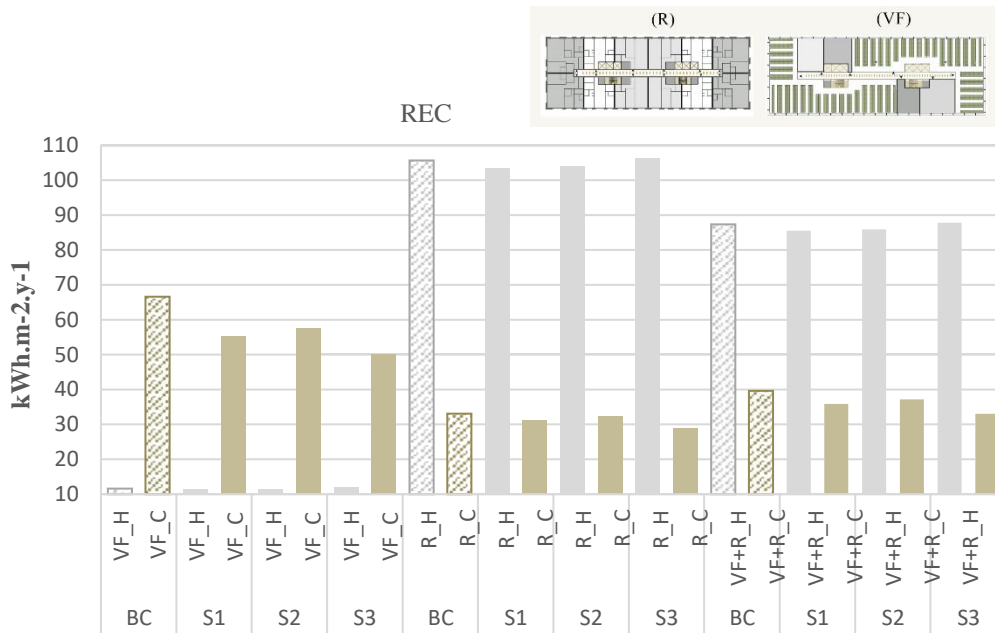


Figure 73. Comparison of Annual Heating and Cooling energy consumption (kWh.m-2Y-1) for each shading typology on REC.

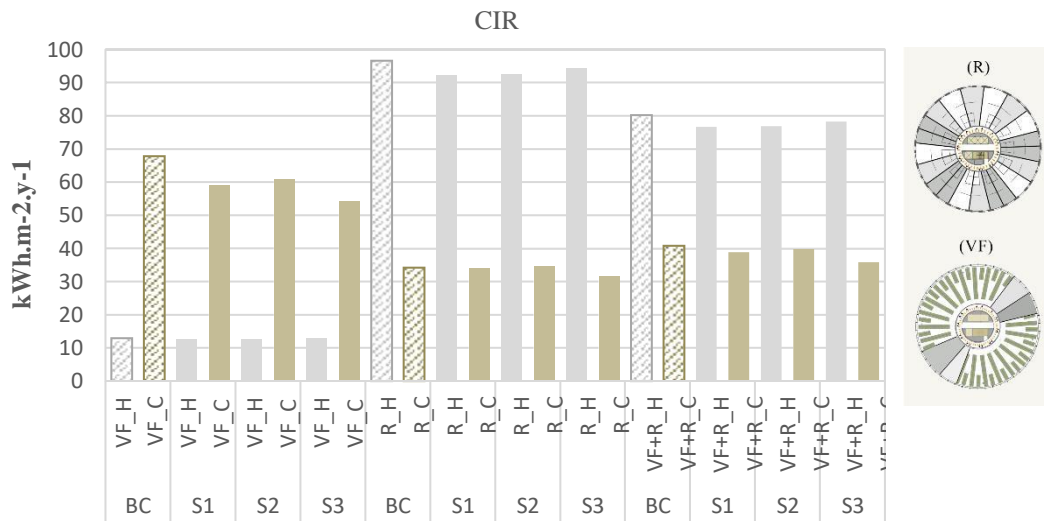


Figure 74. Comparison of Annual Heating and Cooling energy consumption (kWh.m-2Y-1) for each shading typology on CIR.

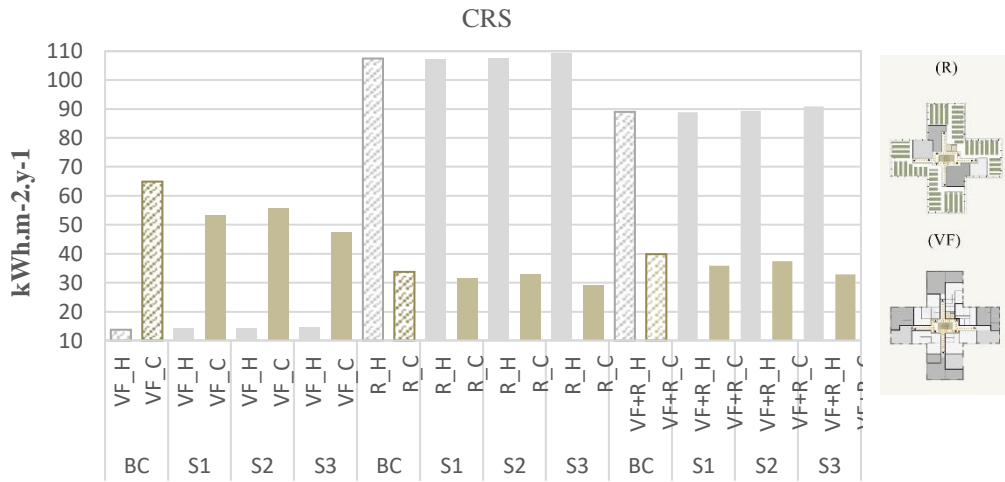


Figure 75. Comparison of Annual Heating and Cooling energy consumption (kWh.m-2Y-1) for each shading typology on CRS.

Figure 75 depict the heating and cooling energy consumption optimization for all shading typologies and their associated building type for CRS morphology. Based on the estimates there is an increase in average heating demands of ± 0.68 kWh.m-2Y-1. among all shading typologies. Conversely, will be an average decrease + 6.51 kWh.m-2Y-1 of cooling energy demand values or 19.5%, 7.2 %, and 11.1% for VF, R and VF+R respectively in which the greatest optimization is provided by S3 shading typology followed by S1 and lastly by S2.

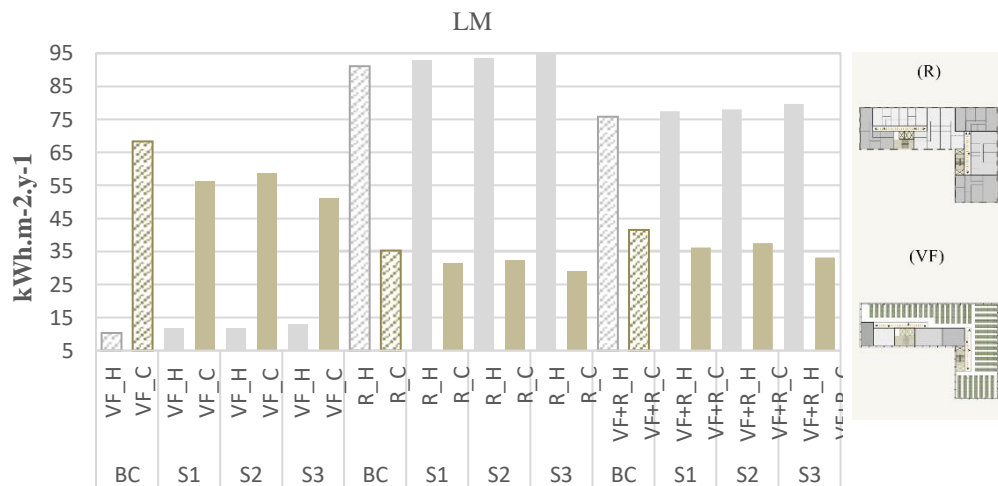


Figure 76. Comparison of Annual Heating and Cooling energy consumption (kWh.m-2Y-1) for each shading typology on LM.

Figure 76 depict the heating and cooling energy consumption optimization for all shading typologies and their associated building type for LM morphology. Based on the estimates there is an increase in average heating demands of ± 2.39 kWh.m-2Y-1. among all shading typologies. Conversely, will be a significant average decrease + 7.71 kWh.m-2Y-1 of cooling energy demand values or 18.8 %, 12.1 %, and 14.2% for VF, R and VF+R respectively in which the greatest optimization is provided by S3 shading typology followed by S1 and lastly by S2.

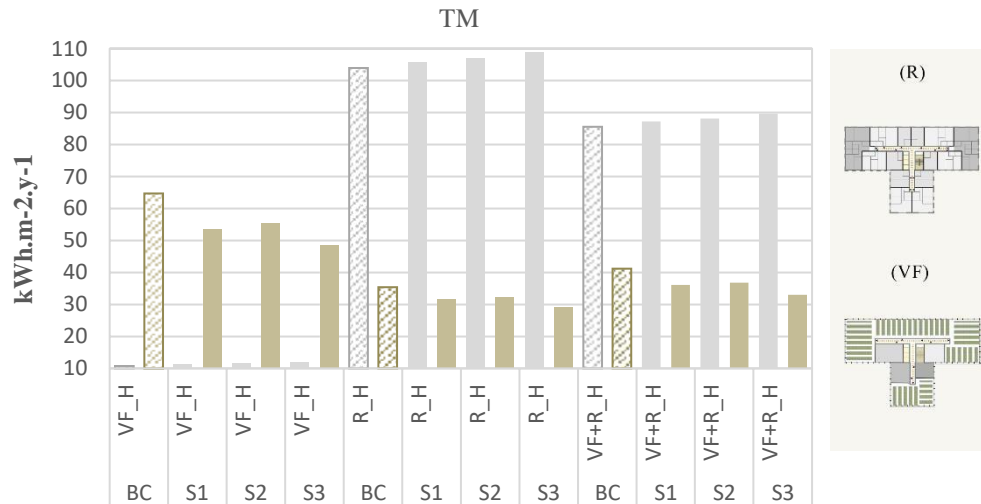


Figure 77. Comparison of Annual Heating and Cooling energy consumption (kWh.m-2Y-1) for each shading typology on TM.

Figure 77 depict the heating and cooling energy consumption optimization for all shading typologies and their associated building type for TM morphology. Similarly to LM, there is an increase in average heating demands of ± 2.32 kWh.m-2Y-1. among all shading typologies. Conversely, will be a significant average decrease + 7.48 kWh.m-2Y-1 of cooling energy demand values or 18.8 %, 12.3 %, and 14.3% for VF, R and VF+R respectively in which the greatest optimization is provided by S3 shading typology followed by S1 and lastly by S2.

R and VF+R respectively.

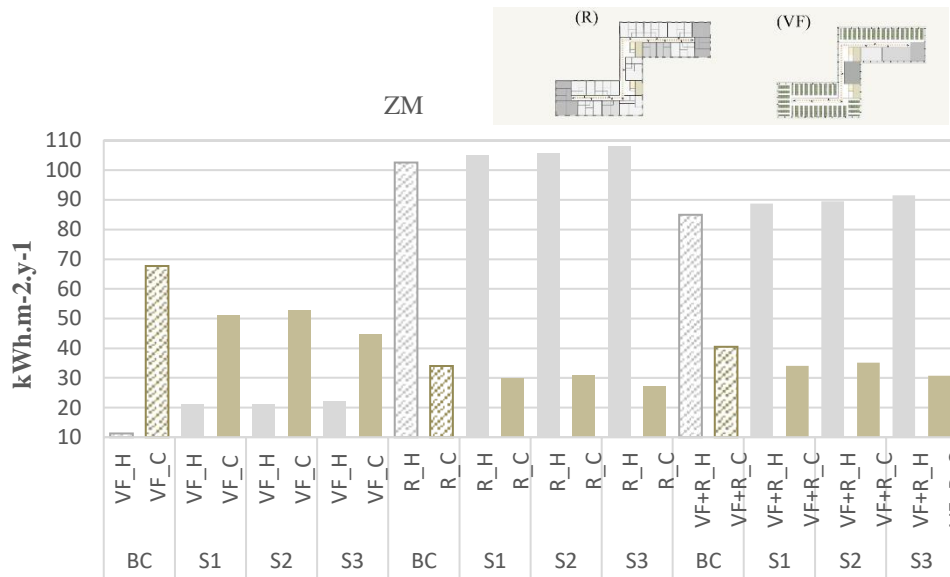


Figure 78. Comparison of Annual Heating and Cooling energy consumption (kWh.m-2Y-1) for each shading typology on ZM.

Figure 78 depict the heating and cooling energy consumption optimization for all shading typologies and their associated building type for ZM morphology. There is a substantial increase in average heating demands of ± 6.29 kWh.m-2Y-1. among all shading typologies. Conversely, will be an average decrease + 9.97 kWh.m-2Y-1 of cooling energy demand values or 26.78 %, 13.5 %, and 17.8 % for VF, R and VF+R respectively in which the greatest optimization is provided by S3 shading typology followed by S1 and lastly by S2.

Figure 79 depict the heating and cooling energy consumption optimization for all shading typologies and their associated building type for UM morphology. There is an increase in average heating demands of ± 3.47 kWh.m-2Y-1. among all shading typologies. Conversely, will be an average decrease + 8.42 kWh.m-2Y-1 of cooling energy demand values or 19.8 %, 13.1 %, and 15.2 % for VF, R and VF+R respectively in which the greatest optimization is provided by S3 shading typology followed by S1 and lastly by S2.

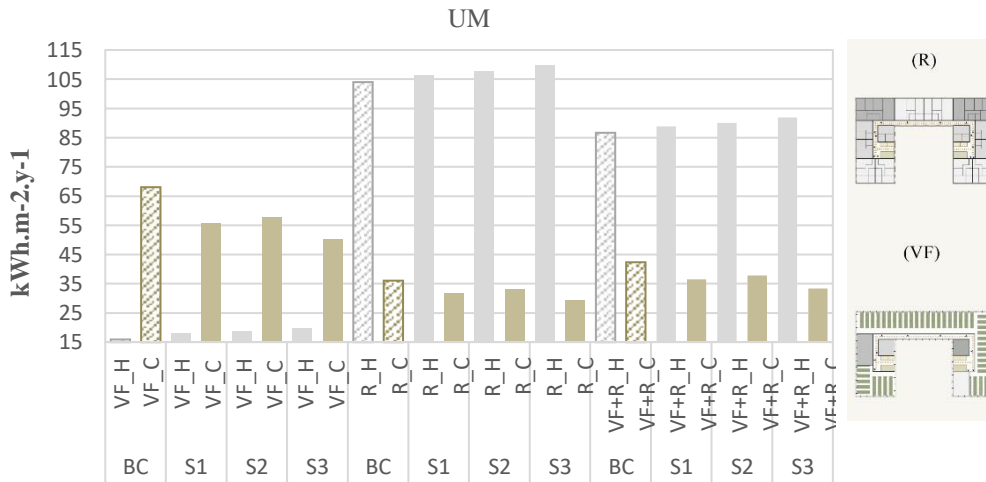


Figure 79. Comparison of Annual Heating and Cooling energy consumption (kWh.m-2Y-1) for each shading typology on UM.

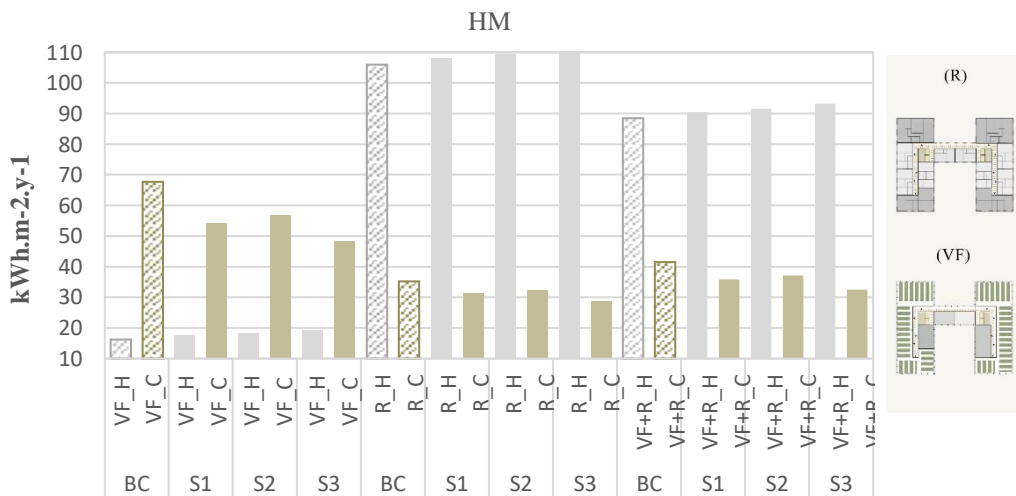


Figure 80. Comparison of Annual Heating and Cooling energy consumption (kWh.m-2Y-1) for each shading typology on HM.

Figure 80 depict the heating and cooling energy consumption optimization for all shading typologies and their associated building type for HM morphology. There is an increase in average heating demands of ± 2.98 kWh.m-2Y-1. among all shading typologies. Conversely, will be an average decrease + 8.42 kWh.m-2Y-1 of cooling

energy demand values or 21.47 %, 12.4 %, and 15.3 % for VF, R and VF+R respectively in which the greatest optimization is provided by S3 shading typology followed by S1 and lastly by S2.

6.2.2 Comparison of Morphological Optimization

The following data depict a clear illustration of the optimization values across all the studied morphologies for VF, R and VF+R typologies respectively. As shown in *Figure 81* the morphology with the most optimization is TM which is followed by REC and CRS whereas the least is depicted to be UM. S3 typology is the most efficient shading scenario with an optimization of around 20 %, and 11.2% 13.6% for S2 and S3. It is noteworthy to mention that the VF typology has the greatest optimization values as opposed to R and VF+R.

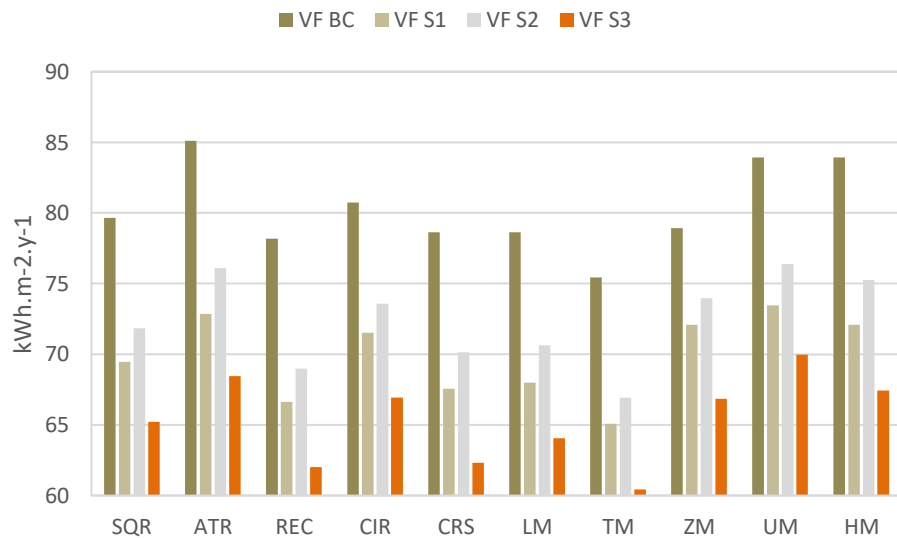


Figure 81. Comparison of Annual Total energy consumption (kWh.m-2Y-1) for each shading scenario according to all morphologies regarding VF.

Figure 82 Conversely illustrates that the morphology with the most optimization for the residential typology is SQR, whereas the least is depicted to be ATR. S3 typology is the most efficient shading scenario with an optimization of roughly 5 %.

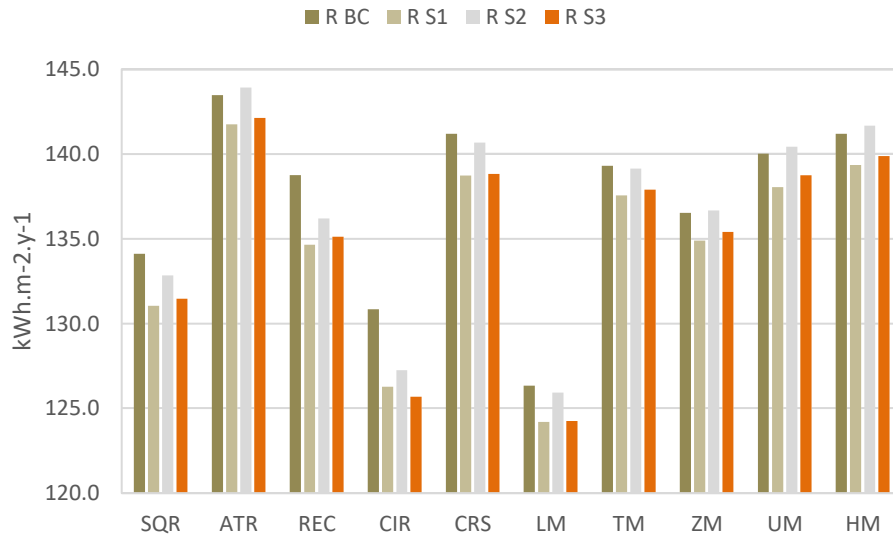


Figure 82. Comparison of Annual Total energy consumption (kWh.m-2Y-1) for each shading scenario according to all morphologies regarding R(Residence).

Similarly, **Figure 83** on the other hand represents that the S3 optimization ranges around 5.7 % for VF+R with REC as the most optimized morphology.

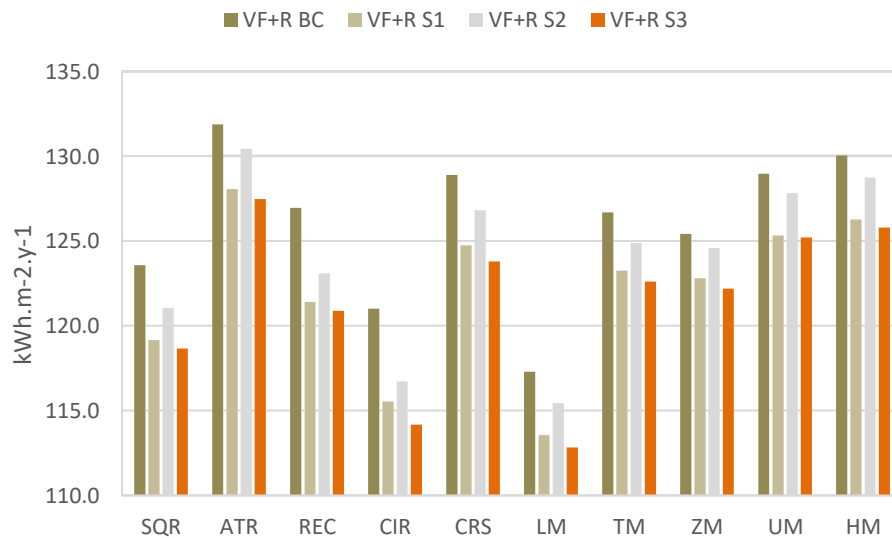


Figure 83. Comparison of Annual Total energy consumption (kWh.m-2Y-1) for each shading scenario according to all morphologies regarding VF+R.

Table 23. Shading efficiency results for the climate of New York (%).

	VF (Vertical farming)				R (Residence)				VF+R (CEA Integrated High-Rise)			
	BC	S1	S2	S3	BC	S1	S2	S3	BC	S1	S2	S3
SQR	-	-	-	-	-	-	-	-	-	-	-	-
ATR	-6.9	-4.9	-6.0	-5.0	-7.0	-8.2	-8.3	-8.1	-6.7	-7.5	-7.8	-7.4
REC	8.1	8.5	9.4	9.4	3.3	5.0	5.4	4.9	3.7	5.2	5.6	5.2
CIR	-3.3	-7.3	-6.7	-7.9	5.7	6.2	6.6	7.0	4.7	4.8	5.2	5.6
CRS	2.6	5.6	4.7	6.9	-7.9	-9.9	-10.5	-10.4	-6.5	-8.0	-8.6	-8.4
LM	0.0	-0.7	-0.7	-2.8	10.5	10.5	10.5	10.5	9.0	9.0	9.0	8.8
TM	4.0	4.3	5.2	5.7	-10.3	-10.8	-10.5	-11.0	-8.0	-8.6	-8.2	-8.7
ZM	-4.6	-10.8	-10.5	###	2.0	1.9	1.8	1.8	1.0	0.4	0.2	0.3
UM	-6.3	-1.9	-3.3	-4.7	-2.6	-2.3	-2.8	-2.5	-2.8	-2.1	-2.6	-2.5
HM	0.0	1.9	1.5	3.6	-0.8	-1.0	-0.9	-0.8	-0.8	-0.7	-0.7	-0.5

Note: (SQR morphology is kept as base case scenario, Darker shades indicate higher optimization values)

6.3 Singapore, Shading Optimization

The following analysis examines the effects of three shading scenarios, namely S1, S2, and S3, on the building morphologies as to the unique climatic circumstances of Singapore, in comparison to the base case scenario BC.

6.3.1 Optimized Energy Performance

In association with the SQR morphology, **Figure 84** shows the data indicating the optimization of heating and cooling energy consumption for various shade typologies and the related building types. It is important to mention once again that there are no heating demands. The cooling energy consumption, on the other hand,

shows a considerable average drop of $\pm 15.47 \text{ kWh.m}^{-2}\text{Y}^{-1}$, or a reduction of 7.6%, 6.5%, and 6.7% for VF, R, and VF+R, respectively. The shading typology of S3 exhibits the highest degree of optimization.

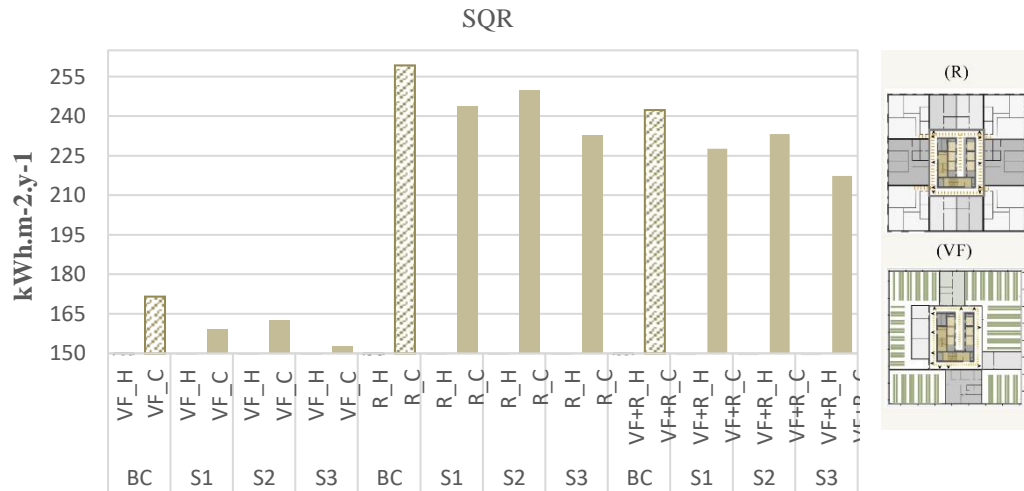


Figure 84. Comparison of Annual Heating and Cooling energy consumption (kWh.m⁻²Y⁻¹) for each shading typology on SQR.

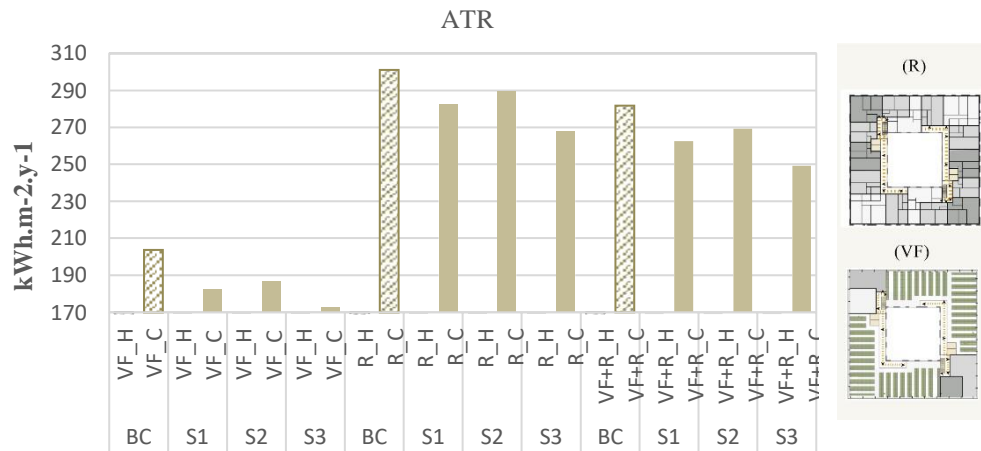


Figure 85. Comparison of Annual Heating and Cooling energy consumption (kWh.m⁻²Y⁻¹) for each shading typology on ATR.

Figure 85 shows the data indicating the optimization of heating and cooling energy consumption for ATR morphology. The cooling energy consumption shows a considerable average drop of ± 21.85 kWh.m-2Y-1, or a reduction of 11.3%, 6.9 %, and 7.6% for VF, R, and VF+R, respectively.

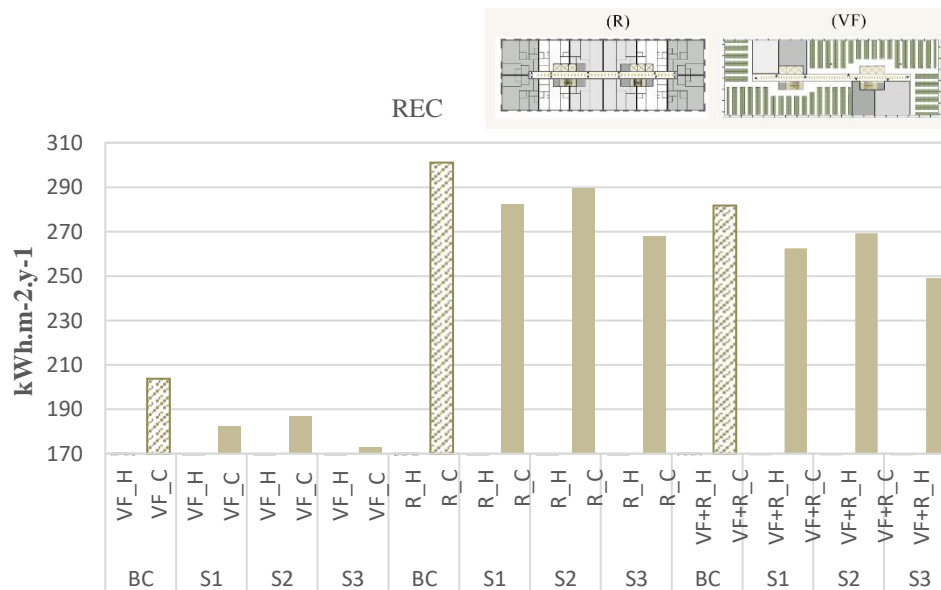


Figure 86. Comparison of Annual Heating and Cooling energy consumption (kWh.m-2Y-1) for each shading typology on REC.

Figure 86 shows the data indicating the optimization of heating and cooling energy consumption for REC morphology. The cooling energy consumption shows a considerable average drop of ± 16.73 kWh.m-2Y-1, or a reduction of 7.5%, 6.5 %, and 6.6% for VF, R, and VF+R, respectively. The shading typology of S3 exhibits the highest degree of optimization.

Figure 87 shows the data indicating the optimization of heating and cooling energy consumption for CIR morphology. The cooling energy consumption shows a considerable average drop of ± 12.56 kWh.m-2Y-1, or a reduction of 6.6%, 4.6 %, and 4.8 % for VF, R, and VF+R, respectively. The shading typology of S3 exhibits the highest degree of optimization.

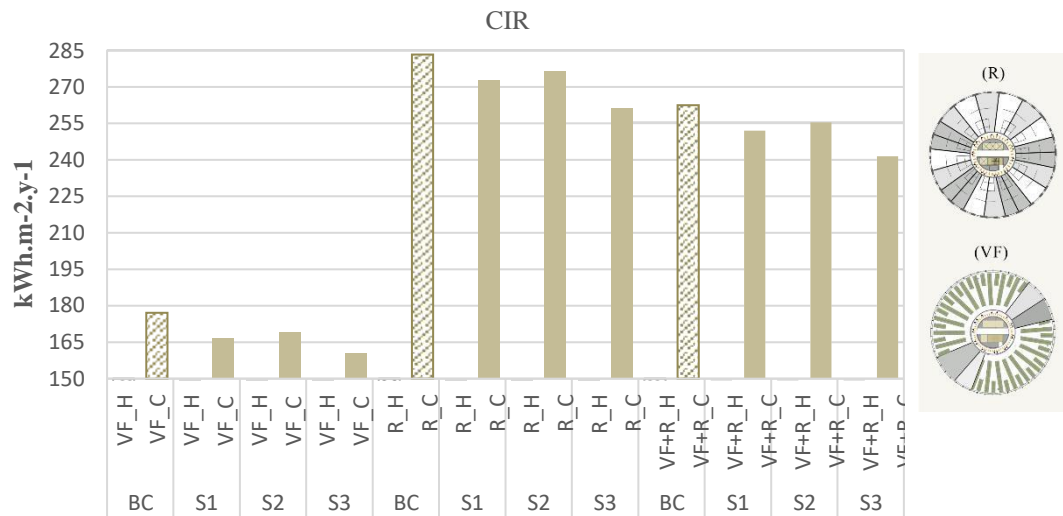


Figure 87. Comparison of Annual Heating and Cooling energy consumption (kWh.m-2Y-1) for each shading typology on CIR.

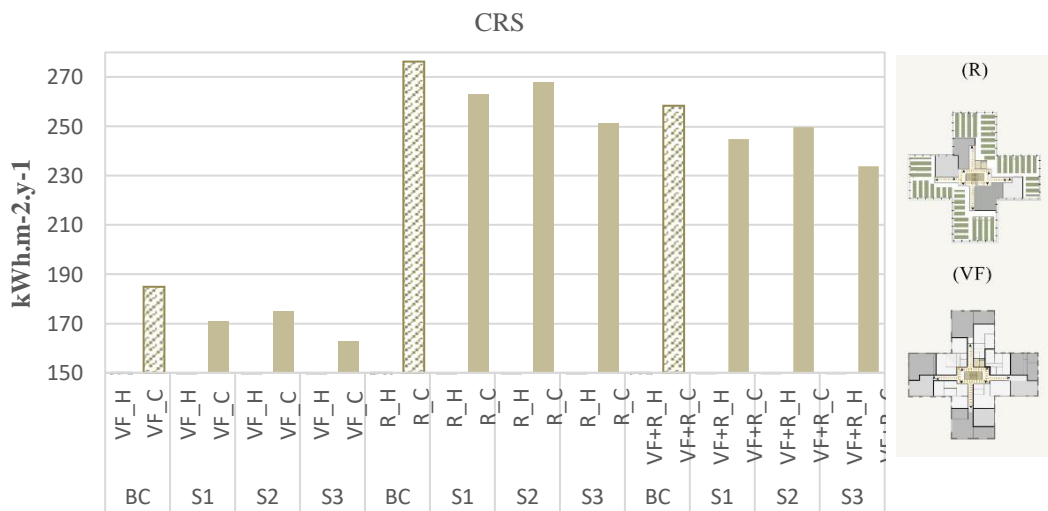


Figure 88. Comparison of Annual Heating and Cooling energy consumption (kWh.m-2Y-1) for each shading typology on CRS.

Figure 88 shows the data indicating the optimization of heating and cooling energy consumption for CRS morphology. The cooling energy consumption shows a considerable average drop of $\pm 15.5 \text{ kWh.m}^{-2}\text{Y}^{-1}$, or a reduction of 8.25%, 5.6 %, and 6 % for VF, R, and VF+R, respectively. The shading typology of S3 exhibits the highest degree of optimization.

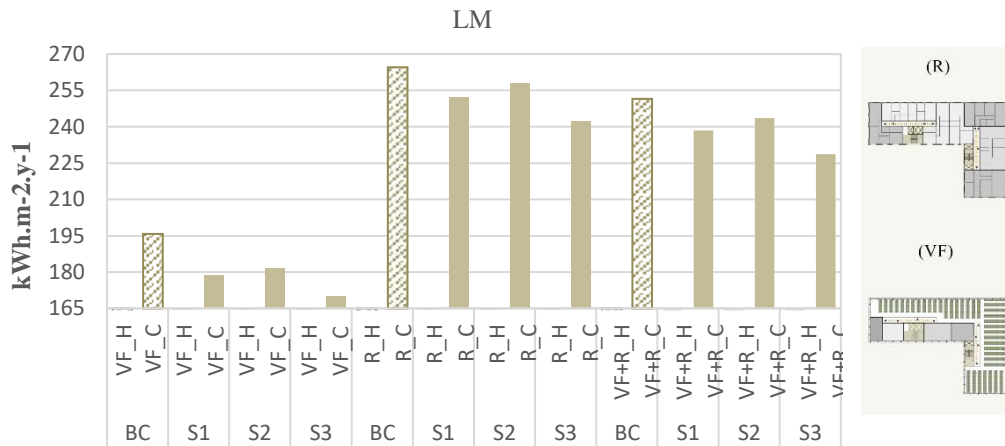


Figure 89. Comparison of Annual Heating and Cooling energy consumption (kWh.m-2Y-1) for each shading typology on LM.

Figure 89 shows the data indicating the optimization of heating and cooling energy consumption for LM morphology. The cooling energy consumption shows a significant average decrease of $\pm 15.7 \text{ kWh.m}^{-2}\text{Y}^{-1}$, or a reduction of 9.7%, 5.1 %, and 5.7% for VF, R, and VF+R, respectively. The shading typology of S3 exhibits the highest degree of optimization.

Figure 90 shows the data indicating the optimization of heating and cooling energy consumption for TM morphology. The cooling energy consumption shows a significant average decrease of $\pm 21.85 \text{ kWh.m}^{-2}\text{Y}^{-1}$, or a reduction of 11.4 %, 7 %, and 7.6 % for VF, R, and VF+R, respectively. The shading typology of S3 exhibits the highest degree of optimization.

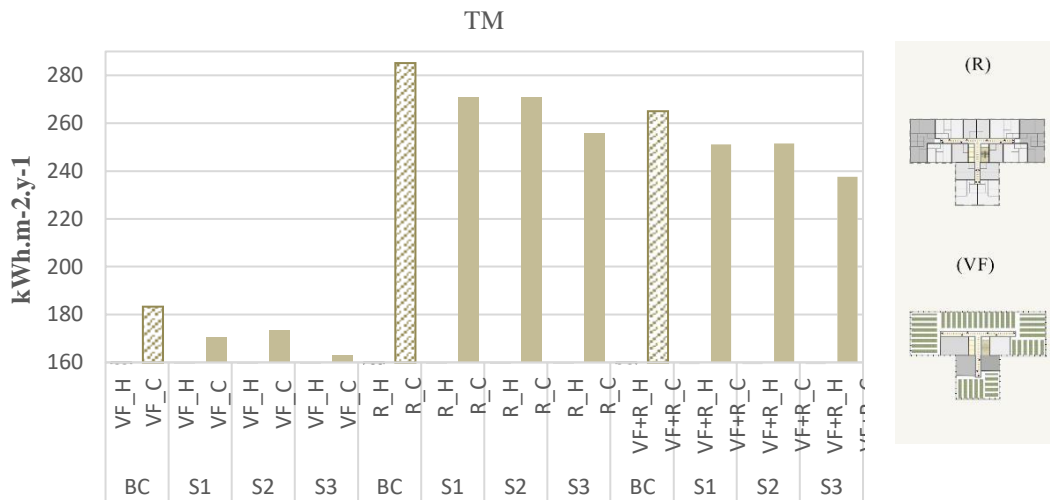


Figure 90. Comparison of Annual Heating and Cooling energy consumption (kWh.m-2Y-1) for each shading typology on TM.

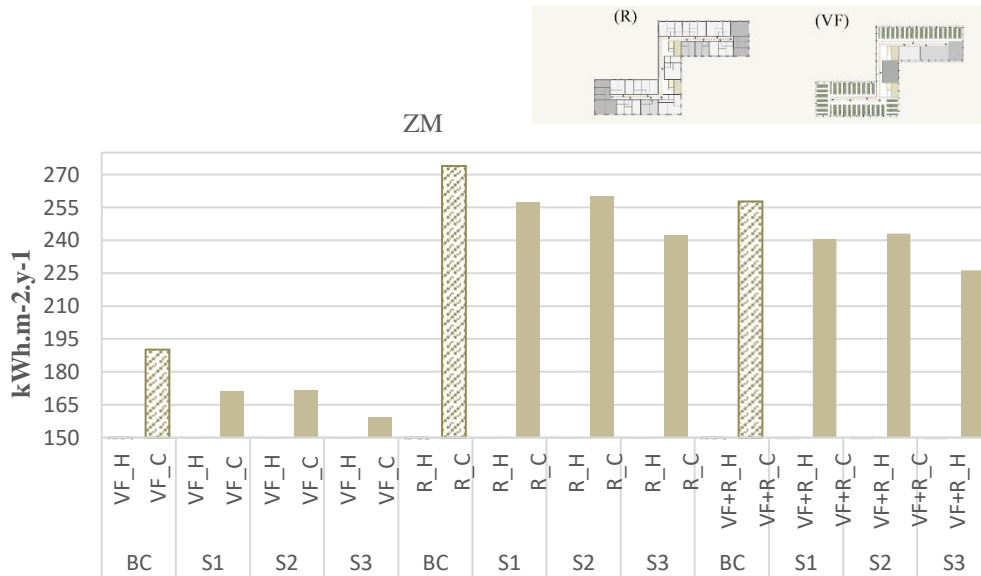


Figure 91. Comparison of Annual Heating and Cooling energy consumption (kWh.m-2Y-1) for each shading typology on ZM.

Figure 91 shows the data indicating the optimization of heating and cooling energy consumption for ZM morphology. The cooling energy consumption shows a significant average decrease of $\pm 21.54 \text{ kWh.m}^{-2}\text{Y}^{-1}$, or a reduction of 12.1 %, 7.5 %, and 8.2 % for VF, R, and VF+R, respectively. The shading typology of S3 exhibits the highest degree of optimization.

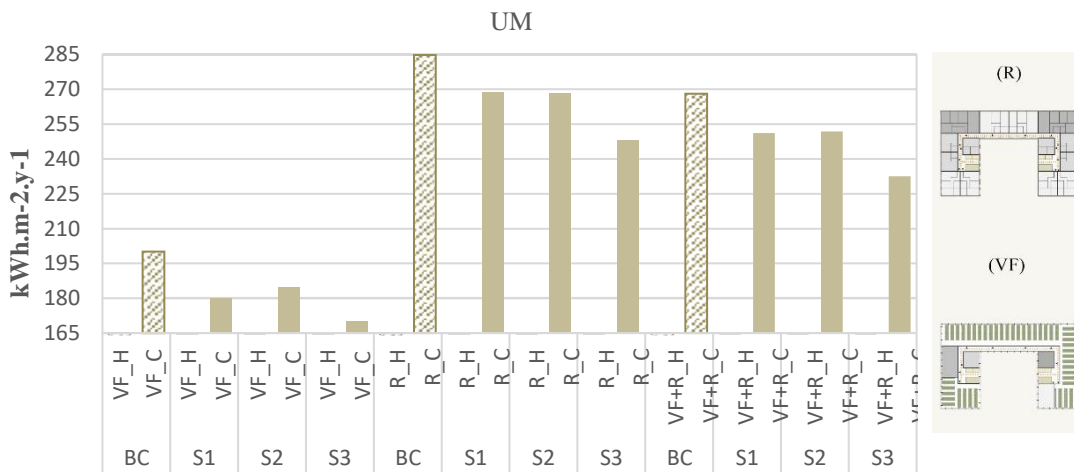


Figure 92. Comparison of Annual Heating and Cooling energy consumption ($\text{kWh.m}^{-2}\text{Y}^{-1}$) for each shading typology on UM.

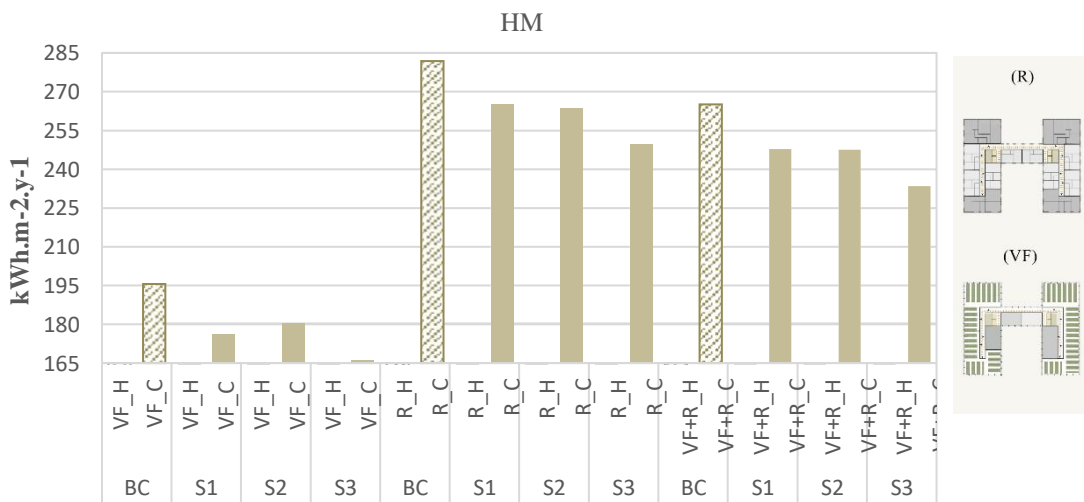


Figure 93. Comparison of Annual Heating and Cooling energy consumption

(kWh.m-2Y-1) for each shading typology on HM.

Figure 92 shows the data indicating the optimization of heating and cooling energy consumption for UM morphology. The cooling energy consumption shows a significant average decrease of ± 22.64 kWh.m-2Y-1, or a reduction of 10.9 %, 8.1 %, and 8.5 % for VF, R, and VF+R, respectively. The shading typology of S3 exhibits the highest degree of optimization.

Figure 93 shows the data indicating the optimization of heating and cooling energy consumption for HM morphology. The cooling energy consumption shows a significant average decrease of ± 22 kWh.m-2Y-1, or a reduction of 10.9 %, 7.9 %, and 8.3 % for VF, R, and VF+R, respectively. The shading typology of S3 exhibits the highest degree of optimization.

6.3.2 Comparison of Morphological Optimization

The following data depict a clear illustration of the optimization values across all the studied morphologies for VF, R and VF+R typologies respectively. *Figure 94* displays again that the best optimizing scenario is S3 by around 15.3%. The morphology with the most optimization surprisingly, in comparison to New York, which was the last ATR morphology is estimated to be the most optimized one as opposed to CIR as the least. S2 has an optimization of at most 9.8 % in this climate setting while S1 is 10.5%.

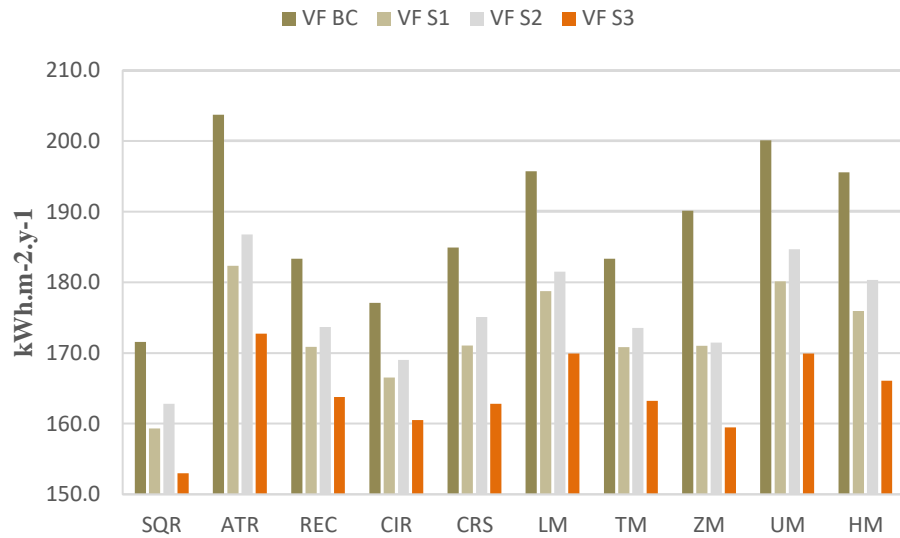


Figure 94. Comparison of Annual Total energy consumption (kWh.m-2Y-1) for each shading scenario according to all morphologies regarding VF.

Figure 95 similarly illustrates that the morphology with the most optimization for the residential typology is UM, whereas the least is depicted to be again CIR. S3 typology is the most efficient shading scenario with an average optimization of approximately 13%. **Figure 96** on the other hand represents that the S3 optimization ranges around 13.5 % for VF+R with UM as the most optimized morphology.

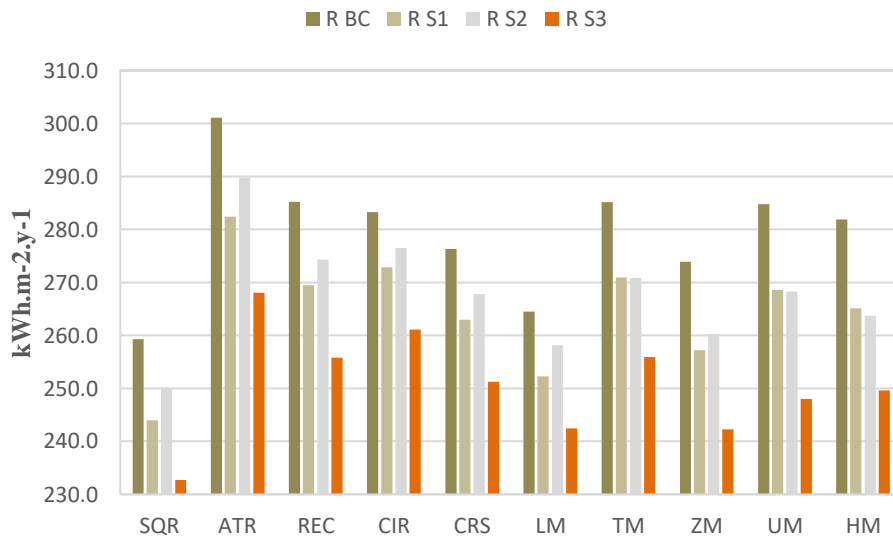


Figure 95. Comparison of Annual Total energy consumption (kWh.m-2Y-1) for each shading scenario according to all morphologies regarding R(Residence).

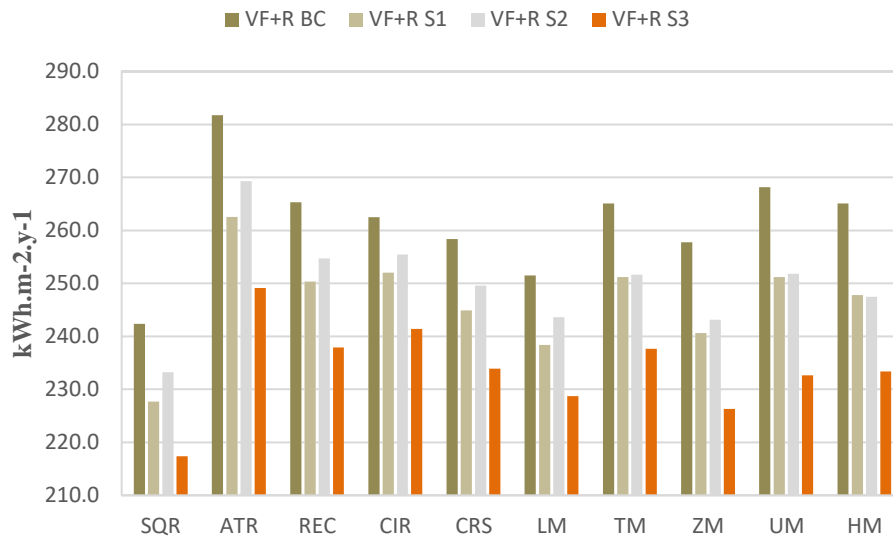


Figure 96. Comparison of Annual Total energy consumption (kWh.m-2Y-1) for each shading scenario according to all morphologies regarding VF+R.

Table 24. Shading efficiency results for the climate of Singapore (%).

	VF (Vertical farming)				R (Residence)				VF+R (CEA Integrated High-Rise)			
	BC	S1	S2	S3	BC	S1	S2	S3	BC	S1	S2	S3
SQR	-	-	-	-	-	-	-	-	-	-	-	-
ATR	-18.8	-14.4	-14.7	-12.9	-16.1	-15.7	-15.9	-15.2	-16.3	-15.3	-15.5	-14.6
REC	10.0	6.3	7.0	5.2	5.3	4.6	5.3	4.6	5.8	4.7	5.4	4.5
CIR	3.4	2.6	2.7	2.0	0.7	-1.2	-0.8	-2.1	1.1	-0.7	-0.3	-1.5
CRS	-4.4	-2.7	-3.6	-1.4	2.5	3.6	3.1	3.8	1.6	2.8	2.3	3.1
LM	-5.8	-4.5	-3.7	-4.4	4.3	4.1	3.6	3.5	2.7	2.7	2.4	2.2
TM	6.3	4.4	4.4	3.9	-7.8	-7.4	-4.9	-5.6	-5.4	-5.4	-3.3	-3.9
ZM	-3.7	-0.1	1.2	2.3	3.9	5.1	3.9	5.3	2.8	4.2	3.4	4.8
UM	-5.2	-5.4	-7.7	-6.6	-4.0	-4.4	-3.1	-2.4	-4.0	-4.4	-3.6	-2.8
HM	2.3	2.3	2.4	2.2	1.0	1.3	1.7	-0.7	1.1	1.3	1.7	-0.3

Note: (SQR morphology is kept as base case scenario, Darker shades indicate higher optimization values)

6.4 Athens, Shading Optimization

The current study focuses on examining the effects of the three different shading situations, fit the particular climatic conditions of Athens, Greece. These shading scenarios of S1, S2, and S3 are compared to the base case scenario BC in a comparison study. This study intends to evaluate the efficacy and possible advantages of various shading systems in maximizing energy efficiency.

6.4.1 Optimized Energy Performance

The following data shown in **Figure 97** depict the heating and cooling energy consumption optimization for all shading typologies and their associated building type for SQR morphology. Based on the estimates there is a slight decrease in average heating demands of ± 1.63 kWh.m-2Y-1. among all shading typologies. Conversely, will be a significant average decrease + 6.5 kWh.m-2Y-1 of cooling energy demand values or 9.2%, 12.9%, and 10.9 % for VF, R and VF+R respectively in which the greatest optimization is provided by S3 shading typology followed by S1 and lastly by S2.

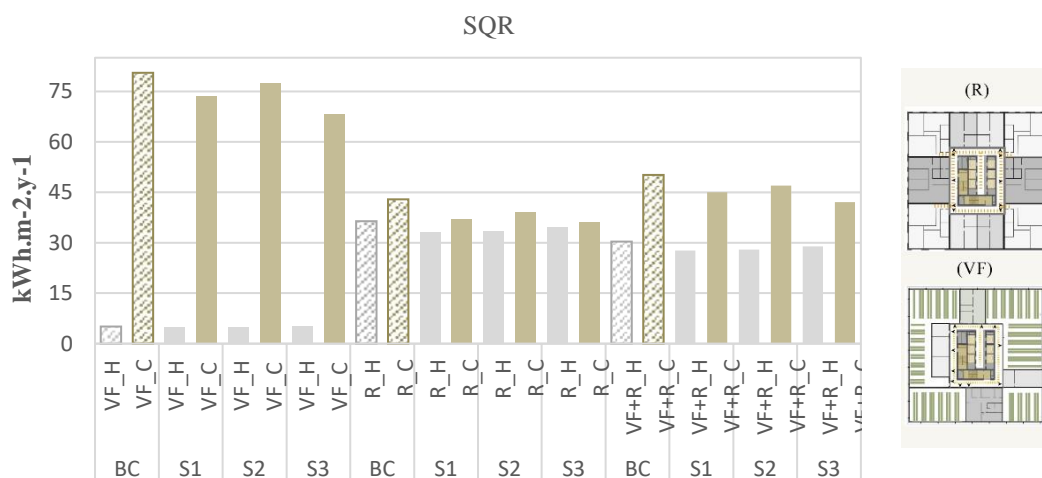


Figure 97. Comparison of Annual Heating and Cooling energy consumption (kWh.m-2Y-1) for each shading typology on SQR.

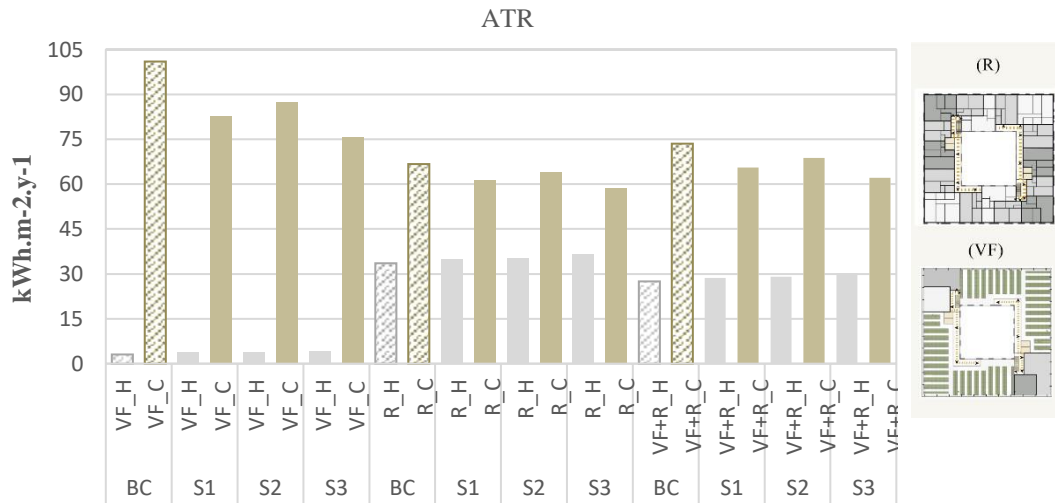


Figure 98. Comparison of Annual Heating and Cooling energy consumption (kWh.m-2Y-1) for each shading typology on ATR.

Figure 98 depicts the data demonstrating how the ATR morphology's heating and cooling energy consumption has been optimized. Surprisingly, the cooling energy consumption shows a notable average reduction of around 10.84 kWh.m-2Y-1, which translates to reductions of 18.9 %, 8%, and 11% for VF, R, and VF+R, respectively. Notably, S3's shading typology stands out as the best option for maximizing energy efficiency. The heating result on the other hand increase by a range of ±1.53 kWh.m-2Y-1 on average.

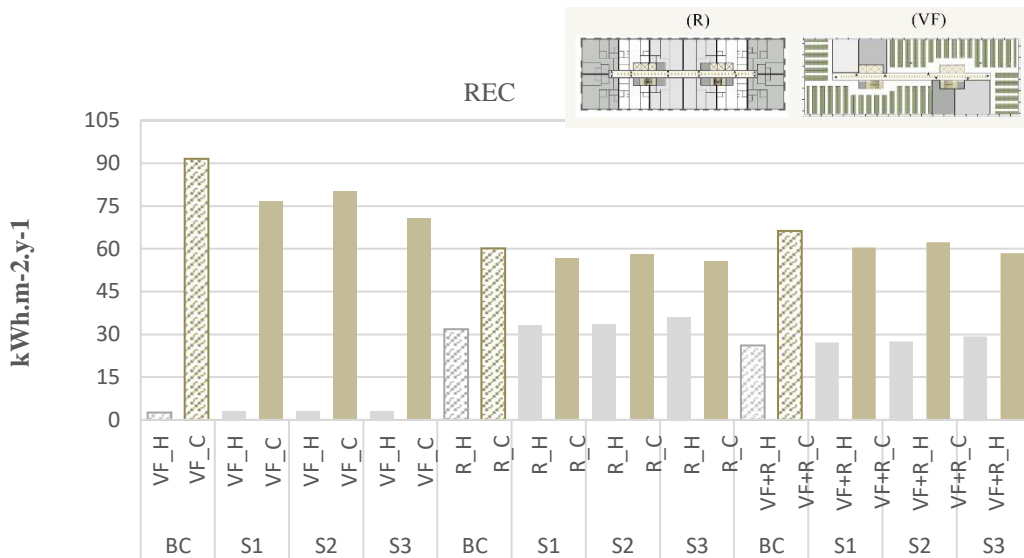


Figure 99. Comparison of Annual Heating and Cooling energy consumption (kWh.m-2Y-1) for each shading typology on REC.

Figure 99 depicts the data display of the REC morphology's heating and cooling energy consumption optimization data. The cooling energy consumption shows a notable average reduction of around 8.3 kWh.m-2Y-1, which translates to reductions of 17.1 %, 5.8%, and 8.8% slightly less than ATR for VF, R, and VF+R, respectively. Conversely, S3's shading typology stands out as the best option for maximizing energy efficiency. Heating results on the other hand increase by a range of ± 1.51 kWh.m-2Y-1 on average.

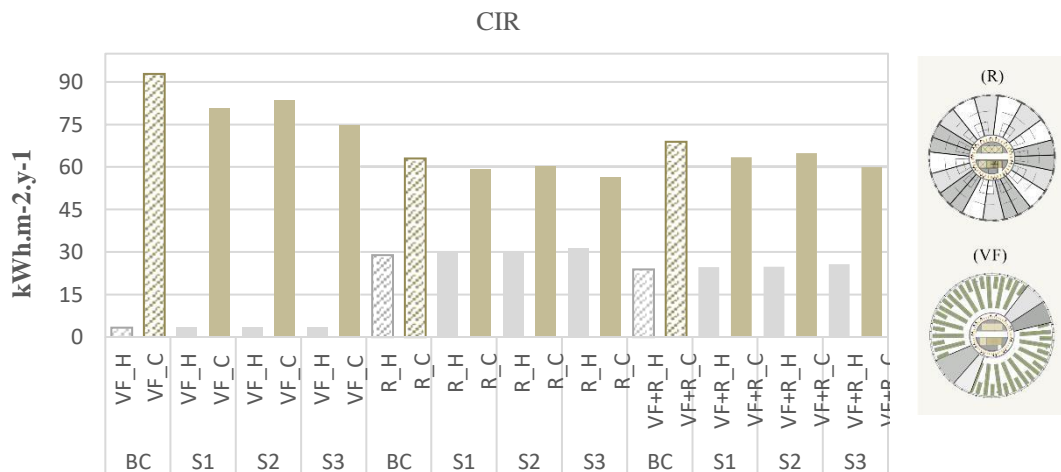


Figure 100. Comparison of Annual Heating and Cooling energy consumption (kWh.m-2Y-1) for each shading typology on CIR.

Figure 100 depicts the data display of the CIR morphology's heating and cooling energy consumption optimization data. The heating result on the other hand increase by an insignificant range ± 0.93 kWh.m-2Y-1 on average. The cooling energy consumption shows a notable average reduction of around 7.96 kWh.m-2Y-1, which translates to reductions of 14.3 %, 7%, and 8.9% for VF, R, and VF+R, respectively.

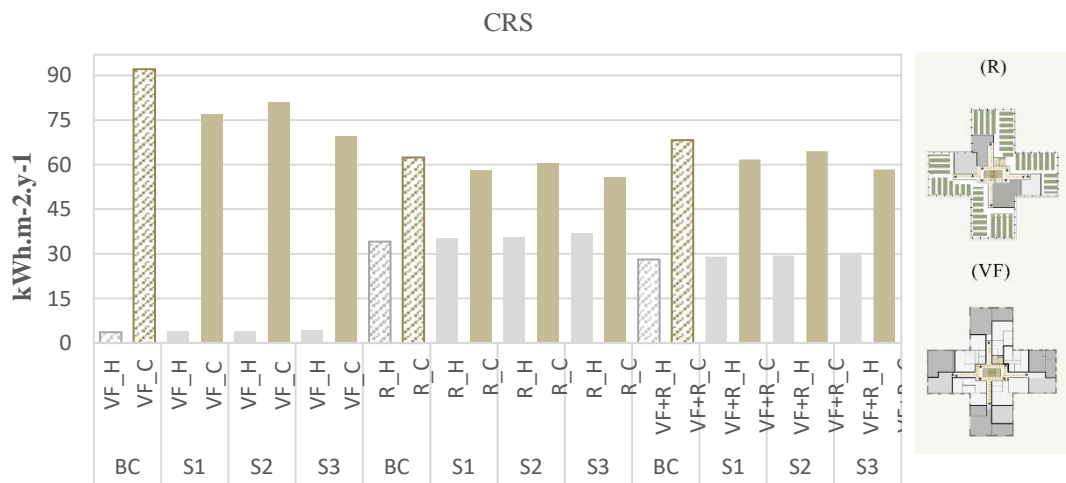


Figure 101. Comparison of Annual Heating and Cooling energy consumption (kWh.m-2Y-1) for each shading typology on CRS.

Figure 101 depicts the data display of the CRS morphology's heating and cooling energy consumption optimization data. The heating result on the other hand increase by an insignificant range ± 1.20 kWh.m-2Y-1 on average. The cooling energy consumption shows a notable average reduction of around 9.11 kWh.m-2Y-1, which translates to reductions of 17.7 %, 6.9%, and 9.7 % for VF, R, and VF+R, respectively

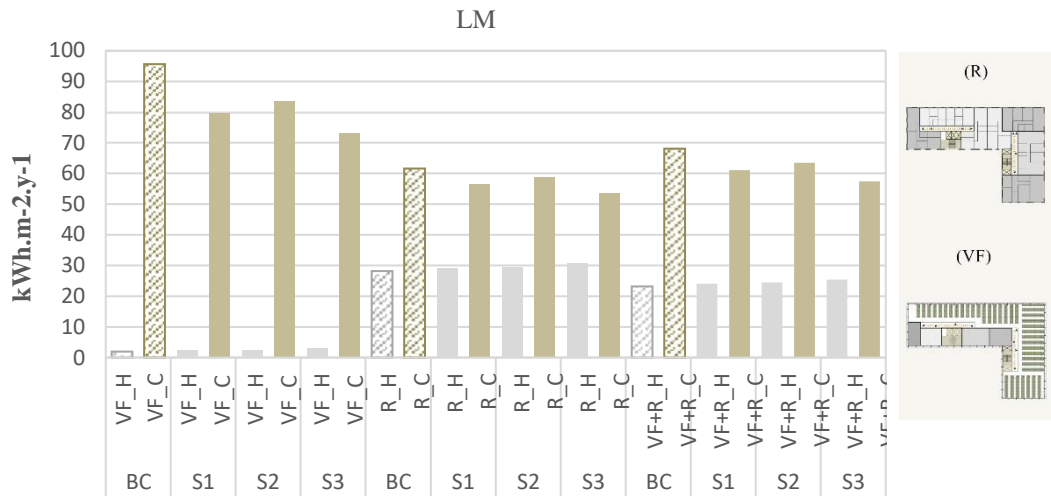


Figure 102. Comparison of Annual Heating and Cooling energy consumption (kWh.m-2Y-1) for each shading typology on LM.

Figure 102 depicts the data display of the LM morphology's heating and cooling energy consumption optimization data. It is noteworthy to mention that the optimization results in this climate setting do change on a very close range in between the morphologies. Heating results for LM increased by an insignificant range ± 1.27 kWh.m-2Y-1 on average. The cooling energy consumption shows a notable average reduction of around 9.11 kWh.m-2Y-1, which translates to reductions of 17.5 %, 8.5 %, and 11 % for VF, R, and VF+R, respectively.

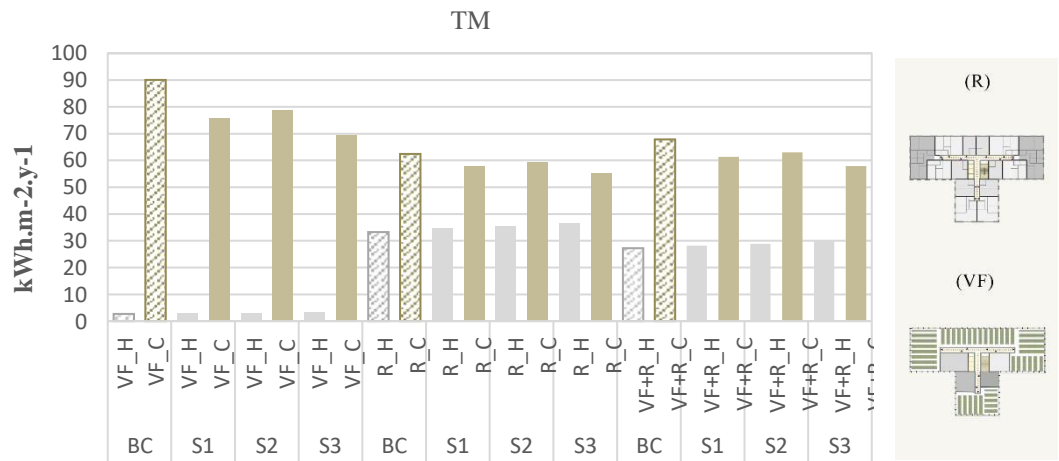


Figure 103. Comparison of Annual Heating and Cooling energy consumption (kWh.m-2Y-1) for each shading typology on TM.

Figure 103 depicts the data display of the TM morphology's heating and cooling energy consumption optimization data. The heating result on the other hand increase by an insignificant range of ± 1.42 kWh.m-2Y-1 on average. The cooling energy consumption shows a notable average reduction of around 9.11 kWh.m-2Y-1, which translates to reductions of 17 %, 8 %, and 10.3 % for VF, R, and VF+R, respectively.

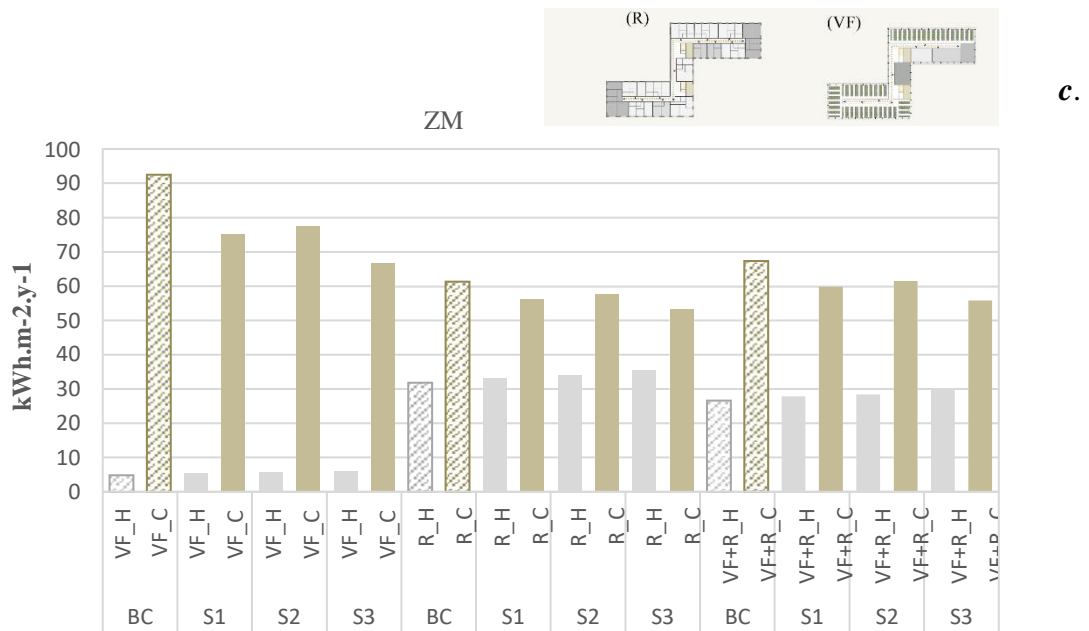


Figure 104. Comparison of Annual Heating and Cooling energy consumption (kWh.m-2Y-1) for each shading typology on ZM.

Figure 104 represents the optimization values of heating and cooling of ZM morphology. The heating result increases by an insignificant range ± 1.42 kWh.m-2Y-1 while cooling does decrease by 11.1 kWh.m-2Y-1 and has the greatest optimization on VF typology by 21%.

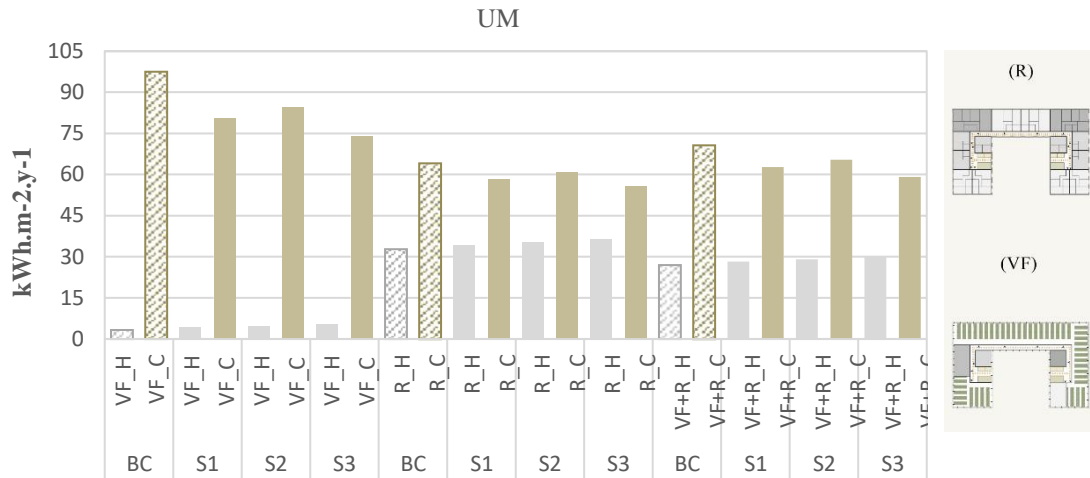


Figure 105. Comparison of Annual Heating and Cooling energy consumption (kWh.m-2Y-1) for each shading typology on UM.

Figure 105 represents the optimization values of heating and cooling of UM morphology. The heating result increases by a range of ± 1.9 kWh.m-2Y-1 while cooling does decrease by 10.7 kWh.m-2Y-1 and has the greatest optimization on VF typology by 18.3%. and last for R by only 9.2%.

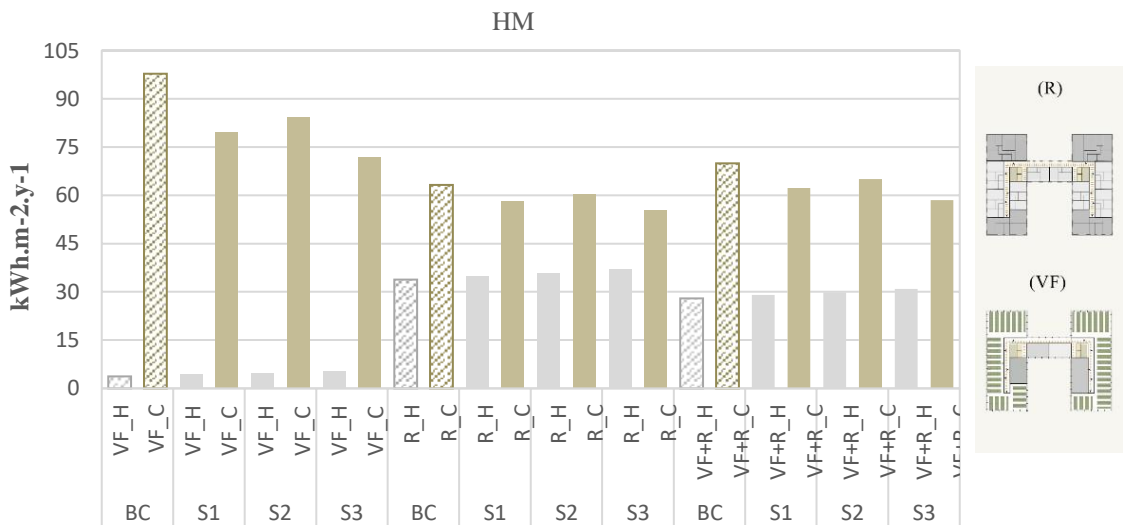


Figure 106. Comparison of Annual Heating and Cooling energy consumption (kWh.m-2Y-1) for each shading typology on HM.

Figure 106 represents the optimization values of heating and cooling of HM morphology which performs very similarly to UM with an average cooling demand decrease of ± 10.8 kWh.m-2Y-1.

6.3.2 Comparison of Morphological Optimization

A thorough review of the optimization values for the VF, R, and VF+R typologies over all examined morphologies is provided by the data shown. **Figure 107** further supports the conclusion that S3 is the most successful optimization scenario, with an improvement of almost 25 % when compared to other shading typologies. Surprisingly, in this specific climatic setting, the SQR morphology demonstrates the maximum amount of optimization for VF+R and R typology and HM for VF and whilst the REC morphology shows generally the least optimization. S3 achieves an optimization of up to 24.9%, followed by S1 which shows an optimization potential of up to 15%. Notably, as compared to R and VF+R, the VF typology exhibits the most substantial optimization values. Notably, as compared to R and VF+R, the VF typology exhibits the most substantial optimization values. These findings demonstrate how different morphologies and shading typologies in a particular climatic environment have variable degrees of optimization potential.

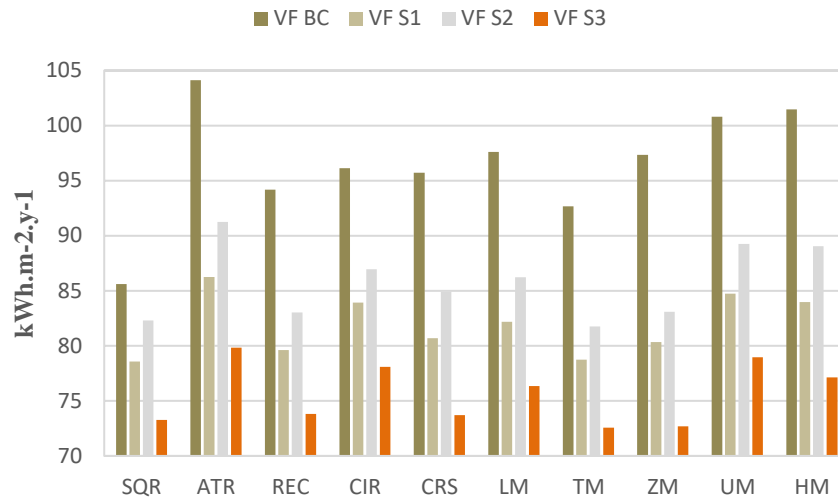


Figure 107. Comparison of Annual Total energy consumption (kWh.m-2Y-1) for each shading scenario according to all morphologies regarding VF.

The configurations with the highest and lowest total optimization for the R typology are shown in **Figure 108**. It shows that the REC morphology has had the least amount of optimization, whereas the SQR morphology has experienced the most amount decrease. The most effective shading typology among them is S3, which achieves an average optimization of about 5%. On the other hand, **Figure 109** shows the S3 optimization, with UM being the most optimal configuration and a range of 8.5% for VF+R morphology. The significance of shading techniques and their effect on maximizing energy efficiency for particular building typologies and morphologies are further highlighted by these figures.

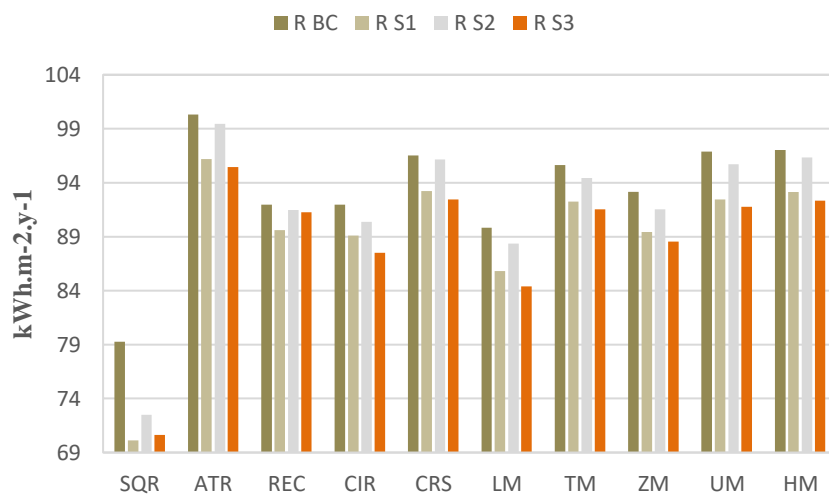


Figure 108. Comparison of Annual Total energy consumption (kWh.m-2Y-1) for each shading scenario according to all morphologies regarding R (Residence).

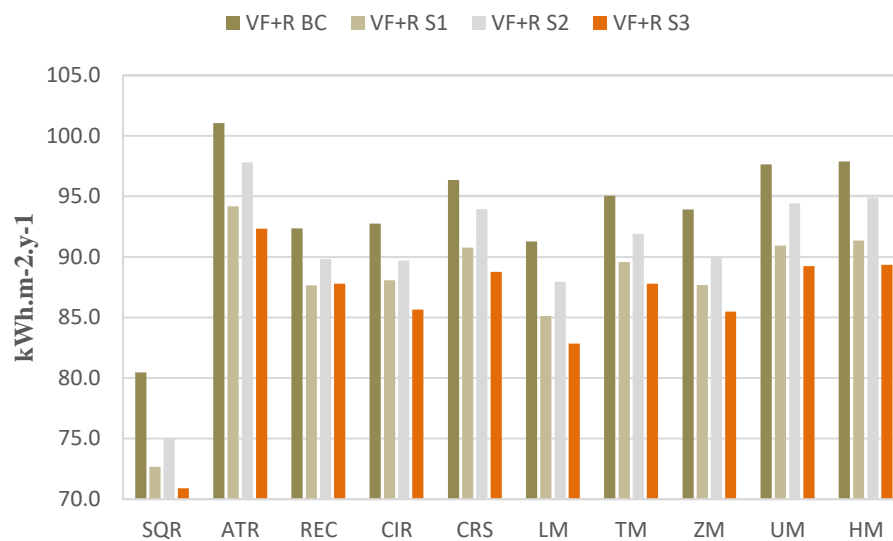


Figure 109. Comparison of Annual Total energy consumption (kWh.m-2Y-1) for each shading scenario according to all morphologies regarding VF+R.

Table 25. Shading efficiency results for the climate of Athens (%).

	VF (Vertical farming)				R (Residence)				VF+R (CEA Integrated High-Rise)			
	BC	S1	S2	S3	BC	S1	S2	S3	BC	S1	S2	S3
SQR	-	-	-	-	-	-	-	-	-	-	-	-
ATR	-21.6	-9.7	-10.9	-8.9	26.6	-37.1	-37.1	-35.2	-25.6	-29.6	-30.4	-30.2
REC	9.5	7.7	9.0	7.5	8.4	6.8	8.0	4.4	8.6	6.9	8.2	4.9
CIR	-2.1	-5.4	-4.7	-5.8	0.0	0.6	1.2	4.1	-0.4	-0.5	0.1	2.4
CRS	0.4	3.8	2.3	5.6	-5.0	-4.6	-6.4	-5.7	-3.9	-3.1	-4.7	-3.7
LM	-2.0	-1.8	-1.5	-3.6	7.0	8.0	8.1	8.7	5.3	6.2	6.4	6.7
TM	5.1	4.2	5.2	4.9	-6.5	-7.5	-6.9	-8.5	-4.1	-5.3	-4.5	-6.0
ZM	-5.0	-2.1	-1.7	-0.2	2.6	3.1	3.1	3.3	1.2	2.1	2.2	2.6
UM	-3.6	-5.4	-7.4	-8.6	-4.0	-3.4	-4.6	-3.7	-4.0	-3.7	-5.1	-4.4
HM	-0.7	0.9	0.2	2.3	-0.1	-0.7	-0.6	-0.6	-0.2	-0.5	-0.5	-0.1

Note: (SQR morphology is kept as base case scenario, Darker shades indicate higher optimization values)

CHAPTER 7

CONCLUSIONS

7.1 Conclusions

The study presented in this paper discusses the underexplored field of employing computational data to evaluate the energy performance and future predictions of vertical farming and high-rise residential design. A complete approach is given in this study, which takes into account many design characteristics such as building form, typology, transparency, and shading devices. The framework integrates analytical and quantitative methodologies to evaluate and optimize the energy efficiency of 10 morphologies in Humid subtropical, Tropical, and Mediterranean climate. By doing so, the novelty of this research focuses on filling the gaps in the existing body of literature, attempting first and foremost to raise the climate and morphological choice consciousness of designers and architects during the decision-making process.

In contrast to previous research, the approach suggested in this work contributes significantly to the evaluation and optimization of energy performance in prevalent and various morphologies of contemporary high-rise residential structures. The process outperforms prior investigations by providing a more thorough and advanced understanding of the complex interplay between design factors. Furthermore, it adds a new dimension by integrating the vertical farming typology, which was previously overlooked in energy simulations. The study provides a new viewpoint and significant insights into the subject of energy efficiency in integrated CEA high-rise residential structures through the following key findings:

- Among the analyzed climates, Singapore's tropical climate has the greatest energy consumption, suggesting the most substantial energy requirements

for cooling and none for heating. Following closely, Athens's Mediterranean climate performs similarly to that of Singapore, nonetheless is at least 27 % more suitable and efficient than the former. Moreover, Athens and secondly New York's climates were found to have the most appropriate conditions for such CEA integrated models with the least energy consumed yearly on an average ± 94.56 and $126.07 \text{ kWh.m-2Y-1}$ respectively across all morphologies.

- ATR morphology is unsuitable, especially for climates comparable to those of Singapore and Athens. However, can be successfully used in cooler climates such as New York. Conversely, in warmer climates of the Mediterranean and tropical, morphologies with higher S/V ratios and lower compactness have the lowest ranking.
- It is feasible to obtain large savings in overall energy usage by carefully selecting the proper morphology at the early design stage, adapted to the unique climatic setting. In the instance of New York, the highest optimization rate is outstandingly 62.1%, similarly, Singapore's climatic environment is 20.7%, and Athens by 26.5% showing a significant reduction in energy use.
- When comparing annual simulated energy demand across different typologies such as VF, R, and integrated VF+R, it is clear that the residential typology consumes the most energy. The residential typology outperforms other typologies in terms of energy needs, with an average of $\pm 169.3 \text{ kWh.m-2Y-1}$ across all climates consuming at least 28.8% more than VF.
- The study found that the SQR typology performed remarkably well in both Singapore and Athens, making it the best-case scenario for energy efficiency. In general, the LM typology outperformed in all three climates, solidifying its status as one of the top rankings. The ATR typology, on the other hand, constantly shows inadequate energy efficiency as compared to other typologies, making it the worst-case scenario in terms of energy

demand.

- The estimated results show that the morphologies can be optimized through shading devices with an energy demand decrease of up to 25 % in which the best performance was provided utilizing shading typology S3 of both horizontal and vertical.
- The future prediction scenarios showed that the energy needed for cooling will be doubled by the year 2011, in addition, demonstrated that the morphological selection will change and need to adapt to these changes.
- The investigated cost estimations for food production depicted that the modeled prototype of vertical farming needs only 30 % of food for the residents yearly, while the rest of 70 % can be used to supply service sectors. The payback time from the initial start-up investing cost is calculated to be in 2.3 years.

7.2 Recommendation for future research

Based on the data and insights gained from this study, various recommendations for future research on the subject of energy consumption and typologies may be made. These proposals seek to increase our understanding and efficacy of energy-efficient building design. The validity and reliability of this research study derive from the use of advanced computational software tools for modelings, such as Design-Builder, Meteonorm, and Energy-Plus. These software platforms made it possible to accurately simulate different features of high-rise residential and vertical farming structures, including accurate construction characteristics, HVAC systems, occupancy patterns, glazing properties, heating/cooling schedules, natural ventilation schedules, and other energy load inputs. Comprehensive findings were acquired by running over 900 simulations, giving a solid foundation for further research in the following crucial areas:

- Renewable Energy System Integration
- Advanced examination of occupant behavior patterns, preferences, and habits, and their impact on this typology's energy consumption
- Embodied Energy and Life-Cycle Assessment: Consideration of the complete life-cycle of typologies, including embodied energy.
- Additional investigation is needed to look into the morphological configuration of High-Rise Integrated CEA buildings, with a focus on their shape and geometric qualities, particularly those with more organic shapes.
- Analysis of aspect ratio optimization of the morphologies
- Including variables of different transparencies.
- Advanced analysis of the cost estimations and profitability of such models and their feasibility.
- Including interior layout in the making and evaluation of simulation results.

REFERENCES

- T. Saroglou, I.A. Meir, T. Theodosiou, B. Givoni, Towards energy efficient skyscrapers, *Energy Build.* (2017), <https://doi.org/10.1016/j.enbuild.2017.05.057>.
- Food and Agriculture Organization of the United Nations (FAO). Database on Arable Land (2021). Available online
- Bogomolova, S., Loch, A., Lockshin, L., and Buckley, J. (2018). Consumer factors associated with purchasing local vs. global value chain foods. *Renew. Agric. Food Syst.* 33, 33–46. doi: 10.1017/S1742170516000375 http://www.fdnearth.org/files/2012/09/Why-verticalfarms_Final.pdf
- Harada, Y., and Whitlow, T. H. (2020). Urban rooftop agriculture: challenges to science and practice. *Front. Sustain. Food Syst.* 4:76. doi: 10.3389/fsufs.2020.00076
- Renmark, A. (2021). The hyped trend is growing – but is it sustainable?
- O’Sullivan C.A., McIntyre C.L., Dry I.B., Hani S.M., Hochman Z., Bonnett G.D. Vertical farms bear fruit. *Nat. Biotechnol.* (2020)
- Appolloni, E., Orsini, F., Michelon, N., Pistillo, A., Paucek, I., Pennisi, G., et al. (2020). From micro garden technologies to vertical farms: innovative growing solutions for multifunctional urban agriculture. doi: 10.17660/ActaHortic.2020.1298.10
- Armanda, D. T., Guinée, J. B., and Tukker, A. (2019). The second green revolution: innovative urban agriculture's contribution to food security and sustainability—a review. *Glob. Food Security.* 22, 13–24. doi 10.1016/j.gfs.2019.08.002
- Pinstrup-Andersen, P. (2018). Is it time to take vertical indoor farming seriously? *Glob. Food Security.* 17, 233–235. doi 10.1016/j.gfs.2017.09.002
- Bryce, E. (2019). The Trouble with the Urban Farming “Revolution.” *Anthropocene.*
- McDougall, R., Kristiansen, P., and Rader, R. (2019). Small-scale urban agriculture results in high yields but requires judicious management of inputs to achieve sustainability. *PNAS-Proc. Nat. Acad. Sci.* 116, 129–134. doi: 10.1073/pnas.1809707115
- Bustamante, M. J. (2020). Using sustainability-oriented process innovation to shape product markets. *Int. J. Innov. Manag.* doi: 10.1142/S1363919620400010
- Butturini, M., and Marcelis, L. F. M. (2020). “—vertical farming in Europe: present status and

- outlook,” in *Plant Factory*, 2nd Edn, eds T. Kozai, G. Niu, and M. Takagakidoi: 10.1016/B978-0-12-816691-8.00004-2
- Khan, R., Aziz, Z., & Ahmed, V. (2018). Building integrated agriculture information modeling (BIAIM): An integrated approach towards urban agriculture.
- Kim, H., Lee, K., Lee, J., & Lee, S. (2018). Exploring outdoor solar potential in high-density living: Analyzing direct sunlight duration for urban agriculture in Seoul’s residential complexes. *Energies*.
- Kosorić, V., Huang, H., Tablada, A., Lau, S. K., & Tan, H. T. (2019). Survey on the social acceptance of the productive façade concept integrating photovoltaic and farming systems in high-rise public housing blocks in Singapore. *Renewable and Sustainable Energy Reviews*.
- Song, X. P., Tan, H. T., & Tan, P. Y. (2018). Assessment of light adequacy for vertical farming in a tropical city. *Urban Forestry & Urban Greening*.
- Palliwal, A., Song, S., Tan, H. T. W., & Biljecki, F. (2021). 3D city models for urban farming site identification in buildings. *Computers, Environment and Urban Systems*, 86. <https://doi.org/10.1016/j.compenvurbsys.2020.101584>
- van Delden, S. H., SharathKumar, M., Butturini, M., Graamans, L. J. A., Heuvelink, E., Kacira, M., Kaiser, E., Klamer, R. S., Klerkx, L., Kootstra, G., Loeber, A., Schouten, R. E., Stanghellini, C., van Ieperen, W., Verdonk, J. C., Violet-Chabrand, S., Woltering, E. J., van de Zedde, R., Zhang, Y., & Marcelis, L. F. M. (2021). Current status and future challenges in implementing and upscaling vertical farming systems. In *Nature Food*. <https://doi.org/10.1038/s43016-021-00402-w>
- Al-Kodmany, K. (2018). The vertical farm: A review of developments and implications for the vertical city. In *Buildings* (Vol. 8, Issue 2). MDPI AG. <https://doi.org/10.3390/buildings8020024>
- Gibson T. Room to grow. *ASEE Prism* ;27(7):26–31. <https://doi.org/10.2307/26820026>.
- O’Sullivan, C.A.; Bonnett, G.D.; McIntyre, C.L.; Hochman, Z.; Wasson, A.P. (2019) Strategies to improve the productivity, product diversity, and profitability of urban agriculture. *Agric. Syst*.
- Avgoustaki, D.D.; Xydis, G (2020). Indoor vertical farming in the urban nexus context: Business growth and resource savings. *Sustainability*.
- Khandaker, M.; Kotzen, B (2018). The potential for combining living wall and vertical farming systems with aquaponics with special emphasis on substrates.

- Popkova, E.G. (2022) Vertical Farms Based on Hydroponics, Deep Learning, and AI as Smart Innovation in Agriculture. *Smart Innov. Syst. Technol.*
- Ng, A.K.; Mahkeswaran, R. (2021) Emerging and Disruptive Technologies for Urban Farming: A Review and Assessment. *J. Phys. Conf. Ser.*
- Krishnan, A.; Swarna, S.; Balasubramanya, H.S. (2020) Robotics, IoT, and AI in the Automation of Agricultural Industry: A Review. In *Proceedings of the 2020 IEEE Bangalore Humanitarian Technology Conference (B-HTC)*
- Sharma, R.; Kamble, S.S.; Gunasekaran, A.; Kumar, V.; Kumar, A. (2020) A systematic literature review on machine learning applications for sustainable agriculture supply chain performance. *Comput. Oper. Res.*
- Talaviya, T.; Shah, D.; Patel, N.; Yagnik, H.; Shah, M. (2020) Implementation of artificial intelligence in agriculture for optimisation of irrigation and application of pesticides and herbicides. *Artif. Intell. Agric.*
- Rohit, R.V.S.; Chandrawat, D.; Rajeswari, D. (2021) Smart Farming Techniques for New Farmers Using Machine Learning.
- Ekici, B., Turkcan, O. F. S. F., Turrin, M., Sariyildiz, I. S., & Tasgetiren, M. F. (2021). Optimising High-Rise Buildings for Self-Sufficiency in Energy Consumption and Food Production Using Artificial Intelligence: Case of Europoint Complex in Rotterdam. *Sustainability*, 13(13), 7162.
- Gan, V.J.; Wong, H.; Tse, K.T.; Cheng, J.C.; Lo, I.M.; Chan, C.M. (2019) Simulation-based evolutionary optimization for energy-efficient layout plan design of high-rise residential buildings. *J. Clean. Prod.*, 231, 1375–1388
- Jayaweera, N.; Rajapaksha, U.; Manthilake, I. (2021) A parametric approach to optimize solar access for energy efficiency in high-rise residential buildings in dense urban tropics. *Sol. Energy*, 220, 187–203.
- Yarbrough, D.W.; Bomberg, M.; Romanska-Zapala, A. (2019) On the next generation of low-energy buildings. *Adv. Build. Energy Res.*, 1–8
- Godoy-Shimizu, D.; Steadman, P.; Hamilton, I.; Donn, M.; Evans, S.; Moreno, G.; Shayesteh, H. (2018) Energy use and height in office buildings. *Build. Res. Inf.*, 46, 845–863.
- Imam, M.; Kolarevic, B. (2018) Towards Resource-Generative Skyscrapers. *Int. J. High-Rise Build.*, 7, 161–170.
- Chen, X.; Huang, J.; Zhang, W.; Yang, H. (2019) Exploring the optimization potential of thermal and power performance for a low-energy high-rise building. *Energy Procedia*,

158, 2469–2474.

- Chen, X.; Yang, H. (2018) Integrated energy performance optimization of a passively designed high-rise residential building in different climatic zones of China. *Appl. Energy*, 215, 145–158.
- Graamans, L.; Tenpierik, M.; van den Dobbelsteen, A.; Stanghellini, C. Plant factories: (2020) Reducing energy demand at high internal heat loads through facade design. *Appl. Energy*
- Chen, X.; Yang, H.; Peng, J. (2019) Energy optimization of high-rise commercial buildings integrated with photovoltaic facades in urban context. *Energy*
- Ref Giouri, E.D.; Tenpierik, M.; Turrin, M. (2019) Zero energy potential of a high-rise office building in a Mediterranean climate: Using multi-objective optimization to understand the impact of design decisions towards zero-energy high-rise buildings. *Energy Build.*, 209, 109666.
- Liu, J.; Wang, M.; Peng, J.; Chen, X.; Cao, S.; Yang, H. (2020) Techno-economic design optimization of hybrid renewable energy applications for high-rise residential buildings. *Energy Convers. Manag.*, 213, 112868
- The European Parliament and the Council of the European Union. (2018) Amending Directive 2010/31/EU on the energy performance of buildings. *Off. J. Eur. Union L*, L153, 13–35.
- Yang, Z.; Chen, Y.; Zheng, Z.; Huang, Q.; Wu, Z. (2020) Application of building geometry indexes to assess the correlation between buildings and air temperature. *Build. Environ.*, 167, 106477.
- Zhang, J.; Cui, P.; Song, H. (2020) Impact of urban morphology on outdoor air temperature and microclimate optimization strategy based on Pareto optimality in Northeast China. *Build. Environ.*, 1
- Boccalatte, A.; Fossa, M.; Gaillard, L.; Menezo, C. (2020) Microclimate and urban morphology effects on building energy demand in different European cities. *Energy Build.*, 224, 110129
- Leng, H.; Chen, X.; Ma, Y.; Wong, N.H.; Ming, T. (2020) Urban morphology and building heating energy consumption: Evidence from Harbin, a severe cold region city. *Energy Build.* 2020, 224, 110143.
- . Zhu, D.; Song, D.; Shi, J.; Fang, J.; Zhou, Y. (2020) The Effect of Morphology on Solar Potential of High-Density Residential Area: A Case Study of Shanghai. *Energies*,
- Feng, J., Luo, X., Gao, M., Abbas, A., Xu, Y. P., & Pouramini, S. (2021). Minimization of

- energy consumption by building shape optimization using an improved Manta-Ray Foraging Optimization algorithm. *Energy Reports*, 7. <https://doi.org/10.1016/j.egy.2021.02.028>
- Jalali, Z., Noorzai, E., & Heidari, S. (2020). Design and optimization of the form and facade of an office building using the genetic algorithm. *Science and Technology for the Built Environment*, 26(2). <https://doi.org/10.1080/23744731.2019.1624095>
- Chen, Y., & Hong, T. (2018). Impacts of building geometry modeling methods on the simulation results of urban building energy models. *Applied Energy*, 215. <https://doi.org/10.1016/j.apenergy.2018.02.073>
- Kumar, D., Alam, M., Zou, P. X. W., Sanjayan, J. G., & Memon, R. A. (2020). Comparative analysis of building insulation material properties and performance. In *Renewable and Sustainable Energy Reviews* (Vol. 131). <https://doi.org/10.1016/j.rser.2020.110038>
- Košir, M., Gostiša, T., & Kristl, Ž. (2018). Influence of architectural building envelope characteristics on energy performance in Central European climatic conditions. *Journal of Building Engineering*, 15, 278–288. <https://doi.org/10.1016/j.job.2017.11.023>
- Mancebo F. (2018) Gardening the city: addressing sustainability and adapting to global warming through urban agriculture. *Environments*;5:38. Mallick, T. (2019). The impact of building form and orientation on the natural ventilation potential of buildings. *Journal of Building Engineering*, 20, 100611.
- Sivakumar, A. (2018). Building form and orientation: A review of their influence on natural ventilation in buildings. *Renewable and Sustainable Energy Reviews*, 92, 609-622.
- Lee, J. and Kim, J. (2017). Building form and orientation effects on natural ventilation in apartment buildings. *Energy and Buildings*, 140, 578-588.
- Petrucci, A. and Barazzetti, L. (2019). Building form and orientation effects on natural lighting in office buildings. *Energy and Buildings*, 193, 186-198.
- Ampim, P.A.Y.; Obeng, E.; Olvera-Gonzalez, E. (2022) Indoor Vegetable Production: An Alternative Approach to Increasing Cultivation. *Plants* 2022, 11, 2843. <https://doi.org/10.3390/plants11212843>
- AYDIN, D., & MIHLAYANLAR, E. (2020). A Case Study on the Impact of Building Envelopes on Energy Efficiency in High-Rise Residential Buildings. *Architecture, Civil Engineering, Environment*, 13(1), 5–18. <https://doi.org/10.21307/acee-2020-001>

- El-Darwish, I., & Gomaa, M. (2017). Retrofitting strategy for building envelopes to achieve energy efficiency. *Alexandria Engineering Journal*, 56(4), 579–589. <https://doi.org/10.1016/j.aej.2017.05.011>
- Li, Liu, et al. (2019) "Effect of Geometric Factors on the Energy Performance of High-Rise Office Towers in Tianjin, China." 166 in *Buildings*, vol. 9, no. 7. doi: 10.3390/buildings9070166.
- Chen, et al. (2021). "Impact of Building Orientation on Passive Cooling Performance in Different Climate Zones." *Energy and Buildings*, vol. 231, pp. 111943.
- Wang, et al. (2018). "Daylighting Performance of Buildings with Different Forms and Orientations." *Energy and Buildings*, vol. 170, pp. 1-10.
- Park, et al. (2020). "Effect of Building Form and Orientation on Energy Consumption of Residential Buildings." *Applied Energy*, vol. 260, pp. 114309.
- Xu, et al. (2019). "Building Form and Orientation: Impact on Greenhouse Gas Emissions of Residential Buildings." *Building and Environment*, vol. 157, pp. 96-107
- Zhu, D. (2020). Building form and energy performance relationship: A review of the impact of building morphology on energy consumption. *Renewable and Sustainable Energy Reviews*, 140, 111336.
- Choi and Roaf (2018) "Reducing Heat Loss in Winter and Heat Gain in Summer by Insulated Walls: A Case Study" *Journal of Building Envelope Construction*.
- Lstiburek (2017) "Insulated Roofs and Energy Efficiency" Building Science Corporation.
- National Fenestration Rating Council (2021) "High-Efficiency Windows" National Fenestration Rating Council.
- Levinson (2010) "The Benefits of Reflective Roofing" Lawrence Berkeley National Laboratory.
- Burdick, A. (2011). Strategy guideline: accurate heating and cooling load calculations. US Department of Energy, Building Technologies Program. Retrieved from <https://www.energy.gov/eere/buildings/downloads/strategy-guideline-accurate-heating-and-cooling-load-calculations>
- Javanroodi, K., Mahdavinejad, M., & Nik, V. M. (2018). Impacts of urban morphology on reducing cooling load and increasing ventilation potential in hot-arid climate. *Applied Energy*, 231, 714–746. <https://doi.org/10.1016/j.apenergy.2018.09.116>

- Touliatos, D., Dodd, I. C., &McAinsh, M. (2016). Vertical farming increases lettuce yield per unit area compared to conventional horizontal hydroponics. *Food Energy Security*, 5(3), 184-191. doi: 10.1002/fes3.83. PMID: 27635244; PMCID: PMC5001193.
- Agriitecture. (2019). Montel's mobile grow systems optimize space vertically and horizontally. Retrieved from <https://www.agriitecture.com/blog/2019/7/12/montels-mobile-grow-systems-optimize-space-vertically-and-horizontally>
- Vartholomaios, A. (2017). A parametric sensitivity analysis of the influence of urban form on domestic energy consumption for heating and cooling in a Mediterranean city. *Sustainable Cities and Society*, 28, 135–145. doi:10.1016/j.scs.2016.09.006
- Gibson T. Room to grow. *ASEE Prism* 2018;27(7):26–31.<https://doi.org/10.2307/26820026>.
- Specht K, Siebert R, Hartmann I, Freisinger UB, Sawicka M, Werner A, Dierich A. (2013)Urban agriculture of the future: an overview of sustainability aspects of food production in and on buildings. *Agric Hum Val* 2013;31(1):33–51. <https://doi.org/10.1007/s10460-013-9448-4>.
- Mancebo F. (2018) Gardening the city: addressing sustainability and adapting to global warming through urban agriculture. *Environments* 2018;5:38.
- Benis K, Reinhart C, Ferrão P. (2017) Development of a simulation-based decision support workflow for the implementation of Building-Integrated Agriculture (BIA) in urban contexts. *J Clean Prod* 2017;147:589–602. <https://doi.org/>
- Liu S, Teng P. (2020) HIGH-TECH plant factories: challenges and way forward. Rep. S. Rajaratnam School of International Studies; 2017. p. 11–7. Retrieved April 6, 2020, from, www.jstor.org/stable/resrep17149.6.
- Tong Z, Whitlow TH, Landers A, Flanner B. (2015) A case study of air quality above an urban rooftop vegetable farm. *Environ Pollut* 2016;208:256–60. <https://doi.org/10.1016/j.envpol.2015.07.006>.
- Raji, Babak, et al. "Early-Stage Design Considerations for the Energy-Efficiency of High-Rise Office Buildings." *Sustainability*, vol. 9, no. 8, 2017, pp. 1-19.
- Naqvi, S.M.Z.A.; Saleem, S.R.; Tahir, M.N.; Hussain, S.; UIHaq, S.I.; Awais, M.; Qamar, S. (2022)Vertical Farming—Current Practices and Its Future. *Environ. Sci. Proc.* 2022, 23, 4. <https://doi.org/10.3390/environsciproc2022023004>
- Chaganti, R., Rustam, F., Daghri, T., de la Torre Díez, I., Vidal Mazón, J. L., Rodríguez, C. L., & Ashraf, I. (2021). Building Heating and Cooling Load Prediction Using Ensemble Machine Learning Model. *Mia*, 1(1), 1-9. doi: 10.3390/mia1010001

- german., & Boubekri, M. (2017). Statistical analysis of Impact of Building Morphology and Orientation on its Energy Performance. *Journal of Engineering and Architecture*, 5(1), 15-25. doi: 10.15640/jea.v5n1a2
- Engler, Nicholas and Krarti, M. (2017) "Review of Energy Efficiency in Controlled Environment Agriculture." *Journal of Sustainable Agriculture*, vol. 41, no. 5, 2017, pp. 514-529.
- Werner Pessenlehner and Ardeshir Mahdavi (2006). Building morphology, transparency, and energy performance, na
- Ramzi Ourghi, Adnan Al-Anzi, Moncef Krarti. "A simplified analysis method to predict the impact of shape on annual energy use for office buildings." *Energy and Buildings*, Volume 38, Issue 7, July 2006, Pages 757-764.
- Camporeale, P. E., & Mercader-Moyano, P. (2019). Towards Nearly Zero Energy Buildings: Shape optimization of typical housing typologies in Ibero-American temperate climate cities from a holistic perspective. *Solar Energy*, 193, 738–765. <https://doi.org/10.1016/j.solener.2019.09.091>
- Ciardello, A., Rosso, F., Dell’Olmo, J., Ciancio, V., Ferrero, M., & Salata, F. (2020). A multi-objective approach to the optimization of shape and envelope in building energy design. *Applied Energy*, 280. <https://doi.org/10.1016/j.apenergy.2020.115984>
- Albatici, R., & Passerini, F. (2010). Building shape and heating requirements: A parametric approach in Italian climatic conditions. In *Proceedings: CESB 2010 Prague - Central Europe towards Sustainable Building “From Theory to Practice”* (pp. 1–14). Czech technical university
- Hassan, A. M., Fatah El Mokadem, A. A., Megahed, N. A., & Abo Eleinen, O. M. (2020). Improving outdoor air quality based on building morphology: Numerical investigation. *Frontiers of Architectural Research*, 9(2), 319–334. <https://doi.org/10.1016/j.foar.2020.01.001>
- IRAM, (2018). IRAM 11900 Energy Performance in Residential Units. Calculation Method.
- AENOR, (2011). UNE-EN ISO 13790: 2011 Energy Efficiency of Buildings, Energy Consumption Calculation for Heating and Cooling of Spaces. (ISO 13790: 2008). Spanish Standardization and Certification Association.
- ASHRAE (2013) Handbook: Fundamentals. American Society of Heating, Refrigerating and Air-conditioning Engineers, Atlanta

APPENDIX

Vertical Farming Case Studies

Appendix A – SKY GREENS: World’s first low-carbon, hydraulic-driven vertical farm located in Singapore

Appendix B – AEROFARM: A Leading Vertical Farming Company Based in Newark, New Jersey

Appendix C – LUFA FARMS: Pioneering World’s largest Rooftop Greenhouse for Fresh Produce in Montreal, Canada

Appendix D – VERTICAL HARVEST: A Breakthrough in Sustainable Agriculture Year-Round Fresh Produce in Wyoming, USA

Appendix E – FREIGHT FARMS: Revolutionizing Urban Farming with Self-Contained Shipping Container Farms in Boston, USA

Appendix F – MIRAI GROUP Leading the Way in Sustainable and High-Tech Farming Practices